



Provided by the author(s) and University of Galway in accordance with publisher policies. Please cite the published version when available.

Title	Targeted Tissue Engineering: Enhancing Mesenchymal Stem Cell Localisation and Therapeutic Support for Cartilage Repair
Author(s)	Bulman, Sarah Elizabeth
Publication Date	2014-01-06
Item record	http://hdl.handle.net/10379/4402

Downloaded 2024-04-25T14:52:30Z

Some rights reserved. For more information, please see the item record link above.



Targeted Tissue Engineering: Enhancing Mesenchymal Stem Cell Localisation and Therapeutic Support for Cartilage Repair



*A thesis submitted to the National University of Ireland as
fulfilment of the requirement for the degree of*

Doctor of Philosophy

By

Sarah Elizabeth Bulman

**Regenerative Medicine Institute (REMEDI),
College of Medicine, Nursing & Health Sciences,
National University of Ireland, Galway**

Thesis Supervisors:

Prof. Frank Barry

Dr. Mary Murphy

Dr. Cynthia Coleman

Date of Submission: August 2013

Table of Contents

Table of Contents	2
Declaration	9
List of Abbreviations	10
Abstract	13
List of Tables	14
List of Figures	15

Chapter 1 *Introduction*

1.1 Osteoarthritis	19
1.1.1 Osteoarthritis	19
1.1.2 Normal Cartilage Biology	19
1.1.3 Normal Functional Physiology of Cartilage	21
1.1.4 ECM Changes in OA	22
1.2 Clinical Cartilage Repair Strategies	25
1.2.1 Clinical Cartilage Repair	25
1.2.2 Tissue Engineering Principles for Cartilage Repair	27
1.2.3 Scaffolds in the Clinic for Cartilage Tissue Engineering	27
1.3 Mesenchymal Stem Cells	28
1.3.1 Mesenchymal Stem Cells	28
1.3.2 MSC Source	29
1.3.3 Bone Marrow MSC Transplantation for Cartilage Repair	30
1.3.4 MSC Support of the Environmental Niche	31
1.4 MSC Retention	33
1.4.1 MSC Retention	33
1.4.2 Enhancing Cellular Retention	36
1.4.3 Antibody-based Localisation	37
1.4.4 Peptide-based Localisation	39

1.5 Thesis Objectives	41
------------------------------	-----------

Chapter 2

Pullulan: A Biocompatible Adhesive for Enhancing MSC Retention and Response at the Degraded Cartilage Surface.

2.1 Introduction	45
2.1.1 Bioadhesion and Bioadhesives for Cell Retention	45
2.1.2 Pullulan	46
2.1.3 Pullulan Properties	47
2.1.4 Pullulan as an Adhesive for Cell Retention	48
2.2 Materials and Methods	49
2.2.1 MSC Isolation	49
2.2.2 MSC Viability and Proliferation	49
2.2.3 MSC Flow Cytometry	50
2.2.4 MSC Differentiation	50
2.2.5 OA Cartilage Explant Culture	53
2.2.6 Explant Culture with MSCs and Pullulan	53
2.2.7 Stereological Assessment of MSC binding	55
2.2.8 Flow Cytometric Analysis of Dectin-2	55
2.2.9 Statistical Analysis	55
2.3 Results	56
2.3.1 MSC Viability and Proliferation in the Presence of Pullulan	56
2.3.2 MSC Surface Phenotype in the Presence of Pullulan	58
2.3.3 MSCs Maintain Differentiation Potential in the Presence of Pullulan	60
2.3.4 Pullulan Enhances MSC Retention to OA Cartilage	63
2.3.5 MSC Dectin-2 Expression Dose Dependently Increases Over Time	65

2.4 Discussion	67
2.5 Conclusion	70

Chapter 3

Design of an Antibody-Peptide Construct for MSC Localisation to Degraded Cartilage

3.1 Introduction	72
3.1.1 Design Specifications	73
3.1.2 Degraded Cartilage Markers as Tissue Targets	76
3.1.2.1 Neoepitopes	76
3.1.2.2 Synthesised Markers of Degraded Cartilage	78
3.1.3 MSC Surface Markers	80
3.1.3.1 MSC specific markers	80
3.1.3.2 The RGD Peptide and Integrin Receptor	82
3.2 Materials & Methods	86
3.2.1 MSC Cytometry	86
3.2.2 Preparation of Human OA Cartilage for Histology	86
3.2.3 Immunohistochemistry of Degraded Cartilage Matrix Epitopes	87
3.2.4 Production of the Polyclonal Collagen 2 3/4 m Antibody	88
3.2.5 RGD Peptide Conjugation to Streptavidin using Sulfo-SMCC chemical linker	88
3.2.6 Non-reduced SDS Page Gel for Protein Analysis	89
3.2.7 Silverstaining	91
3.2.8 Immunohistochemistry of Cells in Monolayer	91
3.2.9 Immunohistochemistry of Polyclonal Coll 2 3/4 m; Biotinylated Antibody and Non-Biotinylated and Collagen Type II	92
3.2.10 Safranin-0 staining	92
3.2.11 Gel Filtration	92
3.2.12 Immunofluorescence	93

3.3	Results	94
3.3.1	Flow Cytometry of MSC Surface Receptors: Selection of MSC Antibody	94
3.3.2	Epitope Staining of Human Degraded Cartilage; Selection of the Collagen 2 3/4m Antibody	95
3.3.3	Conjugation of RGD Peptide to Streptavidin: Silverstain Analysis	97
3.3.4	Immunohistochemical Analysis of RGD Peptide Functionality after Chemical Conjugation	98
3.3.5	Binding of Polyclonal Biotinylated Collagen 2 3/4m Antibody to OA Human Cartilage	99
3.3.6	Immunohistochemical Comparison of Antibody Staining Patterns on Human OA Cartilage	100
3.3.7	Analysis of the Antibody+RGD-Streptavidin Construct by Gel Filtration and Silverstain Analysis	102
3.3.8	Binding of the Biotinylated Antibody-RGD-Streptavidin Construct to the MSC Surface	104
3.4	Discussion	107
3.4.1	Construct Development: MSC specific marker	107
3.4.2	Construct Development: The RGD peptide	108
3.4.3	Design and Function of the Construct	109
3.4.4	Limitations and Further Experiments	118
3.5	Conclusion	119

Chapter 4

A Biocompatible Antibody-Peptide Construct for Enhancing Specific Cell Localisation to Degraded Cartilage

4.1	Introduction	121
4.1.1	Ex Vivo Explant Models	121

4.1.2	Measuring Cell Retention	122
4.1.3	Biocompatibility	123
4.2	Materials & Methods	124
4.2.1	Porcine Cartilage Explants	124
4.2.2	Immunohistochemistry of Porcine Cartilage	124
4.2.3	Safranin O Staining of Porcine Cartilage	124
4.2.4	Collagen 2 3/4m Peptide Blocking of Porcine Cartilage	125
4.2.5	Porcine Meniscus and Muscle Biopsies	125
4.2.6	Immunohistochemistry of Porcine Meniscus and Muscle	125
4.2.7	MSC Isolation	125
4.2.8	MSC Pre-Incubation with Antibody-Peptide Constructs and Porcine Explant Culture	126
4.2.9	Explants and Stereology	127
4.2.10	Fluorescence Imaging of Cartilage Explants and Sections	127
4.2.11	Scanning Electron Microscopy (SEM) Imaging of MSCs Localised on Porcine Explants	127
4.2.12	MSC Morphology	129
4.2.13	MSC Viability and Proliferation	129
4.2.14	MSC Osteogenesis	130
4.2.15	MSC Adipogenesis	130
4.2.16	MSC Chondrogenesis	131
4.2.17	Statistical Analysis	131
4.3	Results	132
4.3.1	Porcine Cartilage Staining of the Polyclonal Collagen 2 3/4m	132
4.3.2	Collagen 2 3/4m Peptide Block on Degraded Cartilage	134
4.3.3	Biotinylated Collagen 2 3/4m Antibody Staining on Porcine Meniscus and Muscle	135
4.3.4	MSC Adhesion to Degraded Cartilage with the RGDStBAb Construct and RGDSt: Fluorescence Imaging	136
4.3.5	MSC Adhesion to Degraded Cartilage with the RGDStBAb Construct and RGDSt: Stereology	138
4.3.6	MSC Adhesion to Non-Degraded Cartilage with the	140

RGDStBAb Construct and RGDSt: Fluorescence Imaging	
4.3.7 MSC Adhesion to Non-Degraded Cartilage with the RGDStBAb Construct and RGDSt: Stereology	141
4.3.8 MSC Morphology after Binding of the RGDStBAb Construct	142
4.3.9 SEM Analysis of MSC Morphology Upon Adhesion to Degraded Cartilage	143
4.3.10 SEM Analysis of MSC Morphology Upon Adhesion to Non-Degraded Cartilage	146
4.3.11 MSC Viability and Proliferation after Binding of the RGDStBAb Construct	147
4.3.12 MSC Osteogenesis after Pre-Incubation with the RGDStBAb Construct	149
4.3.13 MSC Adipogenesis after Pre-Incubation with the RGDStBAb Construct	152
4.3.14 MSC Chondrogenesis after Pre-Incubation with the RGDStBAb Construct	154
4.3.15 MSC Chondrogenesis after Pre-Incubation and Culture with the RGDStBAb Construct	156
4.4 Discussion	158
4.5 Conclusion	166

Chapter 5 *Discussion*

5.1 Enhancing Cellular Retention	168
5.2 Pullulan: A Bioadhesive for Increasing Cellular Retention and the MSC Therapeutic Response	170
5.3 RGDStBAb: An Antibody-Peptide Construct for Enhancing Cellular Retention and MSC Adhesive Properties	171
5.4 Regulatory Aspects for Clinical Translation	174
5.5 Conclusion	177
5.6 Future In Vivo Experiments	177
5.7 In Vivo in a Mouse Model	178

5.8 The Future of Cartilage Repair	179
Bibliography	181

Declaration

I declare that all the work in this thesis was performed personally. No part of this work has been submitted for consideration as part of any other degree or award.

Abbreviations

AC	Articular cartilage
ACI	Autologous chondrocyte implantation
ACLT	Anterior cruciate ligament transection
ADAMTS	A Disintegrin And Metalloproteinase with Thrombospondin Motifs
ANOVA	Analysis of variance
BAb	Biotinylated antibody
bFGF	Basic fibroblast growth factor
BiAb	Bispecific antibody
BSA	Bovine serum albumin
CBFa1	Core-binding factor subunit alpha-1
CCM	Complete chondrogenic medium
CFU-F	Colony forming unit fibroblast
CIA	Collagen-induced arthritis
CILP	Cartilage intermediate layer protein
cm	Centimetre
CO₂	Carbon dioxide
COL2A	Type IIA procollagen
COMP	Cartilage oligomeric matrix protein
c(RADfC)	Cyclic RAD
c(RGDfC)	Cyclic RGD
°C	Degrees celsius
2D	Two dimensional
3D	Three dimensional
DAB	Diaminobenzodine
DAPI	4',6-diamidino-2-phenylindole
diH₂O	Distilled water
DMEM	Dulbecco's modified Eagle's medium
DMM	Destabilisation of the medial meniscus
DMMB	1,9-dimethylmethylene blue
DNA	Deoxyribonucleic acid
dNTPs	Deoxyribonucleotide triphosphates
dsDNA	Double stranded DNA
ECM	Extracellular matrix
EDTA	Ethylenediamine tetraacetic acid
ELISA	Enzyme-linked immune sorbent assay
FACS	Fluorescence-activated cell sorting
FBS	Fetal bovine serum
FITC	Fluorescein isothiocyanate
g	Grams
GAG	Glycosaminoglycan
GRF	Gelatin resorcin formaldehyde
GvHD	Graft versus host disease
hrs	Hours
H₂O	Water
HA	Hyaluronic Acid/Hyaluronan
HCl	Hydrochloric acid
HGF	Hepatocyte growth factor

HRP	Horse radish peroxidase
HSC	Hematopoietic stem cell
ICAM-1	Intercellular adhesion molecule 1
ICM	Incomplete chondrogenic medium
IGD	Interglobular domain
IGF	Insulin-like growth factor
IgG	Immunoglobulin G
IL-6	Interleukin-6
ISCT	International Society for Cell Therapy
kDa	Kilodaltons
kV	Kilovolts
LNGFR	Low-affinity nerve growth factor receptor
M	Molar (moles per L)
mA	Milliamps
mAb	Monoclonal antibody
MACI	Matrix-induced autologous chondrocyte implantation
mAU	Milli-absorbance unit
mbar	Millibar
MCP-1	Monocyte chemoattractant protein-1
α-MEM	Minimum essential medium Eagle alpha
mg	Milligram
μg	Microgram
μl	Microlitre
μM	Micromolar
μm	Micron
min	Minutes
ml	Millilitre
mM	Millimolar
mm	Millimetre
MMP	Matrix metalloproteinase
MRI	Magnetic resonance imaging
MSC	Mesenchymal stem cell
MTS	3-(4,5-dimethylthiazol-2-yl)-5-(3-carboxymethoxyphenyl)-2-(4-sulfophenyl)-2H-tetrazolium
NaCl	Sodium chloride
NFGR	Nerve growth factor receptor
ng	Nanograms
NHS	<i>N</i> -hydroxysuccinimide
NK	Natural killer
nm	Nanometre
OA	Osteoarthritis
OATS	Osteochondral autograft transfer system
P	Passage
PBS	Phosphate buffered saline
PE	Phycoerythrin
Ph-FITC	Phalloidin-FITC
PPARγ	Peroxisome proliferator activated receptor- γ
psi	per square inch

RAD	Arginine-Alanine-Aspartic Acid
RADSt	RAD conjugated streptavidin
RGD	Arginine-Glycine-Aspartic Acid
RGDSt	RGD conjugated streptavidin
RGDStBAb	RGDSt+BAb (biotin-streptavidin linkage)
rhFGF	Recombinant human fibroblast growth factor
RNA	Ribonucleic acid
rpm	Revolutions per minute
RT	Room temperature
RUNX2	Runt-related transcription factor 2
RYDS	Arginine-Tyrosine-Aspartic Acid-Serine
SD	Standard deviation
SDS	Sodium dodecyl sulfate
SEM	Scanning electron microscopy
SLeX	Sialyl Lewis X
SMCC	succinimidyl 4-[<i>N</i> -maleimidomethyl] cyclohexane-1-carboxylate
St	Streptavidin
St-TRITC	Streptavidin-TRITC
STRO-1	
SZP	Superficial Zone Protein
TBS	Tris buffered saline
TE	Tris/EDTA
TGF-β	Transforming growth factor beta
TNF-α	Tumour necrosis factor alpha
TRITC	Tetramethylrhodamine isothiocyanate
VCAM	Vascular cell adhesion molecule
VEGF	Vascular endothelial growth factor
x g	Relative centrifugal force

Abstract

Osteoarthritis, the most common form of arthritis, is a progressive degenerative disease of cartilage and the synovial joint. Since cartilage is an avascular tissue with a limited capacity for self-repair, mesenchymal stem cells (MSCs) are a potential therapeutic for cartilage regeneration. Local intra-articular delivery of MSCs has shown to slow the progression of cartilage degradation, however MSCs likely stimulated repair locally and not by direct engraftment to the cartilage. It is considered that insufficient numbers of cells are retained at the cartilage surface for effective repair and that increasing MSC localisation at the cartilage surface may in turn enhance the efficacy of engraftment and/or creation of a local MSC reparative environment. With an objective to increase cellular localisation at the diseased cartilage surface, methods of cellular targeting to the diseased cartilage surface were investigated. The adhesive 'Pullulan' was assessed for capacity to increase cell localisation in a non-specific manner. MSCs demonstrated biocompatibility and an upregulation of Dectin-2 receptor associated with an immunomodulatory response in the presence of the bioadhesive, with enhanced cell adhesion on pullulan coated degraded cartilage explants. Using a more specific approach, a dual-functioned construct, consisting of an arginine-glycine-aspartic acid (RGD) peptide to pre-coat MSCs and an anti-degraded collagen II antibody for degraded cartilage was developed to target cells, thereby increasing the numbers of cells localized. The peptide/antibody construct demonstrated enhanced MSC adhesion at the degraded cartilage surface; in addition, RGD alone showed comparable targeting efficiency *in vitro* and construct biocompatibility with MSCs was demonstrated. In conclusion, several methods of specific and non-specific viable cellular localisation were shown to have potential for enhancing localisation of MSCs at a degraded cartilage surface with additional beneficial MSC responses observed, such as enhanced proliferation, differential potential and potential immunomodulation.

List of Tables

Chapter 3

- 3.1 List of primary antibodies used for the immunohistochemical analysis of degraded human cartilage. 87**

Chapter 4

- 4.1 Sputter coating conditions for cartilage explants using the Leica EM ACE 600. 128**
- 4.2 Conditions used for imaging samples on the FEI NovaNano200 SEM. 129**

List of Figures

Chapter 1

1.1	The Basic Structure of Articular Cartilage	21
1.2	Normal and OA Human Cartilage	23
1.3	The Role of Cell Retention in Tissue Engineering	36
1.4	Methods of Increasing MSC Adherence to Degraded Cartilage	43

Chapter 2

2.1	Pullulan Conditioned Cartilage	54
2.2	MSC Viability and Proliferation in the Presence of Pullulan	57
2.3	MSC Surface Receptor Expression in the Presence of Pullulan	59
2.4A	MSC Differentiation in the Presence of Pullulan	61
2.4B	MSC Differentiation in the Presence of Pullulan	62
2.5	MSC Retention on Pullulan Conditioned OA Cartilage	64
2.6	Dectin-2 Expression on MSCs in the Presence of Pullulan	66

Chapter 3

3.1	Design Specifications of a Construct for MSC Localisation to OA Degraded Cartilage	75
3.2	Schematic of Antibody-Peptide Construct Design for MSC Localisation	85
3.3	Schematic of the Conjugation Reaction of Sulfo-SMCC with <i>c</i>(RGDfC) and Streptavidin	90
3.4	Selection of an MSC Surface Marker Antibody	94
3.5	Selection of an Antibody for Degraded Cartilage Epitopes	96
3.6	Silverstain Analysis of RGD Peptide Conjugation to Streptavidin	97
3.7	RGD-Streptavidin Conjugate Functionality: Binding Cells in Monolayer	98
3.8	Polyclonal Biotinylated Collagen 2 3/4m Antibody Functionality on OA Human Cartilage	99

3.9	A Comparison of Biotinylated and Non-Biotinylated Polyclonal Collagen 2 3/4m Antibody to Collagen II Staining and GAG Expression	101
3.10	Gel Filtration and Silverstain Analysis of the Biotinylated Antibody and RGD-Streptavidin Combined Construct	103
3.11	Analysis of MSC Surface Binding of Construct after 0 hours by Fluorescence Analysis	105
3.12	Analysis of MSC Surface Binding of Construct after 2 hours by Fluorescence Analysis	106

Chapter 4

4.1	Comparison of Immunostaining of Porcine Cartilage with Polyclonal Collagen 2 3/4m and Collagen II Antibodies	133
4.2	Specificity of the Polyclonal Collagen 2 3/4m Antibody	134
4.3	Polyclonal Collagen 2 3/4m Antibody Staining of Meniscus and Muscle	135
4.4A	Fluorescence Analysis of MSC Adhesion to Degraded Cartilage	137
4.4B	MSC Adhesion at the Degraded Cartilage Surface: Stereological Analysis	139
4.5A	Fluorescence Analysis of MSC Adhesion to Non-Degraded Cartilage	140
4.5B	MSC Adhesion at the Non-Degraded Cartilage Surface: Stereological Analysis	141
4.6	MSC Morphology with RGDStBAb and Components in Monolayer	142
4.7	Analysis of MSC Adherence to Degraded Cartilage Explants with SEM	144
4.8	MSC Surface Topography on Degraded Cartilage Explants with SEM	145
4.9	MSC Adherence to Non-Degraded Cartilage Explants with SEM	146
4.10	MSC Viability and Proliferation after Incubation with RGDStBAb, RGDSt or BAb	148
4.11A	MSC Osteogenesis after Incubation with RGDStBAb, RGDSt or BAb	150

4.11B MSC Osteogenesis after Incubation with RGDStBAb, RGDSt or BAb	151
4.12A MSC Adipogenesis after Incubation with RGDStBAb, RGDSt or BAb	153
4.12B MSC Adipogenesis after Incubation with RGDStBAb, RGDSt or BAb	154
4.13A MSC Chondrogenesis after Incubation with RGDStBAb, RGDSt or BAb	155
4.13B MSC Chondrogenesis after Incubation and Culture with RGDStBAb, RGDSt or BAb	157

Chapter 1

Introduction

1.1 Osteoarthritis

1.1.1 Osteoarthritis

Arthritis is a collective name for a family of musculoskeletal disorders, complex in nature and having different pathologies. In the US alone 50 million adults are affected by the disease and it is the leading cause of disability (CDC, 2010). Osteoarthritis (OA), the most common form of arthritis, is a progressive degenerative disease of the cartilage and synovial joint (Aigner and McKenna, 2002; Sandell and Aigner, 2001). Due to its complex multifactorial nature, OA is a disease that defies early systematic diagnosis and treatment (Becerra *et al.*, 2010; Goldring and Goldring, 2007). The disease is characterized by the breakdown of joint cartilage, proteolysis of the extracellular matrix (ECM) and an uncontrolled remodelling of the affected joint (Goldring and Goldring, 2007; Umlauf *et al.*, 2010). As a consequence, OA is associated with severe pain, physical impairment and significant reduction in quality of life, contributing a high burden to worldwide health systems (Becerra *et al.*, 2010; Umlauf *et al.*, 2010).

1.1.2 Normal Cartilage Biology

There are several types of cartilage found in the body at various locations. Histologically and molecularly these cartilages can be classified as hyaline, elastic and fibrocartilaginous (Naumann *et al.*, 2002; Umlauf *et al.*, 2010). Hyaline cartilage is associated with the appendicular skeleton known as articular cartilage (AC) (Aigner and Stove, 2003; Pearle *et al.*, 2005; Umlauf *et al.*, 2010). AC can be divided further into the superficial zone, transitional zone, radial zone and the calcified zone, the area of the cartilage that interfaces the bone (Becerra *et al.*, 2010; Pearle *et al.*, 2005; Umlauf *et al.*, 2010). The tissue itself is avascular, aneural and alymphatic, comprising a highly specialised and complex structure designed to be high in compressive strength and providing a smooth, gliding surface adjacent to the subchondral bone for joint movement (Aigner and McKenna, 2002; Becerra *et al.*, 2010). The distinct zonal organisation of cartilage and lack of vascular supply limits and complicates the self-regenerative capacity of the tissue (Becerra *et al.*, 2010; Caplan, 2009a).

AC consists of a fibrillar collagen type II matrix, 50% dry weight, embedded into a chondrocyte produced proteoglycan meshwork (Becerra *et al.*, 2010; Pearle *et al.*, 2005). The proteoglycan aggrecan binds to hyaluronic acid (HA) to form large macromolecule aggregates with glycosaminoglycans chondroitin sulphate and keratin sulphate that accumulate water, providing compressive strength and flexibility to the tissue (Mort *et al.*, 2003; Poole *et al.*, 2003; Silbert and Sugumaran, 2002; Umlauf *et al.*, 2010). The collagen network, consisting collagen type II and other collagens (types III, VI, IX, X, XI, XII and XIV) in small amounts, provides tensile strength and further prevents expansion of viscoelastic aggrecan, providing stiffness (Poole *et al.*, 2001). When compressive force is applied cartilage responds by rapidly recovering its elasticity as the hydrophilic aggrecan components draw back water into the matrix (Aigner and McKenna, 2002; Smith, 2007).

The AC has distinct polarity and chondrocytes behave differently depending on their position within the zones of the matrix (Figure 1.1) (Becerra *et al.*, 2010; Klein *et al.*, 2003; Wong *et al.*, 1996). The superficial zone consists of flattened chondrocytes, orientated with collagen type II fibres, secreting a surface superficial zone protein (SZP) or lubricin (Flannery *et al.*, 2009; Schumacher *et al.*, 1994). The middle zone or 'transitional zone' contains collagen type II and aggrecan, with larger, rounder and randomly distributed chondrocytes and collagen fibres in the matrix. In the deep zone or 'radial zone' chondrocytes form columns, facing perpendicular with collagen fibres to the cartilage surface within a mineralised matrix or 'calcified zone' adjacent to the cortical bone (Aigner and McKenna, 2002; Becerra *et al.*, 2010; Pearle *et al.*, 2005).

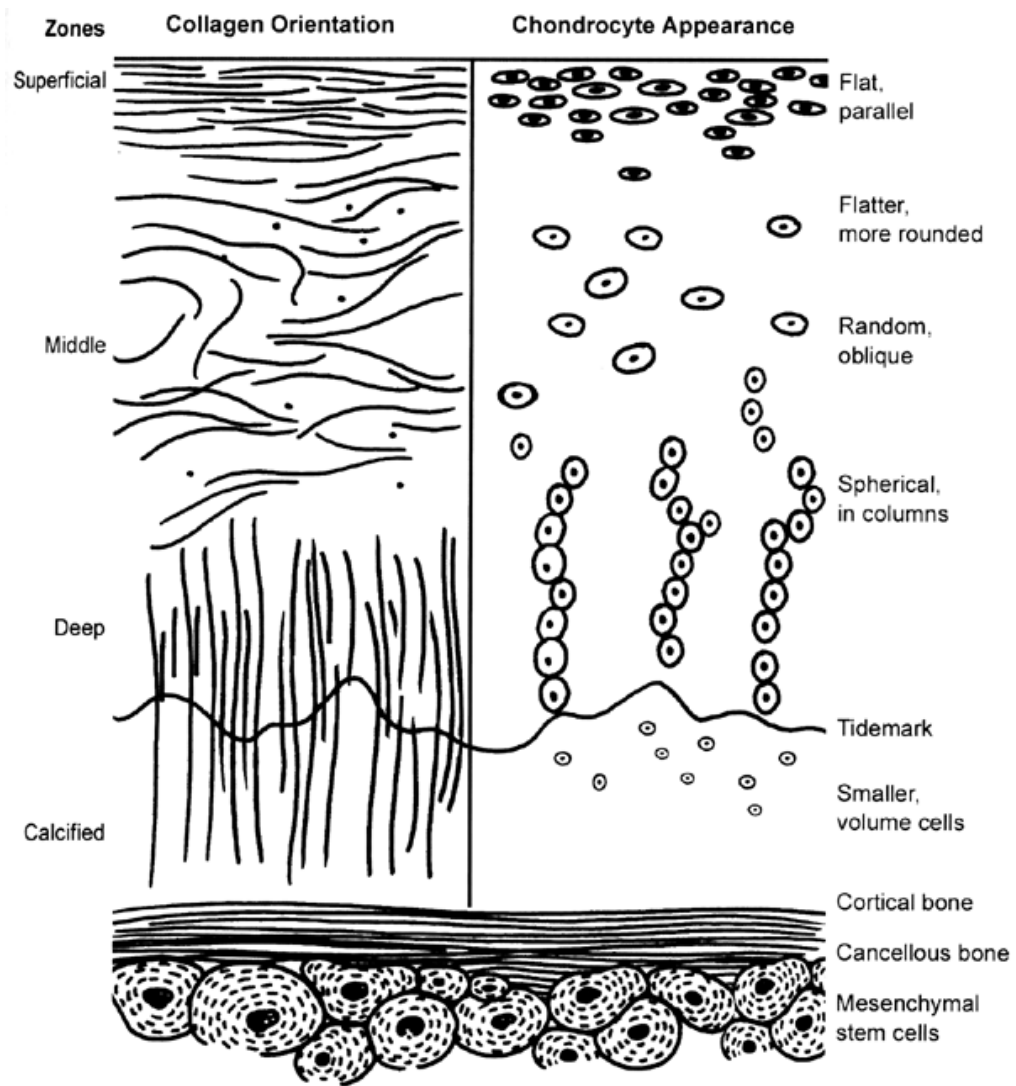


Figure 1.1: The Basic Structure of Articular Cartilage

Schematic of the basic structure of articular cartilage, showing orientation of chondrocytes and collagen fibres within the different zones of the matrix (Browne and Branch, 2000).

1.1.3 Normal Functional Physiology of Cartilage

In normal human articular cartilage, there is a natural turnover of cartilage components. Normally, ECM function is preserved through a balance of turnover of matrix components, critical for the prevention of joint degeneration (Tchetina *et al.*, 2005; Westacott and Sharif, 1996). Aggrecan undergoes a highly regulated proteolysis initiated by matrix metalloproteinases (MMPs), such as MMP3 (Aigner *et al.*, 2006; Blain *et al.*, 2001; Burrage *et al.*, 2006; Lee *et al.*, 2005; Umlauf *et al.*,

2010). The turnover of aggrecan monomers and aggregates can range from days to months to years (Aigner and McKenna, 2002). The collagen type II network in contrast is very stable (Aigner and Stove, 2003; Ap Gwynn *et al.*, 2002; Becerra *et al.*, 2010). The complex structure contributes to the load bearing properties of the tissue and mechanical loading, sustaining cartilage homeostasis and chondrocyte viability (O'Hara *et al.*, 1990; Smith, 2007).

An imbalance in joint homeostasis is thought to be causal in the pathophysiology of OA. Shear and hydrostatic stresses on cartilage are generated from various types of motion at the joint surfaces and influence chondrocyte metabolism. Pro-inflammatory mediators are normally balanced and mechanical stresses can increase or decrease cartilage matrix expression (Lee *et al.*, 2002; Mohtai *et al.*, 1996; Smith, 2007; Smith *et al.*, 2000). Consequently, clinical observations of OA risk factors that alter joint homeostasis such as mechanical injury, obesity and genetics are recognised as causal in cartilage degeneration (Smith, 2007).

1.1.4 ECM Changes in OA

William Hunter was one of the first to recognise the unique, complex structure of cartilage and its limited capacity for repair. In a paper to the Royal Society in 1743 he described the repair of cartilage to be '*a very troublesome disease; that it admits of a cure and more difficulty than a carious bone; and that, when destroyed, it is never recovered*' (William Hunter, 1744 cited in (Buchanan, 2003)).

The earliest known example of OA was observed in the spine of a 100 million year old conmanchean dinosaur showing the microscopic hallmarks of the modern day disease, overgrowth at the articular margins and large vascular spaces (Dequeker and Luyten, 2008). Today, articular cartilage defects caused by either mechanical injury, through lifestyle, age, osteochondral pathology and genetics (Goldring and Goldring, 2007; Kurz *et al.*, 2005; Li *et al.*, 2007a; Valdes *et al.*, 2006), lead to a progressive degeneration of the cartilage and the entire joint (Chiang and Jiang, 2009; Samuels *et al.*, 2008).

Little is known about the initial molecular changes that take place in the early stages of OA and cartilage degradation as a result of the asymptomatic features of this disease (Aigner and McKenna, 2002; Goldring and Goldring, 2007). As a result of the multitude of causal factors, early physical changes in the joint include swelling, increase in water content, fibrillation at the articular surface, loss of matrix and cell division in the form of chondrocyte clusters (Goldring and Goldring, 2007; Squires *et al.*, 2003) (Figure 1.2). In later stages there is an extensive loss of cartilage and exposure to the subchondral bone (Lorenzo *et al.*, 2004).

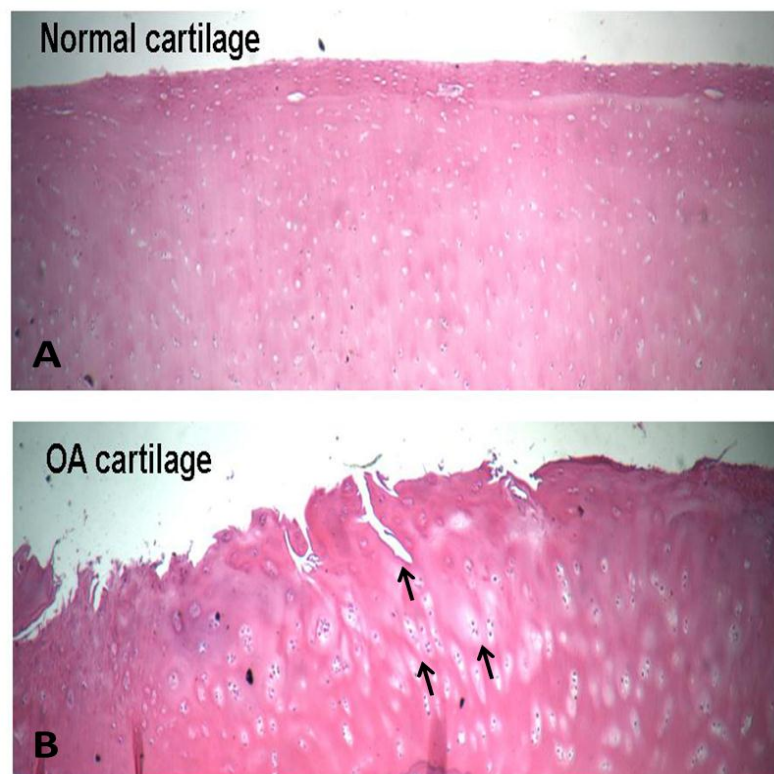


Figure 1.2: Normal and OA Human Cartilage

Haematoxylin and eosin stained sections of human cartilage, normal (A) and OA (B) showing chondrocyte clusters and fibrillations, characteristic hallmarks of degraded OA cartilage (black arrows) (Abramson, 2007).

At a cellular level, there are several observations associated with OA pathology. Some chondrocytes undergo cell death, which is then thought to be compensated for by an increase in proliferation of the remaining chondrocytes. Chondrocytes respond to biomechanical perturbation by upregulating synthetic activity such as anabolic cytokines, Insulin-like growth factor (IGF) and transforming growth factor beta

(TGF β), growth factors that induce matrix production. Conversely, there is also a noted decrease in expression of cartilage matrix proteins that is associated with persistent cartilage trauma (Caterson *et al.*, 2000; Dahlberg *et al.*, 2000; Goldring and Goldring, 2007; Rizkalla *et al.*, 1992; Westacott and Sharif, 1996). Phenotypically, chondrocytes alter with an overall change in gene and protein expression within the tissue to eventually becoming hypertrophic, expressing collagen type X (Aigner and McKenna, 2002; Fuerst *et al.*, 2009; Goldring and Goldring, 2007; Horton *et al.*, 2005; Poole *et al.*, 2002). Although anabolic capacity of the chondrocyte naturally diminishes and OA is associated with age, age is not necessarily associated with OA (Carrington, 2005; Goldring and Goldring, 2007). During aging, collagen type II synthesis and cleavage, normally restricted to pericellular regions, is found throughout the cartilage, extending deeper with age from the surface (Aigner *et al.*, 2007; Hollander *et al.*, 1995; Nelson *et al.*, 1998; Poole *et al.*, 2002). The collagen network is modified during aging with increased stiffness of collagen fibrils, however, healthy aged cartilage shows few molecular changes in collagen and aggrecan content, which are notably changed in OA (Aurich *et al.*, 2002; Poole *et al.*, 2002; Poole *et al.*, 2003).

In association with the alterations in chondrocyte metabolism, there is an upregulation of proteolytic enzymes produced by chondrocytes and associated cell types, such as synovial cells (Hulejova *et al.*, 2007; Sutton *et al.*, 2009; Westacott and Sharif, 1996). Proteases, such as collagenases and aggrecanases, are increased in association with the increase in denaturation of the cartilage framework and collagen type II and aggrecan degradation. This results in the loss of structural integrity and functional load bearing properties of the cartilage (Becerra *et al.*, 2010; Stoop *et al.*, 1999). Natural repair tissue is observed to lack the original network and fibril organisation of AC (Becerra *et al.*, 2010). The induction of increased matrix metabolism is also a symptomatic feature of OA, a defensive response to the degradative turnover of the tissue (Sandell and Aigner, 2001). As a compensation for the loss of superficial components, proteoglycans content increases deeper in the cartilage (Nelson *et al.*, 1998; Poole *et al.*, 2002; Poole *et al.*, 1996; Rizkalla *et al.*, 1992).

The roles of molecules involved in OA have revealed areas to target therapeutically. Pharmacokinetics, through inhibiting destructive pathways, enhancing matrix synthesis by drug administration into the joint or using gene therapy to do both, are some of the areas of therapy being explored (Bakker *et al.*, 2001; Caron *et al.*, 1996; Fernandes *et al.*, 1997; Hayashi *et al.*, 2008; Kobayashi *et al.*, 2005; Krzeski *et al.*, 2007; Nixon *et al.*, 2005; Pelletier *et al.*, 1997). Clinically however, the focus has been on physically replacing or regenerating new tissue with a combination of cells, molecules such as growth factors, or scaffolds (Chiang and Jiang, 2009; Hunziker, 2009; Iwasa *et al.*, 2009).

1.2 Clinical Cartilage Repair Strategies

1.2.1 Clinical Cartilage Repair

Current cartilage treatments only provide temporary relief from pain and do not offer a cure or prevention. Initial surgical strategies were developed with the aim to stimulate repair naturally through abrasion arthroplasty, resulting in a type of temporary fibrocartilage repair (Johnson, 2001) and microfracture, through multiple drilling of the subchondral bone in an attempt to release progenitor cells to in turn stimulate repair (Steadman *et al.*, 2002; Steinwachs *et al.*, 2008).

Patches or chondrocyte grafts used to replace lost tissue in defects encompass more recent strategies, but have many limitations. Chondrocytes have limited viability and restorative potential (Gole *et al.*, 2004; Williams *et al.*, 2004). Once implanted, allograft cartilage generally causes a synovial immune reaction in the host (Phipatanakul *et al.*, 2004). Mosaicplasty or osteochondral autograft transfer system (OATS), an autograft technique, involves the filling of defects with osteochondral plugs taken from non-weight bearing areas of healthy cartilage and bone. Autologous osteochondral grafts yield better clinical outcomes (Gudas *et al.*, 2012; Gudas *et al.*, 2005; Gudas *et al.*, 2006) due to the lack of immune reaction and self-attachment of the graft, reducing damage and invasiveness of the procedure (Hangody *et al.*, 2008). This technique however, is limited by the shortage of autogenous donor cartilage sources, congruency of donor plugs with surrounding cartilage and only applicable for smaller sized defects (Chiang and Jiang, 2009).

Larger defects requiring extra cartilage have led to research for other tissue sources, including artificial construction. Progenitor cells residing in periosteum or perichondrium can be induced environmentally to produce chondrocytes, while the periosteum graft itself acts as a scaffold to support these newly formed cells (Mara *et al.*, 2011; O'Driscoll, 1999; Trzeciak *et al.*, 2006).

Autologous chondrocyte implantation (ACI) was developed to overcome the need for autogenous cartilage by expanding chondrocytes in the laboratory, implanting them into a defect and covering the implant with a sutured periosteal patch (Brittberg, 1999, 2008; Hunziker, 2009). First generation ACI with cells injected into a defect and sealed with a periosteal flap revealed problems of leakage, loss of chondrocyte phenotype, periosteal hypertrophy and was an invasive procedure causing donor site morbidity (Gooding *et al.*, 2006; Muellner *et al.*, 2001). Second generation ACI, matrix-induced autologous chondrocyte implantation (MACI), involves the culture of chondrocytes that are then seeded onto biodegradable matrices that can be implanted. Biomaterials such as collagen type I gels, hyaluronan scaffolds and collagen type I/III membranes are used to secure the chondrocytes in place (Koga *et al.*, 2009; Schinhan *et al.*, 2013). This advancement of the ACI technique improves biological structure of the tissue graft, but conversely introduces issues of scaffold biocompatibility, inflammation and degradation (Brittberg, 1999; Chiang and Jiang, 2009; Hunziker, 2009).

In a 5-year clinical study by Knutsen *et al.*, no advantage was demonstrated when patients received ACI compared to conventional microfracturing (Knutsen *et al.*, 2007). However, a 5-year study by Kon *et al.* demonstrated MACI treated patients showed a better outcome compared to microfracture (Kon *et al.*, 2009). More recently, improved functional outcomes of ACI over mosaicplasty were observed in a 10-year study (Bentley *et al.*, 2012). In all such clinical studies newly regenerated cartilage consisted of fibrous cartilage, different in structure and biological properties to the desired hyaline cartilage (Bartlett *et al.*, 2005; Manfredini *et al.*, 2007; Tins *et al.*, 2005). Furthermore, success in patients over the age of 50 was not demonstrated, since autologous chondrocytes demonstrate a loss of potential over time, suggesting a cohort of patients that do not respond to autologous cell therapy (Hunziker, 2009; Zheng *et al.*, 2007).

1.2.2 Tissue Engineering Principles for Cartilage Repair

Cell-based technology for cartilage repair has evolved over the years in an attempt to improve the efficacy of regenerated tissue. Traditionally, cell-based repair is based upon the principle of the implantation into a defect of cultured or non-cultured, chondrocytes, chondroprogenitor cells or progenitor cells. Transplanted cells are then required to integrate, deposit ECM and/or differentiate to become the building blocks of newly formed cartilage (Chiang and Jiang, 2009).

One current tissue engineering strategy is to construct the regenerated tissue *in vitro* and then subsequently implant the newly constructed graft *in vivo* (Chiang and Jiang, 2009; Vunjak-Novakovic *et al.*, 1999). A second, such as ACI relies on *in vivo* cell-based repair where the intra-articular environment provides a suitable niche for regeneration of implanted cells. For success, a sufficient number of chondrogenic cells that can produce cartilage-like ECM and remain engrafted at the site of repair are essential (Chiang and Jiang, 2009; De Bari and Dell'Accio, 2008). In a third strategy, endogenous cell-based repair is aided by the implantation of a growth factor infused scaffold. Lee *et al.* demonstrated this in a proof of concept study using TGF β 3 adsorbed collagen hydrogels in rabbit condyles (Lee *et al.*, 2010).

The fundamentals in tissue engineering research currently focus on three elements; the cells, the scaffold and the environment with each element being influential and interlinked for an effective outcome (Chiang and Jiang, 2009).

1.2.3 Scaffolds in the Clinic for Cartilage Tissue Engineering

Scaffolds for cartilage repair have several requirements in design. They must be biocompatible with surrounding tissue and the environment in which they are placed with an optimal degradation time, long enough to provide a temporary supportive environment, but short enough to not compromise efficacy. They must be structurally and mechanically stable to be able to withstand compressive load. Secondly, they must allow successful infiltration and attachment of environmental

cues and/or endogenous cells to enable integration with native tissue and promote cellular viability, proliferation and differentiation (Danisovic *et al.*, 2012; Iwasa *et al.*, 2009; Vinatier *et al.*, 2009). Natural and synthetic biomaterials have been used as scaffolds including collagen, hyaluronic acid based polymers, fibrin and synthetic copolymers with natural materials found within cartilage being more favourable (Bulman *et al.*, 2012; Chiang and Jiang, 2009; Iwasa *et al.*, 2009; Sitterling *et al.*, 1994; Tognana *et al.*, 2005; Visna *et al.*, 2004; Wakitani *et al.*, 1994).

In addition to the limitations in phenotype, such as age and health affecting repair efficacy, new scaffolds need to demonstrate a homogenous distribution of cells, retention of sufficient quantities, maintenance of chondrocyte phenotype and ultimately demonstrate a hyaline cartilage structure. Few studies have shown this to date (Bartlett *et al.*, 2005; Iwasa *et al.*, 2009; Nehrer *et al.*, 1998).

1.3 Mesenchymal Stem Cells

1.3.1 Mesenchymal Stem Cells

“We shall need flat, and round, and all shapes of bones. Some of them will be hollow, to make them lighter, except for a little marrow, where the cells live which do the mending, and where new baby soldier cells are born, and live in safety until they are needed in some part of the body”. Sir Wilfred Grenfell, 1924 ‘Yourself and Your Body’ (Grenfell, 1924).

It has long been reported that cells isolated from postnatal bone marrow have differentiation potential *in vitro* and have shown to differentiate into specific cells of mesenchymal tissues, such as bone, cartilage and fat, when implanted *in vivo* (Goshima *et al.*, 1991). Friedenstein first identified the existence of marrow stromal or mesenchymal stem cells (MSCs) as having self-renewal and multi-lineage potential. MSCs can be isolated from an array of adult mesenchymal tissues and expanded in culture, demonstrating extensive proliferative potential, without the loss of potential over several passages (Johnstone *et al.*, 1998; Koga *et al.*, 2009). MSCs are therefore considered to be an attractive cell source for tissue engineering and cartilage repair, overcoming limits of available autologous chondrocytes and donor

site morbidity associated with harvesting chondrocytes (Hunziker, 2009; Koga *et al.*, 2009).

A defined medium for MSC chondrogenesis was first described by Johnstone *et al.*, where micromass/pellet culture was used with TGF- β and dexamethasone to support the *in vitro* differentiation of MSCs into cartilage (Johnstone *et al.*, 1998). In addition, bone morphogenetic proteins (BMPs), such as growth differentiation factor 5 (GDF-5), have been shown to enhance chondrogenesis under these conditions (Coleman and Tuan, 2003; Sekiya *et al.*, 2005). Other growth factors and cytokines such as IGF have also been employed in culture cocktails for enhancing chondrogenesis (Bai *et al.*, 2004; Pei *et al.*, 2008). However, *in vitro* MSC chondrogenesis still does not completely mimic embryonic cartilage development and the properties of mature cartilage as MSCs continue to express collagen type I and increase both collagen type II and collagen type X, a marker of hypertrophy (Barry *et al.*, 2001b; Ichinose *et al.*, 2005). *In vivo* studies of MSC implantation demonstrate that the microenvironment is key in inducing cartilage formation and maintenance of the cartilage phenotype (Caplan, 2009b; Peltari *et al.*, 2006).

1.3.2 MSC source

Since clinical outcomes have shown age to be a factor in repair; a highly proliferative cell with a full capacity to differentiate is sought (Hunziker, 2009). Donor age has previously demonstrated adverse effects on cell proliferative and differentiation capacities (Kretlow *et al.*, 2008; Moerman *et al.*, 2004). Conversely, some studies have found no change in capacity, although MSC titres change with age (Caplan, 2009b; Haynesworth *et al.*, 1994) suggesting that in older patient populations, autologous cells might not always be appropriate. Donor variation has also been shown to play a role in determining MSC differentiation and proliferative capacity (Caplan, 2009b) supporting an allogenic route with cells that are chosen for their purpose.

MSCs can be isolated from many kinds of mesenchymal tissues such as synovium, muscle and adipose tissue (Cao *et al.*, 2003; De Bari *et al.*, 2001; Zuk *et al.*, 2002)

with similar *in vitro* colony forming abilities. However, there are studies demonstrating specific potential of MSCs according to their origin. Synovial tissue has been reported to contain progenitor cells of high differentiating potential for a variety of connective tissues, in particular cartilage (De Bari *et al.*, 2001; Sakaguchi *et al.*, 2005) and bone marrow MSCs have shown higher chondrogenic potential over adipose derived MSCs (Huang *et al.*, 2005; Koga *et al.*, 2007). To date however, most *in vivo* studies have been performed with MSCs from bone marrow origin, currently the most widely accepted MSC source being easier to harvest than other sources such as the synovium (Koga *et al.*, 2009).

1.3.3 Bone Marrow MSC Transplantation for Cartilage Repair

MSCs demonstrate advantages over the use of chondrocytes for transplantation. They can be isolated from a variety of tissues without harvesting healthy cartilage and expanded in culture without the loss of potential at early passages (Matsumoto *et al.*, 2010). Based on promising results of MSC transplantation in a collagen gel in a rabbit osteochondral model (Wakitani *et al.*, 1994), Wakitani *et al.* considered the application of MSCs in the clinical setting (Wakitani *et al.*, 2002; Wakitani *et al.*, 2004). In a study of 24 patients with knee OA and an average age of 63 years, 12 were given autologous bone marrow cell transplants, 1.3×10^7 cells seeded in collagen gels and 12 given cell-free control gels (Wakitani *et al.*, 2002). It was observed that defects were filled with white tissue in treated groups six weeks after transplantation, which after 42 weeks was much harder, but still softer than normal cartilage. Analysis of clinical data 64 months later revealed non-significant clinical scores between cell-transplanted groups and controls. The authors concluded that either longer time was required to see an effect or that cell transplantation was not effective in the OA knee because of poor environmental factors or patient age (Wakitani *et al.*, 2008).

Giannini *et al.* reported positive results for repair of 48 osteochondral defects in both the ankle and knee. Magnetic resonance imaging (MRI) and histologic analysis revealed regenerated tissue of varying degrees; however none showed hyaline cartilage (Giannini *et al.*, 2009a; Giannini *et al.*, 2009b). Further, autologous MSC

transplantation using $10\text{-}15 \times 10^6$ cells in 36 articular cartilage defects, showed comparable results to that of an ACI control, but had an advantage of being a one-step procedure, reducing donor-site morbidity (Nejadnik *et al.*, 2010).

Other published MSC clinical studies have generally included only small patient numbers or younger patients but reported positive clinical outcomes (Kuroda *et al.*, 2007; Wakitani *et al.*, 2004; Wakitani *et al.*, 2007). Despite recent clinical reports showing improvement with intra-articular injection of autologous MSCs in OA knees (Emadedin *et al.*, 2012) and more recently improvement in pain and cartilage quality observed by MRI (Orozco *et al.*, 2013), to date the clinical results of bone marrow MSC transplantation for cartilage repair have been similar to that of other cell-matrix based repair technologies. Mostly repair tissue formed is of a fibrocartilaginous type and variable quality (Hunziker, 2009; Koga *et al.*, 2009; Matsumoto *et al.*, 2010). Additionally, age, donor variation and extent of cartilage degradation contribute to efficacy (Hunziker, 2009; Matsumoto *et al.*, 2010; Punwar and Khan, 2011).

Other than numbers of cells injected or seeded onto scaffolds, most of these studies do not follow up on the number of cells that are retained in the tissue or their length of retention and contribution within the defects post-transplantation. In the clinical setting this can be difficult practically and likely needs to be a focus pre-clinically. Tracking cells for identifying and quantifying cell retention can provide supporting information on efficacy outcomes and identify limitations in current practice (Christian *et al.*, 2008; Rosen *et al.*, 2007).

1.3.4 MSC Support of the Environmental Niche

Over the last five years it has become evident that implanted progenitor cells likely play more of a supportive role in tissue repair processes rather than simply providing the building blocks for regeneration (Caplan, 2009b). MSCs have also demonstrated therapeutic properties by secreting factors that contribute to tissue regeneration, including anti-apoptotic factors and chemoattractants for immunomodulation and homing of native progenitors. This suggests an indirect effect of MSCs on tissue

repair and a role in enriching the repair environment (Bertolo *et al.*, 2011; Meirelles Lda *et al.*, 2009).

Meirelles *et al.* reviewed molecules involved in the paracrine effects of MSCs, based on earlier reports of MSCs secreting bioactive molecules associated with chemoattraction, angiogenesis, anti-apoptosis and immunomodulation (Haynesworth *et al.*, 1996; Majumdar *et al.*, 1998; Meirelles Lda *et al.*, 2009; Pittenger *et al.*, 1999). Paracrine factors include: anti-apoptotic vascular endothelial growth factor (VEGF), hepatocyte growth factor (HGF) and IGF-1; pro-angiogenic, such as basic fibroblast growth factor (bFGF), monocyte chemoattractant protein-1 (MCP-1) and interleukin-6 (IL-6), with various factors having several active roles. For example, VEGF has a role in both angiogenesis and apoptosis and MCP-1 acts in angiogenesis and chemoattraction (Hung *et al.*, 2007; Kinnaird *et al.*, 2004; Parekkadan *et al.*, 2007; Togel *et al.*, 2007). MSCs preferentially home to sites of tissue injury and inflammation which is attributed to the presence of surface receptors that bind molecules such as ECM, growth factors and chemokines. *In vitro*, MSCs have shown to migrate in a dose-dependent manner towards growth factor and chemokines such as tumour necrosis factor alpha (TNF- α) (Ponte *et al.*, 2007).

Based upon assumptions that bone marrow derived MSCs would naturally home to the marrow, MSCs were first used to supplement bone marrow transplantation (Caplan, 2009b; Devine *et al.*, 2001; Koc *et al.*, 2000; Koc *et al.*, 1999). Studies using MSCs to enhance bone marrow transplantation for genetic disorders such as osteogenesis imperfecta have shown mixed results (Horwitz *et al.*, 2002; Horwitz *et al.*, 1999). In those patients with positive MSC effects, it was not clear how long MSCs had been retained, if they remained active, differentiated or whether they contributed through biofactor release (Caplan, 2009b; Horwitz *et al.*, 2002; Horwitz *et al.*, 1999).

Clinical studies using culture expanded MSCs for treating graft-versus host disease (GvHD) by intravenous infusion, demonstrated the potential of MSCs for increasing survival rate of patients who had previously proved therapy resistant (Le Blanc *et al.*, 2008). Infusions reported to date have shown no documented adverse effects

suggesting MSCs provide more of an environmental supportive role than differentiating units. MSCs homing to other organ sites such as the lung have not been shown to differentiate into unwanted phenotypes (Caplan, 2009a, b; Wakitani *et al.*, 2011). However, the environmental niche in which the cells are retained also plays a role in providing the cues for determining cell fate (Caplan, 2009b; Chen *et al.*, 2005; Karp and Leng Teo, 2009).

Immunomodulatory properties of MSCs were first observed after cell transplantation studies, demonstrating an evasion of the immune system (Liechty *et al.*, 2000; Rasmusson *et al.*, 2007). MSCs have been shown to directly inhibit T cell proliferation and function *in vitro* (Bartholomew *et al.*, 2002; Di Nicola *et al.*, 2002; Krampera *et al.*, 2003), inhibit or promote B cell proliferation (Corcione *et al.*, 2006; Traggiai *et al.*, 2008), modulate secretion profiles of macrophages and dendritic cells (Aggarwal and Pittenger, 2005; English *et al.*, 2008; Nemeth *et al.*, 2009) and suppress the actions of natural killer (NK) cells (Sotiropoulou *et al.*, 2006; Spaggiari *et al.*, 2008).

Acting through a variety of mechanisms, MSCs have shown therapeutic potential in providing support and enriching the environmental niche. This alone renders them a highly sought therapy for tissue engineering (Caplan, 2009b; da Silva Meirelles *et al.*, 2008; Karp and Leng Teo, 2009; Yagi *et al.*, 2010).

1.4 MSC Retention

1.4.1 MSC Retention

Scaffolds providing a structure for cell retention and function encompass a large proportion of MSC studies for cartilage regeneration (Chiang and Jiang, 2009; Iwasa *et al.*, 2009; Koga *et al.*, 2009). However, a focus is often placed on scaffold type and functional contribution to efficacy, with less attention on cellular retention and localisation within the scaffold (Bulman *et al.*, 2012).

Few studies to date have been able to demonstrate MSC retention and engraftment at the degraded cartilage surface *in vivo* (Mokbel *et al.*, 2011; Sato *et al.*, 2006; Sato *et al.*

al., 2012). Local delivery of MSCs to the articular joint in a goat model of OA has shown to slow the progression of cartilage degradation. However, MSCs *in vivo* did not engraft to either intact or fibrillated cartilage (Murphy *et al.*, 2003). It was hypothesised that insufficient numbers of cells were retained at the cartilage surface for effective repair and that enhancing retention *in vivo* would increase possible cellular engraftment and/or create a suitable reparative environment for cartilage repair (Coleman *et al.*, 2010; Murphy *et al.*, 2003).

The contribution of implanted cells versus native cells to the repair process is not always clear to interpret, even when cells are tracked (Bulman *et al.*, 2012). It is likely a combination of implanted cells, host cells and stimulated mediators that play a role in the repair process (Coleman *et al.*, 2010). Direct injection of 7×10^6 fluorescently labelled MSCs mixed with HA in a spontaneous OA model (Sato *et al.*, 2012) revealed the presence of MSCs within fibrillated cartilage, but also in the synovial lining and meniscus. Histological findings at 5 weeks demonstrated some partial repair in the HA-MSc treated group and an increase in collagen type II around the implanted MSCs and native chondrocytes, suggesting both differentiation of the implanted cells and also a trophic effect on native cells. Since the MSC and HA alone controls showed poor repair success compared to the HA-MSc group, the authors suggest that the mix of HA and MSCs is potentially beneficial for OA (Sato *et al.*, 2012).

Chen and Tuan 2008, suggested that lack of MSC engraftment at the cartilage surface appears to be specific to the cartilage tissue (Chen and Tuan, 2008). After MSCs were transplanted *in utero* in sheep they were shown to engraft and persist in various different tissues undergoing site-specific differentiation. Cartilage engraftment however, was only observed at a low frequency (Liechty *et al.*, 2000). Similarly, in a mouse model of collagen-induced arthritis (CIA), cells were absent in the joint cartilage (Augello *et al.*, 2007). The loss of available ECM and adhesion molecules that facilitate cell binding at the degraded cartilage surface likely contribute to low cellular adherence, but also the dynamic nature of articular mechanical forces creates a harsh environment for delivered cells (Bulman *et al.*, 2012; Smith, 2007).

In a study by Quintavalla *et al.* survival and persistence of fluorescently labelled MSCs on a gelatin sponge implanted in a goat osteochondral defect were assessed (Quintavalla *et al.*, 2002). MSCs were detected at 1, 2, 7 and 14 days; after this period there was a gradual loss of cells and fragments of the sponge found in marrow spaces, suggesting a dislodgement and fragmentation of the implant (Quintavalla *et al.*, 2002). The study highlights that even with the use of a scaffold, it is challenging to retain transplanted cells within the joint environment (Mauck *et al.*, 2003; Quintavalla *et al.*, 2002).

In the literature, MSC transplantation alone has shown poor engraftment and retention at the site of cartilage repair (Murphy *et al.*, 2003; Sato *et al.*, 2012). Most studies have included scaffolds or delivery carriers as important factors contributing to efficacy (Quintavalla *et al.*, 2002; Sato *et al.*, 2012). However, cell retention and numbers post implantation are often not analysed. It appears that MSCs may contribute by both trophic factor release and differentiation (Augello *et al.*, 2007; Murphy *et al.*, 2003; Sato *et al.*, 2012) depending on the environmental context, with both animal model and cartilage degradation levels influencing MSC contribution (Caplan, 2009a; Chen and Tuan, 2008). Since an enhancement of cell localisation at the cartilage surface would theoretically enhance cell response, environment and scaffold integrity, the localisation of cells should be considered an additional requirement entwined within the basic three elements of scaffold, cell and environment (Figure 1.3) (Bulman *et al.*, 2012; Chiang and Jiang, 2009).

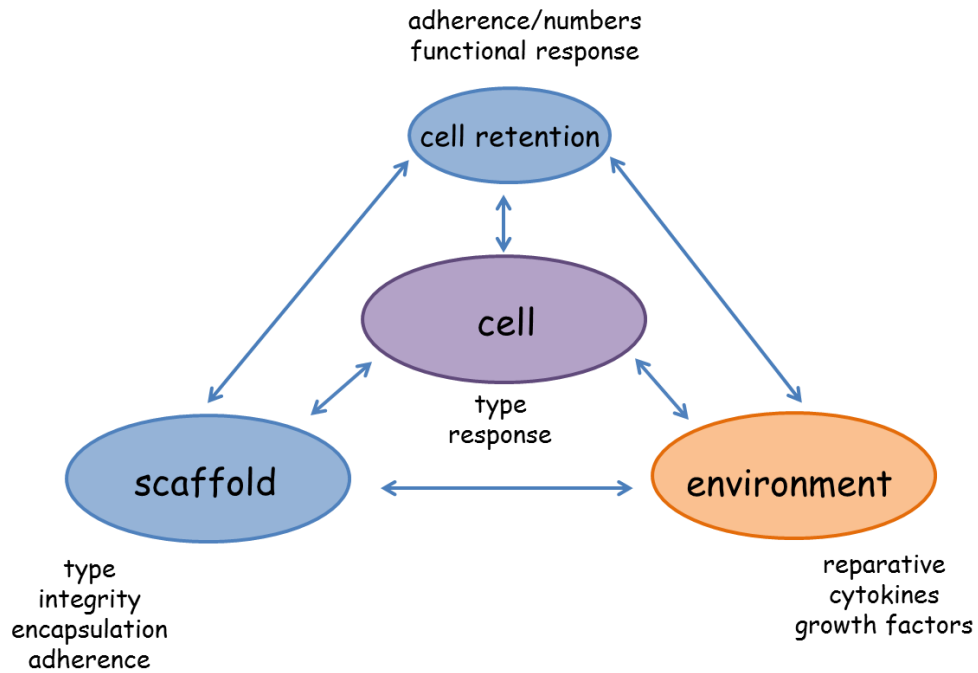


Figure 1.3: The Role of Cell Retention in Tissue Engineering

Schematic demonstrating the role of cell retention within the three principle elements of tissue engineering. Cell retention is influential within all elements, providing an increase in cell function, cell number, environmental enrichment and adherence within the scaffold and integrity. Both scaffold and cell retention can be interchangeable and/or combined elements, where a cell retention technology might replace a scaffold and vice versa.

1.4.2 Enhancing Cellular Retention

Cellular retention may be achieved at the cartilage surface by several methods. Increasing numbers of cells delivered to the joint is not always an economically viable option due to limited sources of progenitor cells and high costs of harvesting and expansion (Mason, 2005, 2007; Mason and Manzotti, 2010). Cells can be encapsulated within a scaffold or hydrogel that can then be delivered to the area of repair, in a type of static retention of cells. However, scaffolds such as hydrogels often lack mechanical properties sufficient for supporting cell retention and tissue regeneration (Kim *et al.*, 2011b) and retaining required numbers and cell viability can influence the efficacy and outcome (Hansen *et al.*, 2012; Issa *et al.*, 2011;

Mauck *et al.*, 2003). Some researchers are using magnetic particles as a means of increasing cellular delivery and localisation (Cheng *et al.*, 2010; Feng *et al.*, 2011).

More recently, nanomaterials enable possibilities of providing a support with cues that can influence cellular responses, maximising the potential of cells retained and also controlling their proliferation (Bulman *et al.*, 2012; Li *et al.*, 2003). Microcarriers have been employed as *in vitro* model systems to increase cell numbers and maintain cell phenotype for cartilage repair applications (Frauenschuh *et al.*, 2007; Freed *et al.*, 1993). By directing cellular behavior and expansion with nanomaterials and microcarriers, enhanced cell localisation might be also achieved (Bouffi *et al.*, 2010; Bulman *et al.*, 2012; Kisiday *et al.*, 2002; Porter *et al.*, 2009; Yang *et al.*, 2007). Although, *in vitro* studies have shown promise, few *in vivo* cartilage specific approaches have been demonstrated (Liu *et al.*, 2011).

1.4.3 Antibody-based Localisation

Antibodies are one of the strongest candidates for cell targeting and enhancing localisation, since they are natural molecular tags. Antibody-based therapeutics represent a growing portion of biopharmaceuticals in current clinical trials (Glennie and Johnson, 2000; Jain *et al.*, 2007; Phillips *et al.*, 2001). A bispecific antibody (BiAb) is considered a man-made antibody able to bind two different antigens. Similarly, a bifunctional antibody is a single antibody that is linked to a diagnostic or therapeutic molecule, such as antibodies that are coupled to drug delivery nanoparticles (Dinauer *et al.*, 2005). The concept of having a dual-functioned antibody that can be tailored to requirements and target a cell specifically to a tissue of interest has many advantages and potential in the field of tissue engineering. Localizing progenitor cells to a site of tissue damage should essentially enhance cell retention, cell utility and possibly reduce the cell numbers required for transplantation (Bulman *et al.*, 2012).

Lum *et al.* adapted a bispecific antibody technology previously employed for cancer therapeutics to target hematopoietic stem cells (HSCs) to damaged myocardium tissue (Lum *et al.*, 2004; Sen *et al.*, 2001). The BiAb consisted of anti-c-kit, a target

for mouse stem cells and anti-vascular cell adhesion protein 1 (VCAM-1), a target antigen upregulated in myocardial injury. The antibodies were joined by traditional chemical heteroconjugation using Sulpho-SMCC (sulphosuccinimidyl 4-(N maleimidomethyl) cyclohexane-1-carboxylate). BiAb pre-incubated HSCs or HSCs alone were injected either systemically or directly into mice post-infarction. Results demonstrated directly-injected BiAb pre-incubated HSCs had increased retention in the myocardium tissue over HSCs alone. Intravenous injection experiments further demonstrated that BiAb pre-incubated HSCs were capable of homing to the injured myocardium, with increased numbers compared to that of cells alone (Lum *et al.*, 2004).

The same research group developed a second BiAb construct, comprising of an anti-CD45 antibody, specific to common leukocyte antigen found on HSCs and an antibody to myosin light chain, an antigen specific to injured myocardium (Lee *et al.*, 2007). In a rat model of ischemic injury, human HSCs pre-incubated with BiAb were injected intravenously two days after injury. Immunohistochemical analysis revealed pre-incubated cells specifically localized to the infarcted region of the heart and improved cell delivery to the injured tissue over cells alone. This targeting also correlated with improved myocardial function (Lee *et al.*, 2007). Such studies described positive pre-clinical evidence demonstrating potential of specifically localising stem cells in increased numbers to a site of tissue injury. A BiAb technology could be specifically tailored for cartilage repair, so that transplanted MSCs might overexpress a peptide moiety to an epitope found specifically on the surface of degenerated cartilage (Bulman *et al.*, 2012). A technology for mobilising or homing native progenitor cells would require absolute specificity for the homing cell type of interest.

In the cartilage repair field, 'cell painting,' first introduced by Chen *et al* and further developed by Dennis *et al.* coated chondrocytes with antibodies to localize to the cartilage extracellular matrix (Chen *et al.*, 2000; Dennis *et al.*, 2004). The technique involved a two-step process; lipidated protein G was intercalated into chondrocyte cell membranes and then incubated with antibodies specific to cartilage matrix antigens, allowing binding of antibodies to protein G on the surface of the cells. Antibody-coated cells were added to cartilage explants taken from a rabbit partial-

thickness defect model. Histological and fluorescent analysis, demonstrated enhanced binding to the cartilage with antibody coated chondrocytes, suggesting a potential method for increasing cell adherence at the site of cartilage injury (Dennis *et al.*, 2004). Using the same technique MSCs pre-coated with lipidated protein G and intercellular adhesion molecule 1 (ICAM-1) antibodies localised to activated human vascular endothelial cells (Ko *et al.*, 2009).

An *in vivo* study using cell painting to localise MSCs to the inflamed bowel in a mouse model of acute colitis demonstrated increased systemic delivery of targeted MSCs to the colon. An increase in clinical efficacy with an observed increase in regulatory T cells was also shown, suggesting a possible MSC mechanism of action (Ko *et al.*, 2010). Interestingly, MSCs labelled with antibody to VCAM demonstrated the highest localisation of cells to the colon, but higher clinical efficacy was demonstrated with MSCs labelled with anti-addressin antibody, suggesting increased efficacy was not a result of increased MSC delivery to the colon since cell delivery within this group was very low. This study demonstrated the different possible mechanisms of action that cells may have depending on the targeting molecule, suggesting that the localisation construct itself can have other supportive functions in addition to providing a method of cell adherence to a target tissue (Ko *et al.*, 2010).

1.4.4 Peptide-based Localisation

In addition to antibodies, peptides and proteins that promote adherence of a cell to a target tissue or scaffold have also been explored for cell delivery. Nuttelman *et al.*, covalently attached the cell adhesion protein fibronectin to poly(vinyl alcohol) hydrogels increasing fibroblastic cell number and rate of attachment to gels (Nuttelman *et al.*, 2001). In a similar approach, alginate gels modified with the fibronectin binding site, arginine-glycine-aspartic acid (RGD) showed 10-20 times higher attachment of chondrocytes compared to an unmodified alginate gel (Genes *et al.*, 2004; Nuttelman *et al.*, 2001) and Jeschke *et al.* demonstrated chondrocytes cultured in monolayer on synthetic materials and coated with RGD peptides demonstrated accelerated binding at both early and late passages (Jeschke *et al.*,

2002). In contrast to the effects of strong adhesion at higher peptide concentrations there is also a decrease in matrix production (Mann and West, 2002). Connelly *et al.* showed that interaction of bone marrow stromal cells with RGD motifs in an alginate hydrogel inhibited chondrogenesis, observed by the inhibition of sulphated glycosaminoglycan (GAG) synthesis that increased with increasing RGD density (Connelly *et al.*, 2007). Mixed results have suggested that the presence of fibronectin or its binding site RGD plays a role in initiating chondrogenesis and maintaining hMSC viability; however, persistence of this molecule inhibits chondrogenic differentiation (Salinas and Anseth, 2008; Salinas *et al.*, 2007). Fibronectin and RGD peptides will therefore also possess a functional role with the cells to be localized and the environment in which they are placed (Bulman *et al.*, 2012).

An alternative approach to selectively deliver progenitor cells is through the alteration of a cell's behaviour, to potentially 'home' cells *in vivo* to a site of tissue damage (Karp and Leng Teo, 2009). Sarkar *et al.* demonstrated that the surfaces of culture expanded MSCs could be chemically modified to possess leukocyte-like adhesion properties, promoting a cell rolling behaviour. The sialyl Lewis X (SLeX) moiety was covalently coupled to the surface of MSCs through biotin-streptavidin modifications that did not compromise cell viability, differentiation potential and cell phenotype (Sarkar *et al.*, 2008). In a more recent study, a system was developed to transiently label the cells using biotinylated lipid vesicles with SLeX. Cell rolling behaviour was observed in a flow chamber assay, showing no effects on viability, proliferation and differentiation (Sarkar *et al.*, 2010). These homing effects have yet to be demonstrated *in vivo*. Engineering MSCs to behave as HSCs to increase cell recruitment to bone was also undertaken by Sackstein *et al.* The MSC native CD44 glycoform was converted through α -1,3-fucosyltransferase preparation to HSC E-selectin/L-selectin ligand. Modified cells demonstrated homing to bone compared to unmodified cells (Sackstein *et al.*, 2008).

Challenges surrounding the use of antibodies and peptides as cell targeting tools include regulatory hurdles placed upon developing a new platform technology of a pharmaceutical nature (Kriangkum *et al.*, 2001). Costs and manufacture on a large scale can further limit these therapeutics (Kriangkum *et al.*, 2001; Mason, 2005);

however, antibodies and peptides have potential in tissue engineering, directing and positioning cells within what is normally an avascular tissue and in functionally influencing efficacy of repair (Bulman *et al.*, 2012).

1.5 Thesis Objectives

Articular cartilage is a multi-layered biological composite structure, with hierarchical organisation. Future repair strategies for cartilage repair must consider mechanical properties, zonal organisation and biological functions of native cartilage and it is likely that a combined approach will be required (Bulman *et al.*, 2012). It was demonstrated by Murphy *et al.* that few cells are retained when injected at the diseased cartilage surface and these authors suggested that enhancing the numbers of cells retained, may contribute to more efficacious repair (Murphy *et al.*, 2003). The various methods by which MSC retention might be enhanced at the cartilage surface need further validation in terms of quantification of cell numbers and functionality with MSCs.

It is hypothesised that increasing the number of cells retained at the diseased cartilage surface will in turn enhance the efficacy of repair. This thesis aims to design, develop and demonstrate biocompatible methods of enhancing MSC retention at the degraded articular surface.

Therefore this research can be divided into 3 specific aims:

1.) Pullulan: A Biocompatible Adhesive for Enhancing MSC Retention and Response at the Degraded Cartilage Surface

Pullulan is a biocompatible alpha-glucan exopolysaccharide that has a history of use in the food and biomedical industry (Rekha and Sharma, 2007). The objective was to demonstrate enhanced MSC retention to degraded cartilage using the bioadhesive pullulan (Figure 1.4C). Using a stereological approach, MSC adherence to pullulan coated human OA cartilage tissue was investigated, alongside a series of tests for pullulan biocompatibility and mode of action with MSCs.

2.) Development and Design of an Antibody-Peptide Construct Specific to MSCs and Degraded Cartilage

It was hypothesised that specifically localising cells through the use of antibodies or peptides would be advantageous for enhancing cell numbers and retention in the target tissue of interest (Figure 1.4B) (Bulman *et al.*, 2012; Dennis *et al.*, 2004). The objective of this study was to design and develop a bispecific antibody-peptide construct that would bind both MSCs and degraded cartilage. The study design involved the chemical conjugation of an RGD peptide to streptavidin in order to form a bridge with a biotinylated coll 2 3/4m antibody. The construct was tested for functionality on MSCs and degraded cartilage by immunohistochemical and immunofluorescent methods.

3.) Enhancing MSC Retention to Degraded Cartilage Using a Biocompatible Antibody-Peptide Construct

The purpose of this study was to demonstrate enhanced adherence of MSCs at the degraded cartilage surface using the bispecific antibody-peptide construct developed and further validate its biocompatibility with MSCs. Using a porcine cartilage explant model, a stereological approach was used to quantify numbers of MSCs retained and further, biocompatibility with MSCs was addressed through tri-lineage differentiation, proliferation and viability assays.

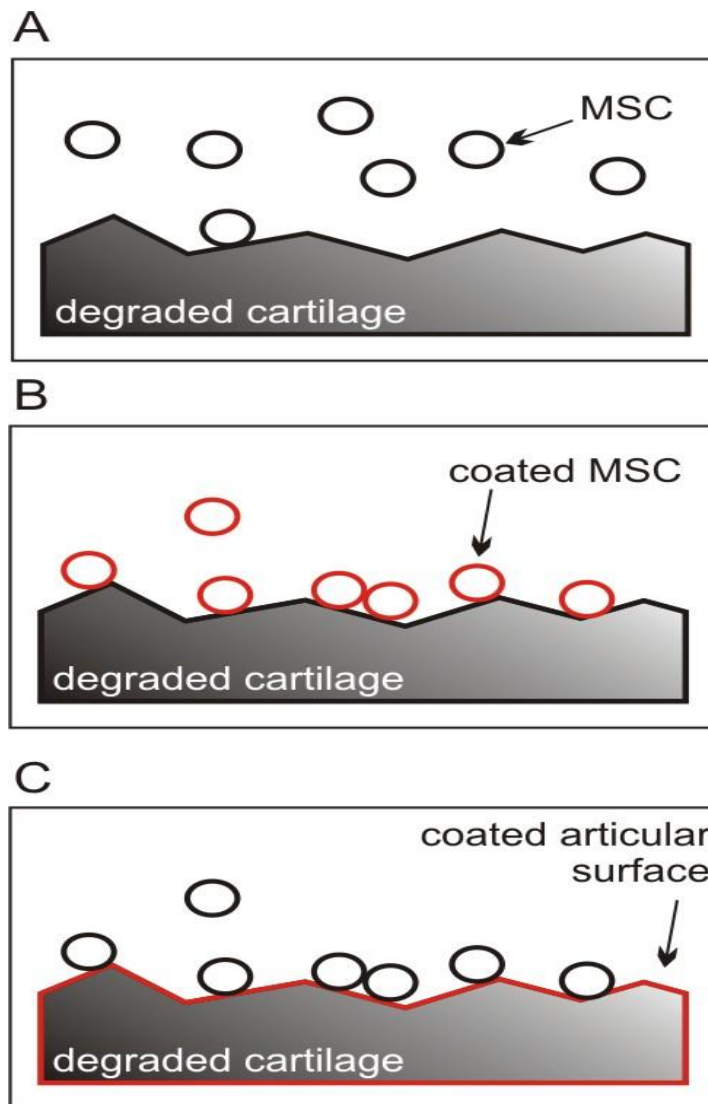


Figure 1.4: Methods of Increasing MSC Adherence to Degraded Cartilage

Cartoon illustrating methods of increasing MSC adherence to degraded cartilage. MSCs alone are retained at the surface of the cartilage in few numbers (A). MSCs coated with a localisation technology such as peptide or antibody show retained enhancement at the surface of degraded cartilage (B). In an alternative method, degraded cartilage coated with a localisation technology such as an adhesive also enhances MSC retention at the degraded cartilage surface (C).

Chapter 2

Pullulan: A Biocompatible Adhesive for Enhancing MSC Retention and Response at the Degraded Cartilage Surface

2.1 Introduction

There is an unmet clinical need in cartilage repair methodologies for strategies to maintain or increase cell numbers at the injury site (Coleman *et al.*, 2010; Murphy *et al.*, 2003). Whether MSCs contribute to repair by direct differentiation or through an indirect supportive role, increasing cell retention will be valuable for repair. There are several approaches through which cellular retention may be increased at the cartilage surface (chapter 1). An alternative method for increasing cell adhesion would be to use a biomaterial to provide an adhesive interface between the cells and the cartilaginous tissue.

2.1.1 Bioadhesion and Bioadhesives for Cell Retention

Adhesion is described as the phenomenon between two surfaces or materials which are held together for a period of time by interfacial forces. Bioadhesion is when one or both surfaces comprise a biological material (Rogue *et al.*, 2011; Shaikh *et al.*, 2011). Traditionally, bioadhesives are used surgically for bonding soft tissues, as gap-filling agents to aid bone fixation in orthopaedic surgery or more recently as drug delivery systems (Donkerwolcke *et al.*, 1998; Jasti, 2003). Transmucosal drug delivery systems involve methods of rapid uptake of a drug systemically via a mucous membrane using mucoadhesives (Jasti, 2003; Vinod *et al.*, 2012). The term ‘mucoadhesive’ is specifically defined as a bioadhesive, usually a polymer, that binds the mucin layer of a biological membrane (Jasti, 2003; Lehr, 1996; Mythri *et al.*, 2011; Vinod *et al.*, 2012). An orthopaedic adhesive must possess adequate strength to hold a tissue bond for a sufficient time, be biocompatible to allow the tissue to regenerate naturally and have a comparable degradation rate with that of the neotissue formation (Chivers, 1997; Donkerwolcke *et al.*, 1998).

Naturally occurring adhesives, developed for bioadhesive applications are often derived from marine plants and animals possessing a combination of proteins and polysaccharides that allow a firm bond of the organism to their substratum (d'Ayala *et al.*, 2008). Soft tissue adhesives such as cyanoacrylates and a combination of gelatin, resorcin and formaldehyde (GRF) have been tested pre-clinically with advantages over acrylic glues in reducing infection and having lasting elasticity. For

strong adherence and effective seals under wet conditions in surgery, mussel-inspired adhesives have anchoring properties suitable for such applications (Hwang *et al.*, 2007; Lee *et al.*, 2011).

In orthopaedic surgeries, fibrin based adhesives are commonly used as sealants in combination with thrombin for clotting with positive and negative results (Donkerwolcke *et al.*, 1998; Kluba *et al.*, 2012; Patel *et al.*, 2010). Fibrin glue has predominantly been used for MSC encapsulation within scaffolds for bone repair (Ho *et al.*, 2006; Liao *et al.*, 2011; Nair *et al.*, 2009; Yamada *et al.*, 2003) and has shown mixed results for its application in cartilage repair. The combination of MSCs with fibrin glue was investigated in full articular cartilage defects clinically. All patients demonstrated an improvement over a 1-year study, but only 3 of 5 procedures resulted in complete defect fill (Haleem *et al.*, 2010). Although, fibrin encapsulated MSCs have shown some potential to remain viable and support chondral repair (Ho *et al.*, 2010; Ting *et al.*, 1998), fibrin hydrogels have demonstrated poor cell retention (Wilke *et al.*, 2007) and compromised osteochondral repair in a rabbit model (Brittberg *et al.*, 1997).

The use of a bioadhesive to bond a cell to a tissue or material surface is an approach that has previously been explored through the use of hydrogels and cellular encapsulation (Biomet, 2013; Jabbari and Khandemhosseini, 2010; Nicodemus and Bryant, 2008; Wang *et al.*, 2007). It is recognized that host tissue integration with newly repaired or transplanted tissue is a vital requisite for any transplant or scaffold and this might be achieved using a bioadhesive approach (Biomet, 2013; Wang *et al.*, 2007).

2.1.2 Pullulan

Pullulan is one of a group of naturally-derived polysaccharides that in nature are hydrophilic, with biochemical structures similar to that of the extracellular matrix (Autissier *et al.*, 2007; d'Ayala *et al.*, 2008; Leathers, 2005; Mano *et al.*, 2007). It is a structurally flexible exopolysaccharide produced from starch fermentation by the fungus *Aureobasidium pullulans* (Leathers, 2003; Singh *et al.*, 2008). There are a

variety of 'exopolysaccharides' produced by microorganisms as an extracellular cell surface attached material, in the form of an amorphous slime (Singh *et al.*, 2008; Sutherland, 1998). Exopolysaccharides are divided into homopolysaccharides, such as neutral glucans like pullulan and heteropolysaccharides, such as xanthan or gellan that are polyanionic (Kumar and Mody, 2009; Sutherland, 1998; Welman and Maddox, 2003). These microbial components are the equivalents of the plant polysaccharides, such as cellulose and pectin, with similar structures but having their own unique and superior physical properties (Singh *et al.*, 2008; Sutherland, 1998). Pullulan is one of only a few fungal polysaccharides that have been documented in the literature with a history of use. Additionally, its commercial properties have been studied, making it an attractive choice for tissue engineering applications (Leathers, 2003; Rekha and Sharma, 2007; Singh *et al.*, 2008).

2.1.3 Pullulan Properties

Pullulan is a maltotriose trimer, α -glucan that comprises repeating units, linked through α -1, 6- and α -1,4-glucosidic bonds (Figure 2.1). This regular structure of pullulan gives it two distinctive properties, structural flexibility and enhanced solubility (Leathers, 2003; Singh *et al.*, 2008). The linkage pattern also offers properties of adhesion, fiber formation and the formation of strong films impermeable to oxygen. Pullulan is highly soluble in water and its solubility can be controlled easily by chemical derivatisation (Akiyoshi *et al.*, 1998; Jeong *et al.*, 1999; Kuroda *et al.*, 2002; Leung *et al.*, 2006; Rekha and Sharma, 2007; Singh *et al.*, 2008).

Multiple cell surface receptors have evolved on animal immune cells in response to surface exposure of fungal cell wall components and are recognized by the innate immune system (Levitz, 2010). Receptors that recognize β -glucans of fungal cell walls include, Dectin-1, complement receptor 3 and scavenger receptors such as CD5, CD36 and SCARF-1 (Levitz, 2010; Saijo and Iwakura, 2011). The Dectin-2 receptor was shown to have specific affinity for α -glucans and mannans (Levitz, 2010; Saijo *et al.*, 2010; Saijo and Iwakura, 2011), thus a potential receptor for demonstrating a pullulan mechanism of action with MSCs.

2.1.4 Pullulan as an Adhesive for Cell Retention

The bioadhesive approach of using pullulan for cell retention has several advantages over other adhesives and retention technologies including low cost production and a history of safe use *in vivo* (Leathers, 2003; Rekha and Sharma, 2007). The polysaccharide is neutral, linear, non-ionic, non-toxic, non-immunogenic, blood compatible and biodegradable making it widely used in the food and biomedical industry (Kimoto *et al.*, 1997; Rekha and Sharma, 2007, 2009). The high adhesion and film forming abilities of pullulan have made it suitable as a mucoadhesive and in more recent developments it has been self-assembled to form nanoparticles for drug/gene delivery (Akiyoshi *et al.*, 1998; Kuroda *et al.*, 2002; Rekha and Sharma, 2007, 2009). Due to its biocompatibility, cost and structural flexibility pullulan was therefore considered an attractive material to be evaluated in this study for enhancing MSC adhesion to human OA cartilage. The effects of pullulan on MSC viability, proliferation, differentiation and surface marker expression were also assessed for demonstration of biocompatibility. Further, an MSC mechanism of action with pullulan was analysed through Dectin-2 receptor expression.

2.2 Materials and Methods

Note: All materials were supplied by Sigma-Aldrich unless otherwise stated.

All experiments were performed in triplicate with 3 biological replicates, unless otherwise stated.

2.2.1 MSC Isolation

MSCs were isolated from the bone marrow of consenting human donors using a protocol approved by the Clinical Research Ethical Committee at University College Hospital, Galway. Traditional methods were used to isolate and expand cells in culture by direct plating (Murphy *et al.*, 2003). Cultures were fed twice weekly with MSC expansion medium: alpha-Minimum Essential Medium Alpha (α -MEM; Gibco), 10% selected fetal bovine serum (FBS; Lonza), 1% penicillin/streptomycin, 2mM L-glutamine, 1% non-essential amino acids and 5ng/ml recombinant human fibroblast growth factor 2 (rhFGF-2, Peprotech) and subcultured at 80% confluence. Cultures were expanded in monolayer to passage 3. For each subsequent assay, 3 biologic replicates were used, ranging in age from 18-35 years.

2.2.2 MSC Viability and Proliferation

For viability assessment, MSCs were seeded at a density of 3.125×10^3 cells/cm² in a 96-well assay plate and exposed to 0, 2 and 5% (w/v) pullulan (Hayashibara International) for 1, 3 and 7 days. Pullulan was UV sterilized prior to use and dissolved in MSC expansion medium. MTS (3-(4,5-dimethylthiazol-2-yl)-5-(3-carboxymethoxyphenyl)-2-(4-sulfophenyl)-2H-tetrazolium), was applied as per the manufacturer's instructions (Promega). Briefly, 20 μ l of Cell Titer96 AQueous One Solution Reagent was added into each well containing 100 μ l of culture medium and the culture incubated for 2 hours at 37°C. Culture media absorbance was evaluated at 490nm on a Wallac Victor™ 1420 Multilabel Counter spectrophotometer.

For DNA quantification, MSCs were seeded at a density of 5.8×10^3 cells/cm² and exposed to 0, 2 and 5% (w/v) pullulan for 1, 3 and 7 days. Cells were lysed using

0.1% Triton x-100, scraped, placed in a microcentrifuge tube and subsequently vortexed to pellet cell debris. The Quant-iT PicoGreen dsDNA assay kit (Molecular Probes) was utilised according to the manufacturer's protocol. Briefly, kit stock solutions were prepared and 100µl of lysed cell solution samples (in triplicate) and kit standards provided (DNA 100 µg/ml diluted in 200 mM Tris-HCl, 20 mM ethylenediamine tetraacetic acid (EDTA), pH 7.5), were added to the wells of a 96-well black flat-bottomed plate, followed by the addition of PicoGreen solution (diluted in Tris-EDTA; TE) and incubated for 3 minutes at room temperature. Samples were evaluated on a Wallac Victor™ 1420 Multilabel Counter spectrophotometer, exciting at 485nm and reading at 538nm.

2.2.3 MSC Flow Cytometry

MSCs were pre-incubated in tissue culture flasks with 0, 2 and 5% (w/v) pullulan for a period of 1, 3 and 7 days. After incubation, the MSCs were trypsinised, resuspended in phosphate buffered saline (PBS) at 5×10^5 cells/ml and incubated with phycoerythrin (PE)-conjugated antibodies, CD44 (Milteny biotech), CD90 (Abcam), CD73 (Abcam), CD105 (Milteny biotech) and an IgG-PE isotype control (Milteny biotech) at a 1:10 dilution for 20 minutes at 4°C. Cells were washed twice in PBS to remove unbound antibody and resuspended in serum free α -MEM for analysis using the ExpressPlus program software on the Guava Cytosoft system (Millipore).

2.2.4 MSC Differentiation

Tri-lineage differentiation of MSCs was assessed after exposure to 0, 2 and 5% (w/v) pullulan in MSC expansion medium for 2 hours. For osteogenic differentiation, MSCs were seeded at 3.2×10^3 cells/cm² for 24 hours in expansion medium. Cultures were incubated with osteogenic medium [low glucose Dulbeccos Modified Eagle's Medium (DMEM) with 10% FBS, 1% penicillin/streptomycin, 50µM ascorbic acid 2-phosphate, 100nM dexamethasone and 10mM β -glycerophosphate. Control cultures were incubated in MSC expansion medium for the duration of the assay and refreshed twice a week for 17 days. To visualize

deposited calcium, MSCs were fixed, washed and stained in 2% Alizarin Red S solution (Sigma) and photographed using an Olympus IX71 inverted brightfield microscope and QImaging (Retiga Exi) camera.

Quantification of calcium was accomplished using the StanBio quantification kit, according to the manufacturer's instructions. Briefly, samples were washed twice with PBS and 0.5 M HCl was added to each well. The wells were scraped and contents placed into separate Eppendorf tubes. This was repeated to ensure all matrix was removed from the wells. Samples were centrifuged at 3,000 rpm for 5 minutes and standards were prepared according to manufacturer's instructions with 0.5 M HCl and deionised water ranging from 0.05 µg to 1.5 µg. Stanbio Calcium (CPC) Liquicolor working solution (1:1 working dye to binding reagent) was added to standards and samples in a 96-well plate (200 µl per well) and incubated at room temperature, in the dark, for 15 minutes. Samples were assayed in triplicate and the absorbance was read on a Wallac Victor^{3™} 1420 Multilabel Counter spectrophotometer at 550 nm.

For adipogenic differentiation, MSCs were seeded at 2.1×10^4 cells/cm² and grown to confluence, changing expansion medium every 3-4 days. Once confluent, adipogenesis was induced by adding induction medium to the culture [high glucose DMEM with 10% FBS, 1% penicillin/streptomycin, 1µM dexamethasone, 1.7µM insulin, 200µM indomethacin and 500µM isobutyl methylxanthine]. Negative control cultures were incubated in MSC expansion medium. MSCs were cultured for 3 days and changed to maintenance medium [high glucose DMEM with 10% FBS, 1% penicillin/streptomycin and 1.7µM insulin] for a further 3 days. Alternating media changes were continued for 3 cycles and then cultures were incubated 5-7 days in maintenance medium. Cultures were prepared for lipid vesicle visualization by washing with PBS and crosslinked in 10% neutral buffered formalin. Oil Red O solution (0.3% in 99% isopropanol) was added to the cells for lipid staining and haematoxylin was used as a counter stain. Cell lipid vesicles were visualised and photographed using light microscopy. For quantification, Oil Red O was extracted using 99% isopropanol and absorbance read at 520nm.

MSCs were induced to chondrogenic differentiation through pellet culture (2.5×10^5 cells per pellet) in complete chondrogenic medium [CCM, high glucose DMEM, 100nM dexamethasone, 173 μ M ascorbic acid 2-phosphate, 340 μ M L-proline, 1% ITS supplement (R&D Systems), 1mM sodium pyruvate, 1% penicillin/streptomycin and supplemented with 10ng/ml TGF- β 3 (R&D Systems)]. Four pellets per treatment group were prepared and controls were placed in incomplete chondrogenic medium (ICM; CCM without TGF- β 3). The culture medium was refreshed twice a week for 21 days. Pellets were histologically processed by cross-linking in 10% formalin in an automated tissue processor (Leica ASP300S) and embedded in paraffin wax. Pellets were sectioned at a thickness of 5 μ m using the Leica RM2235 microtome and rehydrated by passing the slides through a series of histoclear and graded ethanols, followed by haematoxylin, 0.02% fast green, 1% acetic acid (Fischer Scientific) and 0.1% Safranin O to visualize sulfated GAGs. Slides were then hydrated, mounted using histomount solution (National Diagnostics) and imaged by light microscopy.

Quantitative assessment of GAG content was conducted by DMMB (1, 9 dimethylmethylene blue) analysis. Pellets were digested overnight at 60°C in 25 μ g/ml papain, dissolved in DMMB dilution buffer (50mM sodium phosphate, 2mM N-acetyl cysteine and 2mM EDTA, pH 6.5). Samples and chondroitin-6-sulphate standards prepared in DMMB dilution buffer were placed into a 96 well plate with DMMB stock solution (200 μ l) (in 100% ethanol, deionised H₂O (di H₂O), 47mM NaCl, 40mM glycine and 11.6M HCl), then incubated at room temperature for 5 minutes and absorbance was detected at 595nm. The DNA content of each pellet was quantified using the Quant-iT PicoGreen dsDNA assay kit (Molecular Probes) according to the manufacturer's protocol to assess the GAG/DNA ratio of each pellet. Briefly, kit stock solutions were prepared according to the manufacturer's instructions and papain digested samples were diluted 1 in 25 in DMMB dilution buffer. Both samples and kit standards provided (DNA 100 μ g/ml diluted in 200 mM Tris-HCl, 20 mM EDTA, pH 7.5), were added (100 μ l) to the wells of a 96-well black flat-bottomed plate, followed by the addition of PicoGreen solution (diluted in Tris-EDTA; TE) and incubated for 3 minutes at room temperature.

2.2.5 OA Cartilage Explant Culture

Informed consent was given by patients with end-stage OA, undergoing total hip and knee arthroplasty as approved by the Clinical Research Ethical Committee at Merlin Park Hospital, Galway. Cartilage biopsies were taken from the articular cartilage surfaces of the hip femoral head and condyle tibial plateau of the knee. Full thickness cartilage explants were created by biopsy punch (1-2mm thick and 2 mm diameter). The explants were placed in α -MEM, containing 10% FBS for 48 hours at 37°C and subsequently placed in ICM for 24 hours.

2.2.6 Explant Culture with MSCs and Pullulan

MSCs were PKH26 labelled with the PKH26GL cell linker kit following the manufacturer's instructions. Explants were incubated in 0, 2 and 5% (w/v) pullulan for 10 minutes, after which 0.5×10^6 PKH26 labelled MSCs were incubated with each explant on a rocking plate for 20 minutes (Figure 2.1). Unbound MSCs were removed by washing twice with PBS, snap-frozen in OCT embedding medium (RA Lamb) in liquid nitrogen and cryosectioned at 5 μ m using the OTF5000 Bright 5040 microtome cryostat. Sections were coverslipped using Vectorshield containing 4',6-diamidino-2-phenylindole (DAPI) (Vector Laboratories) and visualised using an Olympus BX51 upright fluorescent microscope.

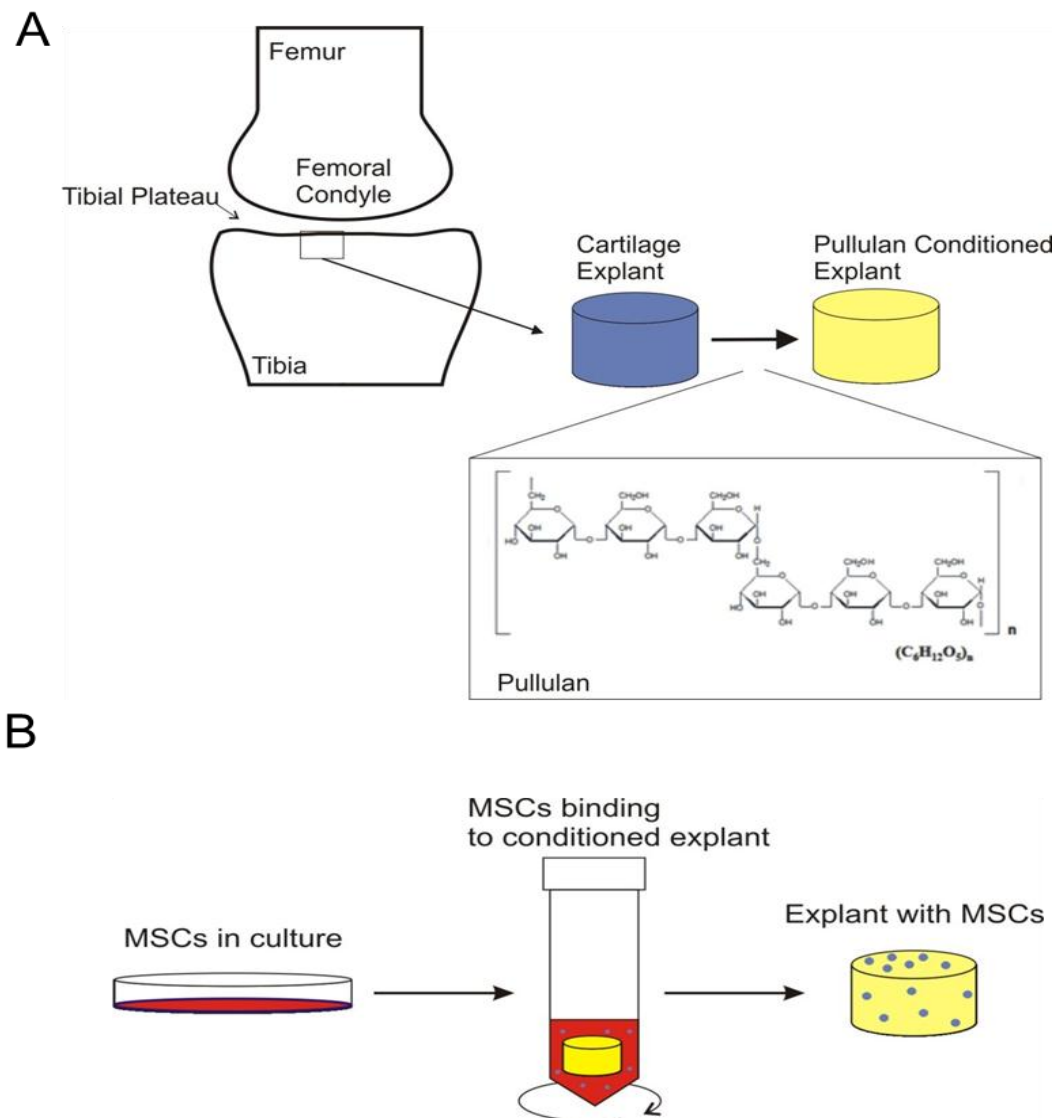


Figure 2.1: Pullulan Conditioned Cartilage

Schematic shows the methodology for conditioning cartilage with the bioadhesive pullulan prior to MSC delivery. Cartilage biopsies are taken from the articular cartilage surfaces of the tibial plateau of the knee or hip femoral head. The explant surface is coated for 10 minutes in pullulan, an α -1-4; α -1-6-glucan polysaccharide consisting of maltotriose units (A). Culture expanded PKH26 labelled MSCs are applied to conditioned cartilage explants and incubated on a rocking plate for 20 minutes. Unbound MSCs in suspension are removed by washing in PBS, leaving MSC bound cartilage which can then be fixed and analysed histologically (B).

2.2.7 Stereological Assessment of MSC binding

Quantification of cell adherence was performed on 5µm cryosections of cell seeded explants. MSCs were identified as dual labelled cells (red, PKH26 and blue, DAPI). Delivered cells were counted manually using the software program Image J. The optical disector method, a three-dimensional sampling method was used to estimate the number of cells on the surface of the explant (Garcia *et al.*, 2007; Gundersen *et al.*, 1988). The disector method relies on observation of the images of two parallel/serial sections. The occurrence of labelled cells present on the cartilage surface in the first image (sampling image) was compared with their occurrence in the second image (look-up image). Only those cells present in the first image and not in the second image were counted. Cells present in both images are not counted. Density estimates were calculated expressed as the number of cells present per square millimetre of explant.

2.2.8 Flow Cytometric Analysis of Dectin-2

Culture expanded MSCs were pre-incubated with 0, 2 and 5% (w/v) pullulan in expansion medium for 2, 24 and 48 hours. MSCs were trypsinised and resuspended in PBS/2% FBS at 0.5×10^4 cells/well in triplicate. Cells were incubated with APC-conjugated Dectin-2/CLEC6A antibody (R&D systems) at a final concentration of 6.25µg/ml for 30 minutes at 4°C, protected from light. Cells were washed twice in PBS/2% FBS to remove unbound antibody and resuspended in a final volume of 400µl of PBS/2% FBS. Immunostaining signal intensity was analyzed with a FACS Canto (BDBiosciences) with FlowJo software.

2.2.9 Statistical Analysis

All values were expressed as the mean \pm standard deviation of the mean (SD). All datasets were tested for significance using the two-way ANOVA. Donor was used as a blocking factor and post hoc analysis (Dunnetts) identified where the difference lay within the groups. For all tests, $p \leq 0.05$ was considered statistically significant. Data analysis was performed on Minitab 16.2.2.0.

2.3 Results

2.3.1 MSC Viability and Proliferation in the Presence of Pullulan

Biocompatibility of pullulan with MSCs was assessed using viability and proliferation; MSCs in monolayer were exposed to expansion medium containing 0, 2 and 5% pullulan and viability and proliferation assessed after 1, 3 and 7 days. A non-significant increase in metabolic activity was observed at day 1 in 2 and 5% pullulan treated cultures as compared to 0% untreated controls. The metabolic activity remained similar to day 1 levels at day 3 and increased at day 7 for all treatment groups. There were no significant changes in metabolic activity in 2 and 5% pullulan treated cultures at day 3 and 7 compared to untreated controls at the same time point (Figure 2.2A).

PicoGreen analysis of DNA content revealed an increase in cell number in all cultures between days 1 and 3, with a greater change observed in 2 and 5% pullulan treated cultures as compared to 0% untreated controls. At day 7, DNA content continued to increase in untreated cultures, however a statistically significant decrease in DNA content was found in 2% pullulan treated cultures as compared to untreated controls (Figure 2.2B).

MSC metabolic activity and DNA content were combined for assessment of activity per cell (Figure 2.2C). At day 1, there was a non-significant initial decrease in the ratio of metabolic activity per cell in 2% treated cultures as compared to untreated controls, and a non-significant increase in metabolic activity per cell in 5% treated cultures as compared to untreated controls. The metabolic activity per cell decreased in all cultures at day 3, remaining consistent in all treatment groups. Metabolic activity non-significantly increased again at day 7, with slight variation between treatment groups.

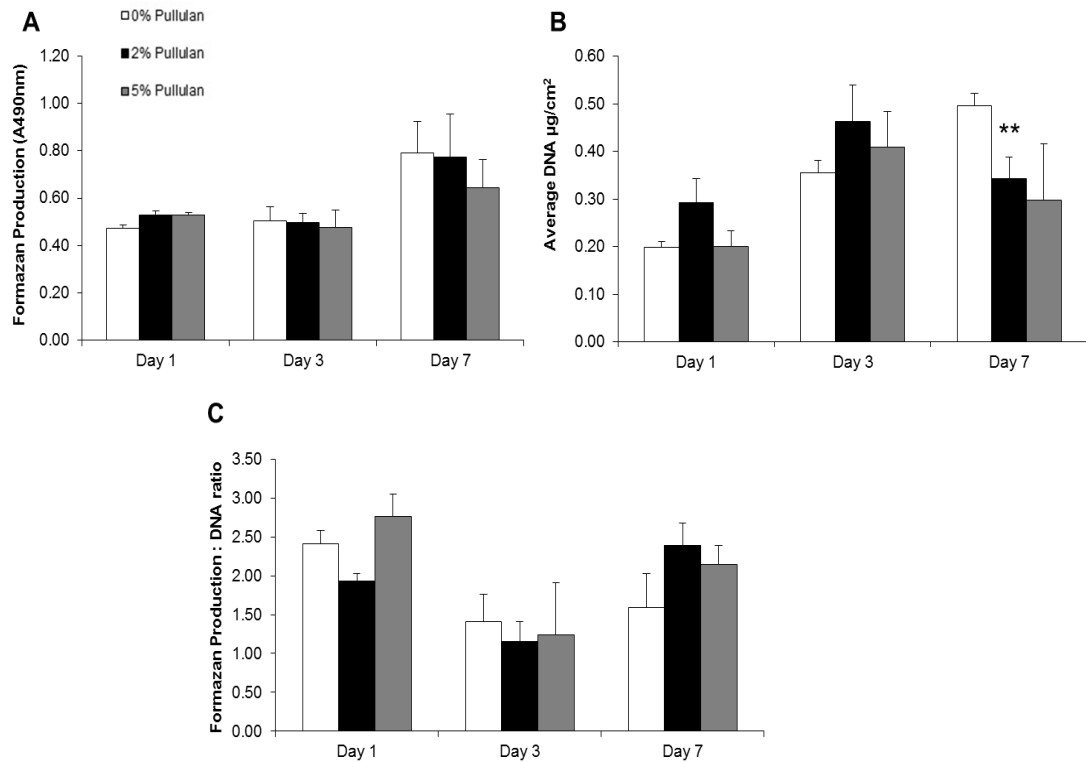


Figure 2.2: MSC Viability and Proliferation in the Presence of Pullulan

MSC metabolic activity was assessed by quantitative formazan production (A490). MSCs were cultured in 0, 2 and 5% pullulan for 1, 3 and 7 days. A non-significant increase in metabolism at day 1 was observed in MSCs cultured in 2 and 5% pullulan as compared to 0% controls. Metabolic activity was maintained at days 3 and 7 in all cultures, but consistently increased over time with no significant change due to pullulan treatment (A). An increase in MSC DNA concentration as assayed by PicoGreen incorporation was observed in all culture conditions between days 1 and 3, with a non-significant increase in proliferation of MSCs cultured in 2% pullulan at day 1 compared to 0% and 5% treated cultures. A statistically significant decrease was observed in 2% pullulan cultures after 7 days as compared to controls at the same time point (B). The ratio of metabolic activity normalised to DNA content indicated a non-significant increase in MSC metabolism at day 1 in MSCs exposed to 5% pullulan, however metabolic activity in all cultures decreased with time, returning to day 1 levels at day 7 (C). Data is presented as the mean \pm SD of $n=3$ biological replicates, generated using triplicate measurements **= $p \leq 0.01$.

2.3.2 MSC Surface Phenotype in the Presence of Pullulan

Confirmation of the traditional MSC surface phenotype after pullulan exposure was performed using flow cytometric analysis of CD44, CD90, CD73 and CD105 expression. After 1 day of exposure, pullulan treated cultures maintained MSC receptor expression of CD44, CD90, CD73 and CD105 at 95-100% expression (Dominici, 2006), similar to that of 0% cultures (Figure 2.3A). Three days after pullulan exposure, expression of CD44, CD90, CD73 and CD105 also remained similar to that of control 0% levels (Figure 2.3B). After 7 days exposure to pullulan, CD44, CD90, CD73 and CD105 receptor expression was decreased in 5% pullulan treated cultures to $\leq 95\%$ compared to 2% treated cultures and 0% controls at $\geq 95\%$ and CD73 expression was statistically significantly decreased (Figure 2.3C).

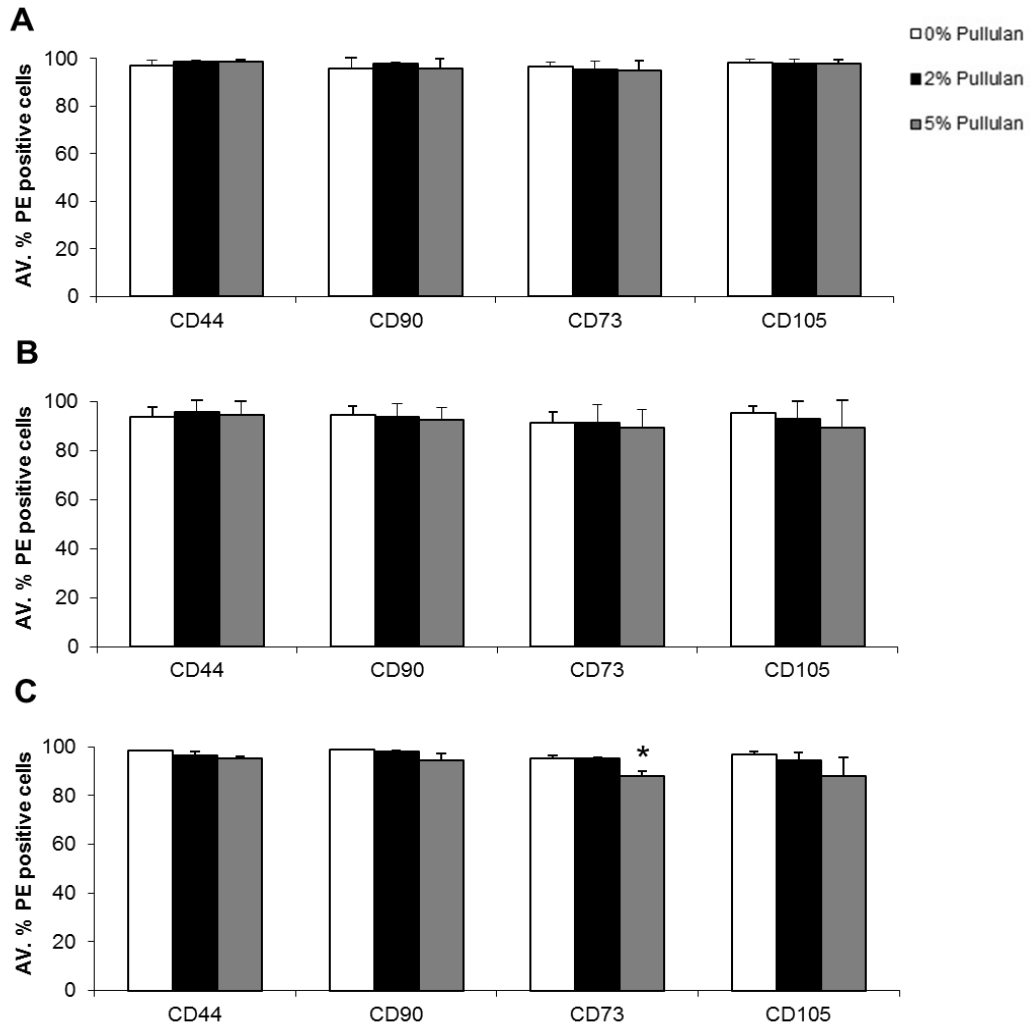


Figure 2.3: MSC Surface Receptor Expression in the Presence of Pullulan

Assessment of CD44, CD90, CD73 and CD105 receptor expression was made by cytometric flow analysis, after 1, 3 and 7 days exposure to increasing concentrations of pullulan. There was no significant difference in receptor expression between MSCs incubated in 2 and 5% pullulan as compared to 0% controls after 1 day (A). There was a decrease in overall receptor surface expression for all groups after 3 days of culture. A small decrease was observed in expression of CD90, CD73 and CD105 for MSCs cultured in 5% pullulan after 3 days, however this was not statistically significant (B). A decrease in CD44, CD90, CD73 and CD105 receptor expression was noted after 7 days of MSC culture in 5% pullulan (C). This was statistically significant for CD73 expression. Data is presented as the mean \pm SD of n=3 biological replicates, generated using triplicate measurements *= $p \leq 0.05$.

2.3.3 MSCs Maintain Differentiation Potential in the Presence of Pullulan

MSC differentiation potential was assessed in the presence of pullulan to ensure maintenance of MSC tripotentiality. MSCs were differentiated in osteogenic, adipogenic and chondrogenic conditions after 2 hours pre-incubation in 0, 2 and 5% pullulan. Alizarin Red staining of calcium deposits in pullulan treated cultures showed increased levels of calcium deposition in pullulan 2 and 5% treated cultures, compared to 0% controls (Figure 2.4A). Calcium quantification in pullulan treated cultures showed a statistically significant increase in calcium content as compared to 0% controls (Figure 2.4BA). Oil Red O staining of lipid droplets in adipogenically primed cultures indicated a similar abundance of lipids in the cytoplasm of adipogenically differentiated cultures for all treatment groups (Figure 2.4A). Oil Red O absorption readings showed that 2 and 5% pullulan treated cultures resulted in a non-significant decrease of Oil Red O with increasing pullulan concentration as compared to 0% controls (Figure 2.4BB). Safranin O staining of chondrogenic pellets showed GAG deposition similar to that of 0% pullulan controls in pullulan pre-treated 2 and 5% MSC chondrogenic pellets (Figure 2.4A). Quantification of sulphated GAGs by DMMB assay was normalised to DNA content per pellet and represented as average fold change in GAG:DNA ratio over 0% pullulan controls. The GAG:DNA ratio normalised to 0% pullulan controls shows a non-significant decrease in GAG:DNA content in 2% pullulan treated MSCs and an increase in 5% treated MSCs (Figure 2.4BC).

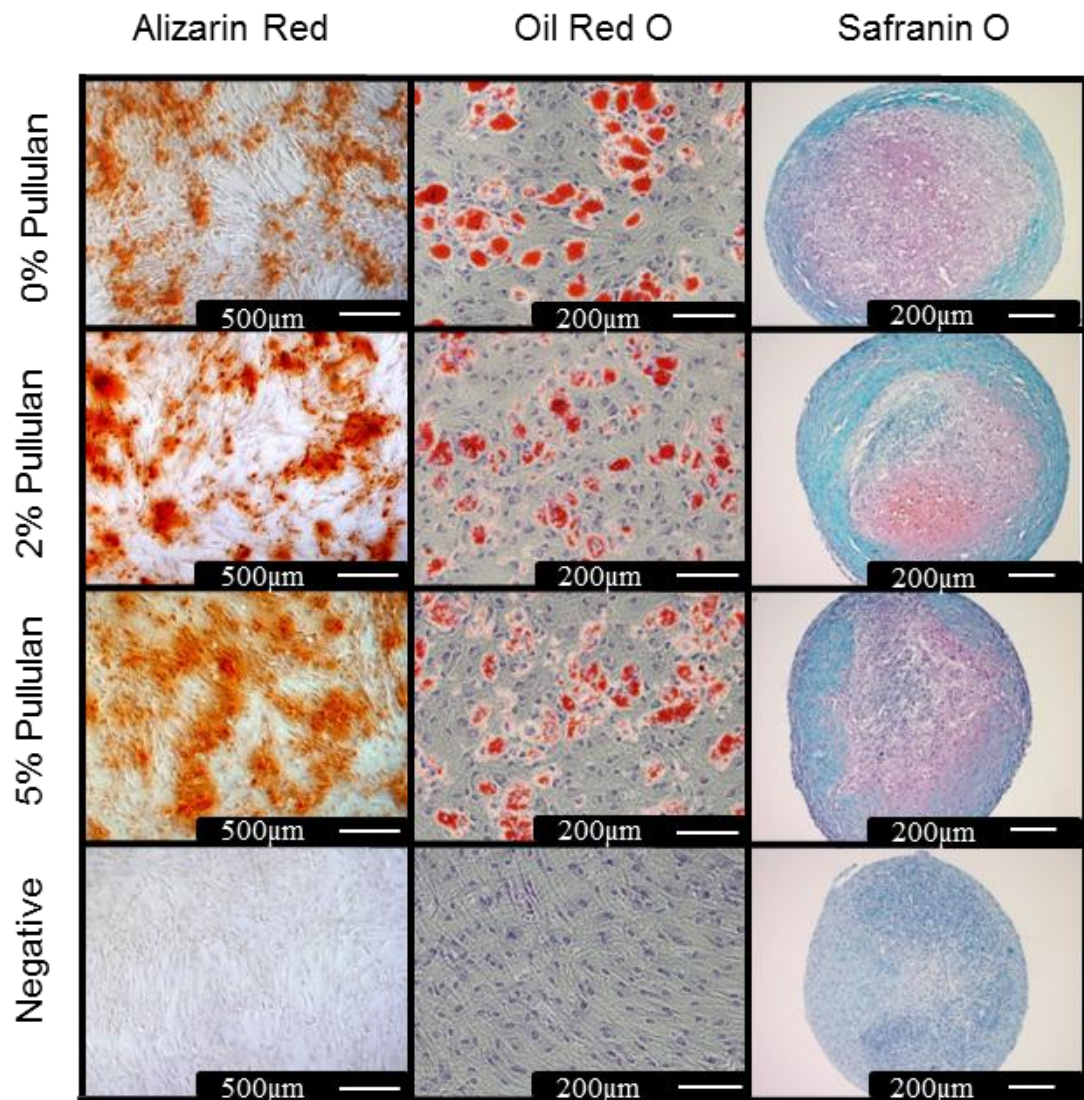


Figure 2.4A: MSC Differentiation in the Presence of Pullulan

Osteogenesis, demonstrated by Alizarin Red stain showed increased mineral deposition in 2% and 5% pullulan treated groups as compared to the 0% control. Oil Red O staining of lipid droplets for adipogenesis showed differentiated MSCs in all pullulan treated groups. Histological assessment by Safranin O of MSCs in pellet chondrogenic culture showed GAG deposition in all pullulan treated groups. Magnification bars = 500µm for Alizarin Red and 200µm for Oil Red O and Safranin O images.

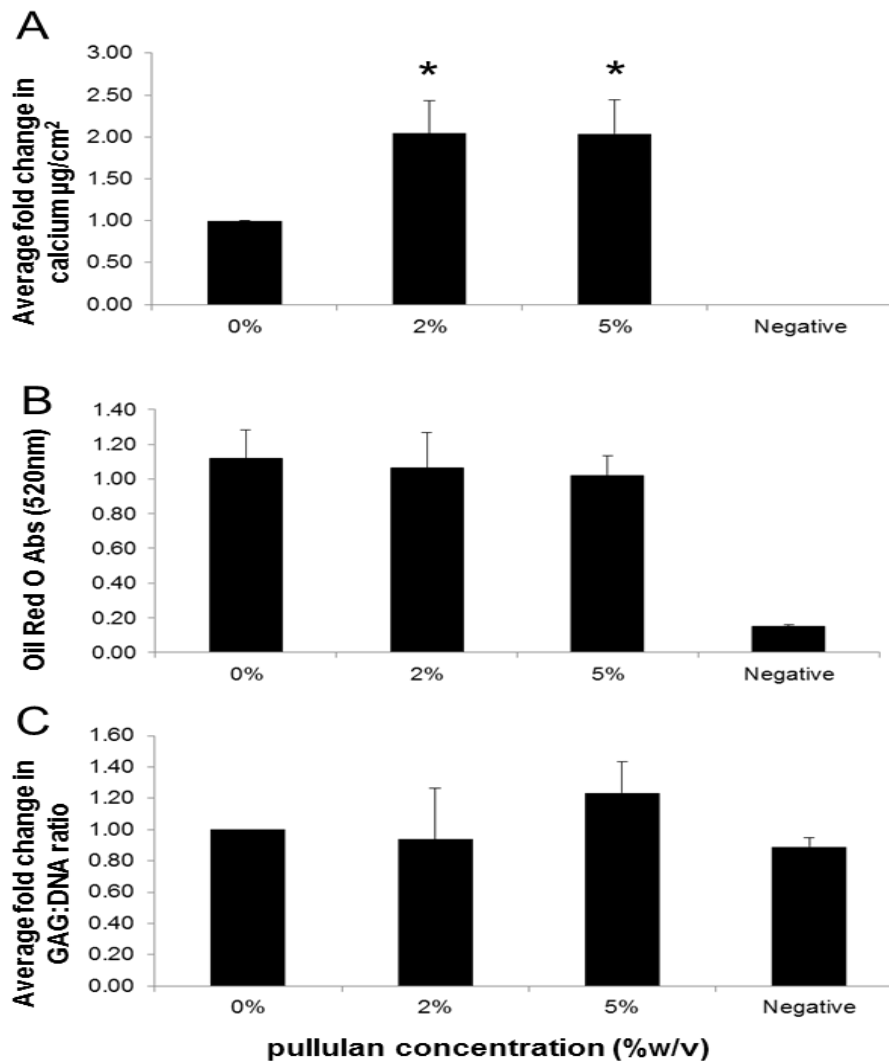


Figure 2.4B: MSC Differentiation in the Presence of Pullulan

Quantification of calcium content, represented as average fold change in osteogenically differentiated MSCs, demonstrated significant increases in calcium deposition after 2 and 5% pullulan pre-exposure as compared to 0% pullulan controls (A). Oil Red O extraction and quantification from adipogenically differentiated MSCs pre-exposed to 2 and 5% pullulan showed a maintenance of adipogenic potential comparable to 0% controls (B). Using DMMB to measure GAG production and PicoGreen to quantify DNA content, the average fold GAG:DNA ratio was unchanged in pullulan treated groups as compared to 0% controls (C). Data is presented as the mean \pm SD of n=3 biological replicates, generated using triplicate measurements *=p \leq 0.05.

2.3.4 Pullulan Enhances MSC Retention to OA Cartilage

In an attempt to increase MSC adhesion at the cartilage surface, pullulan was applied to OA cartilage explants prior to MSC incubation. MSCs incubated with uncoated explants were retained at the cartilage surface at low levels (Figure 2.5A). MSCs incubated with 2% (Figure 2.5B) and 5% (Figure 2.5C) pullulan pre-coated explants resulted in an observed increase in cell retention, as indicated by a greater number of PKH26 positive cells at the fibrillated surface. Quantification of an estimate of MSC retention using stereology showed an increase in MSC retention to OA cartilage when MSCs were incubated with 2% (2876 cells/mm²) and 5% (1491 cells/mm²) pullulan pre-coated explants as compared to 0% (145 cells/mm²) pullulan controls (Figure 2.5D).

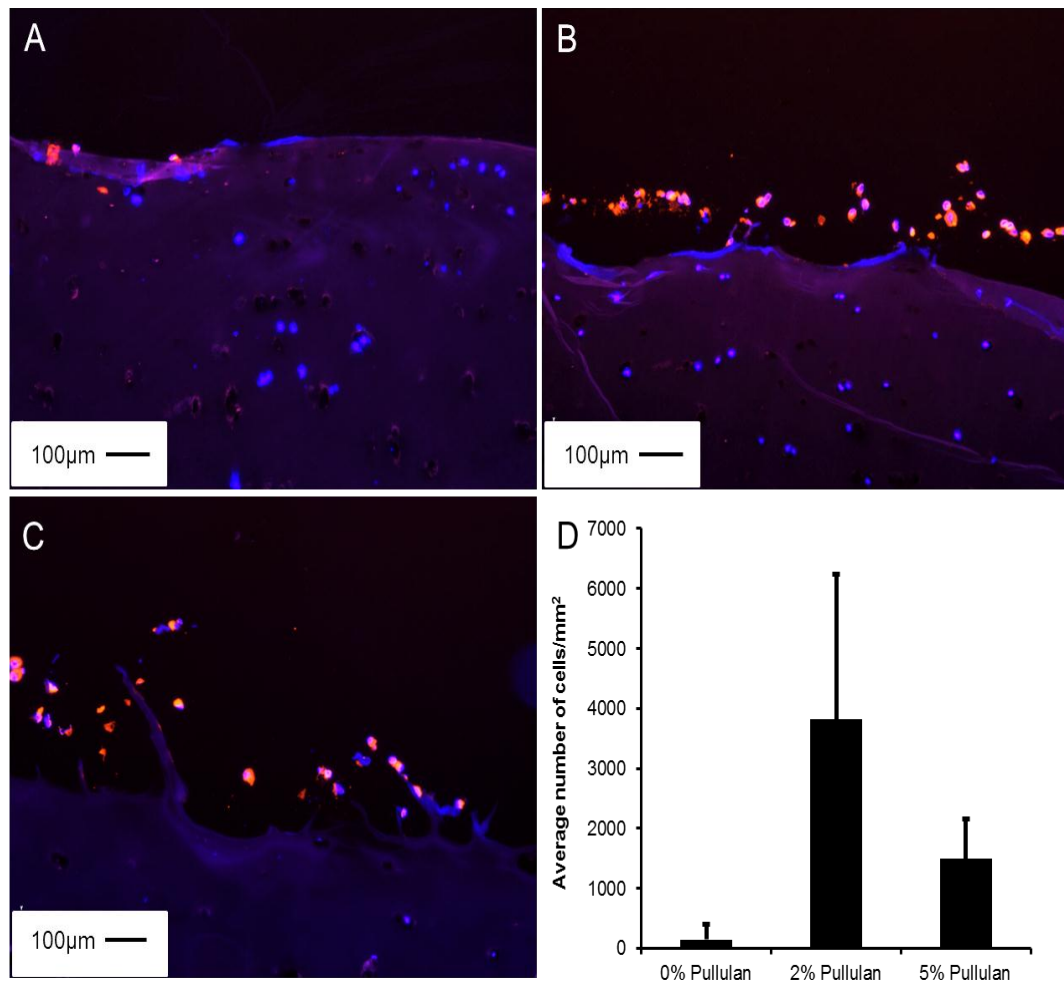


Figure 2.5: MSC Retention on Pullulan Conditioned OA cartilage

PKH26 labelled MSCs (red) bound to fibrillated cartilage on DAPI stained human explanted OA cartilage (blue) (A). MSC retention was increased in 2% (B) or 5% (C) pullulan coated explants. Stereological quantification of MSC retention indicated an estimated increase in the average cell number per mm² on both 2% and 5% pullulan coated explants as compared to 0% untreated controls (D). Data is presented as the mean ± SD of n=3 biological replicates, generated using triplicate measurements. Magnification bars = 100µm.

2.3.5 MSC Dectin-2 Expression Dose Dependently Increases Over Time

MSC expression of the Dectin-2 receptor, normally upregulated on immune cells in response to exposure of alpha-glucans, was analysed to demonstrate a mode of action of MSC binding with pullulan. MSCs were incubated with 0, 2 and 5% pullulan for 2, 24 and 48 hours and Dectin-2 receptor expression analysed by FACs (Figure 2.6). After 2 hours of pullulan exposure, there was a dose-dependant increase in Dectin-2 expression on MSCs. MSCs incubated with 5% pullulan demonstrated an average 15% increase in Dectin-2 expression over 0% pullulan treated MSCs. After 24 hours of pullulan incubation, 2 and 5% pullulan treated MSCs demonstrated an increase in Dectin-2 expression and a statistically significant increase for 5% cultures compared to 0% controls. Positive cells increased to 21 and 38% for 2 and 5% respectively, as compared to 0% controls at 13% positive. After 48 hours of pullulan exposure, 2 and 5% pullulan treated MSCs demonstrated a further increase in expression compared to earlier time points, with a significant increase of 42% in 5% cultures over 0% pullulan controls.

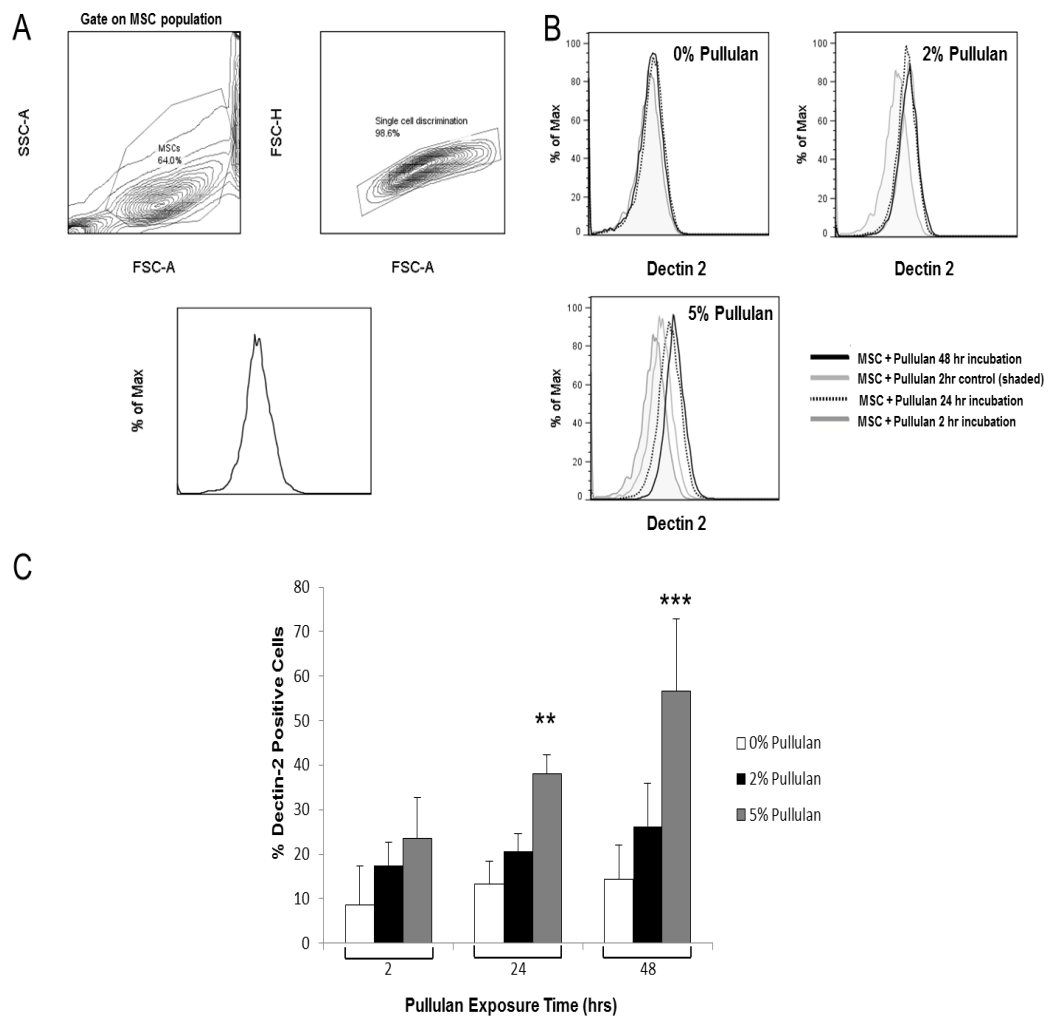


Figure 2.6: Dectin-2 Expression on MSCs in the Presence of Pullulan

MSC gating strategy for receptor surface analysis, showing contour plots of forward and side scatter gating on MSCs (A). Histogram plots for MSCs incubated in the presence of increasing pullulan concentrations at 2, 24 and 48 hours. Graphs show curve shifts with increasing Dectin-2 staining of cells, with increasing concentrations of pullulan and length of exposure (B). Bar chart representation of Dectin-2 expression on MSCs over time as a result of pullulan exposure (hours) (C). At all time points of exposure, there was an increase in Dectin-2 expression with increasing concentration of pullulan. After 24 and 48 hours, the increase in Dectin-2 expression significantly increased in 5% treated cultures compared to 0% controls. Data is presented as the mean \pm SD of $n=3$ biological replicates, generated using triplicate measurements $**=p\leq 0.01$; $***=p\leq 0.001$.

2.4 Discussion

In this study the ability of the bioadhesive pullulan for increasing cell retention at the degraded cartilage surface was assessed. The biocompatibility of pullulan with MSCs was also analysed by assessment of MSC viability, proliferation, differentiation, and surface marker expression. Pullulan cell adhesive potential was demonstrated on human OA cartilage explants and analysis of pullulan specific receptor up-regulation was conducted to assess a specific mode of action at the cell surface.

Pullulan has potential as an adhesive application for cellular retention. However, *in vivo* pullulan is non-specific enabling the adhesion of any cell type within the joint, favouring local application directly to the cartilage, for example, arthroscopy over intra-articular administration. Due to its rapid solubility, the clinical application of pullulan requires chemical modifications to reduce solubility and incur longer term persistence in the fluidic joint (Bruneel and Schacht, 1995; Conca and Yang, 1993; Leathers, 2003; Rekha and Sharma, 2007) enabling more time for cellular adhesion. Alternatively, if MSC reparative mechanisms create a restorative environment, non-specific adhesion to the synovium and menisci may not be an issue.

MSCs incubated with pullulan demonstrated increased metabolic activity and proliferation, however, metabolic activity per cell was not statistically different from untreated controls due to a concurrent increase in cell number. The pullulan-associated increase in metabolism was possibly due to cellular enzymatic breakdown of polysaccharide along with a natural rise in cell proliferation over time (Alberts *et al.*, 1994; Pratt and Cornely, 2004). Bae *et al.* engineered methacrylated pullulan hydrogels for engineering microscale tissues and found that pullulan gels promoted cellular proliferation and aggregation of cells compared to gelatin controls (Bae *et al.*, 2011). With the ultimate goal of enhancing cell retention, an initial pullulan-stimulated increase in MSC proliferation and aggregation at the cartilage surface may be favourable for increasing cell numbers retained and matrix repair. As reduced cellular viability, proliferation and retention can be associated with lack of efficacy in many cartilage scaffold studies (Bulman *et al.*, 2012; Mauck *et al.*, 2003),

the application of pullulan for enhancing proliferation and retention may be considered an advancement over current technologies.

Surface marker analysis demonstrated a decrease in the ISCT-dictated MSC surface receptor phenotype (Dominici, 2006) over time in 5% pullulan. Surface marker expression is maintained in all cultures $\geq 95\%$ at day 1 (Dominici, 2006) but expression decreases in all treatment groups and controls at day 3 to $\leq 95\%$. Expression is increased again at day 7 to $\geq 95\%$ for 0 and 2% treated cultures but remains decreased for 5% treated cultures. The surface receptors CD44, CD90, CD73 and CD105 have previously been documented in the literature as influencing cell proliferation (Abbasi *et al.*, 1993; Fonsatti *et al.*, 2003; Ishiura *et al.*, 2010; Kaya *et al.*, 1997; Khaldoyanidi *et al.*, 1996; Nakamura *et al.*, 2006; Stagg *et al.*, 2011; Trochon *et al.*, 1996; Yegutkin *et al.*, 2011; Zhang *et al.*, 2011). Endoglin (CD105) is required for endothelial cell proliferation and currently used as a tool to measure tumour angiogenesis (Zhang *et al.*, 2011). Similarly, CD73 expression is expressed in several types of cancer and has been associated with increased glioma cell proliferation (Bavaresco *et al.*, 2008; Yegutkin *et al.*, 2011). Since pullulan is exerting a proliferative/metabolic effect on MSCs, the decreased expression levels after 7 days may be due to a down regulation of these receptors as a result of the pullulan exerted proliferation at the earlier time point (Alberts *et al.*, 1994).

Differentiation analysis of MSCs in pullulan-treated cultures demonstrated maintenance of chondrogenic and adipogenic potential and an enhancement of osteogenic potential after pullulan exposure. This increase in osteogenesis potentially relates to the increase in proliferation of MSCs in pullulan treated cultures. Li *et al* described enhanced mineralisation in cell monolayers cultured with high glucose (Li *et al.*, 2007b). Further, osteogenesis has been associated with a proliferative cell phenotype, which is decreased in aging (Moerman *et al.*, 2004). In the application of pullulan for cartilage repair, this enhanced mineralisation is superficially an unfavourable response. However, reparative MSCs *in vivo* are more likely providing more environmental supportive roles rather than directly contributing to new tissue formation (Caplan, 2009b). Since the environment determines cell differentiation, it would be assumed in a cartilage repair environment, cues for chondrogenesis would be present (Caplan, 2009b).

Pullulan is primarily used as an adhesive by *Aureobasidium pullulans* and therefore it is not surprising that a pullulan coated cartilage surface would demonstrate enhanced cellular adhesion (Leathers, 2003; Singh and Ganganpreet, 2008). Similarly, Autissier *et al.*, developed a pullulan-based hydrogel for smooth muscle cell culture (Ramamurthi and Vesely, 2002), observing that smooth muscle cells favourably adhered and formed focal adhesions with the polysaccharide gel (Autissier *et al.*, 2007).

The Dectin-2 receptor, a type II transmembrane protein of the C-type lectin family, is expressed on dendritic cells and macrophages (Sato *et al.*, 2006). Here Dectin-2 was also found expressed on the surface of MSCs, an expression pattern directly relating to pullulan dose and exposure. The function of the Dectin-2 receptor, like Dectin-1 for β -glucans, is to induce intracellular cytokines and reactive oxygen species (ROS) as a protective mechanism from fungal infection (Saijo and Iwakura, 2011). This response is activated through the receptor binding with the Fc receptor γ (Sato *et al.*, 2006) upon α -glucan binding, activating spleen tyrosine kinase and mitogen-activated protein kinase signalling pathways, inducing NF- κ B activation and production of cytokines such as IL-1 β , IL-2, IL-6, IL-10, IL12, IL-17A, IL-23, and TNF α (Robinson *et al.*, 2009; Saijo *et al.*, 2010; Saijo and Iwakura, 2011). MSCs are well documented to express IL-6, which has both supportive, anti-inflammatory (Haynesworth *et al.*, 1996; Majumdar *et al.*, 1998; Tilg *et al.*, 1994; Xing *et al.*, 1998) and angiogenic properties (Hung *et al.*, 2007). Pro-inflammatory cytokine expression traditionally induced with Dectin receptor activation on myeloid cells has been shown to be suppressed by MSCs (Beyth *et al.*, 2005, Duffy *et al.*, 2011, Meirelles Lda *et al.*, 2009). However, IL-6 can be pro-inflammatory depending on environmental context and is documented to be increased in OA synovial fluid (Pelletier *et al.*, 1995, Venn *et al.*, 1993).

The immunomodulatory properties of various polysaccharides have been studied for therapeutic function (Tzianabos, 2000). Pullulan and other dietary fibres have been shown to upregulate colonic peroxisome proliferator activated receptor- γ (PPAR γ) expression and consequently suppress inflammation (Bassaganya-Riera *et al.*, 2011, Ricote *et al.*, 1998). Interestingly, Wong *et al.* developed a pullulan hydrogel for delivery in a mouse ischemic wound model and reported pullulan maintenance of

cell viability and antioxidant properties, protecting cells from toxic levels of hydrogen peroxide (Wong *et al.*, 2011). Therefore, pullulan acting through a possible Dectin-2 receptor mechanism on the MSC surface has the potential to modulate the existing inflammatory environment, resulting in the creation of a cell protective milieu at the tissue surface. Further elucidation of pullulan conditioning within the synovial joint and its effects on MSCs will remain for future analysis.

2.5 Conclusion

Pullulan has demonstrated flexibility and compatibility that can be tailored to a specific therapeutic application. It possesses unique properties such as regular (1→6) linkages that impart structural flexibility and high solubility, allowing pullulan to mimic synthetic polymers, but in a stable, non-harmful composition (Singh and Ganganpreet, 2008). In this study the adhesive application of pullulan was considered and demonstrated its use for enhancing MSC retention at the diseased cartilage surface with the intention of increasing MSC therapeutic efficacy. Pullulan demonstrated biocompatibility with MSCs including enhanced proliferation that may translate to increasing cell numbers *in loco*. Pullulan positively affected MSC osteogenic differentiation while maintaining adipogenesis and chondrogenesis. Furthermore, Dectin-2 receptor surface expression was identified on MSCs and upregulated in response to exposure of pullulan, suggesting a potential mechanism of action by which the MSC binds pullulan and responds with environmental conditioning in support of local cartilage repair. Therefore, pullulan is a versatile bioadhesive, able to secure MSCs at the articular cartilage surface in support of creating a local reparative environment.

Chapter 3

Design of an Antibody-Peptide Construct for MSC Localisation to Degraded Cartilage

3.1 Introduction

Clinical therapies for cartilage repair such as ACI or microfracture show poor fibrous cartilage repair and only initial/temporary healing, with patient age affecting the outcome. MSC therapy is therefore an attractive choice, with the cells possessing multilineage potential with easy harvest and expansion. Still, although MSC implantation has shown to slow the progression of OA, few injected therapeutic cells are retained at the site of cartilage damage for sufficient repair (Coleman *et al.*, 2010; Murphy *et al.*, 2003). Consequently, there is a practical need to enhance cellular retention within the dynamic conditions of an articular joint, where cells alone are likely retained for insufficient lengths of time to have any effect on local repair.

Most attempts to enhance MSC retention and delivery in the cartilage field have been explored using biomaterial scaffolds, statically placing cells and retaining them within a structure at the site of cartilage damage (Amini and Nair, 2012; Bulman *et al.*, 2012; Chiang and Jiang, 2009; Frenkel and Di Cesare, 2004; Nguyen *et al.*, 2011). Scaffold biocompatibility, strength and degradation rate can limit the outcome of these approaches making some researchers focus on more controlled and specific cell localisation methods, including that of antibodies and peptides to enhance cell adhesiveness and/or response (Bulman *et al.*, 2012; Dennis *et al.*, 2004; Grzesiak *et al.*, 1997; Jeschke *et al.*, 2002; Khatayevich *et al.*, 2010; Salinas *et al.*, 2007; Stoop, 2008).

As previously discussed (chapter 1) there are examples of ‘cell painting’ with antibodies for various tissue engineering applications, such as bispecific antibodies for ischemia tissue damage and biotinylation of MSC surfaces to induce MSC homing to sites of inflammation (Dennis *et al.*, 2004; Lee *et al.*, 2007; Sarkar *et al.*, 2008). Adhesion molecules such as RGD peptides have also demonstrated functional roles for enhancing cell adherence, proliferation and differentiation (Jeschke *et al.*, 2002; Ruoslahti, 1996; Salinas and Anseth, 2008; You *et al.*, 2011). Based upon this collection of cell localisation studies, a construct for retaining MSCs to the degraded cartilage surface was developed.

3.1.1 Design Specifications

Figure 3.1 depicts the set of specifications used in the design of the MSC localisation construct. Each box describes the design rationale for the two component targets of the construct, the MSC and the degraded cartilage. An initial step in the design is the analysis of surface markers (1) of both MSC and degraded cartilage. A requirement for both cartilage and MSC markers are targets that are found superficially and external. For MSC, a surface marker that is not lost in culture is ideal, since culture expansion is generally a requirement for sufficient cell numbers. It is envisaged that through specific targeting of cells the numbers required for efficacy will also be minimized and a specific MSC marker will allow the use of MSCs isolated directly from tissue without expansion (Mason, 2005, 2007; Mason and Manzotti, 2010; Medcalf, 2011). Degenerated cartilage requires a target epitope found in the superficial or upper remaining surface zone of the cartilage, ensuring access, and an epitope that is retained in the tissue after subsequent degradation.

The second point for consideration of the markers is specificity (2). For the degraded cartilage this is a requirement for ensuring localisation of the cells to the target tissue and avoiding unwanted localisation in other tissues. For the MSC, specificity as a requirement depends on the application of the construct. If intended for isolating native MSCs from marrow aspirates or for endogenous recruitment of cells from synovium or marrow *in vivo*, then specificity of the marker to an MSC will be required, eliminating the targeting of unwanted cell types (Wagers and Weissman, 2004). However, if MSCs are to be culture expanded first and pre-incubated prior to delivery, then specificity may not be a requirement. Ideally, a specific MSC marker will provide a construct with a wider application for both *in vivo* recruitment and pre-incubation *ex vivo*.

A third specification is that an antibody or other targeting molecule should be commercially available (3). This will ensure a readily available molecule, eliminating the need and cost of producing a molecular target by methods such as phage display technology (Kriangkum *et al.*, 2001). In addition, a commercially

available source also opens an area of patentability, if the use is a novel application (4), thus providing commercial value to the construct (Mason, 2005; Medcalf, 2011). A further practical specification is the use of components that are easy to modify and can be linked to another molecule without compromising functionality of the construct (5). The intent of the construct design was for a proof of principle of MSC localisation to degraded cartilage. However, considering a design with fewer regulatory hurdles for future commercial application was also preferable where possible in the design (6).

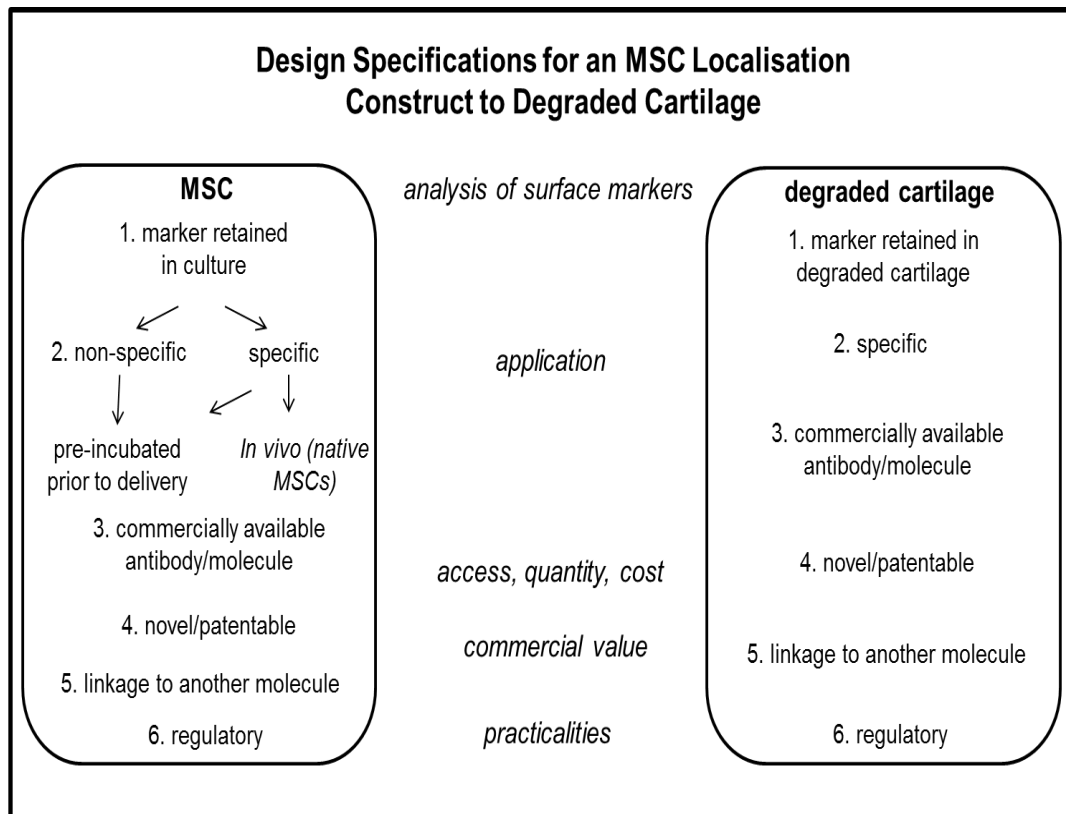


Figure 3.1: Design Specifications of a Construct for MSC Localisation to OA Degraded Cartilage

Diagram depicts the set of specifications used in the design of the MSC localisation construct. Each box describes numerically the design rationale for the two component targets of the construct, the MSC and the degraded cartilage. The first step is the analysis of surface markers (1) of both MSC and degraded cartilage, with a requirement of a retained marker in the cartilage and MSC surface after culture expansion. The cartilage marker requires specificity to degraded cartilage and MSC marker specificity is dependent on application (2). A third design requirement is for a marker that has an antibody or other target molecule that is commercially available (3), additionally allowing patentability of a novel application (4). Both components also require the ability to link to another molecule (5) and ideally a feasible regulatory route (6).

3.1.2 Degraded Cartilage Markers as Tissue Targets

Biomarkers reflect the degradative state of cartilage and are considered a useful way for monitoring tissue health and OA disease progression (Fosang *et al.*, 2003). The appearance of denaturation epitopes or ‘neoepitopes’ as a result of matrix breakdown by proteases is a prominent feature in OA. These neoepitopes can be detected in immunological assays with antibodies recognising terminal amino acid sequences at specific sites in core proteins such as aggrecan and collagen type II (Fosang *et al.*, 2003; Hunter *et al.*, 2007). The imbalance of cartilage homeostasis in OA not only increases cleavage of matrix components but also increases matrix synthesis, presenting potential molecular candidates as targets for MSC localisation (Aigner and McKenna, 2002; Lorenzo *et al.*, 2004).

Selection of appropriate molecular targets depends on zonal location and retention of the molecules in the cartilage. Ideally, selection of a marker representing early OA would be most useful clinically, since it is suggested that targeting an early lesion will give a better therapeutic outcome, preventing further irreversible destruction (Curtin, 2009; Hunziker, 2009). However, there are limitations to obtaining early stage OA cartilage for analysis and a marker present in early and late stages of OA would provide a wider therapeutic application.

3.1.2.1 Neoepitopes

Two families of proteinases are known to be involved in cartilage degradation and the generation of neoepitopes. Matrix metalloproteinases degrade both collagen and aggrecan and aggrecanases or members of the ADAMTS (A Disintegrin And Metalloproteinase with Thrombospondin Motifs) family degrade aggrecan (Baragi *et al.*, 2009; Chubinskaya *et al.*, 1996; Chubinskaya *et al.*, 2001; Dahlberg *et al.*, 2000; Dejica *et al.*, 2008; Fernandes *et al.*, 1997; Fosang *et al.*, 2000; Kafienah *et al.*, 1998; Neuhold *et al.*, 2001; Tetlow *et al.*, 2001; Young *et al.*, 2005). These enzymes are increased during OA and have become targets of inhibition in studies aiming to perturb cartilage degradation (Billinghurst *et al.*, 1997; Conway *et al.*, 1995; Dahlberg *et al.*, 2000; Pelletier *et al.*, 1997; Poole *et al.*, 2003).

Collagenases, MMP1, MMP8 and MMP13 cleave collagen fibrils at G₇₇₅↓L₇₇₆, a conserved site in triple-helical domains yielding α -chain fragments of $\frac{3}{4}$ and $\frac{1}{4}$ length (Fosang *et al.*, 2003), after which fragments are further degraded by gelatinases, collagenases and cathepsins (Fosang *et al.*, 2003). The $\frac{1}{4}$ fragment is particularly unstable and subject to further cleavage (Billinghurst *et al.*, 1997; Vankemmelbeke *et al.*, 1998). However, the $\frac{3}{4}$ fragment is stable and retained in the cartilage matrix. Antibodies have been raised against neoepitope sequences at the C and N terminus of the collagen type II fragments (Billinghurst *et al.*, 1997; Stoop *et al.*, 1999; Vankemmelbeke *et al.*, 1998) and provide a source of potential existing commercial antibodies for developing a cell localisation construct (Hollander *et al.*, 1994; Hunter *et al.*, 2007; Otterness *et al.*, 1999).

Aggrecan, like collagen type II also undergoes several molecular changes in OA making this matrix molecule a potential candidate as a marker within degraded cartilage. As OA progresses there is a loss of aggrecan and break down of the aggrecan complex (Lorenzo *et al.*, 2004). The main site of proteolytic aggrecan cleavage is within the interglobular domain (IGD), found between domains G1 and G2, and peptidase activity releases the glycosaminoglycan-rich C terminus (Little *et al.*, 2002). The site of cleavage by MMPs was shown *in vitro* to be at N₃₄₁ ↓ F₃₄₂, generating C-terminal DIPEN₃₄₁ and N-terminal F₃₄₂FGVG fragments (Buttner *et al.*, 1998; Fosang *et al.*, 1998). The site of cleavage by ADAMTS is the E₃₇₃ ↓ A₃₇₄ bond within the IGD, generating neoepitopes C-terminal NITEGE₃₇₃ and N-terminal A₃₇₄RGSV (Arner, 2002; Fosang *et al.*, 2010) aggrecan fragments. The C-terminal fragments generated from this cleavage have been observed in the synovial fluid of OA patients and are also increased in medium from cartilage explants (Arner, 2002; Fosang *et al.*, 2010; Fosang *et al.*, 2000; Sandy and Verscharen, 2001). Fosang *et al.* reported that cleavage by MMP activity resulted in the retention of DIPEN and the N-terminal FGVG fragments within porcine explant cartilage. These neoepitopes, detected by immunolocalisation, therefore represent suitable targets for cell localisation (Fosang *et al.*, 2000).

Fibronectin is a small component of the cartilage ECM in healthy cartilage; however, OA cartilage can contain 10-fold more fibronectin (Brown and Jones, 1990; Zack *et al.*, 2006). Increases in fibronectin content in cartilage are also

associated with accumulation of fibronectin fragments in synovial fluid (Peters *et al.*, 2003; Zack *et al.*, 2006). The degeneration process is amplified by matrix degradation products such as that of collagen type II and fibronectin, inducing MMPs and subsequently further matrix degradation in a positive feedback loop (Homandberg, 1999; Homandberg *et al.*, 1997; Homandberg and Wen, 1998; Poole *et al.*, 2002; Poole *et al.*, 2003; Yasuda, 2006). Zack *et al.* identified fibronectin neoepitopes retained within cartilage generated by cleavage at A₂₇₁↓V₂₇₂ and developed monoclonal antibodies detecting the C-terminus VRAA₂₇₁ and N-terminus ₂₇₂VYQP (Zack *et al.*, 2006).

3.1.2.2 Synthesised Markers of Degraded Cartilage

Collagen type II, which normally has a slow turnover in healthy cartilage is newly synthesised in OA cartilage, however, these synthesised molecules are eventually damaged (Dahlberg *et al.*, 2000; Rizkalla *et al.*, 1992) and proliferative attempts by chondrocytes are likely curbed by this extensive collagen fibril damage (Horton *et al.*, 2005; Poole *et al.*, 2002). A splice variant of the type II collagen molecule, type IIA procollagen (COL2A), not found in healthy cartilage is also produced in diseased cartilage (Aigner *et al.*, 2006; Aigner *et al.*, 1999; Hermansson *et al.*, 2004; Sandell and Aigner, 2001). Expression of COL2A is increased in early OA cartilage, suppressed in upper zones with progressive matrix degradation and increased all over in late-stage OA cartilage (Aigner *et al.*, 2006). This molecule would be suitable for cell localisation to late stage OA cartilage where expression is not suppressed superficially.

Lorenzo *et al.* observed an increase in synthesis of other cartilage matrix proteins such as fibronectin, cartilage oligomeric matrix protein (COMP) in early and late OA samples and cartilage intermediate layer protein (CILP) and procollagen increased in late stage OA (Lorenzo *et al.*, 2004). Variations in expression of these proteins in zonal regions and stages of OA of the articular cartilage have been observed. COMP binds collagens I/II and IX and was located in the superficial layers while CILP was found mainly located in the middle/deeper layer of articular cartilage (Lorenzo *et al.*, 2004; Yao *et al.*, 2004). Superficial COMP and fibronectin

throughout the matrix in OA could be potential matrix targets. A limitation with fibronectin, found within many other tissues, would be its non-specificity to OA cartilage, (Pankov and Yamada, 2002).

During the OA disease process other molecules barely present in normal articular cartilage such as tenascin (Salter, 1993) and procollagen type III (Aigner *et al.*, 1993) also start to appear, suggesting that chondrocytes start to re-express a chondroprogenitor phenotype at a molecular level (Sandell and Aigner, 2001). Chondrocyte hypertrophy, characterised by the expression of collagen type X and upregulation of runt-related transcription factor 2 (RUNX2) or core-binding factor subunit alpha-1 (CBFa1), binding uniquely to the MMP-13 promoter amongst the MMPs, become prominent within the deeper, calcified zones (Aigner and Stove, 2003). Expression is observed at and close to the remaining articular surface and associated with sites of severe collagen II degradation (Poole *et al.*, 2003). Surface collagen X expression has been suggested the result of degradation and exposure of the deeper calcified layers of cartilage, (Walker *et al.*, 1995).

Collagen type VI, concentrated pericellularly in normal and diseased cartilage, also increases in the interterritorial matrix of OA cartilage following a similar expression pattern to collagen type II (Aigner and McKenna, 2002; Hambach *et al.*, 1998; Poole *et al.*, 1992). Enhanced degradation of this molecule has also been observed, as shown by an abundance of collagen VI aggregates around OA chondrocytes (Aigner and Stove, 2003). Molecules with increased levels in OA cartilage could be useful targets if located in the desired superficial and remaining surface zone and providing they are not expressed in other tissues.

Neoepitopes generated by cartilage matrix degradation, such as coll 2 3/4m, fibronectin and epitopes VRAA, VRQP and aggrecan epitopes DIPEN and NITEGE provide potential targets within cartilage for antibodies to localise and position reparative cells. Cartilage components that are increased in degraded cartilage such as fibronectin, procollagen, COMP and collagen type X may also be targets for cellular adhesion, requiring suitable location within the cartilage and specificity to cartilage for precise localisation.

3.1.3 MSC Surface Markers

MSCs have been shown to constitute a heterogeneous population when considering morphology, physiology and surface marker expression. Adhesion molecules, extracellular matrix molecules, cytokines, growth factor receptors and antigens associated with numerous cell types are all associated with MSC cell interactions and functions (Bobis *et al.*, 2006). Due to this heterogeneous nature of MSCs, to date, there is not a single marker that reliably identifies MSCs *in vitro* within the bone marrow and other tissue sources (Bobis *et al.*, 2006; Dominici, 2006). Guidelines from the International Society for Cell Therapy (ISCT), suggested using a selection of several markers for FACs; $\geq 95\%$ of the cell population must express the markers CD105, CD73 and CD90 and in addition ($\leq 2\%$) the cells must lack the expression of haematopoietic antigen expression CD45, CD34, CD14 or CD11b, CD79 α or CD19 and HLA class II (Dominici, 2006). These common markers used for identifying MSCs *in vitro* have broad cell reactivity and are therefore not suitable alone for the detection of MSCs *in vivo* (Barry *et al.*, 2001a; Barry *et al.*, 1999; Cho *et al.*, 2001; Jones *et al.*, 2002). For an MSC localisation strategy, the use of several markers would be too complex and a single marker is therefore sought.

3.1.3.1 MSC specific markers

Gronthos *et al.* showed that nerve growth factor receptor (NGFR) antibodies could be used to purify the colony-forming units-fibroblast from the STRO-1+ fraction of human bone marrow cells (Gronthos and Simmons, 1995). More recently known as the anti-low affinity nerve growth factor receptor (LNGFR, p75 or CD271), this receptor isolates primitive MSCs directly from the bone marrow (Quirici *et al.*, 2002). Antibodies for LNGFR previously showed specific selection of bone marrow stromal cells, excluding hematopoietic and endothelial cells (Gronthos and Simmons, 1995; Quirici *et al.*, 2002). Quirici *et al.* enriched for MSCs using immunomagnetic selection for LNGFR, selecting a small homogeneous subpopulation comprising approximately 10% of the whole bone marrow. Colony-forming unit-fibroblast (CFU-F) assays showed LNGFR positive enriched fractions were higher in clonogenic precursors and maintained for 2 months, without addition

of bFGF. LNGFR expression was down-regulated after growth factor addition (Colter *et al.*, 2001; Quirici *et al.*, 2002).

Jones *et al.*, using D7-FIB, a marker for human epithelial fibroblasts, purified freshly isolated bone marrow progenitor cells positive for markers CD105, LNGFR, HLA-DR, CD10, CD13, CD90, STRO-1 and BMPRIA and negative for CD14, CD34, CD117 and CD133. The cell fraction was shown to be capable of proliferating and undergoing multilineage differentiation, however at passage 4 (P4) the LNGFR marker disappeared with STRO-1 (Jones *et al.*, 2002). The loss of this marker upon culture adherence and in the presence of bFGF would represent a limitation if it was to be used as a cell marker for localisation of cultured MSCs that are likely to undergo several passages.

The neural ganglioside GD2, found expressed on cells of the nervous system and on tumours of neuroectodermal origin, was investigated as a novel surface receptor marker for bone marrow MSCs, (Martinez *et al.*, 2007). MSCs freshly isolated from bone marrow using GD2 were also shown positive for CD271 and D7-FIB, and expansion over 8 passages showed continuation of high levels of GD2 expression (Martinez *et al.*, 2007). Lack of GD2 expression was observed in the marrow hematopoietic cell fraction and RNA analysis revealed lack of expression of GD2 synthase in peripheral blood cells. GD2-expanded MSCs showed multilineage potential and typical MSC morphology and plastic adherence (Martinez *et al.*, 2007). Neural markers such as GD2 and LNGFR that have further distance in terms of lineage compared to common MSC markers such as CD105, CD73 and CD90 may be preferable for direct MSC isolation, thus avoiding a hematopoietic cell lineage fate (Dominici, 2008; Jones *et al.*, 2002; Martinez *et al.*, 2007). Conversely, consistent expression of a neural marker at late passage, might also suggest over the long term an undesirable fate of cells isolated with this marker.

In search of additional markers, Buhning *et al.* screened monoclonal antibodies (mAbs) by flow cytometry for their specific reactivity with the CD271+ population. The new MSC-specific molecules identified included the platelet-derived growth factor receptor (CD140b), HER-2/erbB2 (CD340), frizzled-9 (CD349) and the W8B2 antigen. Other cell surface antigens were identified by the antibodies W1C3,

W3D5, W4A5, W5C4, W5C5, W7C6, 9A3, 58B1, F9-3C2F1 and HEK-3D6 (Buhring *et al.*, 2007), highlighting a panel of antibodies that might be suitable components of an MSC localisation technology.

Many research groups have looked into potential novel MSC markers but often disparities between methods of isolation and culture can make the use of markers less comprehensive (Docheva *et al.*, 2008; Dominici, 2006). There are also limitations to using freshly isolated MSCs from marrow (autologous MSCs), such as limits on the amount of MSCs isolated and donor variations that exist in potential and possible impairments with disease (Caplan, 2009a; Meirelles Lda *et al.*, 2009). Allogeneic MSCs have the advantage of providing a possible ‘off-the-shelf’ therapeutic, ensuring sufficient numbers and efficacious cells (Caplan, 2009b; Hunziker, 2009; Zhou *et al.*, 2010). For these reasons, the MSC localisation construct for this project was designed with intent for pre-incubation with cultured MSCs. However, a marker tailored for both applications would have been advantageous.

3.1.3.2 The RGD Peptide and Integrin Receptor

The cell adhesion sequence, RGD was originally found as a sequence of the protein fibronectin by Pierschbacher and Ruoslahti (1984) and soon confirmed to be the cell attachment site for many other adhesive proteins (Ruoslahti, 1996). Integrins are a large family of cell adhesion receptors that bind RGD, consisting of non-covalently linked, heterodimeric molecules that contain an α and β subunit, the most common being β 1 and α V (Ruoslahti, 1996). Integrins display a range of functions, including coordination of cytoskeletal polymers and signalling complexes in the cytoplasm. Extracellularly, integrins interact with matrix macromolecules or receptors on opposing cell surfaces imposing spatial restrictions and matrix assembly, thereby controlling and integrating cells within their microenvironment (Brooks *et al.*, 1996; Fisher *et al.*, 1993; Grzesiak *et al.*, 1997; Ruoslahti, 1996). Studies of both natural and engineered genetic mutations in these receptors has confirmed important roles for integrins in tissue patterning, differentiation and cell trafficking (Humphries *et al.*, 2006). Some of the proteins that contain the RGD sequence include adhesion

proteins such as vitronectin, fibrinogen, von Willebrand factor, laminin, tenascin and collagen. It was suggested that these proteins are active *in vitro* because the RGD sequence is presented in the right contextual environment, but are not necessarily likely to serve an *in vivo* integrin binding role (Ruoslahti, 1996).

Cell adhesion is an important biological process involved in guiding cells to appropriate locations within the body, anchoring cells to a specific site and controlling various functions such as proliferation, apoptosis and differentiation (Gumbiner, 1996; Hynes, 1999; Maheshwari *et al.*, 2000; Maheshwari *et al.*, 1999). Peptides and proteins that can be used to improve cell adhesion therapeutically are a current area of research. Adhesive peptides may be used to promote cell attachment and tissue integration when applied to a surface (Grzesiak *et al.*, 1997; Hwang *et al.*, 2007; Re'em *et al.*, 2010; Vonwil *et al.*, 2010), or used to promote cell attachment *in vivo* through an application of therapeutic cell delivery (Janssen *et al.*, 2002; Kibria *et al.*, 2011; Smolarczyk *et al.*, 2006; Tagalakis *et al.*, 2010; Zitzmann *et al.*, 2002). In tissue engineering, hydrogels modified with RGD peptides have demonstrated high efficiency in cell adherence (Genes *et al.*, 2004; Jeschke *et al.*, 2002; Nuttelman *et al.*, 2001) and have shown functional roles with MSCs, influencing differentiation with a dependence on timing, concentration and length of exposure (Connelly *et al.*, 2007; Mann and West, 2002; Salinas and Anseth, 2008; Salinas *et al.*, 2007). MSCs have been shown to express various integrin receptor subunits including the alpha subunits $\alpha 1$, $\alpha 2$, $\alpha 3$, $\alpha 5$, $\alpha 6$ and αV , and $\beta 1$, $\beta 3$ and $\beta 5$ (Docheva *et al.*, 2008; Docheva *et al.*, 2007); through these it is possible to influence cellular attachment and function via RGD peptides.

In the field of cancer research, previous vehicles for tumour targeting have been engineered antibodies, such as bispecific antibodies (Kriangkum *et al.*, 2001). However, more recently targeting peptides offer smaller and less complex alternatives. Developments in this field have been based on the finding that $\alpha V\beta 3$ has been shown to be selectively expressed on endothelial cells involved in the process of angiogenesis (Dubey *et al.*, 2004; Kok *et al.*, 2002; Ruegg *et al.*, 1998; Serini *et al.*, 2006). RGD peptides and anti-integrin antibodies have been demonstrated *in vivo* to inhibit tumour growth through the interference of the angiogenic process (Brooks *et al.*, 1994; Kok *et al.*, 2002; Schraa *et al.*, 2002). RGD

peptides have also been shown to prevent and delay tumour growth when injected directly into *in vivo* models (Humphries *et al.*, 2006; Janssen *et al.*, 2002; Ruoslahti, 1996; Schraa *et al.*, 2002; Smolarczyk *et al.*, 2006; Zitzmann *et al.*, 2002). Additionally, RGD peptides can be used for gene therapy and to selectively deliver therapeutic drugs via carriers to a tumour site (Dubey *et al.*, 2004; Kibria *et al.*, 2011; Nallamothe *et al.*, 2006; Tagalakakis *et al.*, 2010). The field of cancer and immunotherapy is therefore full of potential cell localisation and versatile targeting strategies that can be applied to the field of cartilage repair and applicable in all fields of medicine (Huang *et al.*, 2008). Due to the flexibility and functionality of the RGD peptide, the molecule was chosen as an alternative to a specific MSC receptor.

Using the construct design of a bispecific antibody (Kriangkum *et al.*, 2001; Lum *et al.*, 2004), employing a biotin-streptavidin linkage system (Diamandis and Christopoulos, 1991; Sarkar *et al.*, 2008; Tsai and Wang, 2005) and a functional RGD peptide (Khatayevich *et al.*, 2010) a bispecific antibody-peptide construct was developed. This chapter will focus on the design approach and validation of the antibody-peptide construct that will bind according to two separate entities, both an MSC and the degraded cartilage surface (Figure 3.2).

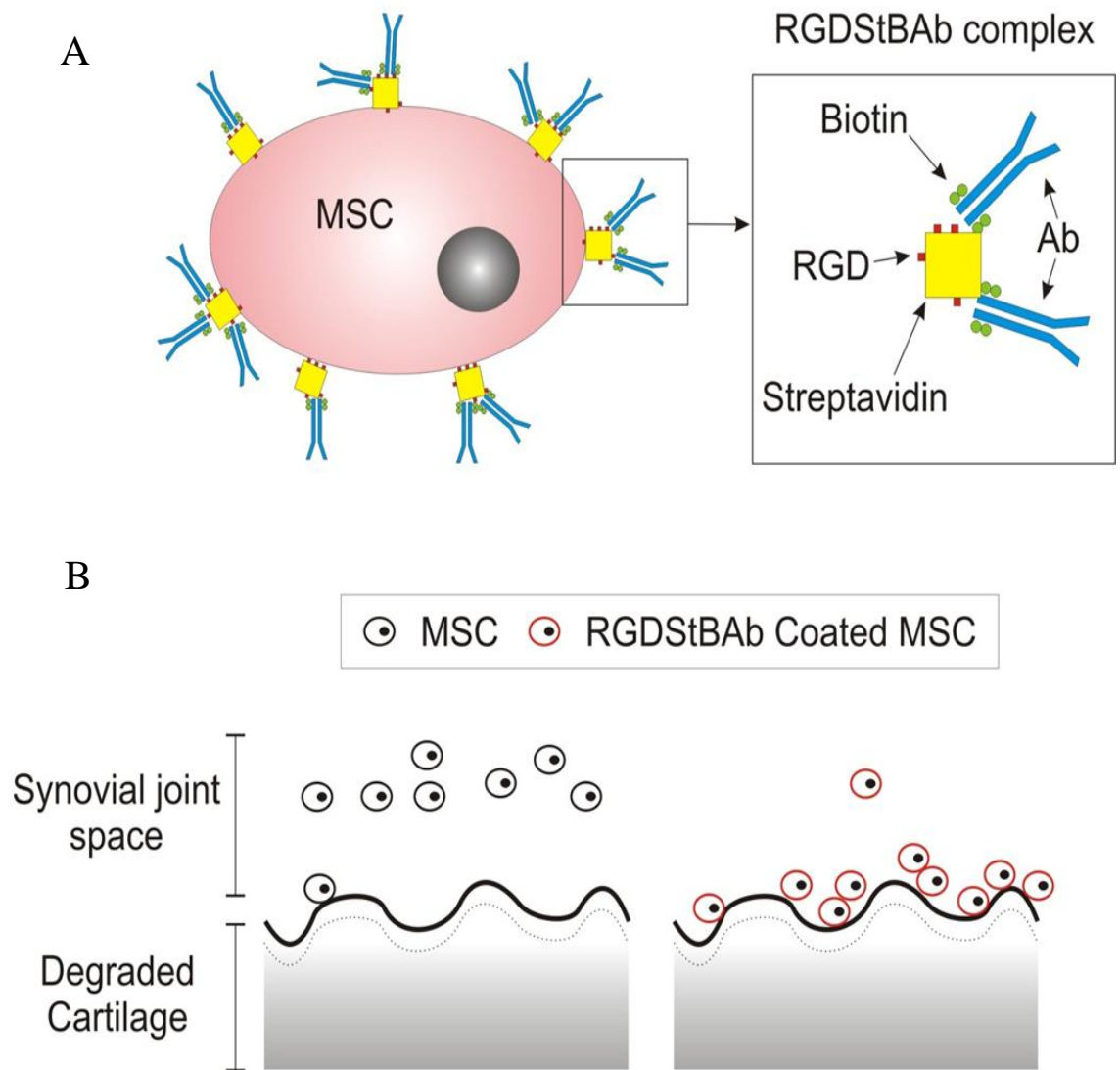


Figure 3.2: Schematic of Antibody-Peptide Construct Design for MSC Localisation

MSC binding to the construct is facilitated through surface integrins. Cyclic RGD peptides (■) are chemically conjugated to the streptavidin surface (■) (RGDSSt). Biotinylated (●) degraded cartilage antibody (—) (BAb) conjugates to RGD peptides via non-covalent biotin-streptavidin linkages (RGDSStBAb) (A). MSCs coated with the RGDSStBAb construct (red) are retained at the degraded cartilage surface in higher numbers compared to uncoated MSCs (B).

3.2 Materials & Methods

Note: All materials were supplied by Sigma-Aldrich unless otherwise stated.

All experiments were performed in triplicate with 3 biological replicates, unless otherwise stated.

3.2.1 MSC Cytometry

Culture expanded MSCs were trypsinised (P6), resuspended in PBS at 5×10^5 cells/ml in a 96-well plate and incubated with PE-conjugated antibodies CD105 (Milteny biotech), CD44 (Milteny biotech), CD271 (Milteny biotech), W3D5 (Biolegend) and W5C5 (Biolegend) primary and an IgG-PE isotype control (Milteny biotech) at a 1:10 dilution for 20 minutes at 4°C, protected from light. Cells were washed twice in PBS to remove unbound antibody and resuspended in 200µl DMEM for analysis using the ExpressPlus program software on the Guava Cytosoft system (Millipore).

3.2.2 Preparation of Human OA Cartilage for Histology

Human OA cartilage sections were prepared from cartilage biopsies taken from the articular cartilage surfaces of the hip femoral head and condyle tibial plateau of the knee of consenting patients with end-stage OA undergoing total hip and knee arthroplasty. The procedure was approved by the Clinical Research Ethical Committee at Merlin Park Hospital, Galway. Full thickness cartilage explants were created by biopsy punch (1-2mm thick and 2 mm diameter), washed in PBS and fixed in 10% formalin for 20 minutes. Explants were histologically prepared in an automated tissue processor (Leica ASP300S) and embedded in paraffin wax prior to sectioning at a thickness of 5µm using the Leica RM2235 microtome.

3.2.3 Immunohistochemistry of Degraded Cartilage Matrix Epitopes

The following monoclonal antibodies were tested on OA cartilage by immunohistochemistry:

Antibody	Concentration	Manufacturer	Reference
VYQP (degraded fibronectin epitope)	1µg/ml	Pfizer (non-commercial)	Zack <i>et al.</i> 2006
VRAA (degraded fibronectin epitope)	1µg/ml	Pfizer (non-commercial)	Zack <i>et al.</i> 2006
FN1 (full length matrix fibronectin)	5.6µg/ml	MYBioSource	www.mybiosource.com
DIPEN (degraded aggrecan epitope)	unspecified concentration 1:100 dilution	Abcam	
NITEGE (degraded aggrecan epitope)	1µg/ml	Abcam	
Coll 2 3/4m (degraded collagen type II epitope)	unspecified concentration. 1:200 dilution	IBEX	Hollander <i>et al.</i> 2004

Table 3.1: List of primary antibodies used for the immunohistochemical analysis of degraded human cartilage.

Immunostaining was carried out on paraffin sections using a horse radish peroxidase (HRP)-Diaminobenzodine (DAB) kit (EnVision Dako Cytomation Kit) as per the manufacturer's instructions. Briefly, sections were deparaffinised and hydrated before incubation with 40mU/ml of chondroitinase ABC in 0.1M tris/acetate pH 7.6 containing 1% BSA for 30 minutes at 37°C to attain antigen retrieval. Slides were then washed 3 times in tris buffered saline (TBS) for 3 minutes. Peroxidase block (EnVisionTM+ Kit) was added for 5 minutes, and slides were then washed in TBS and blocked with 2.5% bovine serum albumin (BSA) for 30 minutes at room temperature (RT). Sections were drained prior to the addition of primary antibody or TBS as a negative control for 30 minutes at RT (Table 3.1). Slides were washed in TBS-0.5% Tween and secondary antibody (EnVisionTM + Kit-peroxidase labelled polymer) was added for 30 minutes at RT. Substrate chromagen (EnVisionTM + Kit) was added for 6 minutes to develop colour. Slides were further washed in TBS-Tween and diH₂O, counterstained in Mayer's Haemotoxylin for 10 seconds, washed

in diH₂O and tap water, and then dehydrated and coverslipped using histomount solution (National Diagnostics). Imaging was performed using an Olympus BX51 upright brightfield microscope and QImaging (Retiga Exi) camera.

3.2.4 Production of the Polyclonal Collagen 2 3/4 m Antibody

Polyclonal collagen 2 3/4m antibody production was outsourced to Harlan Laboratories to ensure supply of sufficient antibody for preparation of the construct and future experimental analysis. The peptide sequence of the commercially available Coll 2 3/4m antibody (IBEX), a 21-amino acid sequence of the alpha chain of collagen II (-Gly-Lys-Val-Gly-Pro-Ser-Gly-Ala-Hyp-Gly-Glu-Asp-Gly-Arg-Hyp-Gly-Pro-Hyp-Gly-Pro-Gln-) (Hollander *et al.*, 1994), was used to immunize rabbits. Serum was collected, tested for antigen by enzyme-linked immuno sorbent assay (ELISA) and further processed by affinity purification at Harlan Laboratories.

3.2.5 RGD Peptide Conjugation to Streptavidin using Sulfo-SMCC chemical linker

Sulfo-SMCC (succinimidyl 4-[*N*-maleimidomethyl]cyclohexane-1-carboxylate), a water soluble analog of SMCC, is a heterobifunctional crosslinker containing *N*-hydroxysuccinimide (NHS) esters and maleimide groups for the covalent conjugation of amine and sulfhydryl containing molecules (Marko *et al.*, 2008; ThermoScientific).

1mg/ml of streptavidin (protein-NH₂) prepared in PBS (pH 7.2) was incubated with 4.8mg/ml of cross-linker sulfo-SMCC (Thermo Scientific) in PBS at 4°C for 2 hours (following manufacturer's instructions). Excess crosslinker was removed by desalting on 5ml Zeba™ Desalt spin columns (Thermo Scientific), previously equilibrated with PBS. Briefly, sample was loaded into the column and a stacker of 100µl PBS added after the sample was absorbed in the resin bed. The column was then centrifuged at 1000 x g for 2 minutes to collect the sample. Cyclic RGD [cyclo (Arg-Gly-Asp-D-Phe-Cys), *c*(RGDfC)] (Peptides International; M.W. 578.65) or control cyclic RAD peptide [cyclo (Arg-Ala-Asp-D-Phe-Cys) or *c*(RADfC)]

(Peptides International; M.W. 592.68) both containing sulfhydryl groups were incubated with streptavidin (protein NH₂) in an equal ratio. The reaction mix was incubated for 2 hours at 4°C and then passed through a desalting column as before (Figure 3.3).

Conjugate concentration was measured using the nanodrop 2000 spectrophotometer (Thermo Scientific), measuring 1µl of protein solution at 280nm absorbance and repeated three times. Conjugates, both consisting of a heterogenous mix of streptavidin bound with varying densities of either RGD or RAD peptides gave average readings of ~0.5mg/ml.

3.2.6 Non-reduced SDS Page Gel for Protein Analysis

NuPAGE® (Novex®) Bis-Tris pre-cast gradient (4-12%) mini-gels (Invitrogen) were placed in an XCell SureLock Mini-Cell and the upper (inner) buffer chamber was filled with 200ml of 1X NuPAGE® sodium dodecyl sulphate (SDS) running buffer (Invitrogen). The lower (outer) buffer chamber was then filled with 600ml of 1X NuPAGE® SDS running buffer. Samples; RGD-streptavidin, streptavidin, biotinylated polyclonal collagen 2 3/4m antibody and the combined construct RGD-streptavidin-biotinylated antibody were prepared at a concentration of 0.5µg/ml. The samples were prepared in a total volume of 10µl; 1µl of sample, 2.5µl of NuPAGE (Invitrogen) and 7.5µl of diH₂O. Magic mark protein ladder (Invitrogen) was used to provide a measurement of size. Non-reduced samples and the ladder were then heated at 70°C for 10 minutes. After heating, samples and ladder were loaded onto the gel and run at 200V for 45-60 minutes, allowing more time for larger protein complexes to run further down the gel. Once the gel had run, gels were then removed and stained following the silverstain protocol.

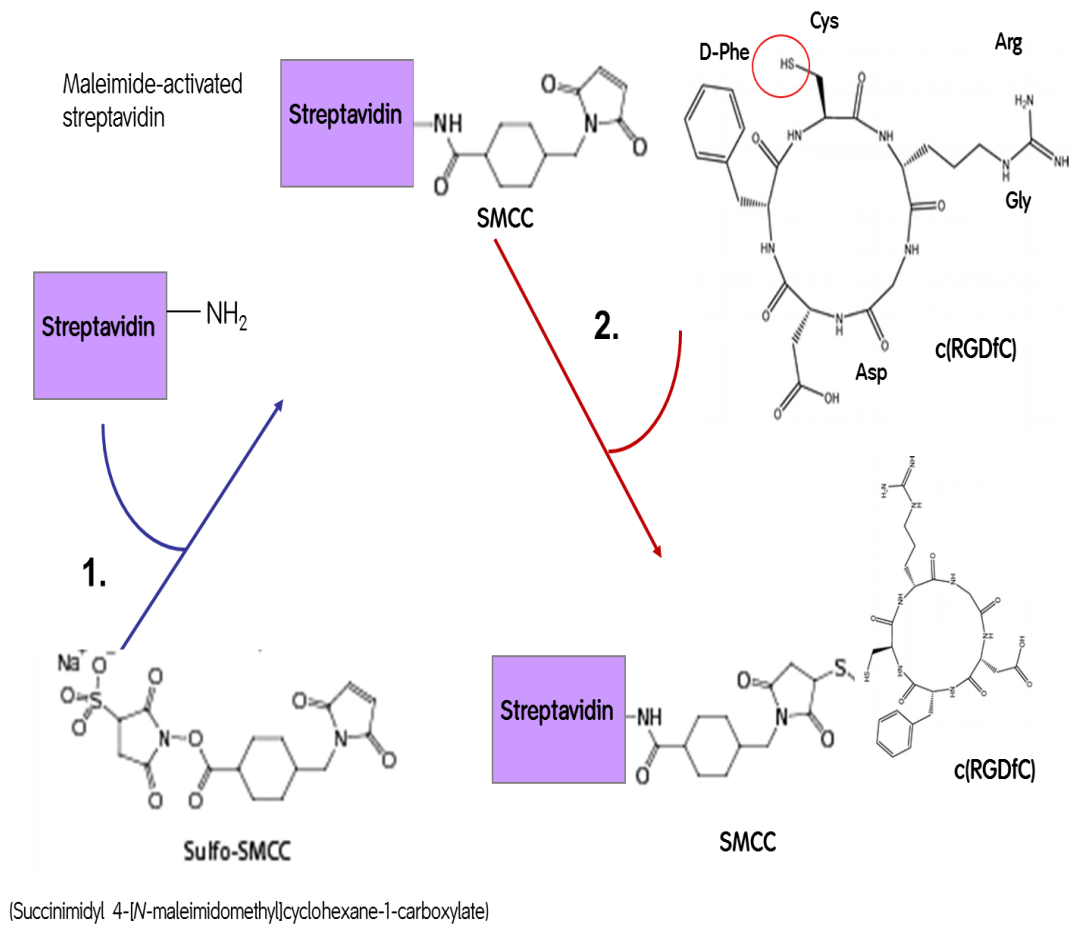


Figure 3.3: Schematic of the Conjugation Reaction of Sulfo-SMCC with *c*(RGDfC) and Streptavidin

A two-step reaction scheme for conjugating *c*(RGDfC) and streptavidin with Sulfo-SMCC was required. The crosslinker was first reacted with streptavidin available amine groups to produce a maleimide-activated protein (Reaction 1, blue arrow). Excess non-reacted crosslinker and by-products were removed and the maleimide-activated streptavidin reacted with an appropriate molar ratio of *c*(RGDfC) containing a cysteine sulfhydryl group (Reaction 2, red arrow) (Marko *et al.*, 2008) (<http://www.piercenet.com>, Thermo Scientific).

3.2.7 Silverstaining

The silverstain protocol was as described by Invitrogen. Briefly, gels were fixed in a solution of 90ml ultra-pure water (18 megaohm/cm resistance), 100ml methanol and 20ml glacial acetic acid for 10 minutes. The fixing solution was then removed and the gels incubated in two changes of sensitising solution for 30 minutes (SilverXpress® Silver Staining Kit). The solutions were then removed and gels rinsed with ultra-pure water twice for 10 minutes. The gels were next incubated in staining solution (SilverXpress® Silver Staining Kit) for 15 minutes and then removed and washed twice in ultra-pure water for 5 minutes. Developing solution (SilverXpress® Silver Staining Kit) was added for a period of 3-15 minutes. As soon as the desired staining intensity was attained, the stopping solution (SilverXpress® Silver Staining Kit) was added for 10 minutes and then removed and washed 3 times in ultra-pure water prior to photography and analysis using a Syngene GeneGenius system.

3.2.8 Immunohistochemistry of Cells in Monolayer

MSCs were seeded in a 48-well plate at a density of 1.33×10^4 cells/cm² until confluent. At confluency, medium was removed and cells washed with PBS. MSCs were then fixed in methanol (-20°C) for 10 minutes and washed in PBS. MSCs were incubated for 20 minutes with RGD (1mg/ml), streptavidin (1mg/ml), RGD-streptavidin (0.5mg/ml) and PBS alone control and then washed for 5 minutes with PBS twice. Biotinylated secondary antibody (HistoMark-KPL) was incubated with MSCs for 30 minutes and then MSCs were washed in PBS for 5 minutes twice. Streptavidin peroxidase (HistoMark-KPL) was added for 30 minutes and MSCs subsequently washed in PBS for 5 minutes twice. DAB substrate chromagen (Envision-DakoCytomation) was added for 5-10 minutes to develop colour and washed in PBS for 5 minutes twice. Cells were counterstained in Mayer's Haemotoxylin for 10 seconds, washed in diH₂O and tap water and imaged using an Olympus BX51 upright brightfield microscope and QImaging (Retiga Exi) camera.

3.2.9 Immunohistochemistry of Polyclonal Coll 2 3/4 m; Biotinylated Antibody and Non-Biotinylated and Collagen Type II

The immunohistochemistry protocol (3.23) was used to test the functionality of the Harlan produced polyclonal coll 2 3/4m antibody and its biotinylated form. Polyclonal antibody was incubated with cartilage sections at a concentration of 5µg/ml. Polyclonal collagen type II antibody (Abcam) was also tested at 5µg/ml following the same procedure.

3.2.10 Safranin O staining

Sectioned samples were rehydrated by passing the slides through a series of histoclear and graded ethanols, followed by exposure to haematoxylin, 0.02% fast green, 1% acetic acid (Fischer Scientific) and 0.1% Safranin O to visualize sulfated glycosaminoglycans (GAG). Slides were hydrated, mounted and coverslipped using histomount solution and imaged using an Olympus BX51 upright brightfield microscope and QImaging (Retiga Exi) camera.

3.2.11 Gel Filtration

Separation of proteins was achieved by gel filtration with proteins eluting off a column in order of decreasing molecular size (Amersham Biosciences). A superdex 200 10/300 GL (GE Healthcare) pre-packed column was equilibrated with PBS (filtered) on the ÄKTAEplorer 100 Air (GE Amersham Pharmacia), prior to addition of the samples through the column. Next, 200µl of either RGD-streptavidin, biotinylated antibody or RGD-streptavidin mixed with biotinylated antibody was added to the column on the ÄKTAEplorer 100 Air for 45 minutes. Read-out of the chromatogram for each sample was visualised on the ÄKTExpress software at an absorbance of 280mAU (GE Amersham Pharmacia).

3.2.12 Immunofluorescence

MSCs were trypsinised and resuspended in α -MEM media and placed at 37°C for 2 hours to allow integrin re-expression. MSCs were then washed twice in serum free α -MEM medium and diluted to a cell concentration of 1×10^6 cells/ml. All antibody/peptide incubations were performed in a 96-well cell-titre plate with each well containing 200 μ l of the cell suspension. Cells were blocked with goat serum for 20 minutes at 4°C and then incubated at 4°C for 20 minutes with the RGD-streptavidin conjugate (0.1mg/ml) or appropriate controls; serum-free medium alone, RAD-streptavidin conjugate (0.1mg/ml). Cells were then spun down (500 x g) for 5 minutes and washed twice with serum-free medium. Cells were next incubated with the biotinylated antibody or control serum-free medium alone at 4°C for 20 minutes. Cells were spun down and washed as before. Next, the cells were incubated with TRITC (tetramethylrhodamine isothiocyanate) labelled streptavidin (Pierce, Thermo Scientific) for 20 minutes at 4°C and covered with tin foil to minimise exposure to light and avoid bleaching of the fluorochrome. The TRITC-streptavidin was used to label the construct bound to the surface of the cells, with the purpose of binding the biotinylated antibody already bound to the RGD-streptavidin conjugate on the MSC surface.

The MSCs were spun down and washed as before, fixed in 10% formalin for 10 minutes and excess removed by spinning down and washing twice in medium. The cells were then stained with phalloidin-FITC (fluorescein isothiocyanate) at a dilution of 1:200 (5 μ g/ml) for 10 minutes and washed as before. Cells were stained with 15 μ l of DAPI (Vectorshield) mounting solution and the cell suspension was placed on slides and coverslipped. Slides were visualised on the Andor Revolution Spinning Disc Confocal Microscope (Andor Technology).

3.3 Results

3.3.1 Flow Cytometry of MSC Surface Receptors: Selection of MSC Antibody

MSC surface receptors were analysed on late passage MSCs (P6) using flow cytometric analysis for an array of antibodies for markers CD105, CD44, GD2, W5C5, W3D5 and CD271 (Figure 3.4). Markers CD105, CD44 were used as standard controls for MSC surface expression. GD2 showed high expression on the MSC surface with approx. 70% cells positive and comparable to expression levels for the standard markers CD105 and CD44 with 80-100% cells positive. CD105 expression was lower than levels normally observed on early passage cells. W5C5, W3D5 and CD271 all showed very low levels of expression at <5%.

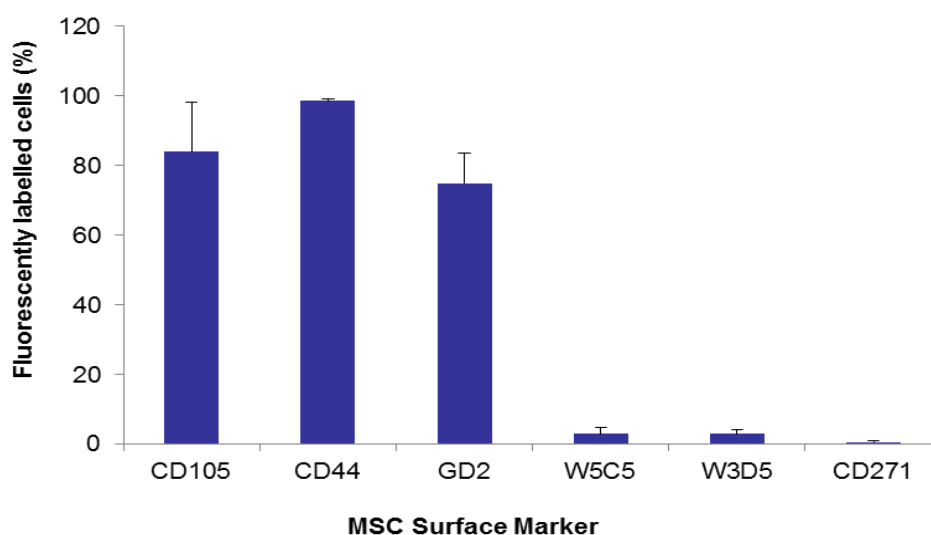


Figure 3.4: Selection of an MSC Surface Marker Antibody

MSC surface markers CD105, CD44, GD2, W5C5, W3D5 and CD271 were assessed using cytometric flow analysis on late passage MSCs (P6). CD105 and CD44 expression levels were > 80% as expected. GD2 demonstrated expression of > 70% and W5C5, W3D5 and CD271 markers were < 5%. Results represent the mean \pm SD of 2 donors with 3 technical replicates.

3.3.2 Epitope Staining of Human OA Cartilage; Selection of the Collagen 2 3/4m Antibody

Immunohistochemical staining of degraded OA cartilage sections with different antibodies specific to matrix epitopes revealed variations in the extent of staining (Figure 3.5). Full length fibronectin antibody staining revealed intense staining throughout surface and middle zones on positive sections (A-C). The fibronectin epitope VYQP antibody showed a small amount of staining at the top surface of the cartilage; this was only evident in one region and not throughout the surface region (D-F). The fibronectin epitope VRAA antibody stained positive throughout the surface zone of the cartilage (G-I). The aggrecan epitope DIPEN antibody demonstrated pericellular staining in the upper zone of the degraded cartilage (J-L). A second aggrecan antibody, specific to the epitope NITEGE, showed very weak staining at the cartilage surface (M-O). The degraded collagen II antibody Coll 2 3/4m demonstrated positive surface staining of the degraded cartilage, extending into the midzone.

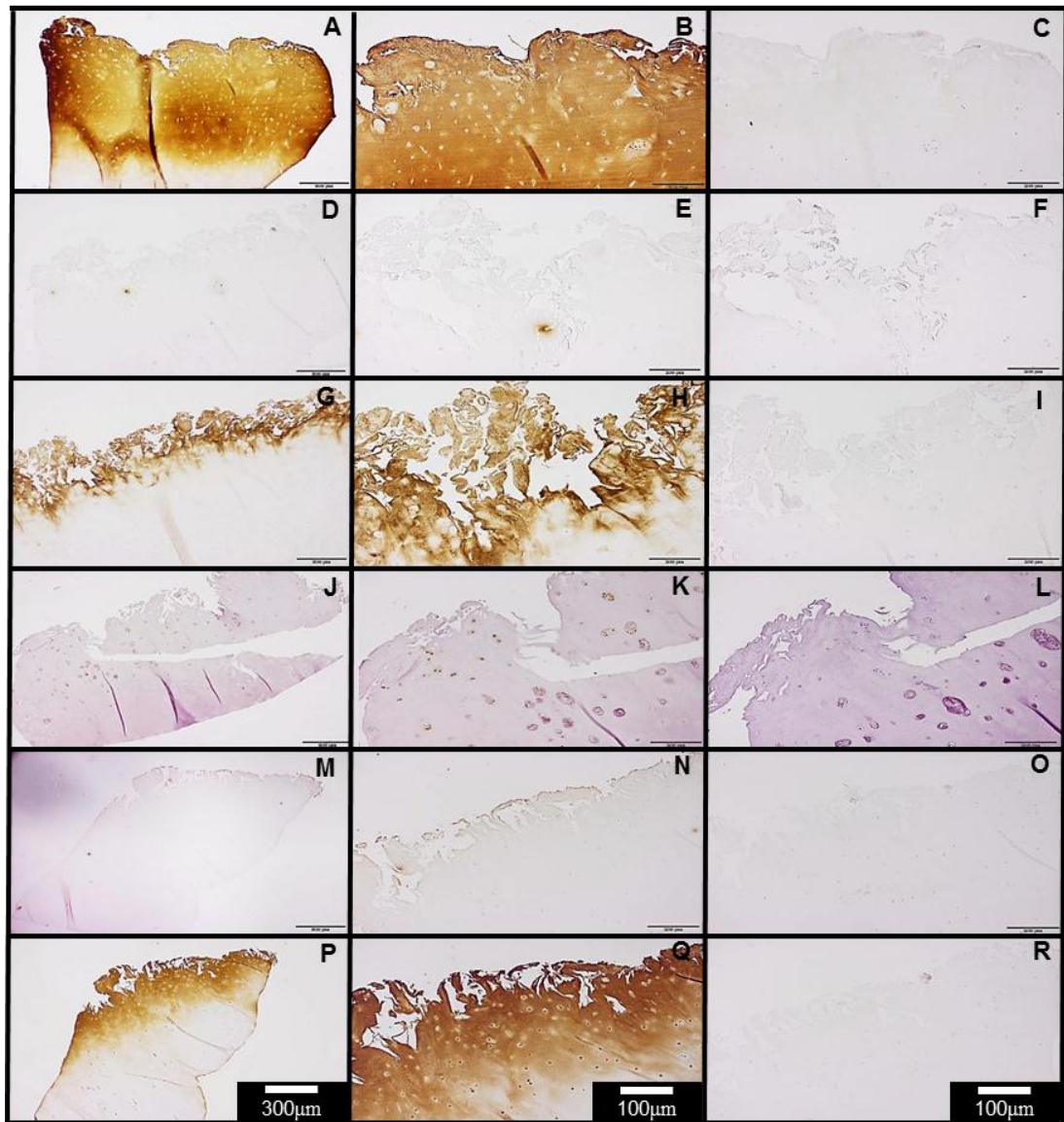


Figure 3.5: Selection of an Antibody for OA Cartilage Epitopes

Immunohistochemical ECM Staining Profiles of human OA cartilage. Intense positive staining for full length fibronectin was found in upper and middle zones of the cartilage (A, B) with no staining in the negative control (C). A small amount of staining for VYQP fibronectin epitope was detected (D, E) whereas positive surface zone staining of the VRAA fibronectin epitope was seen (G, H). Pericellular staining of DIPEN aggrecan epitope (J, K) with weak articular surface staining of the NITEGE aggrecan epitope (M, N). Positive surface staining of Coll 2 3/4m collagen II epitope (P, Q) was also evident. All negative controls were found to be unstained (C, F, I, L, O & R). Scale bar, 300µM for A, D, G, J, M and P; Remaining images, 100µm.

3.3.3 Conjugation of RGD Peptide to Streptavidin: Silverstain Analysis

Cyclic RGD peptides were covalently conjugated via sulfo-SMCC chemical linker to streptavidin molecules and analysed by silverstaining on a non-reducing SDS gradient gel (4-12%) (Figure 3.6). RGD + streptavidin conjugate (lane B) demonstrated a gel shift in size of an average ~20kDa compared to streptavidin alone (60kDa) (lane A). Based on a weight of 579 daltons for each peptide, an average of 35 RGD molecules were found to be covalently linked to streptavidin.

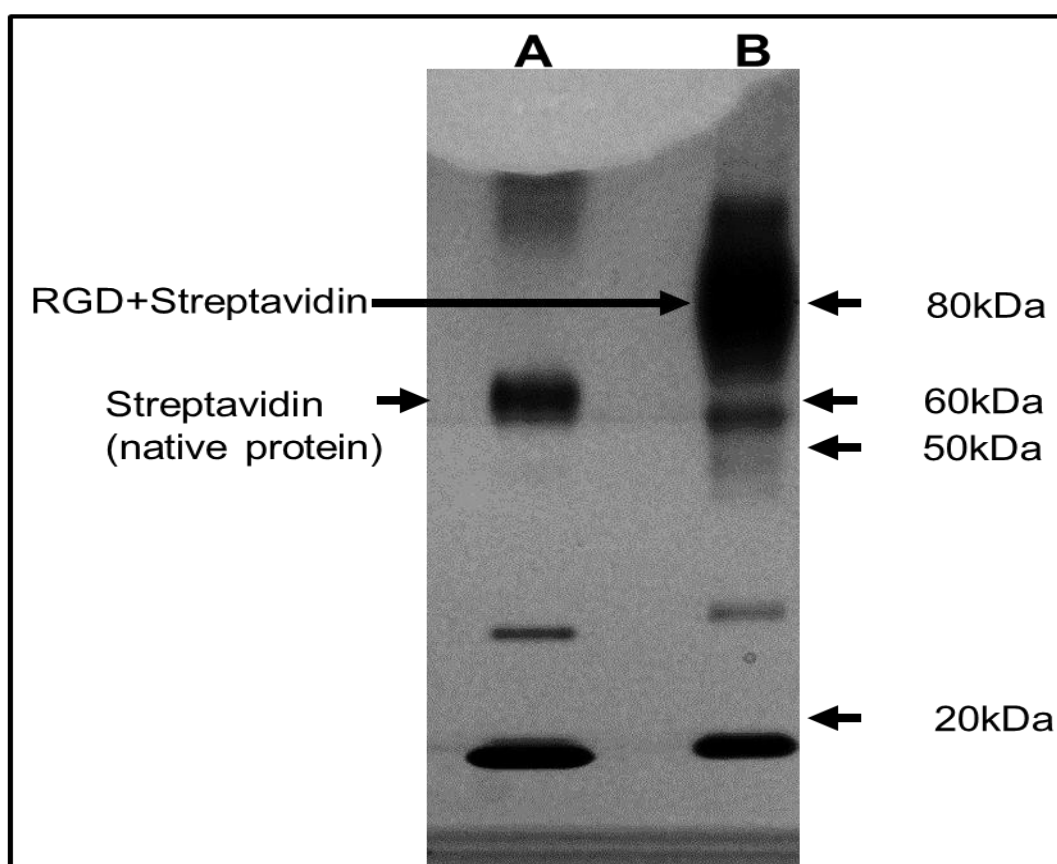


Figure 3.6: Silverstain Analysis of RGD Peptide Conjugation to Streptavidin

Silverstaining of RGD peptides covalently conjugated to streptavidin on a non-reducing SDS gradient gel (4-12%). RGD + streptavidin conjugate (lane B) demonstrated successful conjugation success by a gel shift of an average ~20kDa compared to streptavidin alone (lane A).

3.3.4 Immunohistochemical Analysis of RGD Peptide Functionality after Chemical Conjugation

Functionality of the RGD-streptavidin conjugate was analysed by a biotin/streptavidin-HRP system (Figure 3.7). Using a biotinylated secondary antibody, streptavidin peroxidase and DAB substrate, a brown colour was produced only in wells incubated with RGD-streptavidin (D) and was absent in wells incubated with RGD (C), and cells alone (A). Streptavidin incubated wells stained faintly brown (B).

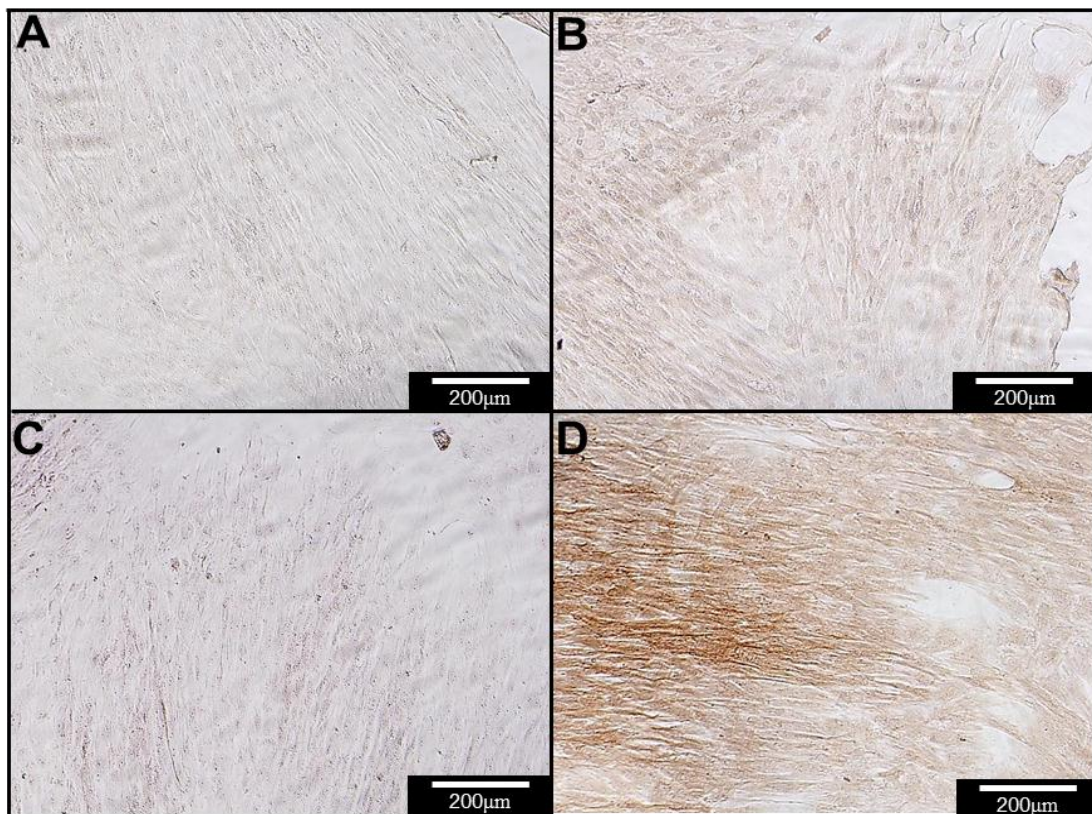


Figure 3.7: RGD-Streptavidin Conjugate Functionality: Binding Cells in Monolayer

MSCs in monolayer were incubated with RGD-streptavidin construct, RGD, streptavidin or PBS control. Using a biotin/streptavidin-HRP staining system, a brown colour was produced in wells incubated with RGD-streptavidin (D) and was absent in wells incubated with RGD (C) and cells alone (A). Streptavidin demonstrated a small amount of staining (B). Scale bar, 200µm.

3.3.5 Binding of Polyclonal Biotinylated Collagen 2 3/4m Antibody to OA Human Cartilage

Binding of the polyclonal biotinylated collagen 2 3/4m antibody to human OA cartilage was analysed by immunohistochemistry to demonstrate functionality (Figure 3.8). Positive staining of the 2 3/4m epitope was evident on sections of OA human cartilage with different levels of OA (A, C). Milder OA was demonstrated by section A with section C showing later signs of OA with superficial fissures, fibrillations and chondrocyte clusters. Positive staining was observed peripherally around chondrocytes (A, C), and observed in deeper zones of the cartilage, with some loss at the surface (C). Negative sections without biotinylated collagen 2 3/4m antibody staining demonstrated no positive staining of the epitope (B, D).

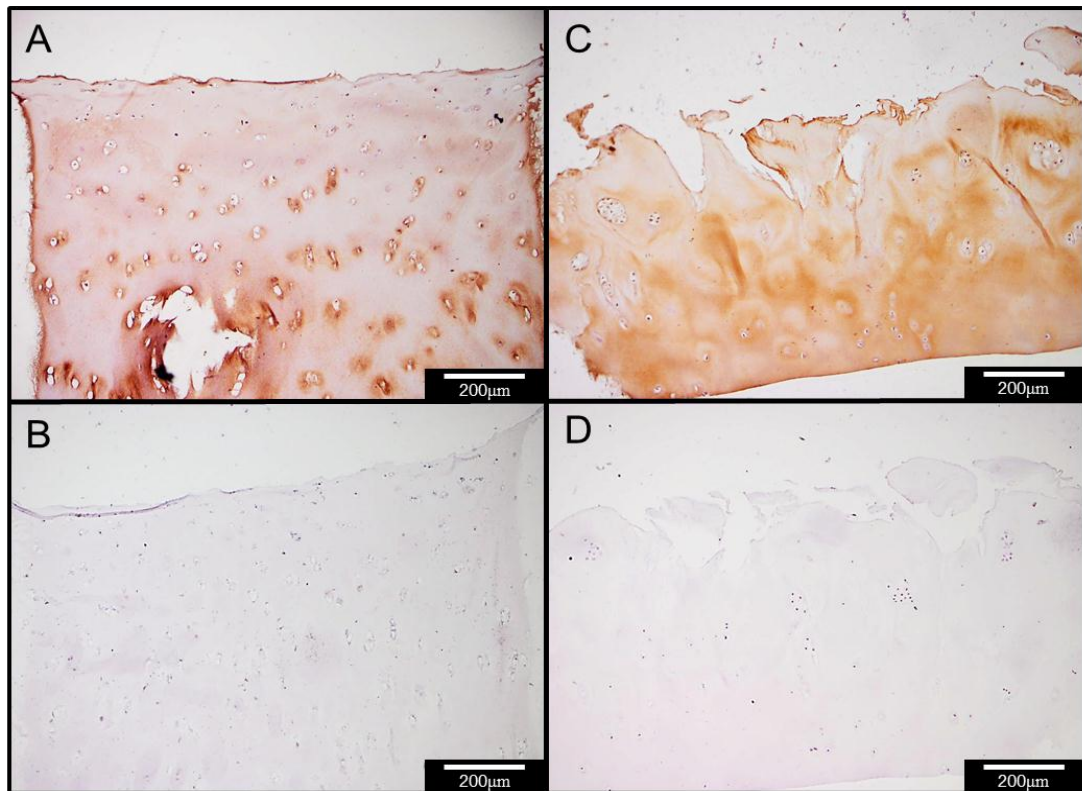


Figure 3.8: Polyclonal Biotinylated Collagen 2 3/4m Antibody Functionality on OA Human Cartilage

Immunohistochemical staining of human OA cartilage using the biotinylated collagen 2 3/4m antibody. Two different human OA sections demonstrated positive, specific staining of the degraded collagen 2 3/4m epitope (A, C). Staining can be observed both at the surface and in deeper zones and around chondrocytes. Negative staining of sections without biotinylated collagen 2 3/4m antibody (B, D). Scale bar, 200µm.

3.3.6 Immunohistochemical Comparison of Antibody Staining Patterns on Human OA Cartilage

A comparison of the polyclonal collagen 2 3/4m antibody, biotinylated polyclonal collagen 2 3/4m antibody and collagen II antibody staining was made using immunohistochemistry on human OA cartilage sections (Figure 3.9A, B, C, F, G, H). Safranin O staining for GAG was also used for a visual comparison of cartilage degeneration (D, I). Comparable positive superficial/surface staining patterns were observed for both the biotinylated (A, F) and non-biotinylated (B, G) collagen 2 3/4m antibody. Staining was stronger in intensity in sections incubated with the non-biotinylated antibody (B, G). Collagen 2 3/4m antibody staining, both biotinylated and non-biotinylated appeared to correlate with areas of loss of GAG (A, B, F, G, D, I). Sections stained intensely for collagen II in the superficial layer and throughout deeper cartilage layers, suggesting collagen II was still present in its native form (C). A reduced intensity in collagen II staining in the surface layer of H correlated with the presence of collagen 2 3/4m staining in surface layers (F, G) and loss of GAG (I). Sections stained for Safranin O demonstrated loss of GAG in the superficial/surface layer (D) and in specific areas in the upper zone (I). Peripheral areas of chondrocytes stained positively for GAG (I). Negative staining was observed on control sections not incubated with antibody (E, J).

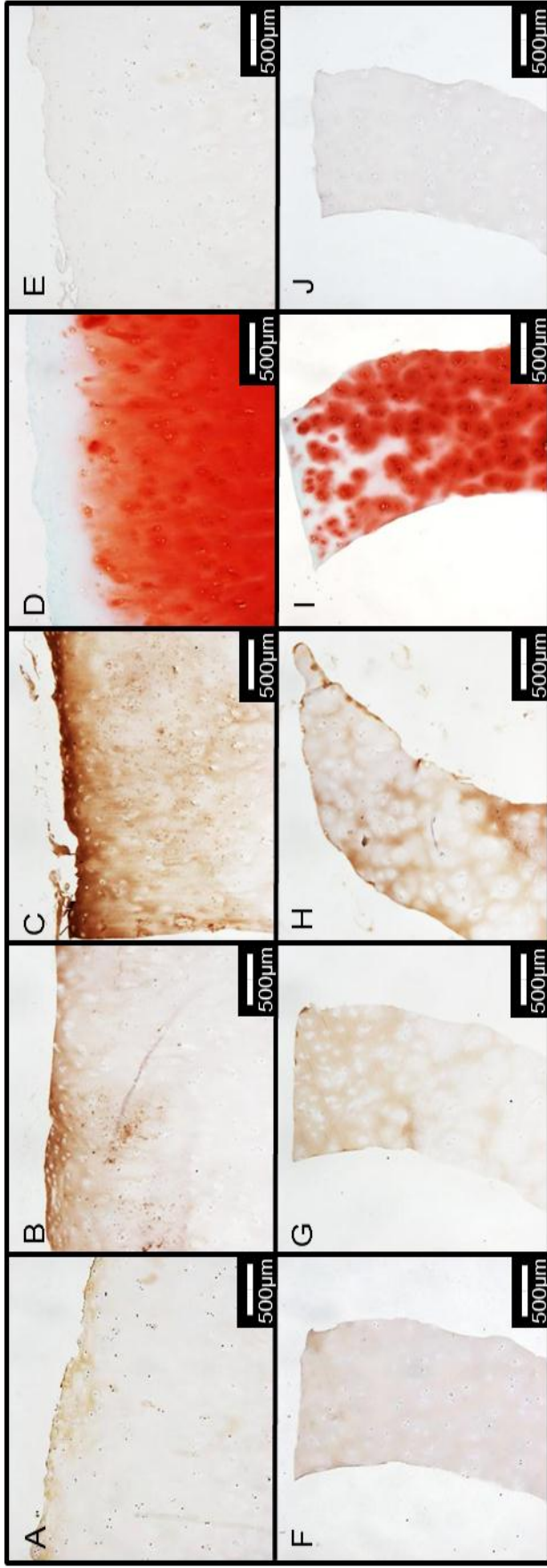


Figure 3.9: A Comparison of Biotinylated and Non-Biotinylated Polyclonal Collagen 2 3/4m Antibody, to Collagen II staining and GAG Expression

Immunohistochemical staining of the polyclonal collagen 2 3/4m antibody, with and without biotinylation, and collagen II on sections of human OA cartilage (A-C, F-H). Safranin O staining was used to detect GAG (D, I). Biotinylated (A, F) and non-biotinylated (B, G) polyclonal collagen 2 3/4m staining was comparable but stronger in non-biotinylated incubated sections. Sections stained superficially and in matrix areas juxtaposing chondrocytes. Intense native collagen II staining was observed in C but weaker staining was observed in H showing loss of collagen II in the upper zone and at the surface. Sections stained positive for GAG in middle to lower zones of the cartilage and around chondrocytes, negatively correlating with staining of the collagen 2 3/4m antibodies (D, I). Control sections with absence of antibodies stained negative (E, J). Scale bar, 500µm.

3.3.7 Analysis of the Antibody+RGD-Streptavidin Construct by Gel Filtration and Silverstain Analysis

Biotinylated antibody and RGD-streptavidin were delivered through a gel filtration column, either pre-mixed or separately, and their elution profile analysed (Figure 3.10A-C). Peak heights indicated efficiency of elution from the column and the width was indicative of molecule purity. The polyclonal biotinylated antibody alone eluted in two peaks (A) indicative of the polyclonal nature of the protein sample. The combined construct demonstrated a unique elution profile compared to the biotinylated antibody and RGD-streptavidin profiles, with a higher peak height and absorbance, as predicted from the biotin-streptavidin linkage of the two molecules (B). The RGD-streptavidin eluted later from the column indicating a smaller molecular weight of the conjugate (C).

Biotinylated antibody, RGD-streptavidin and their combined construct pre-mixed together were analysed by separation and silverstaining on a non-reducing SDS gradient gel (4-12%) (Figure 3.10D). The larger molecular size of the partially separated combined biotinylated antibody and RGD-streptavidin construct (lane 1) is illustrated compared to the components alone (lane 2 and 3 respectively). A shift in size was seen when comparing the combined construct (lane 1) to the biotinylated antibody alone (lane 2). The biotinylated antibody demonstrated staining of several bands, indicating its polyclonal nature (lane 2). RGD-streptavidin partial separation (lane 3) showed the characteristic 'smear' seen previously (Figure 3.6). The lower bands in this instance were not evident.

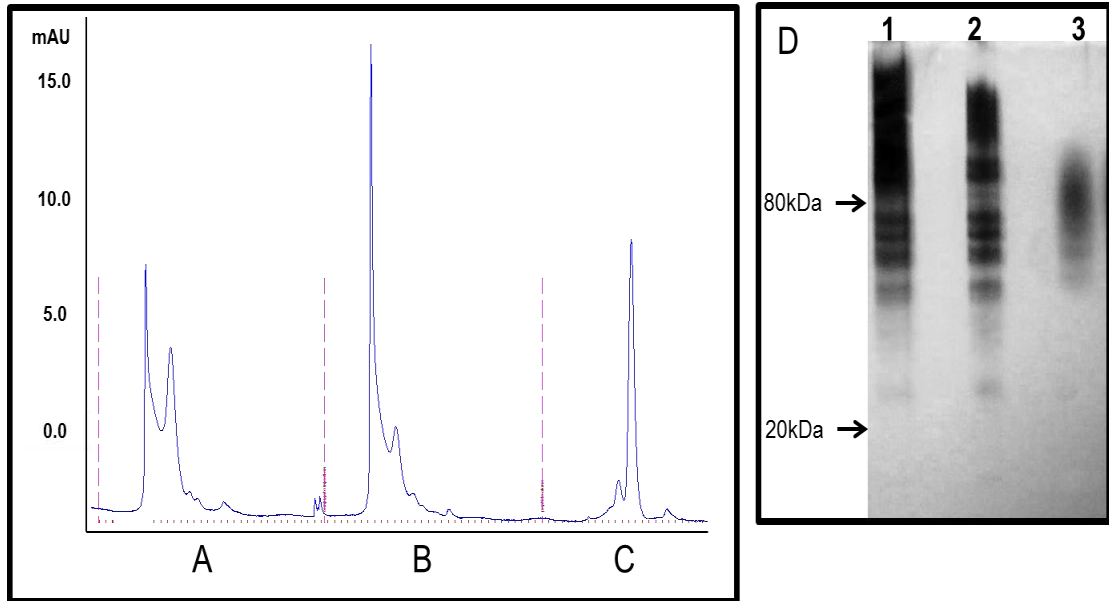


Figure 3.10: Gel Filtration and Silverstain Analysis of the Biotinylated Antibody and RGD-Streptavidin Combined Construct

Biotinylated antibody and RGD-streptavidin pre-mixed together (B) or individually (A, C) were separated on a gel filtration column for 45 minutes. The polyclonal biotinylated antibody showed two distinct peaks of elution from the column (A). The RGD-streptavidin peak eluted from the column after the antibody, indicating a smaller molecular weight of protein (C). The combined construct demonstrated a high elution peak and absorbance, indicating a profile specific to the biotin-streptavidin linkage of the components (B) (Injection time points indicated by pink slashed line). Silverstaining was performed of the biotinylated antibody and RGD-streptavidin pre-mixed and separate on a non-reducing SDS gradient gel (4-12%) (D). Combined construct showing a gel shift and increase in molecular size (lane 1). Biotinylated antibody shows a series of bands representing the polyclonal IgG (lane 2). RGD-streptavidin conjugate showing a molecular weight of ~80kDa (lane 3).

3.3.8 Binding of the Biotinylated Antibody-RGD-Streptavidin Construct to the MSC Surface

MSCs were incubated with biotinylated antibody and RGD-streptavidin, separately or combined. RAD-streptavidin was used as a control peptide. Streptavidin-TRITC was incubated with MSCs after construct incubations to label bound biotinylated antibody and followed by phalloidin-FITC for cytoplasmic labelling and DAPI nuclear staining. MSCs were incubated with constructs or PBS alone, 0 (Figure 3.11A-F) and 2 (3.12A-F) hours after trypsinisation. MSCs alone demonstrated no TRITC labelling after both time points and showed only cytoplasmic and nuclear staining (3.11A, 3.12A). Biotinylated antibody (3.11B, 3.12B), RAD-streptavidin (3.11C, 3.12C), RGD-streptavidin (3.11D, 3.12D) and biotinylated antibody-RAD-streptavidin construct (3.11E, 3.12E) also showed an absence of TRITC labelled cells after both time points as expected, however a small amount of background TRITC was observed. Biotinylated antibody-RGD-streptavidin construct incubation after 0 hours showed a small amount of TRITC labelled cells (3.11F) demonstrating binding of construct to the surface of the MSCs. After 2 hours of incubation, MSCs incubated with the biotinylated antibody-RGD-streptavidin construct were evidently labelled with TRITC in increased numbers and intensity compared to the 0 hour time point (3.12F). MSCs incubated after 2 hours showed more aggregations (3.12A-F).

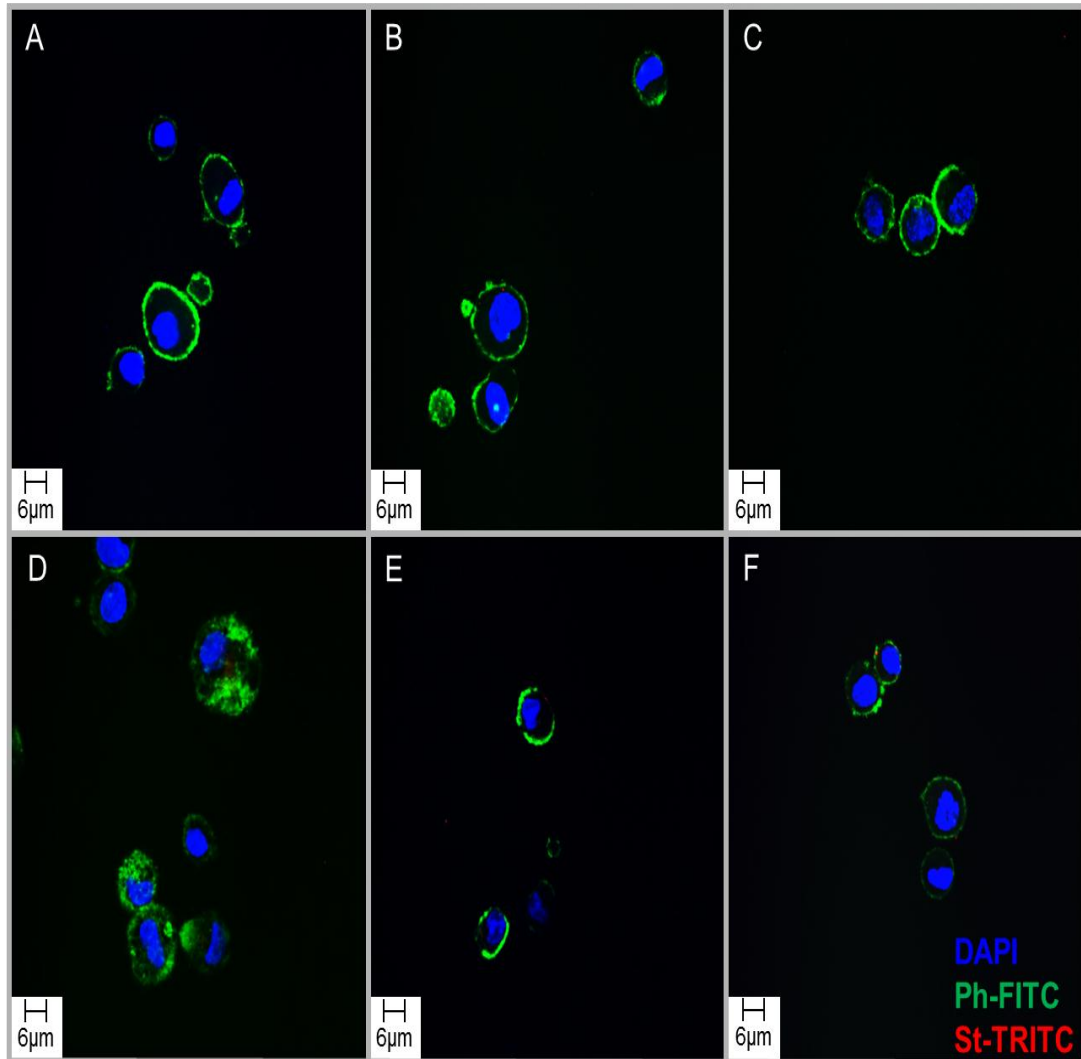


Figure 3.11: MSC Surface Binding of Construct after 0 hours by Fluorescence Analysis

MSCs incubated with biotinylated antibody and RGD-streptavidin separately or combined for 0 hours after trypsinisation, were fluorescently analysed using streptavidin-TRITC, phalloidin-FITC and DAPI for surface binding. MSCs alone demonstrated no TRITC labelled cells (A), only phalloidin FITC and DAPI stain. Biotinylated antibody (B), RAD-streptavidin (C), RGD-streptavidin (D) and biotinylated antibody-RAD-streptavidin construct (E) demonstrated a small amount of background stained TRITC labelled cells. Biotinylated antibody-RGD-streptavidin construct incubation after 0 hours, showed small numbers of construct bound cells, labelled with TRITC (F). Scale bar, 6µm, DAPI nucleus stain (blue), Phalloidin-FITC stain (green) and Streptavidin-TRITC stain (red).

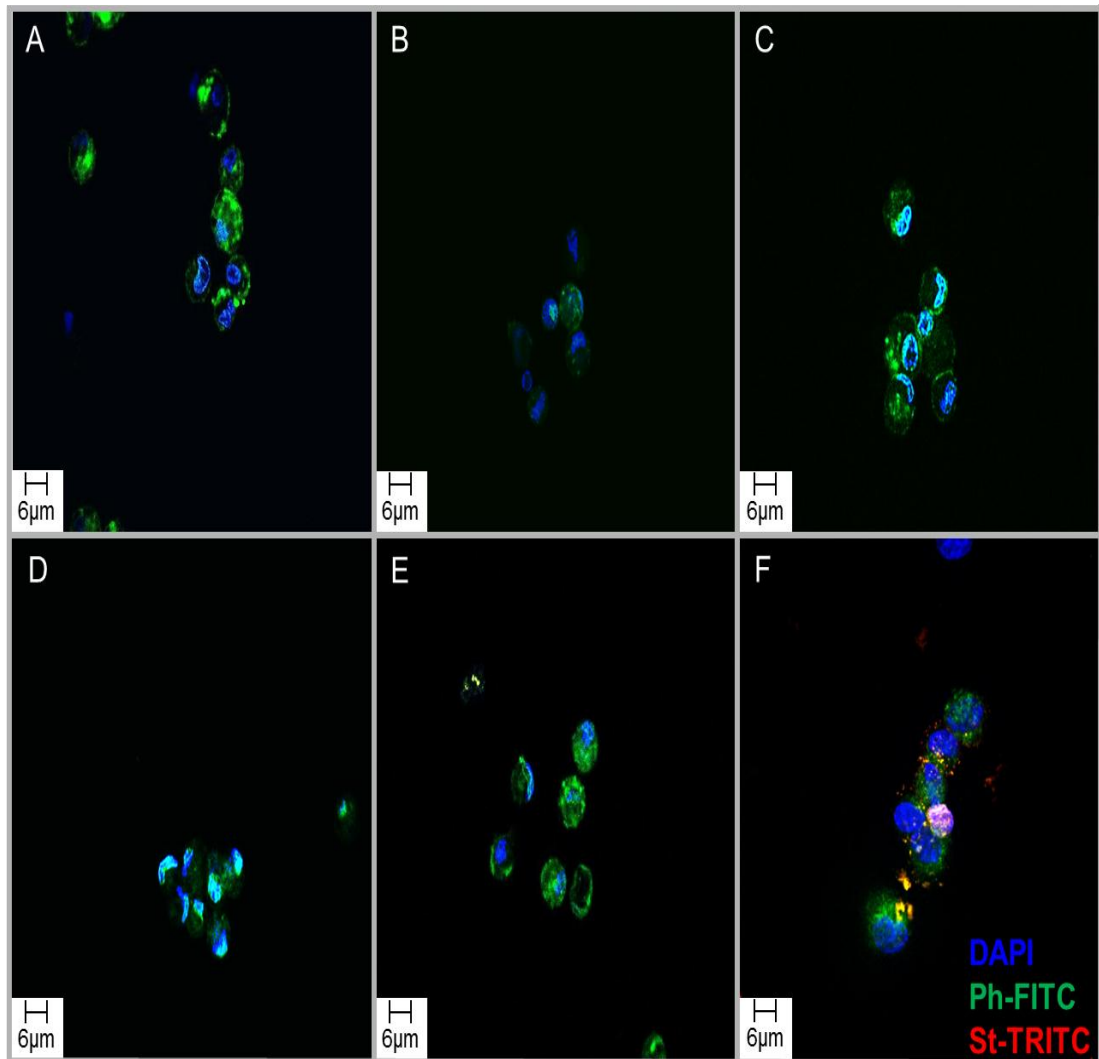


Figure 3.12: MSC Surface Binding of Construct after 2 hours by Fluorescence Analysis

MSCs incubated with biotinylated antibody and RGD-streptavidin separately or combined for 2 hours after trypsinisation, were fluorescently analysed using streptavidin-TRITC, phalloidin-FITC and DAPI for surface binding. MSCs alone demonstrated no TRITC labelled cells (A), only phalloidin FITC and DAPI stain. Biotinylated antibody (B), RAD-streptavidin (C), RGD-streptavidin (D) and biotinylated antibody-RAD-streptavidin construct (E) also demonstrated no TRITC labelled cells, only phalloidin FITC and DAPI stain. Biotinylated antibody-RGD-streptavidin construct incubation after 2 hours, showed an increased number of TRITC labelled cells and also surface bound construct appeared increased per cell (F) as compared to 0 hours (3.11F). Scale bar, 6µm, DAPI nucleus stain (blue), Phalloidin-FITC stain (green) and Streptavidin-TRITC stain (red).

3.4 Discussion

This chapter addressed the development and design of an antibody-peptide construct for localisation of MSCs to degraded cartilage. A series of successive steps were taken to design and develop the construct and demonstrate functionality with both cartilage and cells. These steps included choosing the appropriate target molecules as described in the design specification, followed by a series of tests for confirmation of conjugation, biotin/streptavidin linkage and also functionality with binding to cartilage and MSCs.

3.4.1 Construct Development: MSC specific marker

Early in the design phase, there was a focus on selection of a MSC specific marker. The concept was to develop a bispecific construct: a dual functionalised antibody that would be specific to MSCs and also degraded cartilage. A comparison was made of commercially available antibodies for the markers GD2, CD271, W3D5 and W5C5 alongside the general standard MSC surface markers CD105 and CD44. GD2 was selected based on its documented high expression levels on cultured MSCs (Martinez *et al.*, 2007). CD271 was selected as a recent standard MSC marker with a history of MSC expression in the literature (Quirici *et al.*, 2002). W3D5 and W5C5 antibodies target unknown antigens on the MSC surface and were selected based on their novelty at the time, making them potentially more interesting candidates over known antigens.

GD2 marker expression levels were favorably high and closer to that of CD105 and CD44. In contrast the CD271, W3D5 and W5C5 markers were detected at very low levels on cultured MSCs. CD271 is documented in the literature to lose expression after culture and also to be down regulated after the addition of the growth factor bFGF (Quirici *et al.*, 2002). Both W3D5 and W5C5 are documented to be expressed on freshly isolated MSCs (Buhring *et al.*, 2007). GD2 was selected as an ideal MSC marker, not expressed on hematopoietic cells and showing high expression levels on MSCs at early and late passage (Martinez *et al.*, 2007), therefore allowing greater flexibility for practical application (Mason and Manzotti, 2010). In order to obtain

sufficient amounts of antibody for bioconjugation, the hybridoma for the GD2 antibody was sought. However, this was not commercially available and was unobtainable, due to its current use in clinical trials (Cheung *et al.*, 2012; Kushner *et al.*, 2001).

3.4.2 Construct Development: The RGD peptide

The integrin receptor, known to bind RGD is one of the most ancient and widely expressed receptors found on most cell types of metazoans (Campbell and Humphries, 2012; Humphries, 2000; Kim *et al.*, 2011a; Millard *et al.*, 2011) and therefore not MSC specific. In terms of application, the designed construct was therefore intended to be pre-incubated with cultured MSCs prior to application to the degraded cartilage. Ideally, an MSC specific marker would have been preferred allowing the flexibility of selecting MSCs from fresh marrow, however, since culture expansion is generally required for sufficient numbers (Mason and Manzotti, 2010) specificity was not an absolute requirement. Because of generic integrin expression on most cell types, the construct also has the advantage of being applicable for localisation of any cell type (Humphries *et al.*, 2006).

Use of the RGD peptide and integrin receptor as a target for MSCs also adds several other advantages. The RGD peptide is characteristically known for its adhesive properties, a natural molecular glue that enables cells to form a spatial position within a tissue (Maheshwari *et al.*, 2000; Marko *et al.*, 2008; Ruoslahti, 1996; Vonwil *et al.*, 2010). Additionally, RGD not only has this physical influence with cells, but upon binding integrin receptors stimulates intracellular signaling, influencing gene expression and subsequently cell survival, proliferation, migration and differentiation (Grzesiak *et al.*, 1997; Hersel *et al.*, 2003; Humphries *et al.*, 2006; Ruoslahti, 1996; Salinas and Anseth, 2008; You *et al.*, 2011). Therefore, using a functional molecule such as RGD as part of an MSC localisation construct will be advantageous, if cell function, either MSC or other potentially reparative cells, can be positively influenced to enhance the repair efficacy. The RGD peptide alone may also be useful as a target molecule to enhance MSC retention to the degraded cartilage itself, since integrins are documented in the extracellular matrix

of cartilage and chondrocytes have been reported to shed integrins (Loeser, 2000; Schulze-Tanzil *et al.*, 2001; Shakibaei *et al.*, 2008; Shakibaei and Merker, 1999). Other cartilage matrix proteins have also been reported to bind RGD *in vitro* (Ruoslahti, 1996). The use of a peptide, small in size, compared to an antibody for the construct also ensures a smaller molecular complex that may be more sterically favourable for MSC binding. The cyclic RGD choice was also based upon its low cost, commercial availability and potential novel application for localising MSCs in the cartilage repair field (Dubey *et al.*, 2004; Khatayevich *et al.*, 2010; Kibria *et al.*, 2011; Tagalakis *et al.*, 2010).

3.4.3 Design and Function of the Construct

The design and application of the antibody-peptide construct, demonstrates a process that is tailored for amplification. The specific streptavidin-biotin linkage between the antibody and peptide was chosen based upon its characterized non-covalent binding affinity constant of $K_d = 10^{-15}M$, among one of the highest known formation constants in nature (Diamandis and Christopoulos, 1991). Streptavidin possesses four biotin binding sites per molecule, making it possible to use multiple biotinylated moieties, thereby amplifying the intended application (Diamandis and Christopoulos, 1991). Use of the biotin-streptavidin linkage, joining both components together, adds further flexibility and application to the construct. The construct can be tailored for any cell localisation application by combining the RGD coated streptavidin with a biotinylated antibody or targeting molecule of choice.

Sulfo-SMCC was chosen as a suitable chemical linker for protein-protein coupling (ThermoScientific). The linker is a heterobifunctional reagent, that can be employed to create an amine-thiol link between two proteins. Heterobifunctional linkers have the advantage of offering greater control over the reaction compared to homobifunctional and direct coupling conjugate chemistry (Hermanson, 2008). Numerous coupling agents are commercially available at a low cost and with the addition of the sulfonic acid group allowing for water solubility, conjugation is relatively simple (Hermanson, 2008). Lum *et al.* and Lee *et al.* demonstrated

successful use of the Sulfo-SMCC chemical linker for creating bispecific antibodies (Lee *et al.*, 2007; Lum *et al.*, 2004).

The cyclical RGD peptide c(RGDfC) was chosen for conjugation to streptavidin based on its available linker addition via a cysteine residue. A variety of cyclical RGD peptides are commercially available with additional linkers for conjugations (Goodman *et al.*, 2002; Marko *et al.*, 2008). Many cyclic peptides can be tailored for specificity and have demonstrated enhanced affinity for specific integrin receptors (Docheva *et al.*, 2008; Goodman *et al.*, 2002; Marko *et al.*, 2008; Nallamotheu *et al.*, 2006; Pfaff *et al.*, 1994). The c(RGDfC) was shown to have high affinity for integrin receptor $\alpha V\beta 3$ (Nallamotheu *et al.*, 2006), of which both subunits have been identified previously on MSCs (Docheva *et al.*, 2008; Docheva *et al.*, 2007). The sulfhydryl group available on the c(RGDfC) peptide is specifically required in the maleimide reaction of the chemical linker sulfo-SMCC. The streptavidin molecule is conjugated through available amines that react with NHS esters in the sulfo-SMCC (ThermoScientific). Through conjugation of the peptide to streptavidin, the peptide can be made available in sufficient numbers on one streptavidin molecule, thereby further amplifying the construct.

It was more practical to conjugate the RGD to streptavidin and biotinylate the degraded cartilage antibody. Conjugating the antibody to streptavidin would have created a larger molecular complex, that upon amplification would have possibly limited the biotin-streptavidin binding affinity due to steric hindrance (Clark and Hemsley, 1994). Antibodies, much larger in molecular weight compared to streptavidin, would have compromised streptavidin binding to biotinylated RGD when coated with antibodies. Also, standard biotinylation of the antibody avoids any compromise of function that might be caused by chemically linking the antibody to another molecule. The RGD peptide could have also been chemically linked to the antibody itself, without the need for the biotin-streptavidin linkage, thereby reducing molecular size of the conjugate. However, as previously described, the use of the biotin-streptavidin linkage provides a technology with flexibility for application, without compromising function of the construct.

Selecting the most appropriate epitope for MSC localisation to OA degraded cartilage was based upon staining intensity, specificity to cartilage and location. In addition, the commercial availability of the antibody targeting the epitope was a requirement. The staining pattern was required to be intense and throughout the superficial zone or what remained of the surface zone. Full length fibronectin, found to be upregulated during OA (Brown and Jones, 1990; Jones *et al.*, 1987) demonstrated intense surface and mid-zone staining. However, fibronectin is a major ubiquitous glycoprotein component of the extracellular matrix (Singh *et al.*, 2010) and therefore not an ideal candidate with specificity to degenerated cartilage. The fibronectin epitope, peptide sequence VYQP is representative of a fragment isolated from human OA cartilage by Zack et al and previously shown to be present in abundance in OA cartilage and at the surface of chondrocytes. This fibronectin epitope was only found in small amounts in areas of the surface zone precluding this antibody as a candidate for therapeutic targeting where staining would need to be strongly evident throughout the entire surface and fibrillated regions. The fibronectin epitope, peptide sequence VRAA, also isolated from human OA cartilage by Zack et al, in contrast demonstrated an ideal staining pattern; intense staining throughout the fibrillated surface zone and an ideal target for localizing MSCs at the surface of the cartilage (Zack *et al.*, 2006). The antibodies for peptides VRAA and VYQP were kindly provided from Mark Zack at Pfizer for staining analysis. Because these antibodies were not commercially available and other commercially available antibodies provided the required staining profiles, a decision was made to not continue with these antibodies.

The aggrecan epitope, DIPEN demonstrated pericellular staining only. The staining pattern did not demonstrate any fibrillation or surface staining, suggesting this epitope would not be suitable for MSC localisation and would not be readily available for targeting *in vivo*. Staining of the NITEGE aggrecan epitope demonstrated a more suitable staining profile throughout the surface fibrillations, however staining was very weak in intensity compared to other epitopes such as fibronectin and collagen. Fosang et al reported some superficial staining of NITEGE, although mainly intracellular, and DIPEN was found to be cell-associated (Fosang *et al.*, 2000). Embry Flory *et al.* also reported the intracellular accumulation of the DIPEN and NITEGE neoepitopes within bovine chondrocytes

(Embry Flory *et al.*, 2006) suggesting a possible cause for the reduced visualization and pericellular staining of these epitopes. The collagen 2 3/4m epitope demonstrated an ideal staining profile following the design specifications for the construct. Intense staining was observed at the surface to mid-zone and throughout fibrillations. As this collagen 2 3/4m antibody was available commercially and demonstrated this superior staining pattern, it was selected as optimal for anchoring of the MSC targeting construct to degraded OA cartilage.

Silverstain analysis of the RGD-streptavidin construct was used to analyse the conjugation of the RGD peptide to streptavidin. Confirmation of the conjugation was demonstrated by the gel shift of the streptavidin molecule from a 60kDa band to an 80kDa band. The smear of bands in the conjugate lane indicated a mixed population of conjugates of varying molecular weights. In practice the extent of conjugation per molecule is not controlled and in this case, more than one amine group was available on the streptavidin, inevitably leading to formation of multiple labelled molecules (Hermanson, 2008). Lum *et al.* similarly demonstrated analysis of conjugation of two antibodies by a gel-shift silverstain analysis, describing the presence of a higher band in the conjugated sample (Lum *et al.*, 2004). An average estimation was made of 35 RGD peptides per streptavidin; based on a known size of the c(RGDfC) peptide having a molecular weight of 578.65 daltons. This estimation suggested a sufficient number of peptides were conjugated to streptavidin, ensuring RGD binding to integrins on MSCs, with the possibility of several MSCs being bound to one or more streptavidin.

The chemical linker Sulfo-SMCC covalently conjugates both amine and sulfhydryl molecules. The cyclic RGD-peptide contained the amino acid cysteine that provided the sulfhydryl for the sulfo-SMCC maleimide reaction and therefore stability of the RGD peptide sequence function was guaranteed. However, the N-hydroxysuccinimide reaction with primary amines on the streptavidin molecule did not guarantee stability of the streptavidin molecule, since the reaction could have occurred anywhere on the molecule. Therefore, an analysis of streptavidin function was required.

To test functionality, a biotin/streptavidin-HRP immunohistochemistry method was deployed that enabled testing of both the RGD peptide and streptavidin molecule to be analysed at the same time, in addition to confirming successful conjugation. The presence of a brown colour in the well of MSCs incubated with RGD-streptavidin was created by the reaction of the secondary biotinylated-HRP antibody and the DAB substrate. This indicated that the streptavidin was functional, since the biotinylated antibody was able to bind the molecule. This also indicated that the RGD was functional and able to bind the MSC surface, since strong positive staining was only evident in the RGD-streptavidin well. Only the RGD-streptavidin conjugate had the presence of the streptavidin to bind the biotinylated antibody and therefore also demonstrated that the chemical conjugation itself was successful.

Some weak staining observed in the well incubated with streptavidin alone was likely a consequence of the streptavidin molecule also binding the MSC surface. Streptavidin, has been shown to be an example of a bacterial protein that mimics the RGD sequence, a potential mechanism for interfering with immune responses mediated by integrin receptors (Alon *et al.*, 1990; Alon *et al.*, 1993). Indeed the protein is known to contain a peptide sequence arginine-tyrosine-aspartic acid-serine (RYDS) site, which has high homology to the RGD cell adhesion domain of ECM molecules (Alon *et al.*, 1990, 1992; Bayer *et al.*, 1990; D'Souza *et al.*, 1991). Competition studies with RGD peptides indicated streptavidin binds to cells using this sequence and is distinct from the biotin-binding site. The RYDS site is also shown to undergo a conformational change upon biotin binding and becomes functional in promoting cell adhesion (Alon *et al.*, 1990, 1992; Bayer *et al.*, 1990). Further studies by Alon *et al.* showed that immobilized streptavidin supported activated human CD4⁺ T cell adhesion in a $\alpha 5\beta 1$ specific manner and soluble streptavidin inhibited T cell adhesion to fibronectin. In addition, streptavidin interfered with the co-stimulatory effect on tumour necrosis factor- α , secreted by T cell and macrophage cultures (Alon *et al.*, 1993). This additional property of streptavidin is favorable for enhancing MSC binding to the conjugate. The conformational change and promotion of cell adhesion upon biotin binding is an advantage for using the streptavidin-biotin linkage system. Because the staining of the cells incubated with streptavidin was weak, it may be that the protein is not as

efficient alone at binding the MSC surface as the cyclic RGD peptide and protein combined.

The functionality of the polyclonal collagen 2 3/4m antibody after biotinylation was tested on human OA cartilage using immunohistochemistry. Two sections of OA cartilage with different levels of OA, a milder form of OA with less degradation and fibrillation (Hollander *et al.*, 1995), as demonstrated by a relatively flat surface, compared to a more severe case of OA, with superficial fissures and chondrocyte clusters were selected to demonstrate functionality. Positive staining is observed in both sections, suggesting the biotinylated collagen 2 3/4m antibody is functional and unaffected by the biotinylation. The staining pattern of the severe case of OA is more preferable for MSC localisation, with some surface and mid zone fibrillated staining. However, there is some loss of staining at the articular surface. This suggests the antibody ideally provides a better target for moderate to severe stages of OA, where some degeneration is present for epitope availability, until the loss of matrix depletes the epitope superficially.

Hollander *et al.* used the monoclonal collagen 2 3/4m antibody to investigate sites of denaturation of collagen type II. In non-arthritic cartilages, staining was observed to be superficial and in the midzone. In OA specimens, increased staining was observed extending into the deeper zones. Severity of degeneration and deep fissures were progressively accompanied by loss of staining at the articular surface and likely due to the loss of collagen. Staining was confined to deeper layers around the chondrocytes and in early stages also to pericellular sites. It was suggested that initial damage to collagen II is always seen around chondrocytes (Dejica *et al.*, 2012; Hollander *et al.*, 1995). Since chondrocytes make an initial attempt at restoring the matrix, this pericellular staining may also be associated with the generation of new collagen type II by the chondrocytes (Aigner *et al.*, 1992).

Further immunostaining comparisons with a collagen type II antibody and the non-biotinylated polyclonal collagen 2 3/4m antibody on two different human OA cartilage sections, demonstrated similar staining patterns for the polyclonal collagen 2 3/4m antibody, with or without biotinylation and similar to that of the staining patterns observed by the commercial collagen 2 3/4m antibody. However, by

observation, the amount of staining and intensity was higher for the non-biotinylated antibody, suggesting some partial loss of functionality by biotinylation. A comparison of the regions stained with the collagen 2 3/4m antibody (both biotinylated and non-biotinylated), and the Safranin O staining shows a loss of GAG in regions where the epitope is present.

Collagen type II staining was strongly positive, in particular in the surface layer, suggesting that the full length, healthy form of collagen type II was still present in the cartilage matrix, although signs of degradation were evident as indicated by the collagen 2 3/4m antibody staining. However, collagen type II staining was lost at the articular surface in the second section of higher OA severity, particularly in the matrix juxtaposing the chondrocytes, where the collagen 2 3/4m epitope staining appears. The Safranin O staining in contrast remains peripheral to the chondrocytes and is lost in the matrix. These staining patterns are indicative of the degradative cartilage changes in OA, where the degradation of the collagen network accompanies the loss of proteoglycans, the aggrecan complex consisting of the GAGs, chondroitin and keratin sulfate (Hollander *et al.*, 1995; Wu *et al.*, 2002).

Gel filtration was performed to analyse the elution profile of the streptavidin-biotin linkage of the targeting construct. The streptavidin-biotin linkage was demonstrated to be functional by the individual elution profile of the combined construct, showing a high efficiency elution peak and absorbance. The two peaks in the elution profile of the biotinylated antibody reflected the polyclonal nature of the antibody, suggesting a mixed population of IgGs within the solution. In addition to the gel filtration analysis, a protein profile of the construct and its components was performed by silverstain. The construct demonstrated larger protein bands compared to the antibody and RGD-streptavidin alone as expected. Again, the characteristic smears of the antibody, RGD-streptavidin and the construct indicated the mixed nature of the construct and its components. The components, the RGD-streptavidin and antibody were not purified. For proof of principle, it was decided to use the components in their non-purified form. A study by Lee *et al.*, using bifunctional antibody constructs for targeting HSCs to the injured myocardium, demonstrated that the use of non-purified conjugates were successful at enhancing HSC localisation and myocardium functional outcome in a rat ischemic model. It was

reported by the same group that previous experience in preclinical and clinical studies had shown no significant difference or limitations in binding and specificity between purified and unpurified conjugates (Lee *et al.*, 2007).

After confirming functionality of the individual components the next step was to assess the ability of the construct to bind the surface of MSC. Initially, attempts were made to quantitatively analyse the number of MSCs bound with the construct using a streptavidin-TRITC to label bound biotinylated antibody by flow cytometry. An unsuccessful attempt was also made to label the biotinylated antibody with a fluorescent secondary antibody, but it was likely that the biotinylation affected binding. The aggregated nature of MSCs when bound to the RGD construct may also have contributed to the lack of success with these methods. Several MSCs are potentially bound together when bound with the RGD-streptavidin conjugate and further, several biotinylated antibodies may bind one streptavidin to form large complexes, making a single cell analysis difficult to achieve.

Immunofluorescence analysis was performed as an observational approach for analysing surface binding of the construct, using a ratio of 1:1 of RGD-streptavidin and biotinylated antibody (RGDSt:BAb) and streptavidin-TRITC to label bound cells. Initially, surface binding was observed on MSCs in monolayer (data not shown); however, it was evident that fluorescent binding could also be observed by the streptavidin-TRITC marker alone. This was likely a consequence of the streptavidin protein alone binding the surface of the MSCs, as observed previously. By observation, there appeared to be an increased amount of TRITC fluorescence in monolayers incubated with the RGDStBAb construct, suggesting that there was some binding of the construct on the MSC surface. However, due to the high background of the streptavidin-TRITC alone, these results were not sufficient enough to confirm potential binding. Since it was envisaged that the construct would be bound to MSCs in suspension, prior to delivery to the tissue, immunofluorescence was then performed on MSCs bound with the construct in suspension.

Immunofluorescence of MSCs in suspension was initially performed immediately after trypsinisation. MSCs were trypsinised and incubated with the various

components and control groups, followed by incubation with the streptavidin-TRITC. Some fluorescent binding was observed on the surface of cells bound with the construct; however, this was not as efficient as expected. There was a small amount of background TRITC staining observed on other groups, likely due to streptavidin-TRITC binding to the cell surface. To enhance construct binding, MSCs were left for a period of time prior to incubation, since enzymatic cell dissociation results in degradation of surface proteins (Tarone *et al.*, 1982). Tarone et al observed the adhesion of fibroblastic cells on fibronectin coated plates was completely abolished by pronase digestion and inhibited in varying degrees by other enzymes such as proteinase K and papain. However, after prolonged trypsin treatment cells remained adhesive, even after inhibition of protein synthesis. Further analysis, identified glycoproteins gp120 and gp80 remaining on the cell surface, suggesting a role for these proteins in fibronectin-mediated cell adhesion (Tarone *et al.*, 1982). Since, the RGD peptide is known to specifically bind integrins and various matrix molecules on cell surfaces (Ruoslahti, 1996), it is possible that the removal of integrin receptors by trypsin played a role in the inefficiency of construct binding observed immediately after trypsinisation.

Incubation of the construct and various controls two hours after trypsinisation, demonstrated enhanced construct present on the surface of the cells as shown by enhanced TRITC labelled MSCs. Also noticed was an enhanced aggregation of MSCs incubated for two hours. These observations are indicative of a recovery of integrin receptors on the surface of the MSCs, where protein synthesis restores surface proteins after proteolysis for adhesion (Tarone *et al.*, 1982). Additionally, MSCs left in suspension aggregate as a result of cell-cell contact, in turn inducing integrin receptor clustering and enhancing integrin receptor functionality (Campbell and Humphries, 2012; Humphries, 2000; Kim *et al.*, 2011a).

3.4.4 Limitations and Further Experiments

Initial attempts were made to incubate the RGDStBAb as a complete construct with the MSCs, rather than incubating the components separately and sequentially. However, these attempts proved to be unsuccessful and were likely the result of

large complexes being formed by the construct, as seen in the gel filtration experiment. Large complexes would cause problems sterically for the RGD peptides to successfully bind to the MSC surface and furthermore the large complexes with strong biotin-streptavidin binding affinities, would make it difficult to mix with MSCs. Both restoration of the integrin receptors and the separate incubations of the RGDSt and BAb are limitations to the design of the construct since they add several steps and extra time in the labelling of the MSCs with the construct prior to delivery.

Another issue in the design of the construct is the multiple RGDs bound to one streptavidin molecule. A consequence of this is the possibility of more than one MSC bound to a streptavidin molecule that may then interfere with the efficiency of the binding of the biotinylated antibody to the streptavidin. One way to improve efficiency of bound antibody to the streptavidin would be to reduce the amount of RGD conjugated to the streptavidin, such as reducing the concentration of RGD peptide added during the sulfo-SMCC reaction. In an optimization experiment, the RGD peptide concentration was halved and quartered during the sulfo-SMCC chemical conjugation and a comparison was made with the original concentration (1:1) of binding the construct to the MSC surface. There was no difference observed between the different peptide concentrations by fluorescence analysis (data not shown) and since by observation the results of the construct surface binding after two hours were optimal, no further optimization of the RGDSt conjugation was pursued.

A further useful experiment for optimization purposes would have been a quantification of the amount of construct bound to the MSC surface. Unsuccessful attempts made by FACs analysis were intended to provide quantitative data. Another experimental attempt to quantify the amount of construct bound to the MSC surface used a cell-based ELISA method (O'Kennedy and Reading, 1990). This methodology also proved to be problematic, with induction of cell death by endogenous peroxidase blocking, loss of cells during centrifugation and consequently large variability among replicates making results very inconsistent.

Using the fluorescence method, a semi-quantitative measure of fluorescence and cells could have been attained by a random selection of counts of the number of

MSCs labelled with TRITC, or using a microscopic measure of fluorescence. This would need to take into account the number of cells counted to normalise the data, since intensity and amount of bound construct would be variable on the cell surface. This method, as with all fluorescence based counts would be open to subjectivity, and in the cell suspension experiments would have been difficult to achieve due to aggregations of cells that would make cell counts unclear and inconsistent among groups.

3.5 Conclusion

An antibody-peptide construct specific for localising MSCs to OA degraded cartilage was designed, following a set of design specifications. Antibody and peptide choice was based upon literature searches and screens for appropriate markers. Development of the construct was employed using a series of tests for functionality, which demonstrated successful conjugation of RGD and streptavidin components, functionality of the biotinylated polyclonal coll 2 3/4m antibody, the streptavidin-biotin bridge and successful binding of the construct to the surface of MSCs. Quantification of construct bound to MSCs proved to be a challenge and ultimately an observational approach was achieved. The next step was to assess the binding of the labelled MSCs on degraded cartilage, as detailed in chapter 4.

Chapter 4

A Biocompatible Antibody-Peptide Construct for Enhancing Specific Cell Localisation to Degraded Cartilage

4.1 Introduction

Enhancing the numbers of reparative cells at the cartilage surface may improve the efficacy of cartilage repair (Coleman *et al.*, 2010; Murphy *et al.*, 2003). Specific localisation of cells may be considered an appropriate way of not only controlling the location of cells but also the number retained, since MSCs have been shown not to specifically localise to cartilage tissue in high numbers, even after local intra-articular injection (Augello *et al.*, 2007; Liechty *et al.*, 2000; Murphy *et al.*, 2003). The use of antibodies or peptides enables control of the localisation of cells and further provides functional assistance, thereby enhancing the cellular therapeutic response (Kean *et al.*, 2011).

4.1.1 *Ex Vivo* Explant Models

To enable testing of a targeting technology, a reproducible tissue model that can be controlled and tailored is required. In some instances adherence of cells to the target cells of the tissue can be attempted in 2D culture (Gerasimou *et al.*, 2009). Adhesion assays can also be employed to observe and measure attachment of labelled cells to a matrix or polymer (Anamelechi *et al.*, 2007). Sarkar *et al.* observed MSC adhesion and rolling behaviour in a flow cell chamber following biotinylation and addition of the sialyl Lewis X protein (Sarkar *et al.*, 2008; Sarkar *et al.*, 2010).

Naturally, *in vivo* models offer the required environmental conditions to test a localisation technology, however, the next best model would be an *ex vivo* system. An *ex vivo* system has the advantages over *in vitro* of allowing testing in 3D in less artificial conditions and using the same tissue as *in vivo*. However, the tissue is placed external to the natural conditions. Additionally it offers a less complex and more controlled study platform compared to *in vivo* conditions, whereby environmental factors cannot be controlled (Rezvan *et al.*, 2011). Human cartilage for research purposes is often sourced during late stage OA or after injury and can also show wide variability depending on injury, patient age and donor (Hollander *et al.*, 1995). The use of human cartilage for an explant model can therefore create

variability within an experiment, since the extent of cartilage degradation cannot be controlled and a focus is placed solely on the end stage of the disease, which can often be resistant to therapeutic benefit (Hollander *et al.*, 1995; Hunziker, 2009).

Various studies have used *ex vivo* animal cartilage explant culture models as a means of controlling different amounts and types of degradation and to observe early stage events in the OA disease process (Ashwell *et al.*, 2008; Fosang *et al.*, 2000; Phitak *et al.*, 2012; Yasumoto *et al.*, 2003). Cartilage progenitor cells have also been observed and found active within human and equine explants (Henson and Vincent, 2007; Henson *et al.*, 2005; Khan *et al.*, 2009). In an example of using ‘*ex vivo*’ explants to test a cell localisation technology, Dennis *et al.* used cartilage explants from a rabbit partial-thickness defect model to test the localisation of antibody labelled chondrocytes (Dennis *et al.*, 2004). Koga *et al.* delivered Dil-labelled MSCs to full thickness osteochondral defects *ex vivo* and determined a time-dependent increase in cell numbers adhered to the defect (Koga *et al.*, 2008). In both examples, explants containing defects were used, having the advantage of favourably retaining cells within an existing depression in the cartilage surface.

4.1.2 Measuring Cell Retention

Other than observational approaches (Lum *et al.*, 2004; Quintavalla *et al.*, 2002), few studies have quantified numbers of cells retained within a tissue and instead used semi-quantitative methods as measures for cell retention. Dennis *et al.* demonstrated enhanced cell localisation of ‘cell painted’ chondrocytes to *ex-vivo* rabbit explants. Cells were fluorescently labelled and fluorescence intensity was measured (Dennis *et al.*, 2004). Lee *et al.* measured cell density in a rat *in vivo* model of myocardial infarction, by counting fluorescently labelled cells on histological sections of the infarct area (Lee *et al.*, 2007; Sato *et al.*, 2012). In another 2D approach, the number of annexin V labelled MSCs bound to bovine aortic endothelial cells *in vitro* were analysed by confocal microscopy; MSCs present in 5 randomly selected fields were determined (Gerasimou *et al.*, 2009).

4.1.3 Biocompatibility

A requirement in the design of any medical repair technology, either scaffold or antibody focused is for biocompatibility with the cells and tissue with which it is to be used. MSCs demonstrate tri-lineage potential and possess a proliferative and fibroblastic adherent capacity, therefore, it is important to determine whether this normal functioning of the cells is maintained (Dominici, 2006). Sarkar et al demonstrated that MSC functionality was not compromised after biotinylation of the cell surface (Sarkar *et al.*, 2008). Similarly, Dennis *et al.* showed that cell growth, viability and chondrogenic potential were not affected after the surface of chondrocytes were intercalated with protein G and labelled with antibody (Dennis *et al.*, 2004). Lee *et al.* tested the impact of bispecific antibody (CD45, MLC) on the growth and differentiation of CD34+ cells. *In vivo* bispecific antibody labelled cells persisted in myocardial infarcts, expressed muscle specific antigens and contributed to improved left ventricular function (Lee *et al.*, 2007).

The focus of this chapter was to assess the ability of the antibody-peptide construct and peptide alone for enhancing cell localisation using an *ex vivo* porcine cartilage explant model. Biocompatibility of the construct with MSCs was also assessed by observing morphology, viability, proliferation and differentiation after incubation with the construct and components.

4.2 Materials & Methods

Note: All materials were supplied by Sigma-Aldrich unless otherwise stated.

All experiments were performed in triplicate with 3 biological replicates, unless otherwise stated.

4.2.1 Porcine Cartilage Explants

Biopsies were taken from the tibial plateau of porcine knee joints (A Traves & Son Ltd). Full thickness cartilage explants were created by biopsy punch (1-2mm thick and 2 mm diameter). The explants were placed in α -MEM containing 10% FBS, prior to being placed in 0.02% collagenase (Collagenase Type II, Worthington) in α -MEM for 1 hour or placed in α -MEM alone as a control. Explants were then washed twice in PBS and either placed in a 15 ml falcon tube ready for cell application or fixed for histological processing.

4.2.2 Immunohistochemistry of Porcine Cartilage

Explants with and without collagenase digestion were prepared for histological processing by washing twice in PBS and then cross-linking in 10% formalin for 20 minutes. Explants were placed in an automated tissue processor (Leica ASP300S), embedded in paraffin wax and sectioned at a thickness of 5 μ m using the Leica RM2235 microtome. Immunostaining was carried out using the polyclonal collagen 2 3/4m, biotinylated and unbiotinylated antibody and collagen type II antibody (Abcam), using the HRP-Diaminobenzodine (DAB) kit (Envision Dako Cytomation Kit). The procedure was carried out as described in section 3.2.2 and 3.2.3.

4.2.3 Safranin O Staining of Porcine Cartilage

Cartilage sections were stained following the protocol as in section 2.2.4.

4.2.4 Collagen 2 3/4m Peptide Blocking of Porcine Cartilage

Porcine collagenase digested cartilage sections were prepared for immunohistochemistry as in section 3.2.2 and 3.2.3. Prior to antibody incubation, sections were blocked with the collagen 2 3/4m peptide (Harlan), prepared in PBS at a concentration of 20µg/ml for 20 minutes at room temperature, alongside a control slide incubated in TBS. Sections were washed twice in TBS and then the protocol for immunostaining continued as described in in section 3.2.3.

4.2.5 Porcine Meniscus and Muscle Biopsies

Biopsies of meniscus and muscle were taken from porcine knee joints. Meniscus was taken by biopsy punch (1-2 mm thick and 2 mm diameter) and muscle of similar dimensions by scalpel. Samples were placed in α -MEM and washed twice in PBS prior to fixation for histology.

4.2.6 Immunohistochemistry of Porcine Meniscus and Muscle

Biopsy samples of meniscus and muscle were prepared for histological processing by washing twice in PBS and then cross-linking in 10% formalin for 20 minutes. Samples were placed in an automated tissue processor (Leica ASP300S), embedded in paraffin wax and sectioned at a thickness of 5µm using the Leica RM2235 microtome. Immunostaining was carried out using the polyclonal biotinylated collagen 2 3/4m antibody on meniscus and muscle sections using the HRP-Diaminobenzodine (DAB) kit (Envision Dako Cytomation Kit) as in section 3.2.2 and 3.2.3.

4.2.7 MSC Isolation

MSCs were isolated from the bone marrow following previous methods in section chapter 2.2.1.

4.2.8 MSC Pre-Incubation with Antibody-Peptide Constructs and Porcine Explant Culture

MSCs were trypsinised and labelled with Cell Tracker Red (Molecular Probes). The Cell Tracker Red stock solution was diluted to a final working concentration of 15µM in serum-free medium. MSCs were resuspended in the pre-warmed working solution at a cell concentration of 1×10^6 cells/ml and incubated for 45 minutes at 37°C, 5% CO₂ and 90% humidity. The cells were protected from light at all times. Following incubation, MSCs were centrifuged and washed in PBS twice and then placed in α-MEM at 37°C for a further 75 minutes prior to antibody-peptide incubation to allow time for integrin re-expression.

MSCs were next washed twice in serum-free α-MEM medium and incubated sequentially with RGD-streptavidin at 3 different concentrations, 500µg/ml, 10µg/ml and 5µg/ml at 37°C for 20 minutes. After washing twice in serum-free medium the MSCs were incubated with biotinylated collagen 2 3/4m antibody at 500µg/ml, 10µg/ml and 5µg/ml at 37°C for 20 minutes. MSCs were then washed twice in serum-free medium and 200µl of cell suspension applied to triplicate collagenase digested porcine explants for 20 minutes on a rocking platform at 37°C. Explants were washed in serum-free medium prior to MSC incubation. Controls of RGD-streptavidin alone at concentrations of 10µg/ml and 5µg/ml and MSC alone were also prepared.

After MSC incubation on porcine explants, explants were again washed twice in serum-free medium to remove any unbound MSCs and fixed in 10% formalin for 20 minutes. After fixation, explants were washed in PBS and left at room temperature until required for histological processing and paraffin embedding as described in section 3.2.2.

In addition, MSCs were pre-incubated with 5µg/ml of antibody-peptide construct and controls, 5µg/ml of RGD-streptavidin and MSCs alone and delivered on non-digested cartilage and processed as in section 3.2.2. Extra samples of digested and

non-digested explants incubated with MSCs pre-incubated with 5µg/ml of construct and peptide alone were also prepared for SEM analysis.

4.2.9 Explants and Stereology

After histological processing, sections were coverslipped using Vectorshield mountant containing DAPI (Vector Laboratories) and visualised using a Leica DMLB upright fluorescent microscope with a QImaging (Retiga Exi) camera. Quantification of cell adherence, identified as a dual labelled MSC (red and blue) was performed on 5µm sections. To exclude bias during counting, images were renamed by a colleague prior to cell counting and delivered cells were counted manually in software program Image J. The Disector method (Garcia *et al.*, 2007; Gundersen *et al.*, 1988) was used to estimate the number of cells on the surface of the explant. The density estimates were expressed as number of cells per square millimetre of explant using a stereological assessment as in section 2.2.7.

4.2.10 Fluorescence Imaging of Cartilage Explants and Sections

Higher quality images were taken using the Leica DM4000 B microscope and camera Leica DFC 450 C. Mosaic images were created by performing scans at an overall magnification of x252 using LAS software and Leica DFC4050 digital camera attached to the Leica DM4000 B microscope.

4.2.11 Scanning Electron Microscopy (SEM) imaging of MSCs Localised on Porcine Explants

Explants containing MSCs were placed in sealable glass vials containing 2% glutaraldehyde in PBS and left to fix for 2-4 hours at room temperature. Each explant was then washed/rinsed for 60 minutes in PBS, three times. A final rinse was carried out overnight at 4°C. Explants were then transferred to a series of alcohols for 20 minutes for dehydration, starting at 10% v/v and exchanging in 10% increments up to 100%. Explants were washed three times in 100% alcohol and

then left overnight. Ethanol was finally exchanged for 100% acetone, rinsed three times and left overnight in acetone prior to critical point drying.

Dehydration was completed via a transition fluid of supercritical liquid carbon dioxide in a Leica EM CPD 030 critical point drier. The ethanol infiltrated specimens were transferred to the pressure vessel of the critical point drier and ethanol was exchanged for CO₂ over 9 rinse cycles at approximately 9°C/800psi, ensuring specimens remained submerged in liquid throughout each exchange. The temperature of the specimens and liquid CO₂ was increased to 40°C within 10 minutes to allow the phase transition to gaseous CO₂ to occur (pressure rising to approximately 1200 psi). The excess pressure was vented gently and the dehydrated specimens were removed and stored at room temperature in a sealed container prior to mounting and sputter coating.

Dehydrated specimens from each sample group were mounted on individual 25mm diameter aluminium pin stubs by means of electrical conduction colloidal silver paint (Agar Scientific UK Ltd.). The paint mountant was allowed to dry overnight at room temperature prior to sputter coating with approximately 7nm of platinum. Sputter coating was carried out using a Leica EM ACE 600 high resolution sputter coater (supplied by Leica Microsystems GmbH, Germany) – the following coating conditions were used:

Material	Platinum
Vent after Process	FALSE
Sputter Current	22mA
Pre-Process Vacuum	2.3E-5 mbar
Sputter Vacuum	2.5E-2mbar
Thickness	7.0 nm
Source	1
Purge Cycles	3
Sample Height	12.0 mm
Rotation	3
Working Distance	50 mm
Tilt	0.0°

Table 4.1: Sputter coating conditions for cartilage explants using the Leica EM ACE 600.

An FEI NovaNano200 SEM, Scanning Electron Microscope was used to image the mounted samples; the following conditions were used throughout:

Accelerating voltage	3kV, 5kV and 15kV
Spot size	2.0
Working distance	≤5.0mm
Detectors	ETD (high resolution), TLD (ultra-high resolution)
Vacuum mode	High Vacuum

Table 4.2 Conditions used for imaging samples on the FEI NovaNano200 SEM.

4.2.12 MSC Morphology

MSCs, incubated in suspension for 2 hours at 37°C after trypsinisation, were pre-incubated with 5µg/ml of RGD-streptavidin, followed by 5µg/ml of biotinylated antibody. Controls of 5µg/ml of RGD-streptavidin, RAD-streptavidin, streptavidin, RGD, biotinylated antibody and MSCs alone were set up. MSCs were plated down in monolayer at a seeding density of $1 \times 10^4/\text{cm}^2$ and images were taken at 3 days using the Olympus BX51 upright brightfield microscope and QImaging (Retiga Exi) camera.

4.2.13 MSC Viability and Proliferation

MSCs, incubated in suspension for 2 hours at 37°C after trypsinisation, were subsequently pre-incubated with two different concentrations of RGD-streptavidin (10µg/ml and 5µg/ml) for 20 minutes and then incubated with equal concentrations of biotinylated antibody. Controls of RGD-streptavidin, biotinylated antibody and MSCs alone were also set up. MSCs were seeded in monolayer in 96-well plates at a cell concentration of $1 \times 10^4/\text{cm}^2$ and cultured in α -MEM and 5ng/ml rhFGF-2 for a period of 3 days. For viability assessment, WST-1 reagent (stable tetrazolium salt; Roche) was added to each sample well following the manufacturer's instructions. Briefly, 10µl of WST-1 reagent was added to each culture well containing 100µl of

medium and plates incubated for 2 hours at 37°C. Plates were then read using the Multiskan Ascent plate reader at 450nm.

To assess proliferation, MSCs were prepared and incubated following the same procedure as for the viability assay. Cells were seeded at a density of $1 \times 10^4/\text{cm}^2$ in a 96-well plate and cultured for 3 days in α -MEM and 5ng/ml rhFGF-2. Cells were lysed using 0.1% Triton x-100 (Sigma), scraped and then placed in a microcentrifuge tube and subsequently vortexed to pellet cell debris. The Quant-iT PicoGreen dsDNA assay kit (Molecular Probes) was utilised according to the manufacturer's protocol. Briefly, kit stock solutions were prepared and 100 μ l of lysed cell solution samples (in triplicate) and kit standards provided (DNA 100 μ g/ml diluted in 200 mM Tris-HCl, 20 mM EDTA, pH 7.5), were added to the wells of a 96-well black flat-bottomed plate, followed by the addition of PicoGreen solution (diluted in Tris-EDTA; TE) and incubated for 3 minutes at room temperature. Samples were evaluated on a Multiskan Ascent plate reader, exciting at 485nm and reading at 538nm.

4.2.14 MSC Osteogenesis

MSCs, previously incubated in suspension for 2 hours at 37°C, were pre-incubated with 500 μ g/ml, 10 μ g/ml and 5 μ g/ml RGD-streptavidin, and then equal concentrations of biotinylated antibody. Controls of the same concentrations of RGD-streptavidin alone and biotinylated antibody were also prepared, including MSCs alone. For osteogenic differentiation of the MSCs, the same methods were followed as described in section 2.2.4, measuring calcium content and Alizarin Red staining for mineralisation. Alizarin Red images were taken using Olympus CK40 light microscope and digital camera, Olympus camera (C-3030 zoom).

4.2.15 MSC Adipogenesis

MSCs, previously incubated in suspension for 2 hours at 37°C after trypsinisation, were pre-incubated with 500 μ g/ml, 10 μ g/ml and 5 μ g/ml of RGD-streptavidin and biotinylated antibody and then induced to undergo adipogenic differentiation using

the Lonza adipogenic bullet kit. MSCs were seeded in a 24-well plate at a concentration of 8.4×10^4 /ml. The MSCs were fed every 2-3 days with fresh adipogenic maintenance medium (Lonza, Poietics™) and then exposed to 3 cycles of induction/maintenance adipogenic medium (Lonza, Poietics™), with each cycle consisting of changing the medium every 3 days. Non-induced adipogenic controls were given maintenance medium only for the duration of the culture period. After 3 cycles, the MSCs were left in culture for a further 7 days in adipogenic maintenance medium, replacing the medium every 2-3 days. Differentiation was analysed by Oil Red O visualization and quantification of lipid vacuoles in the induced cells as described previously in section 2.2.4.

4.2.16 MSC Chondrogenesis

MSCs, previously incubated in suspension for 2 hours at 37°C, were pre-incubated with 10µg/ml of RGD-streptavidin and then 10µg/ml of biotinylated antibody. Controls with RGD-streptavidin and biotinylated antibody and MSCs alone were set up. MSCs were induced to chondrogenic differentiation through pellet culture following previous methods as described in section 2.2.4 and analysed by DMMB for GAG analysis and Safranin O staining. Pellet images were taken using the Leica DMLB upright microscope (brightfield) and QImaging (Retiga Exi) camera.

In an attempt to analyse the transient persistence of RGD-streptavidin during chondrogenesis, MSCs pre-incubated with 10µg/ml of construct and controls were subsequently placed in culture at a seeding density of 0.5×10^4 /cm² with expansion medium until confluent. MSCs cultured separately for each group were then trypsinised and induced to chondrogenic differentiation through pellet culture as described in section 2.2.4

4.2.17 Statistical Analysis

All values were expressed as the mean \pm standard deviation of the mean (SD). Datasets were tested for significance using the two-way ANOVA as in previous methods 2.2.9.

4.3 Results

4.3.1 Porcine Cartilage Staining of the Polyclonal Collagen 2 3/4m

Immunohistochemical staining was performed on porcine cartilage sections with and without collagenase digestion. Sections were incubated with biotinylated collagen 2 3/4m antibody, non-biotinylated collagen 2 3/4m antibody and a collagen type II antibody. Additionally, sections were stained with Safranin O stain and negative controls were stained without antibody incubation (Figure 4.1). The biotinylated collagen 2 3/4m antibody demonstrated superficial positive staining on sections digested with collagenase for 1 hour (A) and non-superficial staining on non-digested sections (F). The non-biotinylated collagen 2 3/4m antibody showed a similar staining pattern on digested cartilage with higher signal intensity (B); similarly, non-digested sections stained non-superficially (G). The collagen type II antibody demonstrated a similar staining pattern on digested cartilage, comparable to the polyclonal biotinylated and non-biotinylated collagen 2 3/4m antibody. However, staining was less intense (C). Staining on non-digested cartilage showed an intense, superficial staining pattern, different to that of the polyclonal biotinylated and non-biotinylated collagen 2 3/4m antibody (H). Safranin O staining showed a characteristic osteoarthritic cartilage staining pattern, the loss of GAGs superficially with staining observed in the middle and deeper zones (D). Staining of non-digested cartilage showed an intense stain, demonstrating maintenance of GAG (I). Negative controls for both digested and non-digested cartilage showed no positive staining (E,J).

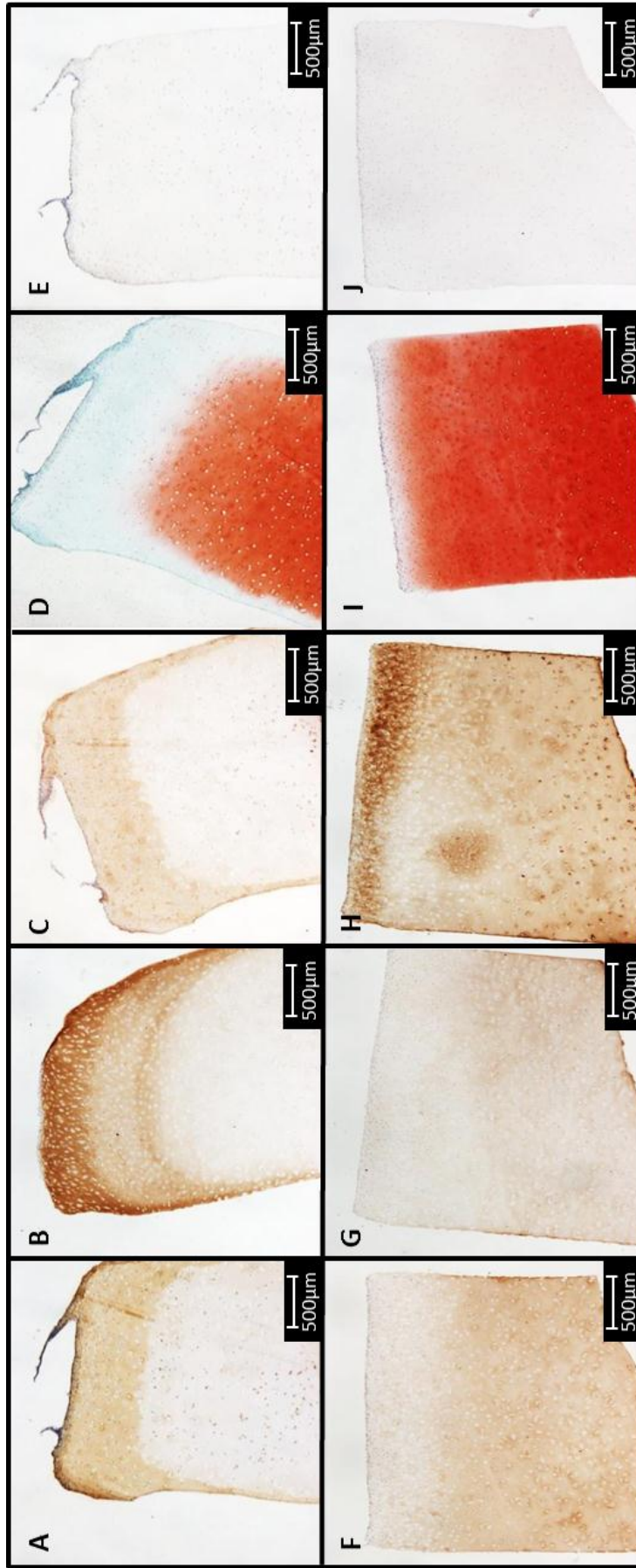


Figure 4.1: Comparison of Immunostaining of Porcine Cartilage with Polyclonal Collagen 2 3/4m and Collagen II Antibodies

Porcine cartilage sections with (A-E) and without (F-G) collagenase digestion were immunostained for the collagen 2 3/4m epitope using both biotinylated and non-biotinylated antibody and collagen type II. Superficial positive staining for the biotinylated and more intense staining by the non-biotinylated collagen 2 3/4m antibody was observed (A, B respectively). Non-superficial, weak staining using the polyclonal antibody on non-digested sections was demonstrated (F, G biotinylated and non-biotinylated antibody respectively). Superficial positive staining of collagen type II was observed on both collagenase and non-collagenase digested sections (C, H respectively), with intensity and distribution throughout greater however on non-digested sections (H). Safranin O staining of cartilage sections (D, I) shows loss of GAG superficially in digested sections (D) as compared to a maintenance of GAG in non-digested sections (I). No staining is observed for antibody negative sections, (E, J, representative of all antibodies). Scale bar, 500µM.

4.3.2 Collagen 2 3/4m Peptide Block on Degraded Cartilage

Immunohistochemical staining of the biotinylated collagen 2 3/4m antibody was performed on porcine collagenase digested cartilage sections with or without collagen 2 3/4m peptide blocking (Figure 4.2). Peptide blocking demonstrated no positive antibody staining (A) with only minimal non-specific staining compared to the negative control (C). Sections stained without peptide block showed a strong positive staining pattern as observed previously (B). The negative control section showed no signs of positive staining but artifactual staining was visible (C).

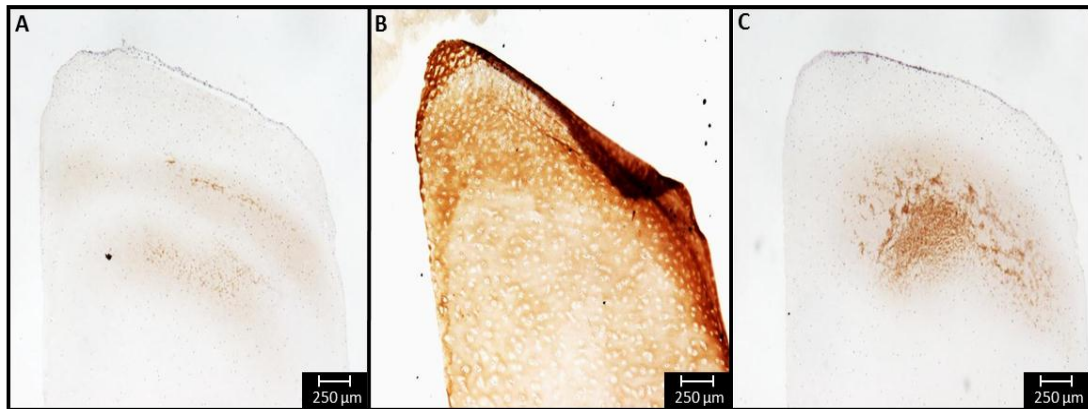


Figure 4.2: Specificity of the Polyclonal Collagen 2 3/4m Antibody

Porcine collagenase digested cartilage sections were blocked with the collagen 2 3/4m peptide prior to biotinylated collagen 2 3/4m antibody staining. Blocked sections demonstrated no positive staining of antibody (A). Un-blocked sections showed positive staining (B) and negative sections without antibody demonstrated no staining (C). Scale bar, 250μM.

4.3.3 Biotinylated Collagen 2 3/4m Antibody Staining on Porcine Meniscus and Muscle

Immunohistochemical staining of the biotinylated collagen 2 3/4m antibody was performed on porcine meniscus and muscle sections (Figure 4.3). Positive staining was observed in small, specific areas on porcine meniscus (A), however, no positive staining was evident on muscle sections as expected (C). Negative control sections, without antibody incubation demonstrated no positive staining (B, D).

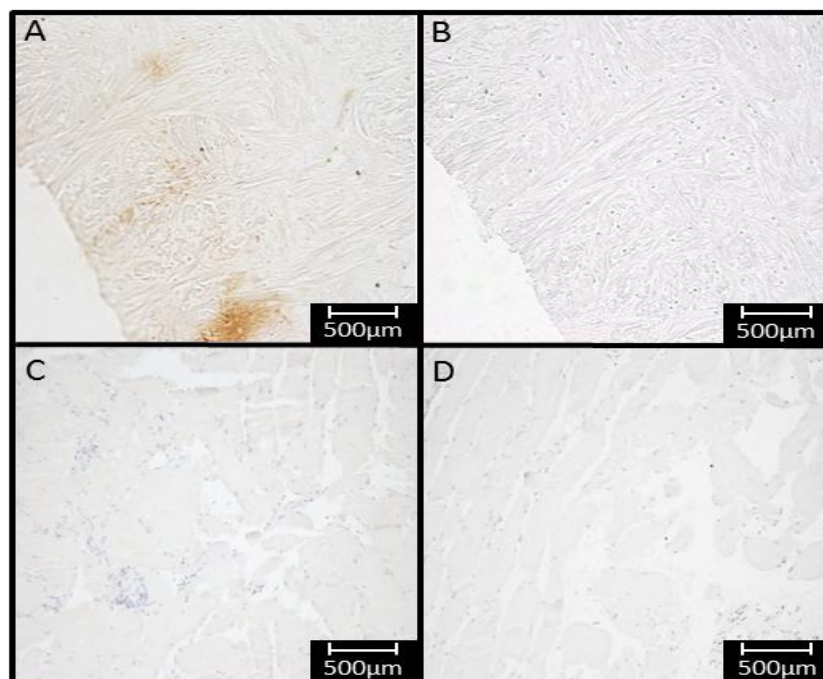


Figure 4.3: Polyclonal Collagen 2 3/4m Antibody Staining of Meniscus and Muscle

Porcine meniscus and muscle sections were immunostained with the biotinylated collagen 2 3/4m antibody. Meniscus sections stained positively in small areas (A) and muscle sections demonstrated an absence of positive staining (C). Negative sections (B, D) showed no positive staining of antibody. Scale bar, 500µM.

4.3.4 MSC Adhesion to Degraded Cartilage with the RGDStBAb Construct and RGDSt: Fluorescence Imaging

MSC adhesion after incubation with varying concentrations of RGDStBAb construct and RGDSt construct to the top surface of collagenase digested cartilage was visualised fluorescently (Figure 4.4A). MSCs were labelled with cell tracker red and sections mounted with DAPI nuclei stain, staining both MSCs and cartilage sections. The MSC alone control (A, B) showed some adherence of cells to the cartilage surface, but only in small isolated areas. MSCs pre-incubated with the lowest concentration of RGDStBAb (5µg/ml), demonstrated the highest amount of adhered MSCs that were consistently spread over the surface of the cartilage explant (C, D). MSCs pre-incubated with 10µg/ml of RGDStBAb, showed an increase in adherence over the 500µg/ml concentration and MSC alone control. However, adherence of MSCs occurred as aggregations on the cartilage surface (E, F). The highest concentration of RGDStBAb construct (500µg/ml) demonstrated the lowest adherence of MSCs which was observed in small areas, but with an increase over that of the MSC alone controls (G, H). MSC pre-incubation with the lowest concentration of RGDSt (5µg/ml) demonstrated increased MSC adhesion, more consistently spread across the surface of the cartilage (I, J). However, numbers of MSCs adhered were lower than that of the 10µg/ml RGDSt concentration. MSCs pre-incubated with RGDSt construct at a concentration of 10µg/ml also demonstrated an increased adhesion of MSCs in aggregations at the surface of the cartilage, higher than all other groups, but less than with 5µg/ml of the RGDStBAb construct (K, L). All MSCs pre-incubated with either RGDStBAb or RGDSt alone demonstrated overall, flatter adhered cell morphologies as compared to MSCs alone that were rounder in shape. Observations of the entire explant for each treatment group (Figure A, C, E, G, I, K) also show adherence of MSCs to the sides and bottom of the explants, however only the articular top surface was analysed.

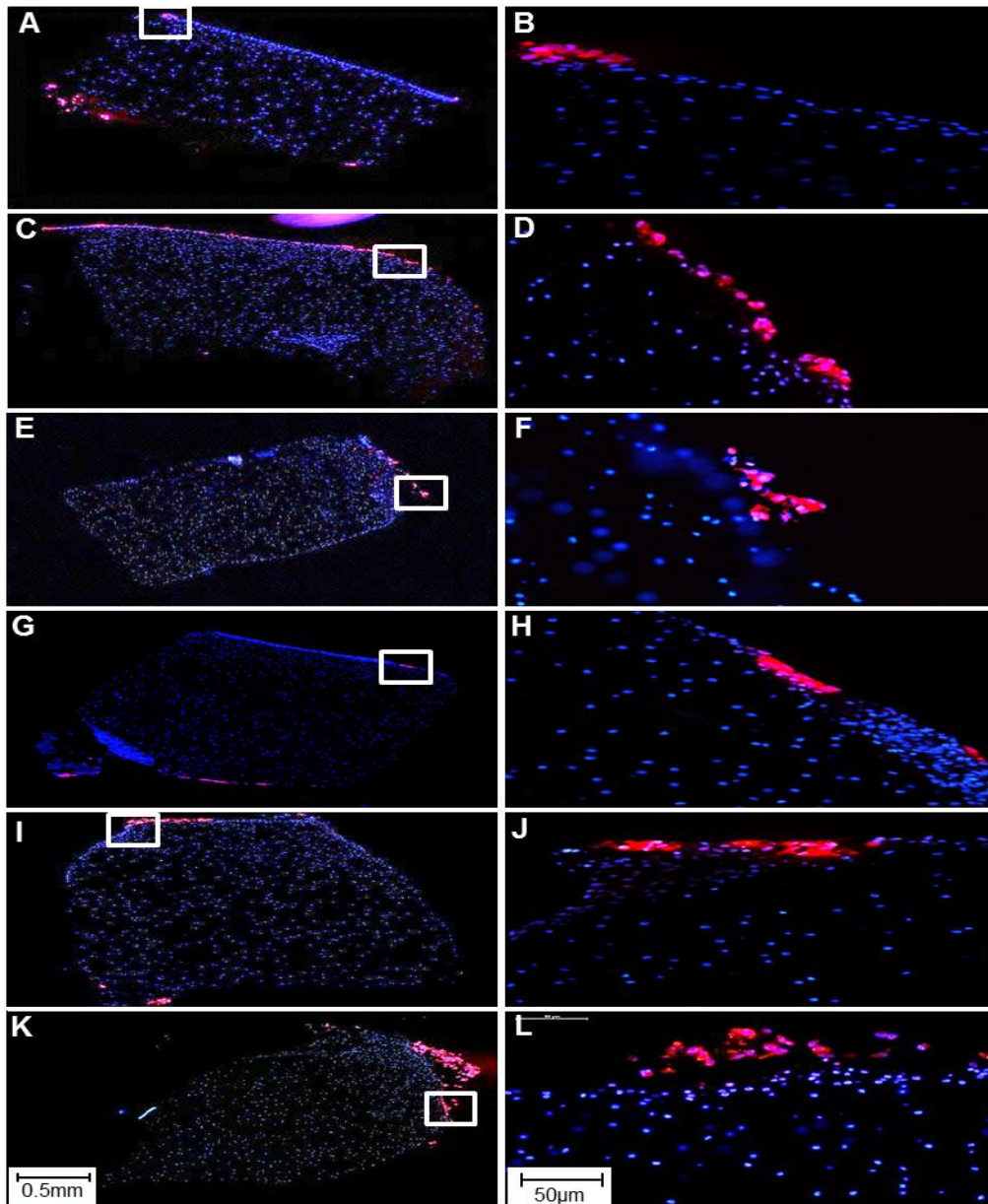


Figure 4.4A: Fluorescence Analysis of MSC Adhesion to Degraded Cartilage

MSCs labelled fluorescently with cell tracker red, pre-incubated with RGDStBAb and RGDSt constructs delivered to the degraded porcine cartilage surface were photographed and a mosaic image of the entire explant was constructed (A, C, E, G, I, K). Adhered MSCs are shown as red with DAPI labelling both chondrocytes and MSCs. MSCs alone showed a small amount of adherence to the cartilage surface (A, B). A small increase in adherence compared to MSCs alone was shown with 500µg/ml of RGDStBAb construct (G, H). An increase in adherence was observed with both 5µg/ml and 10µg/ml RGDStBAb construct (C-F, respectively), with an even spread of MSCs over the cartilage surface for the 5µg/ml concentration (C, D). Both concentrations of RGDSt demonstrated an increase in MSC adherence (I-L) with an even spread at 5µg/ml (I, J) compared to aggregated MSCs observed using 10µg/ml (K, L). Scale bars, 0.5mm for A, C, E, G, I and K; 50µm for B, D, F, H, J and L.

4.3.5 MSC Adhesion to Degraded Cartilage with the RGDStBAb Construct and RGDSt: Stereology

A stereological analysis of cell number was performed for the top surface of collagenase digested porcine cartilage explants cultured with MSCs for 20 minutes. MSCs were pre-incubated with 5µg/ml, 10µg/ml or 500µg/ml of RGD-streptavidin conjugate, followed by the same concentration of biotinylated collagen 2 3/4m (RGDStBAb). Additional controls included 5µg/ml or 10µg/ml of RGD-streptavidin construct (RGDSt) and a count was also performed on MSCs alone retained on the cartilage surface (Figure 4.4B). MSC adhesion was demonstrated in small numbers by MSCs alone. Pre-incubation of MSCs with 5µg/ml of RGDStBAb construct showed a significant increase of adhered MSCs compared to MSCs alone. MSCs pre-incubated with 10µg/ml of RGDStBAb construct also demonstrated an increase in MSC adhesion over MSCs alone at levels higher than the 500µg/ml treated explants, where MSC adhesion was only slightly increased over MSCs alone. Treatment of collagenase digested porcine cartilage explants with 10 or 500µg/ml construct was not statistically significant compared to the control MSC alone group. Pre-incubation of MSCs with concentrations of 5µg/ml or 10µg/ml RGD-streptavidin construct alone also demonstrated enhanced MSC adhesion and similar to the 10µg/ml concentration of the RGDStBAb construct.

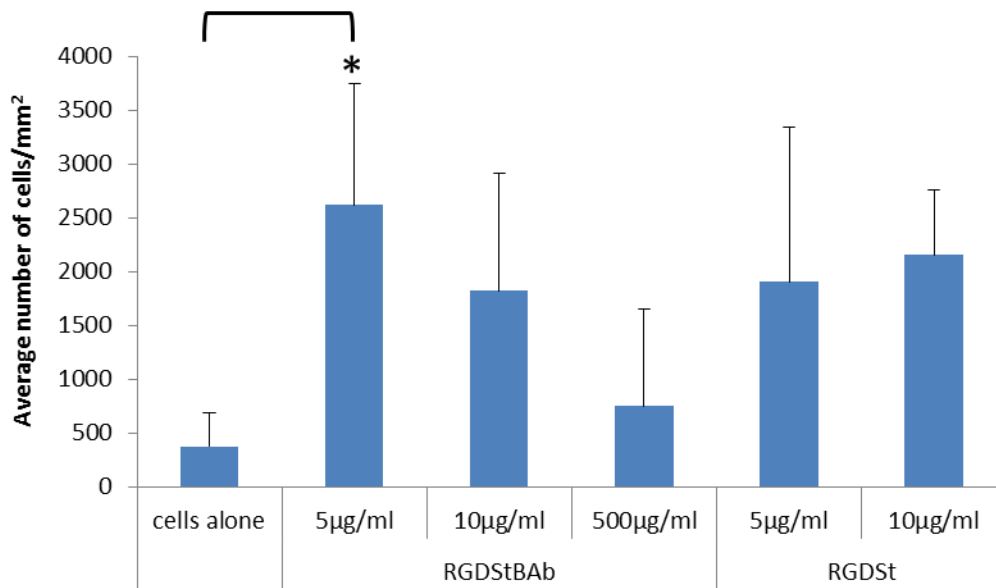


Figure 4.4B: MSC Adhesion at the Degraded Cartilage Surface: Stereological Analysis

MSCs labelled fluorescently with cell tracker red, pre-incubated with RGDStBAb construct and delivered to the degraded porcine cartilage surface were quantified for adherence by stereology. MSCs alone showed small amounts of adherence to the degraded cartilage surface. MSCs pre-incubated with RGDStBAb construct demonstrated enhanced adhesion with decreasing concentration. A statistically significant increase was shown with RGDStBAb construct at a concentration of 5µg/ml compared to cells alone. MSCs pre-incubated with RGDSt demonstrated enhanced adhesion, with 10µg/ml on average higher. Data is presented as the mean \pm SD of n=3 biological replicates, generated using triplicate measurements *= $p \leq 0.05$.

4.3.6 MSC Adhesion to Non-Degraded Cartilage with the RGDStBAb Construct and RGDSt: Fluorescence Imaging

MSCs were pre-incubated with 5 μ g/ml concentrations of RGDStBAb and RGDSt construct and adhesion to the top surface of non-degraded cartilage was visualised by fluorescence (Figure 4.5A). MSCs were labelled with cell tracker red and sections mounted with DAPI nuclei stain, staining both MSCs and cartilage sections. MSCs alone, demonstrated very little adhesion to the non-degraded cartilage surface (A, B). MSCs pre-incubated with RGDStBAb construct demonstrated comparable adhesion to that of MSCs alone, with only a small increase in adhesion (C, D). Pre-incubation of MSCs with RGDSt construct showed a higher number of adhered MSCs in small aggregations (E, F).

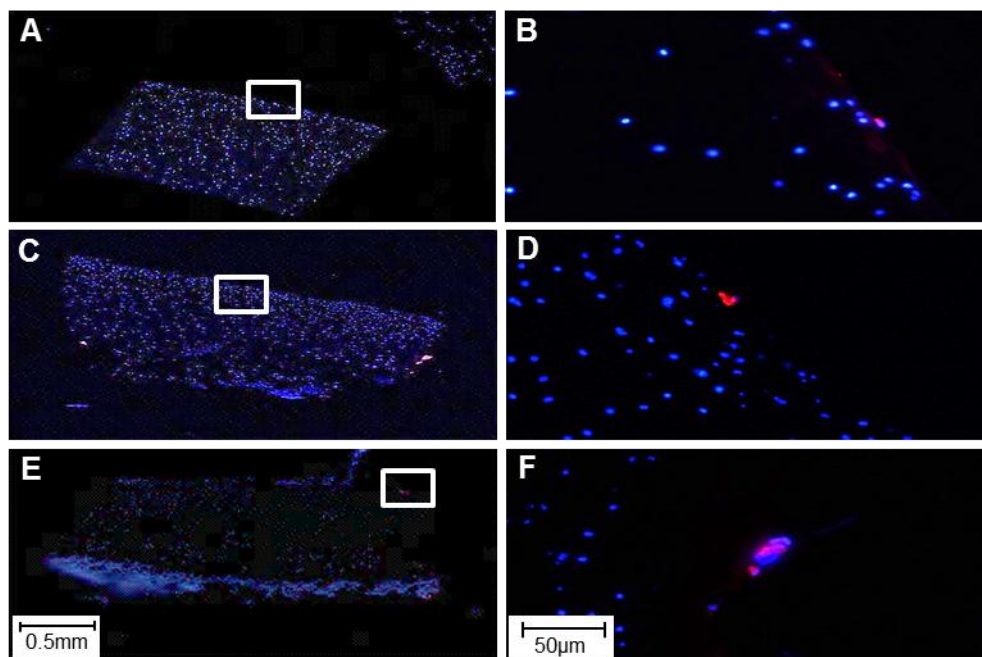


Figure 4.5A: Fluorescence Analysis of MSC Adhesion to Non-Degraded Cartilage

MSCs labelled fluorescently with cell tracker red, pre-incubated with 5 μ g/ml RGDStBAb construct or RGDSt alone and delivered to the degraded porcine cartilage surface, were photographed at the cartilage surface and a mosaic image of the entire explant was constructed (A, C, E). Adhered MSCs are labelled red and DAPI nuclei stain labelled both chondrocytes and MSCs. MSCs alone showed a small amount of adherence to the cartilage surface (A, B). A small increase in MSC adherence was observed with the RGDStBAb construct (C, D) and the highest amount observed with the RGDSt alone (E, F). Scale bars, 0.5mm for A, C and E; 50 μ m for B, D and F.

4.3.7 MSC Adhesion to Non-Degraded Cartilage with the RGDStBAb Construct and RGDSt: Stereology

A stereological cell count was performed on the top surface of non-degraded porcine cartilage explants cultured with MSCs for 20 minutes. MSCs were pre-incubated with 5µg/ml of RGDSt, followed by the same concentration of BAb (RGDStBAb). Controls included 5µg/ml of RGDSt construct alone and a control of MSCs alone (Figure 4.5B). MSCs alone demonstrated a small amount of adhesion (average 66.948/mm²), however this was much lower than previously seen on degraded cartilage (average 226.1561/mm²). MSCs pre-incubated with 5µg/ml of RGDStBAb construct demonstrated a non-significant increase in MSC adhesion over MSCs alone, however still at lower levels compared to that on degraded cartilage. The highest amount of MSC adhesion was observed on explants cultured with MSCs pre-incubated with 5µg/ml of RGDSt construct. However, this increase was not statistically significant over the MSC alone control.

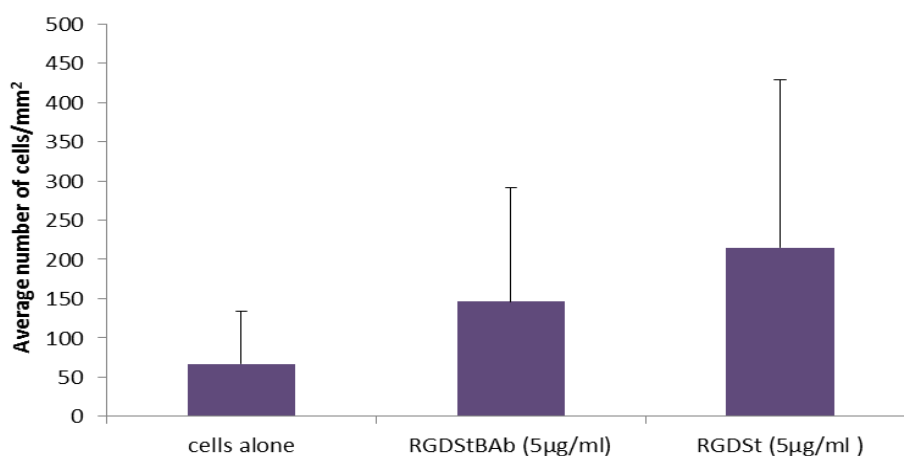


Figure 4.5B: MSC Adhesion at the Non-Degraded Cartilage Surface: Stereological Analysis

MSCs labelled fluorescently with cell tracker red and pre-incubated with 5µg/ml RGDStBAb construct or RGDSt alone were delivered to the non-degraded porcine cartilage surface and quantified for adherence by stereology. MSCs alone showed a small amount of adherence to the cartilage surface. A non-significant increase of MSC adherence was shown with the RGDStBAb construct and a further increase observed with RGDSt alone. Data is presented as the mean ± SD of n=3 biological replicates, generated using triplicate measurements.

4.3.8 MSC Morphology after Binding of the RGDStBAb Construct

MSCs were pre-incubated with 5 μ g/ml of RAD-streptavidin (RADSt), RGDSt, BAb, streptavidin (St), RGD alone or RGDStBAb. MSCs were then cultured in monolayer and morphology observed at day 3 of culture (Figure 4.6). All MSCs demonstrated the characteristic fibroblastic, spindle-shaped morphology, typical of MSCs (A-G). It was observed that MSCs pre-incubated with RGDSt, BAb, RGDSt alone and the RGDStBAb construct also demonstrated small aggregations of MSCs (indicated by red arrows) (C, D, F, G).

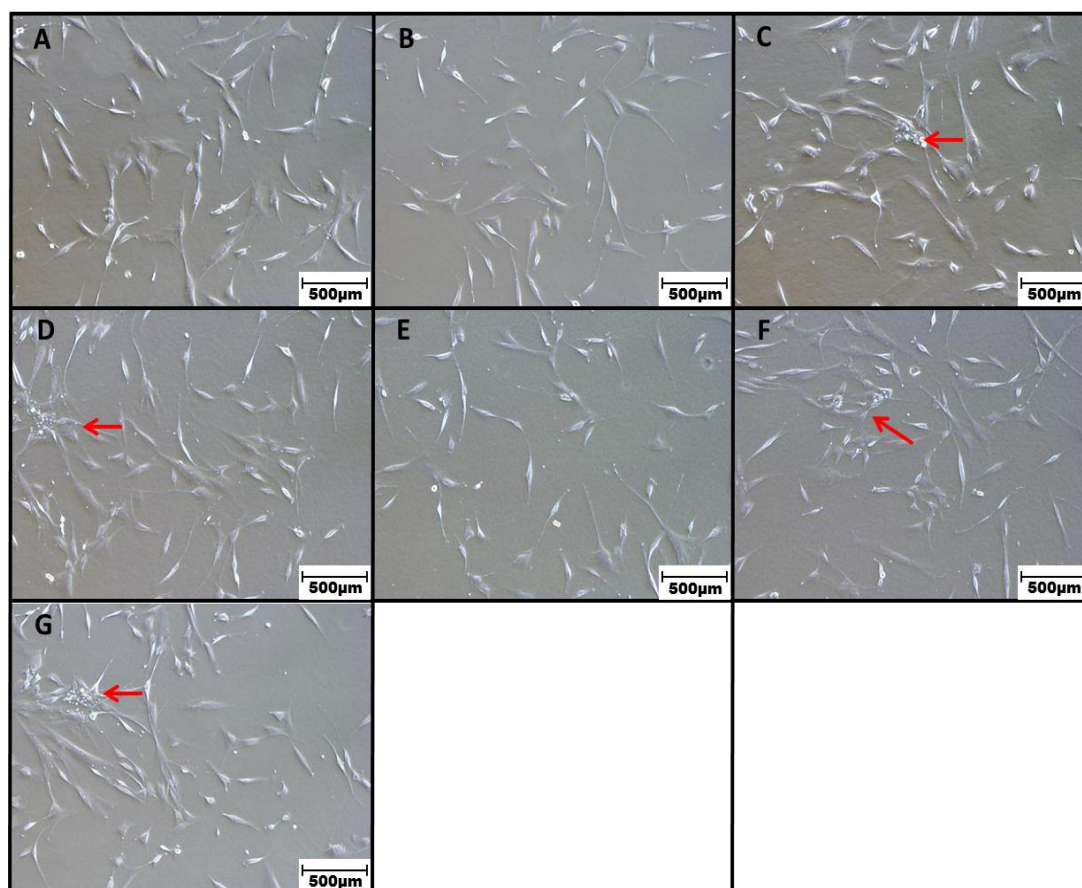


Figure 4.6: MSC Morphology with RGDStBAb and Components in Monolayer
MSCs were pre-incubated with 5 μ g/ml RGDStBAb construct (G), RADSt (B), RGDSt (C), BAb (D), St (E) and RGD (F) alone. An MSC alone control (A) was included and cultured in monolayer for 3 days before photography. All MSCs showed characteristic MSC fibroblastic morphology (A-G). MSCs pre-incubated with RGDSt, BAb, RGD and RGDStBAb demonstrated small aggregations (C, D, F, G respectively, red arrows). Scale bar 500 μ M.

4.3.9 SEM Analysis of MSC Morphology Upon Adhesion to Degraded Cartilage

MSCs were pre-incubated with 5µg/ml concentrations of RGDStBAb construct, RGDSt and incubated with collagenase digested porcine cartilage explants for 20 minutes. An MSC alone control was included (Figure 4.7). Explants were fixed in glutaraldehyde and analysed by SEM. MSCs alone (A-D) bound to the degraded cartilage surface to a lesser extent (A) and demonstrated mostly a typical rounded morphology (B-D) than MSCs incubated with the RGDStBAb construct (E-H). The construct promoted binding of the MSCs (E) with bound cells demonstrating more of a flattened, spread morphology on the cartilage surface (F-H). MSCs incubated with RGDSt alone (I-L), also showed a higher number of adhered cells compared to MSCs alone (I), a similar flattened morphology with MSCs adhered in aggregates (J-L).

Images at higher magnification, (20µm D, H, and L) demonstrated differences in morphology of MSCs between groups. MSCs alone (D) demonstrated rounded MSC morphology with some projections of pseudopodia and surface protein projections. MSCs with RGDStBAb at higher magnification (H), showed more pseudopodia/filapodia, suggesting enhanced MSC adhesion to the cartilage. Higher magnification of MSCs incubated with RGDSt (L), also demonstrated surface protein projections and increased pseudopodia/filapodia projections compared to MSCs alone. Low magnification overviews (A, E, I) show that MSCs can also be seen on the vertical sides of the biopsied tissue cylinder, adhering to the artificial cut surface of the cartilage explant.

Higher magnification images (Figure 4.8), reveal all MSC surfaces showing proteins (A-I) and some evidence of membrane blebbing (B, D). Pseudopodia attachment to the articular surface was observed in MSCs alone (A-C), however MSCs incubated with either RGDStBAb construct (D-F) or RGDSt (G-I) alone demonstrated more surface proteins and pseudopodia.

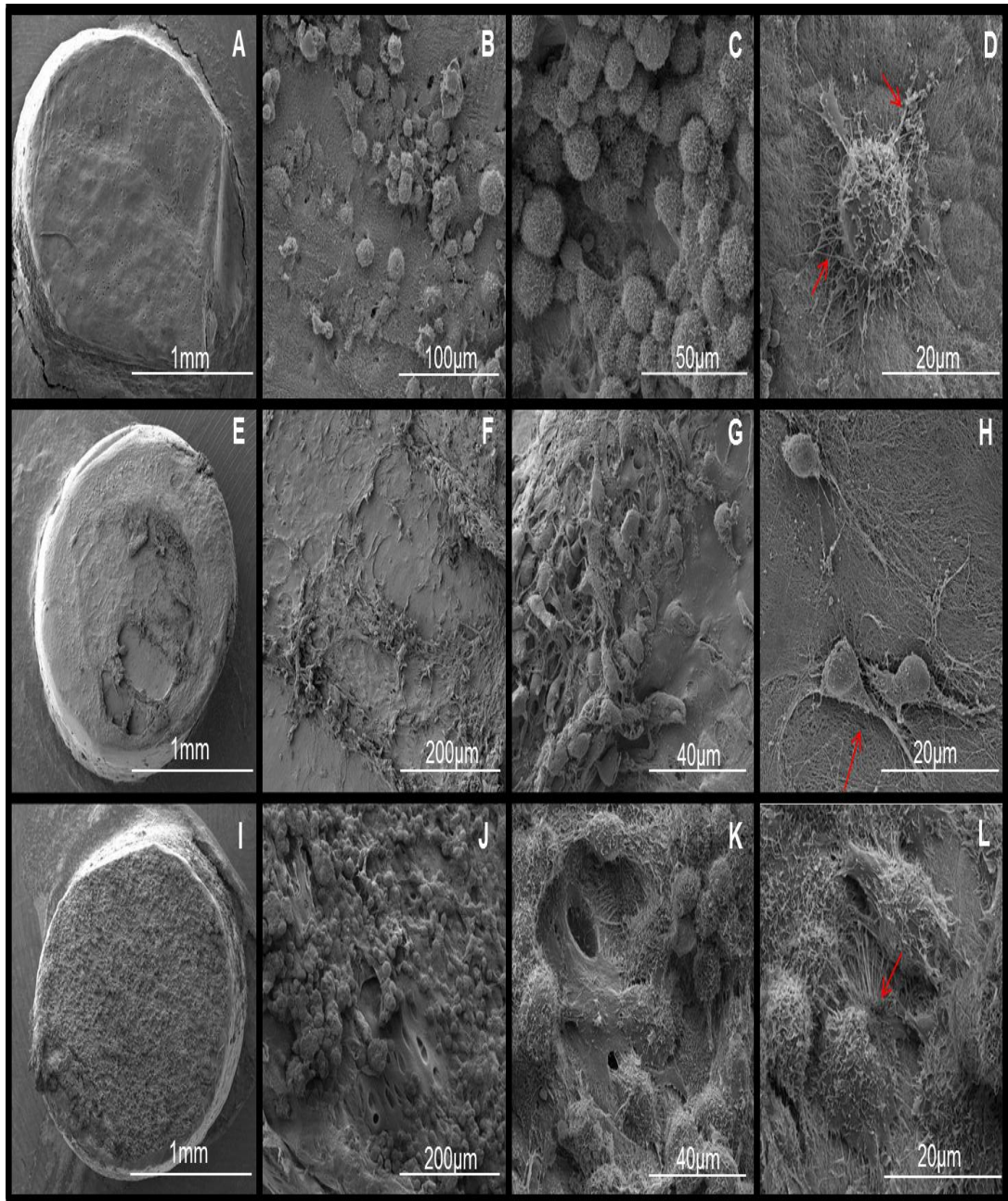


Figure 4.7: Analysis of MSC Adherence to Degraded Cartilage Explants with SEM

MSCs were pre-incubated with 5µg/ml with RGDS_tBAb or RGDS_t alone and delivered to collagenase digested porcine cartilage explants for 20 minutes and analysed by SEM. A range of images at different magnifications are shown (A-L). Low magnification views of articular surface of explants show a topical overview of numbers of MSCs bound, alone or with RGDS_tBAb or RGDS_t (A, E, I respectively). MSCs alone showed a predominantly rounded morphology at the articular surface with fewer numbers bound compared to cells pre-treated with RGDS_tBAb and RGDS_t (A-D). MSCs incubated with RGDS_tBAb demonstrated a more flattened, spread morphology at the articular surface with higher numbers bound (E-H). At higher magnification many filapodia/pseudopodia were observed (H, red arrow). MSCs incubated with RGDS_t demonstrated a flattened morphology with higher numbers at the articular surface (I-L) and showed projections of many filapodia on adhered, flattened MSCs (L). Scale bars, 1mm for A, E and I; 100µm for B; 200µm for F and J; 50µm for C; 40µm for G and K; 20µm for D, H and L.

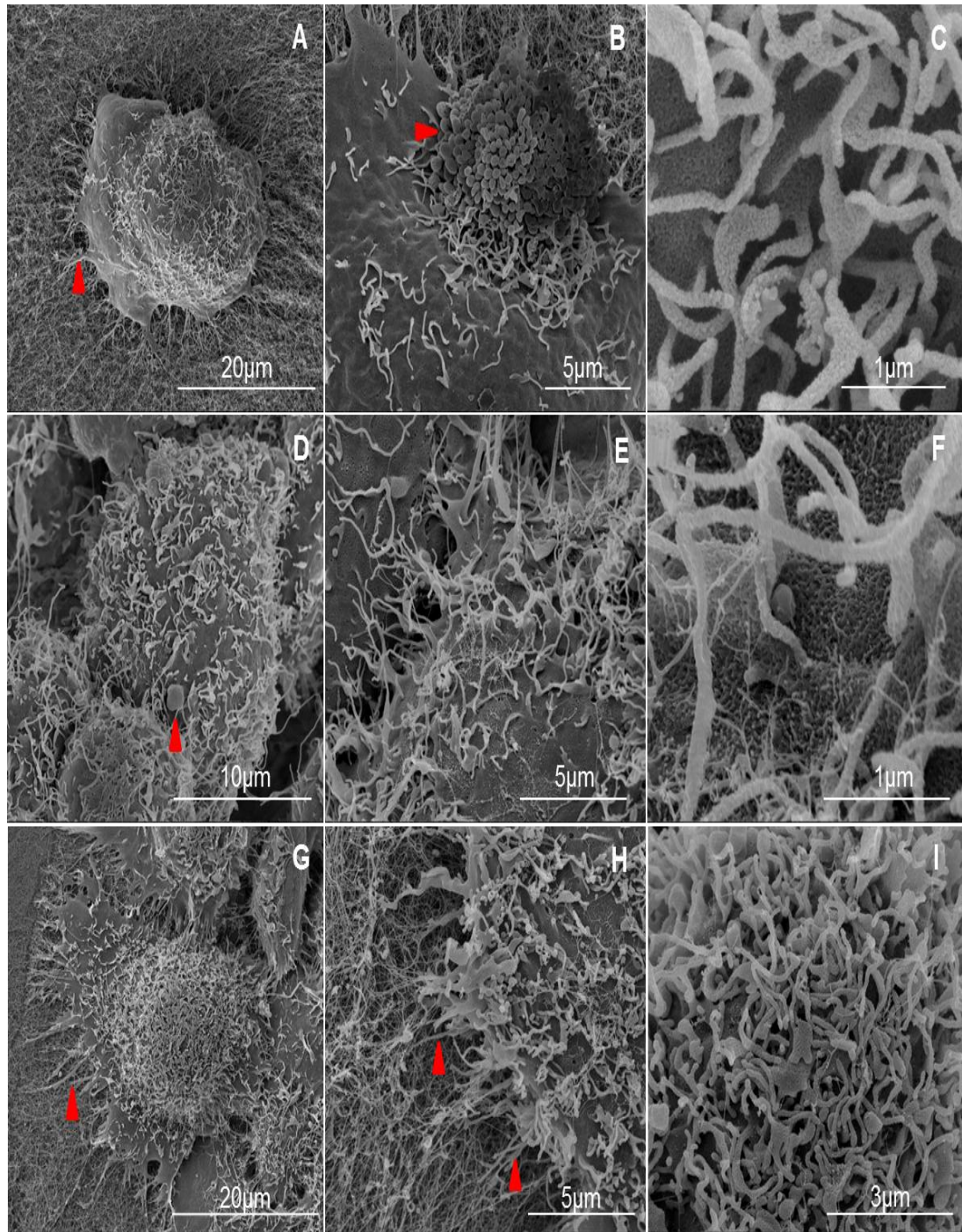


Figure 4.8: MSC Surface Topography on Degraded Cartilage Explants with SEM

MSCs were pre-incubated with 5µg/ml with RGDStBAb or RGDSt alone and delivered to collagenase digested porcine cartilage explants for 20 minutes and analysed by SEM. A range of high magnification images are shown (A-I). All MSC surfaces show proteins (A-I) and some evidence of membrane blebbing (B, D, red arrows). MSCs alone (A-C), showed some pseudopodia attachment (red arrow head) to the articular surface. MSCs incubated with either RGDStBAb construct (D-F) or RGDSt (G-I) alone demonstrate more surface proteins and pseudopodia. Scale bars, 20µm for A and G; 10µm for D; 5µm for B, E and H; 1µm for C and F; 3µm for I.

4.3.10 SEM Analysis of MSC Morphology Upon Adhesion to Non-Degraded Cartilage

MSCs were pre-incubated with 5 μ g/ml concentrations of the RGDStBAb construct, RGDSt and incubated with non-degraded porcine cartilage explants for 20 minutes. A MSC alone control was also included (Figure 4.9). MSCs showed morphologies similar to that of MSCs adhered to degraded cartilage; MSCs alone demonstrated a rounded morphology (A) compared to the flattened, spread morphology that can be seen of the MSCs over the articular surface when incubated with RGDStBAb construct and RGDSt alone (B, C).

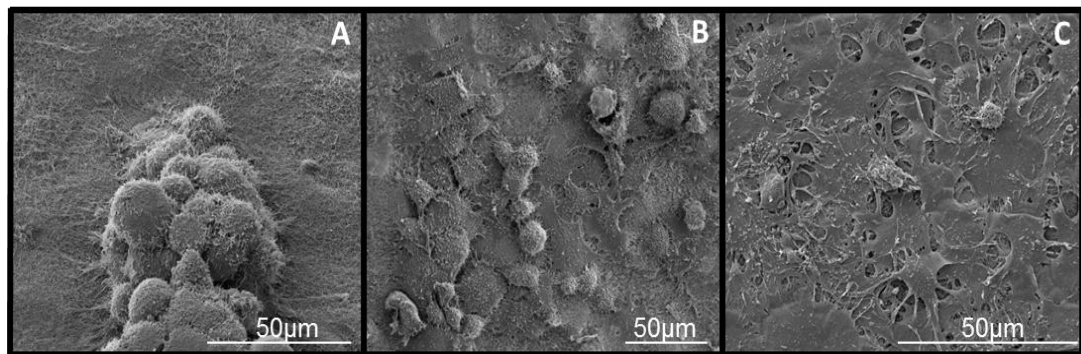


Figure 4.9: MSC Adherence to Non-Degraded Cartilage Explants with SEM

MSCs were pre-incubated with 5 μ g/ml with RGDStBAb or RGDSt alone and delivered to non-degraded porcine cartilage explants for 20 minutes and analysed by SEM. MSCs alone demonstrated a rounded morphology at the articular surface (A). MSCs incubated with RGDStBAb demonstrated a mixed morphology of flattened and rounded cells at the surface of the cartilage (B). In contrast MSCs incubated with RGDSt showed a flattened, spread morphology over the articular surface (C). Scale bars, 50 μ m.

4.3.11 MSC Viability and Proliferation after Binding of the RGDStBAb Construct

MSCs were pre-incubated with 5µg/ml and 10µg/ml concentrations of RGDSt, followed by the same concentrations of BAb (RGDStBAb) for 20 minutes and then cultured in monolayer for 3 days. Controls included MSCs alone, RGDSt at 5µg/ml and 10µg/ml and biotinylated antibody at 5µg/ml and 10µg/ml. Viability was assessed by WST-1 assay and a PicoGreen assay for DNA concentration (Figure 4.10). MSCs pre-incubated with RGDStBAb and the separate components demonstrated higher metabolic activity at all concentrations compared to MSCs alone, however this was not statistically significant (A). Pre-incubations with both concentrations of biotinylated antibody and RGDSt alone demonstrated highest levels of metabolic activity over MSC alone control and RGDStBAb construct (A). RGDSt incubation with MSCs at a concentration of 10µg/ml, showed the highest amount of formazan production as compared to all other treatment groups, however, this was not statistically significant.

MSCs alone demonstrated the highest concentration of DNA compared to all other treatment groups but results were not statistically significant (B). Analysis of the ratio of metabolic activity to DNA concentration (C), showed an increase in activity of MSCs pre-incubated with RGDStBAb construct and separate components as compared to the MSC alone control. RGDSt at a concentration of 10µg/ml again demonstrated the highest metabolic activity (C).

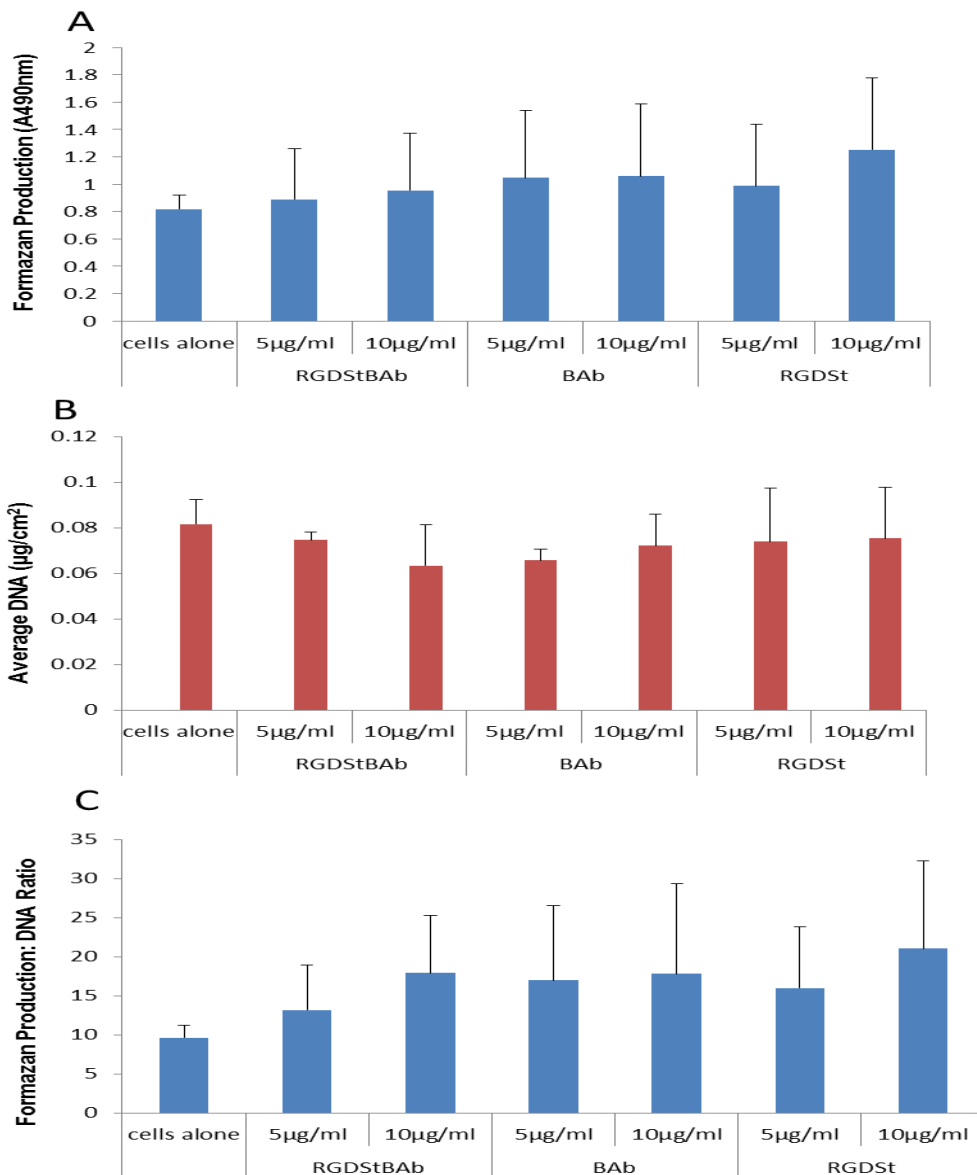


Figure 4.10: MSC Viability and Proliferation after Incubation with RGDStBAb, RGDSt or BAb

MSCs were pre-incubated with 5 or 10µg/ml RGDStBAb, RGDSt or BAb, cultured for 3 days in monolayer and analysed by WST-1 and PicoGreen assays for viability and DNA content. All groups demonstrated non-significant increases in metabolic activity per cell compared to MSCs alone (C). MSCs incubated with BAb and RGDSt alone demonstrated highest levels of metabolic activity (A). MSCs alone demonstrated a non-significant higher concentration of DNA compared to treatment groups (B). Data is presented as the mean \pm SD of n=3 biological replicates, generated using triplicate measurements.

4.3.12 MSC Osteogenesis after Pre-Incubation with the RGDStBAb Construct

MSCs were pre-incubated with varying concentrations of RGDSt followed by the same concentration of BAb (RGDStBAb) for a period of 20 minutes each. MSCs were then plated and cultured in osteogenic medium for 21 days, after which calcium was analysed as a measure of mineralisation. Controls were set up of RGDSt, BAb and MSCs alone (Figure 4.11B). Pre-incubations of MSCs with RGDStBAb construct at concentrations of 5µg/ml, 10µg/ml and 500µg/ml demonstrated maintenance of osteogenic potential. Calcium concentrations were comparable to the MSC alone control. Pre-incubation of MSCs with the same concentrations of biotinylated antibody alone demonstrated a trend of increased mineralisation. In contrast, pre-incubation of MSCs with RGDSt construct alone at all three concentrations showed a trend for a decrease in mineralisation, however these observations were not statistically significant.

MSC mineralisation was also visually observed by Alizarin Red stain for each treatment group (Figure 4.11A). MSCs alone cultured in osteogenic medium for 21 days demonstrated red staining indicating mineralised deposits (B) in contrast to the negative control where MSCs cultured in non-osteogenic media demonstrated no staining (A). MSCs pre-incubated with varying concentrations of RGDStBAb construct, 5µg/ml, 10µg/ml and 500µg/ml (C-E respectively), also demonstrated staining for mineralised deposits comparable to that of the MSC alone positive control. MSCs pre-incubated with biotinylated antibody alone at concentrations of 5µg/ml (F), 10µg/ml (G) and 500µg/ml (H) showed an increase in Alizarin Red staining as compared to the MSC alone positive control. Concentrations of 5µg/ml and 10µg/ml of antibody (F, G) demonstrated a visual increase in red staining with the lowest concentration of 5µg/ml showing red staining covering the entire culture (F). MSCs pre-incubated with RGDSt alone at concentrations of 5µg/ml (I), 10µg/ml (J) and 500µg/ml (K) demonstrated a

decrease in staining, showing a trend of reduced mineralisation correlating with calcium content.

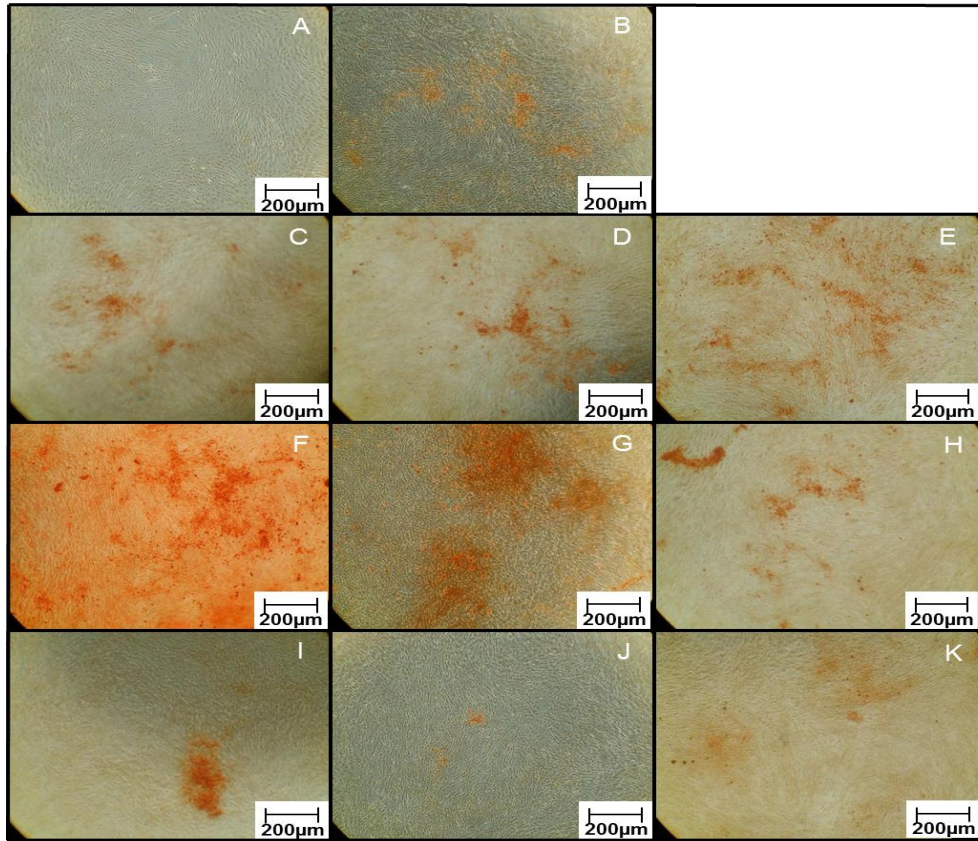


Figure 4.11A: MSC Osteogenesis after Incubation with RGDStBAb, RGDSt or BAb

MSCs pre-incubated with different concentrations of RGDSt or BAb, combined or separately were cultured to undergo osteogenesis for 21 days and analysed by Alizarin Red stain. Negative controls showed an absence of red staining of mineralised deposits (A). MSCs alone demonstrated positive red staining of mineralised deposits (B). MSCs pre-incubated with RGDStBAb construct at 5, 10 and 500µg/ml showed positive staining of mineralised deposits (C-E respectively). MSCs pre-incubated with BAb at 5, 10, 500µg/ml showed increased positive staining of mineralisation (F-H respectively). An evident visual increase in red staining was observed at 5 and 10µg/ml (F, G). MSCs pre-incubated with 5, 10 and 500µg/ml RGDSt alone demonstrated visually lower amounts of positive red staining (I-K respectively). Scale bar, 200µM.

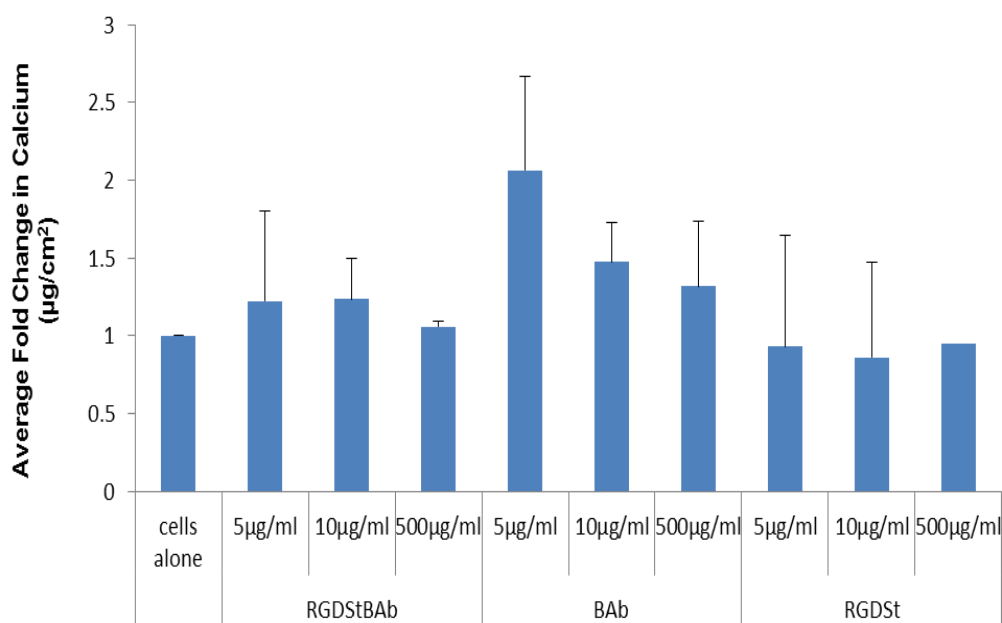


Figure 4.11B: MSC Osteogenesis after Incubation with RGDStBAb, RGDSt or BAb

MSCs pre-incubated with 5, 10 or 500 µg/ml RGDStBAb, RGDSt or BAb were induced to undergo osteogenesis for 21 days and analysed by calcium quantification. Osteogenesis was maintained in all treatment groups. A non-significant increase in mineralisation was observed in cultures incubated with all BAb concentrations. Data is presented as the mean \pm SD of n=3 biological replicates, generated using triplicate measurements.

4.3.13 MSC Adipogenesis after Pre-Incubation with the RGDStBAb Construct

MSCs were pre-incubated with 5 μ g/ml, 10 μ g/ml and 500 μ g/ml concentrations of RGDSt, followed by the same concentration of BAb (RGDStBAb) for a period of 20 minutes each and then induced to undergo adipogenic differentiation. Controls were set up with RGDSt, BAb and MSCs alone. Quantification of Oil Red O staining of lipid droplets demonstrated a trend of a decrease in lipid accumulation in all treatment groups as compared to the MSC alone control; this trend was not statistically significant (Figure 4.12B). Oil Red O visualisation of lipid droplets in adipogenic treatment cultures indicated maintenance of lipid droplet accumulation in all treatment groups (Figure 4.12A, A-K). The negative MSC alone control showed an absence of lipid vacuoles (A). MSC alone positive control (B) demonstrated lipid accumulation. MSCs pre-incubated with RGDStBAb at 10 μ g/ml showed lipid accumulation similar to that of the MSC alone positive control (D) and a decrease was observed at 5 μ g/ml and 500 μ g/ml concentrations (C, E). Further decreases in lipid vacuoles were observed with MSCs pre-incubated with all 3 concentrations of biotinylated antibody and RGDSt construct (F-K).

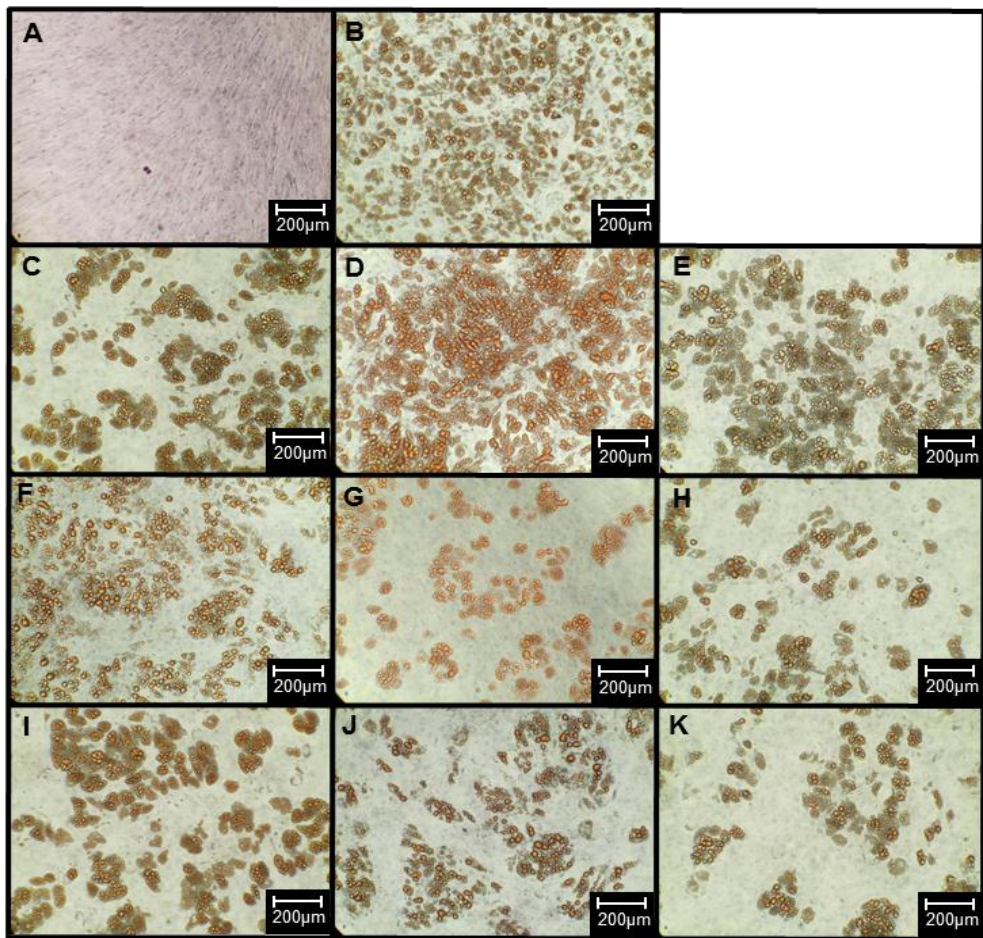


Figure 4.12A: MSC Adipogenesis after Incubation with RGDSStBAb, RGDSSt or BAb

MSCs pre-incubated with 5, 10 or 500µg/ml RGDSStBAb (C-E respectively), RGDSSt (F-H respectively) or BAb (I-K respectively) were cultured to undergo adipogenesis and analysed by Oil Red O Staining of lipid droplets. Negative control showed an absence of lipid droplets (A). Positive staining was observed in the MSC alone control (B). Maintenance of adipogenesis was observed in all treatment groups (C-K). Comparable lipid droplet staining with MSC alone control was observed with MSCs incubated with 10µg/ml RGDSStBAb (D). A visual decrease in lipid droplet staining was observed in all other treatment groups and concentrations (C, E-K). Scale bar, 200µM.

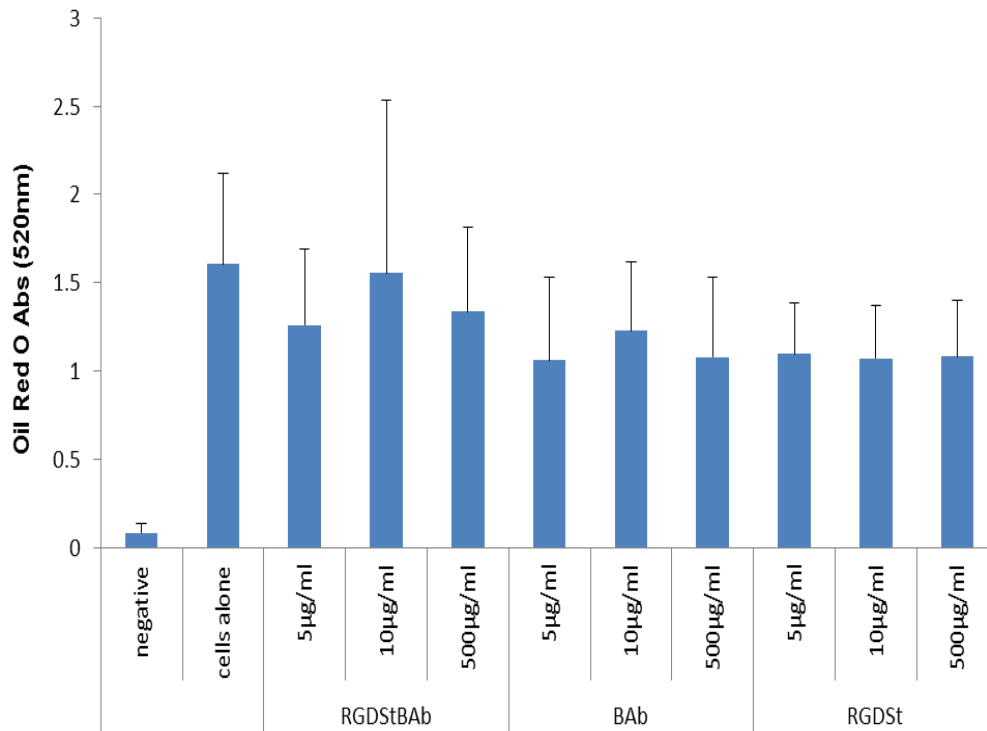


Figure 4.12B: MSC Adipogenesis after Incubation with RGDStBAb, RGDSt or BAb

MSCs pre-incubated with 5, 10 or 500µg/ml RGDStBAb, RGDSt or BAb, were cultured to undergo adipogenesis and analysed by Oil Red O Staining of lipid droplets. Quantification of Oil Red O staining demonstrated maintenance of lipid droplet formation, showing a non-significant decrease in all treatment groups compared to MSC alone control. Data is presented as the mean \pm SD of n=3 biological replicates, generated using triplicate measurements.

4.3.14 MSC Chondrogenesis after Pre-Incubation with the RGDStBAb Construct

MSCs were pre-incubated with 10µg/ml concentrations of RGDSt, followed by 10µg/ml of BAb (RGDStBAb) for a period of 20 minutes each. Controls of BAb, RGDSt and MSCs alone were included in the experiment. MSCs were then induced to undergo chondrogenic differentiation by pellet culture for 21 days. Analysis was performed by Safranin O staining and sulphated GAGs quantified by DMMB assay normalised to DNA content per pellet and represented as average fold change in GAG:DNA ratio (Figure 4.13A).

There was a trend for a decrease in the average fold change of GAG:DNA ratio of MSCs pre-incubated with RGDStBAb construct, RGDSt and BAb as compared to the MSC alone control, however this was not statistically significant (A). Safranin O staining of pellets demonstrated maintenance of staining across groups, showing a visual reduction in staining for both RGDStBAb construct and RGDSt alone (B-E).

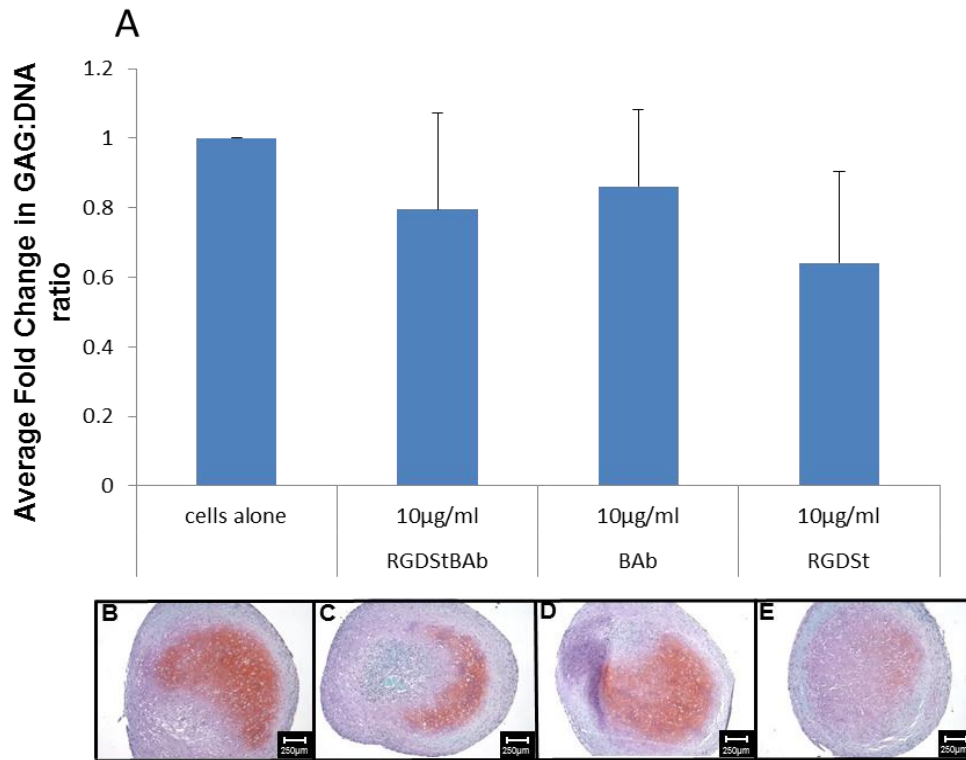


Figure 4.13A: MSC Chondrogenesis after Incubation with RGDStBAb, RGDSt or BAb

MSCs pre-incubated with 10µg/ml concentrations of RGDStBAb, RGDSt or BAb were cultured to undergo chondrogenesis for 21 days and analysed by DMMB assay and Safranin O stain for GAG analysis. Chondrogenesis was maintained in the presence of RGDStBAb, BAb and RGDSt alone (A-E). Average fold change in GAG:DNA ratio was decreased non-significantly in all treatment groups compared to MSC alone control (A). Pellet images show comparable Safranin O staining of MSCs alone and BAb with a small reduction in RGDStBAb and RGDSt (B-E, respectively). Data is presented as the mean \pm SD of n=3 biological replicates, generated using triplicate measurements.

4.3.15 MSC Chondrogenesis after Pre-Incubation and Culture with the RGDStBAb Construct

MSCs were pre-incubated with 10µg/ml concentrations of RGDSt, followed by BAb (RGDStBAb) for a period of 20 minutes each. Controls of BAb, RGDSt and MSCs alone were included in the experiment. MSCs were re-plated and cultured until confluence and then induced to undergo chondrogenic differentiation by pellet culture for 21 days (Figure 4.13B). MSCs pre-incubated and cultured with RGDStBAb demonstrated maintenance of chondrogenic potential as compared to the MSC alone positive control. Similarly, MSC pre-incubation and culture with biotinylated antibody alone demonstrated maintenance of chondrogenic potential, however revealing a non-significant reduction in GAG:DNA ratio. MSCs pre-incubated and cultured with RGDSt alone demonstrated a significant increase in average fold change in GAG:DNA ratio as compared to the MSC alone control. Safranin O staining of pellets demonstrated maintenance of GAG for MSCs pre-incubated with RGDStBAb construct and BAb alone as compared to MSCs alone (B-D). An increase in Safranin O staining of GAG was observed in pellets of MSCs incubated with RGDSt alone as compared to MSC alone control (E).

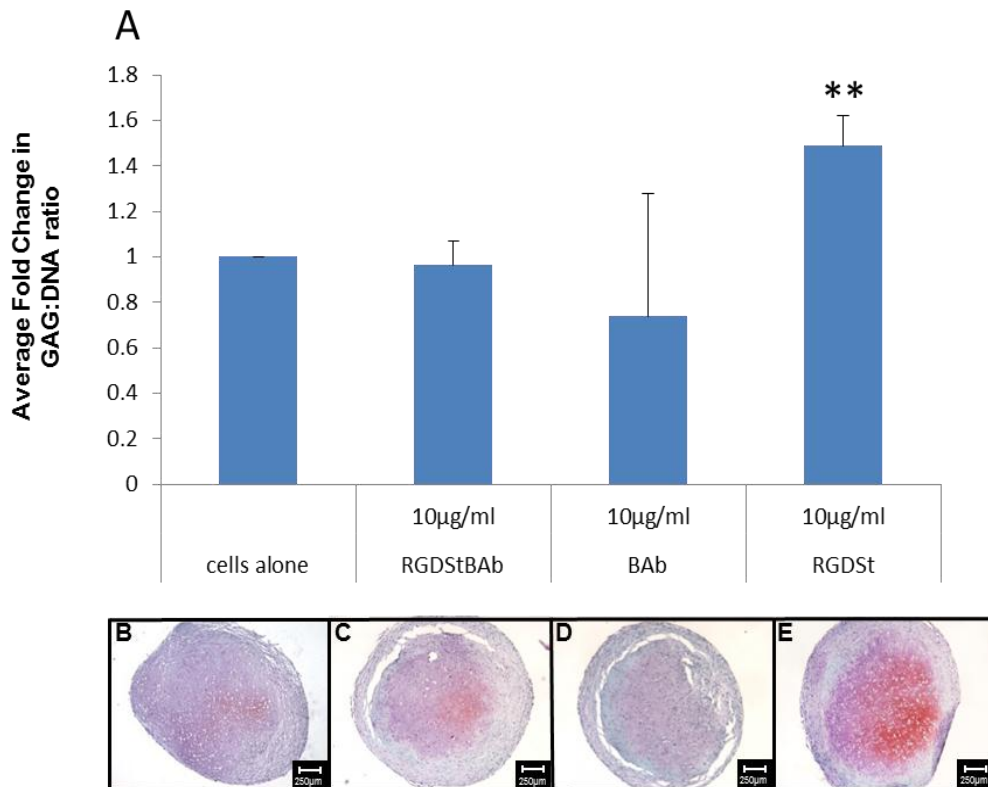


Figure 4.13B: MSC Chondrogenesis after Incubation and Culture with RGDSStBAb, RGDSSt or BAb

MSCs pre-incubated with 10µg/ml concentrations of RGDSStBAb, RGDSSt or BAb were re-plated until confluent and pelleted to undergo chondrogenesis for 21 days. Pellets were analysed by DMMB assay and Safranin O stain for GAG analysis. Average fold change in GAG:DNA ratio demonstrated maintenance of chondrogenesis across all groups (A-E) with a significant increase in GAG observed with MSCs pre-incubated with RGDSSt (A, E). A non-significant decrease was observed with MSCs pre-incubated with BAb alone (A). Data is presented as the mean \pm SD of n=3 biological replicates, generated using triplicate measurements $**=p\leq 0.01$.

4.4 Discussion

The porcine explant model demonstrated a robust and reproducible method of testing cell adhesion *ex vivo*; the coll 2 3/4m epitope was conserved in porcine cartilage and the polyclonal coll 2 3/4m antibody was compatible with the model. The RGDStBAb construct demonstrated significant potential for enhancing MSC retention at the articular surface. Interestingly, RGDSt alone also demonstrated its potential as a localisation method for MSCs at the cartilage surface. However, this would be considered a less specific technology. Importantly, the construct was biocompatible and non-toxic with MSCs. Adherence on plastic culture and on cartilage demonstrated normal, viable, fibroblastic morphologies of MSCs, with the potential for enhanced adherence, spreading and flattening on the articular surface of MSCs localized with RGDStBAb and RGDSt constructs. Proliferative potential was maintained, with an increase in metabolic activity per cell. MSCs also maintained their osteogenic, chondrogenic and adipogenic potential in the presence of the RGDStBAb construct and individual components.

Due to the cost, time and source limitations associated with obtaining human tissue, a readily available source of porcine tissue was instead used to design and implement a set of experiments for testing the antibody-peptide construct on a collagenase digested porcine explant model. Collagenases, are a collection of enzymes specific to breaking the peptide bonds of collagen and are often used for cell isolations from tissues (Atala and Lanza, 2002). Collagenase was therefore chosen as the enzyme of choice for specifically degrading the collagen on the porcine cartilage surface. The porcine explant model could also be considered more reproducible over human tissue, as the same treatment is applied to every explant and every donor. In addition, non-digested tissue was used as a normal control whereas it was not possible to source healthy human cartilage.

The IBEX monoclonal collagen 2 3/4m antibody cross reacts with several different species, including human (Hollander *et al.*, 1995). Due to the conservation of collagen across species (Boot-Handford *et al.*, 2003; Huxley-Jones *et al.*, 2007), it was assumed that the collagen 2 3/4m epitope would indeed be conserved in porcine cartilage after collagenase digestion. Testing the polyclonal antibody on porcine cartilage sections was therefore a requirement in order to proceed with the porcine explant model.

Immunostaining of the collagen 2 3/4m epitope demonstrated the functionality of the polyclonal collagen 2 3/4m antibody on digested porcine tissue and in contrast, non-digested sections showed its absence superficially. There was staining observed in the deeper zones of the non-digested tissue which may be attributed to background staining. Polyclonal antibodies are a heterogenous mix that recognise many different antigenic epitopes (Lipman *et al.*, 2005). Due to the polyclonal nature of the collagen 2 3/4m antibody, it is possible that within the mix of IgGs there are also potential antibodies that recognise elements of the collagen 2 3/4m epitope and account for some of this background staining.

The difference in staining pattern and intensity between the biotinylated polyclonal antibody and non-biotinylated polyclonal antibody on non-digested cartilage suggested some staining is likely non-specific and again possibly a consequence of the polyclonal nature of the antibody. The biotinylated antibody showed stronger staining in areas either weakly stained or where there was an absence of staining in the non-biotinylated antibody section. It is possible also that biotinylation contributed to the non-specific staining through a possible modification of antibody functionality (Bayer and Wilchek, 1990; Diamandis and Christopoulos, 1991). However, this background staining was not significant as there was an absence of stain superficially in the non-digested sections compared to digested sections, following the expected epitope staining pattern as previously seen (Figure 3.8). Human cartilage staining intensity was higher for the non-biotinylated antibody, suggesting some partial loss of functionality by biotinylation.

Comparison of the staining patterns of the collagen 2 3/4m polyclonal to the collagen type II antibody indicated intense superficial staining of collagen type II in non-digested sections and also in the deeper zones of the cartilage. Weak superficial collagen type II staining was in contrast observed in the digested sections. These observations follow the pattern of degradation as described by Hollander *et al.* where an early degradation of collagen II around chondrocytes was noted starting in the superficial and upper mid zone and extending to the lower mid and deep zones with increasing degeneration. Severely damaged matrix demonstrated deep fibrillation, accompanied by loss of staining at the remaining articular cartilage surface, suggesting the loss of the collagen epitopes (Hollander *et al.*, 1995). The digested porcine cartilage sections therefore, could be described as demonstrating moderate levels of degeneration, since epitope staining is noted in the superficial and upper mid-zones as seen in early to moderate stages of OA, but with more severe degeneration there is a loss of staining at the articular surface, accompanied with deep fissures and fibrillation (Hollander *et al.*, 1995).

In an attempt to demonstrate the specificity and functionality of the polyclonal collagen 2 3/4m antibody for the collagen 2 3/4m epitope on porcine cartilage, the peptide sequence (Hollander *et al.*, 1994) used to produce the polyclonal antibody was used to block porcine digested sections. The peptide successfully blocked the polyclonal collagen 2 3/4m antibody with staining in sections comparable to that found in the absence of the antibody.

In addition to demonstrating specificity of the antibody, staining for the degraded cartilage epitope was also tested on two other tissues, meniscus and muscle. Meniscus is a fibrocartilaginous tissue found adjacent to hyaline cartilage and containing 75% collagen, including collagen type II (Brindle *et al.*, 2001). Muscle, a tissue of mesodermal origin is predominantly composed of protein fibres, with a small proportion of collagen representing just 1-2% found of the endomysium (Alberts *et al.*, 1994). Positive biotinylated antibody staining was observed within the porcine meniscus sections, suggesting a staining due to the polyclonal nature of the antibody.

Since the sections were not degraded it is likely that the antibody stained a related epitope within the tissue as observed in non-digested cartilage sections. No positive staining was observed in the muscle tissue as expected, since the tissue contains very little collagen.

In an experiment localising MSCs to the surface of collagenase digested porcine explants it was observed that the addition of the RGDStBAb construct resulted in an increase in MSC adhesion with decreasing concentration of the construct. This suggested that there was steric hindrance or a 'prozone effect' (Butch, 2000) with the increased concentrations of construct forming larger molecular complexes and the smaller concentrations allowing better access to the antibody epitope on the cartilage and/or the ability of the RGD peptide to bind to integrins on the MSCs. The RGDSt alone conversely showed an opposite trend with increasing concentration of RGDSt correlating with binding to MSCs. Chondrocytes are documented to shed integrins into the extracellular matrix and other matrix molecules can also bind RGD (Loeser, 2000; Ruoslahti, 1996; Schulze-Tanzil *et al.*, 2001). The increase in MSC adherence with increasing RGDSt concentration is a possible result of either more RGD molecules bound to the surface of MSCs, increasing the number of MSCs that are localised and/or an increased RGD concentration was made available for enabling binding of the MSCs to the cartilage. It was observed that MSCs also adhered to the sides and bottom of the cartilage explants. These cut edges provide available ligands for the cells to bind with or without antibody-peptide constructs. These surfaces were not analysed stereologically since they were artificially produced and only the original articular surface was of interest experimentally.

It was of interest to examine if MSCs would also localise to non-digested cartilage further testing the specificity of the coll 2 3/4m antibody to degraded cartilage. MSCs adhered alone to non-digested cartilage but in a lower number compared to degraded cartilage. Similarly, as for digested cartilage, an increase in adherence was observed with both the RGDStBAb and RGDSt compared to MSCs alone. However, this binding was considerably lower compared to the numbers of MSCs that adhered to

degraded cartilage. In contrast to a ligand/epitope revealing the articular surface that would be present on degraded cartilage, non-degraded cartilage should possess little or no degraded epitopes and fewer available matrix ligands for binding MSCs. The RGDSt demonstrated the highest number of MSCs bound and was likely a consequence of RGD binding to integrins or full length matrix molecules present in the cartilage matrix (Loeser, 2000; Ruoslahti, 1996; Shakibaei *et al.*, 1993; Shakibaei and Merker, 1999). The RGDStBAb construct binding was dependent on the collagen 2 3/4m epitope being present at the articular surface and in non-degraded cartilage the epitope should not be evident as observed. It is possible that the RGDStBAb incubated MSCs bound to the non-degraded cartilage via non-specific coll 2 3/4m antibody binding, but it is also possible that the RGDSt component played a role in binding.

MSC morphology was examined as part of a series of steps to analyse MSC potential in terms of proliferation, viability and differentiation after incubation with the RGDStBAb construct and the various component controls. Morphology was analysed in monolayer culture, demonstrating the ability of cells to adhere to tissue culture plastic and maintain MSC morphology. It was evident that the RGD peptide and BAb caused MSCs to aggregate or cluster, as can be seen in the images of MSCs cultured with RGDStBAb, BAb, RGDSt and RGD alone. However, the BAb would not be expected to bind the MSC cell surface, but it is possible the antibody bound either specifically to a surface molecule with sequence similarity to degraded collagen type II (Silva and Mooney, 2004) or non-specifically as a result of biotinylation.

Furthermore, MSC morphology was analysed by SEM on cartilage explants demonstrating MSC viability and morphological spread over the articular surface. MSCs showed superior spread and a flattened, adhered morphology when pre-incubated with both RGDStBAb and RGDSt constructs compared to MSCs alone. This was evident in not only the shape of the cells but also by the observation of many pseudopodia projections. This suggests that not only do the RGDStBAb and RGDSt constructs have the advantage of

enhancing the numbers of MSCs localised to the articular surface but functionally they may induce MSC adherence and further cell activities such as migration, signalling, proliferation and differentiation (Grzesiak *et al.*, 1997; Humphries *et al.*, 2006; Khatayevich *et al.*, 2010; Maheshwari *et al.*, 2000; Maheshwari *et al.*, 1999; Ruoslahti, 1996; Vonwil *et al.*, 2010).

MSCs pre-incubated with RGDSt and delivered to non-degraded cartilage also demonstrated a flattened and spread morphology suggesting the peptide was able to bind integrin receptors at the surface. The observed mixed morphology of flat and rounded cells, with MSCs pre-incubated with the RGDStBAb construct suggest an absence of the coll 2 3/4m epitope in the non-degraded surface matrix and that binding was a possible result of RGDSt binding through integrins or non-specific antibody binding.

MSCs pre-incubated with the RGDStBAb construct and its components showed a trend for higher metabolic activity over cells alone. This was possibly the result of the induction of internal cell-signalling activities as a consequence of RGD peptide binding the MSC surface (Alberts *et al.*, 1994; Humphries *et al.*, 2006). Although the BAb would not be expected to bind the MSC surface, incubations with MSCs alone indicated a trend for an increase in metabolism suggesting the antibody does in some way interact with the cell to stimulate activity and supporting previous MSC aggregations with BAb observed in culture. There was a trend for a decrease in DNA content of wells containing MSCs pre-incubated with constructs. This was a possible consequence of surface bound proteins reducing the numbers of cells binding to tissue culture plastic.

Osteogenic analysis of MSCs pre-incubated with RGDStBAb combined or separately demonstrated a maintenance of potential with observed increases when MSCs were incubated with BAb alone as compared to MSC alone controls. This again supports the possibility that the antibody alone also has a functional role with the MSCs (Hall and Miyake, 2000; Sundelacruz and Kaplan, 2009). Since results demonstrated no change in osteogenic potential with RGDStBAb construct or RGDSt alone, this enhanced mineralization

with BAb alone should not be a problem *in vivo* since BAb alone would not be used and where also environment would play a large part in determining MSC fate (Caplan, 2009b).

Adipogenic differentiation of MSCs pre-incubated with RGDStBAb combined or separately demonstrated maintenance of adipogenic potential, although a trend for a decrease in lipid droplet formation was observed, more so when MSCs were cultured with BAb or RGDSt alone. Fibronectin has been implicated in inhibiting adipocyte differentiation (Wang *et al.*, 2010) and Lin *et al* demonstrated that adipogenic phenotype was inhibited using RGD-dependant disintegrins on primary cultured pre-adipocytes (Lin *et al.*, 2005). Therefore RGD MSC surface binding may have contributed to this non-significant decrease in adipogenesis. MSC surface binding of the BAb through a similar mechanism may also influence adipogenesis.

Chondrogenic differentiation of MSCs pre-incubated with RGDStBAb combined or separately also demonstrated maintenance of differentiation, although there was a trend for a decrease in GAG compared to the MSC control. RGD is known to have a functional role in chondrogenesis and can influence the process at different times, depending on the stages of chondrogenesis and concentration (Mann and West, 2002). Contrasting results have suggested that RGD plays a role in initiating chondrogenesis and maintaining hMSC viability, however it appears that the persistence of this molecule inhibits chondrogenic differentiation (Salinas and Anseth, 2008; Salinas *et al.*, 2007). Normally, fibronectin protein expression is regulated during embryonic chondrogenesis; it is increased at condensation and decreased in quantity during maturation (Salinas and Anseth, 2008; Shakibaei *et al.*, 1995). It is possible that the trend for a decrease in GAG with MSCs pre-incubated with RGDStBAb and RGDSt correlates with persistence of the molecule in the pellet, since the MSCs were pre-incubated and immediately put into pellet culture (Shakibaei *et al.*, 1995). An explanation for the BAb alone effect is that in a similar mechanism, persistence of this antibody at the MSC surface or in the medium might block

cell interactions or medium and supplement infiltration required for differentiation.

A further experiment was conducted to observe if the transient presence of RGD was sufficient to increase chondrogenesis as has been reported in the literature in cell seeded scaffolds (Re'em *et al.*, 2010; Salinas and Anseth, 2008). Chondrogenic differentiation was analysed after MSCs were pre-incubated with RGDStBAb combined or separately, placed back in culture until confluent and then placed into pellet culture. Results demonstrated that there was maintenance of differentiation potential for both RGDStBAb and BAb alone, however there was a significant increase in GAG with MSCs cultured with RGDSt alone. This suggested that the transient exposure of RGDSt to the MSCs was potentially advantageous, allowing a period of time for the cells to process the peptide prior to putting them into pellet culture. Because RGD effects are also suggested to be concentration dependent a future experiment following this would be to observe the effects of different concentrations. Importantly, the RGDStBAb construct did not compromise chondrogenic differentiation. The BAb alone showed a non-significant decrease compared to MSCs alone, but as a control this would not be used separately with MSCs *in vivo*.

4.5 Conclusion

The antibody-peptide construct demonstrated non-toxicity with MSCs and successfully enhanced the number of MSCs localized to the degraded cartilage surface. In addition, the construct components alone revealed interesting functionalities with the MSCs, suggesting further potential for the construct beyond cell localisation. These results complement the novel technology as a method of functional cell localisation, suggesting the technology may be considered both a ‘bispecific’ and ‘bifunctional’ antibody-peptide (Kriangkum *et al.*, 2001). Chapter 5 will discuss limitations, refinements of *in vitro* experiments and further *in vivo* experiments that would determine pre-clinical efficacy of the technology as the next step in development.

Chapter 5

Discussion

5.1 Enhancing Cellular Retention

Cartilage tissue is a complex, avascular and zonal tissue that consequently demonstrates an inability to repair itself (Aigner and McKenna, 2002; Becerra *et al.*, 2010). Despite containing progenitor cells within the surface zone (Dowthwaite *et al.*, 2004), the progressive loss of surface layers at the degraded articular surface, contribute to a possible loss of potential for repair (Archer *et al.*, 2012). Although, osteoarthritic cartilage has since demonstrated the presence of migratory progenitor cells that postulate self-repair attempts and potential for therapeutic manipulation (Khan *et al.*, 2009; Koelling *et al.*, 2009), the transplantation of progenitor cells remains an attractive option with advantages over ACI, including availability and expansion. It has been previously shown that MSC transplantation has potential to slow the progression of OA, but that further efficacy was possibly compromised by the insufficient retention of MSCs within the joint and at the articular surface (Murphy *et al.*, 2003).

The objective of this thesis was to design, demonstrate and validate ways to enhance cellular retention, whether MSC, chondrocytes or cartilage progenitor cells, at the diseased cartilage surface. Enhanced MSC retention was demonstrated by two different methods using human and porcine *ex vivo* models. One method made use of the natural adhesive properties of the polysaccharide pullulan for coating cartilage prior to cell application. In a second more designed approach, a construct consisting of antibody and peptide was designed to pre-coat cells and target MSCs specifically to degraded cartilage. The biocompatibility of both technologies with MSCs was assessed, revealing additional functionalities that may enhance MSC therapeutic potential.

5.2 Pullulan: A Bioadhesive for Increasing Cellular Retention and the MSC Therapeutic Response

The use of pullulan as a bioadhesive for attaching MSCs to the cartilage surface has the advantage of being an inexpensive, regulatory-favourable and relatively straightforward method. The adhesive already has an established history of use in both the food and medical industry highlighting the ease by which this method could be introduced and used in the clinic (Leathers, 2003; Rekha and Sharma, 2007). The bioadhesive demonstrated potential for enhancing cellular adhesion to cartilage. In addition to its intended use as a localisation method, it also demonstrated many favourable properties that would enhance MSC therapeutic potential. It showed an advantage for a trend of increased cellular proliferation, further contributing to increased numbers.

Pullulan incubation with MSCs showed a decrease in MSC surface receptor phenotype over 7 days, although this is unlikely to be an issue *in vivo* where the rapid solubility of pullulan would prevent persistence of the material. If the solubility properties of the adhesive were modified for longer persistence, then this decrease in surface receptor phenotype might need further consideration, since it might suggest differentiation of the MSCs (Diaz-Romero *et al.*, 2005; Jin *et al.*, 2009). Lee *et al.* reported the decrease in expression of MSC surface markers including CD105, CD44 and CD90 when MSCs were subjected to chondrogenic differentiation in 3D alginate cultures (Lee *et al.*, 2009).

Differentiation was maintained in the presence of pullulan, even increased in the case of osteogenesis. The osteogenic potential of MSCs with pullulan may not be a concern if the correct environmental cues for chondrogenesis are presented *in vivo* (Caplan, 2009b). However, the potential of pullulan to influence mineralisation and hypertrophy, already existing in OA cartilage, might require further analysis (Aigner and McKenna, 2002; Fuerst *et al.*, 2009; Horton *et al.*, 2005). Further MSC surface receptor analysis revealed

the presence of the Dectin-2 receptor on MSCs. The Dectin-2 receptor has only previously been documented on immune cells and was shown upregulated on MSCs in association with increasing pullulan concentration, suggesting a potential for enhancing MSC immunosuppressive properties through pullulan conditioning.

Limitations to the pullulan method of cellular retention include non-specificity to cartilage. However, this lack of specificity could be overcome by arthroscopic placement of the cell/bioadhesive construct in areas of cartilage degradation or in the joint cavity. An *in vivo* study would be valuable to show whether this strategy could be effective in enabling a MSC therapeutic response, whether in contributing to cartilage repair by a direct cartilage replacement or trophic effects. The non-specificity however, provides a wider application for use of the bioadhesive in other tissue engineering fields. As previously described, pullulan has the advantage of being a flexible adhesive that can be modified to tailor its application. A cross-linked form of the adhesive might be more favourable to decrease solubility and increase retention time within the joint and an option for future *in vivo* studies (Autissier *et al.*, 2007; Rekha and Sharma, 2007; Wong *et al.*, 2011). The presence of Dectin-2 receptor expression on MSCs suggests a possible mechanism of action through which pullulan may elicit an immunosuppressive response at the articular surface. To further explore a possible pullulan immunosuppressive potential with MSCs through the Dectin-2 receptor, a mixed lymphocyte reaction (MLR) experiment could be used. In a further experiment, an antibody block of the Dectin-2 receptor and MLR would confirm the suggested Dectin-2 receptor mechanism of action for this response.

The use of a bioadhesive for targeting and retaining cells at the cartilage surface and within the joint, is a novel approach in the cartilage field. Pullulan provides many advantages as a unique cell adhesive, such as an accessible route to the clinic, ease of application through arthroscopy, biocompatibility and ease of modification. In addition, the bioadhesive

appears to beneficially influence the MSC response with the potential for contributing to an environment suitable for repair.

5.3 RGDStBAb: An Antibody-Peptide Construct for Enhancing Cellular Retention and MSC Adhesive Properties

Antibody and peptide therapeutics represent a significant element of current clinical trials, most of which concentrate on the field of cancer therapy (Carlson *et al.*, 2007; Kriangkum *et al.*, 2001). There are fewer examples within the regenerative medicine field, but it has been demonstrated that the specific localisation of cells efficiently enhanced cell delivery and retention, contributing to repair efficacy (Dennis *et al.*, 2004; Ko *et al.*, 2010; Lee *et al.*, 2007; Lum *et al.*, 2004).

The antibody-peptide construct in contrast to the bioadhesive method of localising cells is designed to be specific to degraded cartilage, consisting of an antibody recognising the coll 2 3/4m epitope in degraded cartilage and an RGD peptide that binds integrin receptors on delivered cells. The RGDStBAb construct demonstrated enhanced adhesion of cells compared to MSC alone control and showed biocompatibility as shown by viability, differentiation and proliferation of MSCs pre-incubated with the construct and individual components. The non-specific RGDSt peptide alone also demonstrated enhanced retention of MSCs at the cartilage surface, providing another method of localising cells, with a wider application. Additionally, localising solely with the RGD peptide might have potential in the cartilage field due to its positive influences on chondrogenesis (Jeschke *et al.*, 2002; Salinas and Anseth, 2008; You *et al.*, 2011). Pre-incubation and culture of MSCs with RGDSt prior to chondrogenic culture demonstrated significant increased GAG compared to MSCs alone.

The construct has the advantage of localising MSCs specifically to the cartilage, avoiding unwanted retention elsewhere in the joint. However, specificity of the construct needs to be demonstrated *in vivo*. It remains to be

shown if efficacy is compromised by cell retention elsewhere in the joint such as the meniscus or synovium (Caplan, 2009b; Wagers and Weissman, 2004). If MSCs exert a response by trophic factor release, then direct attachment to the cartilage itself might not be necessary. Indeed results demonstrated that collagen 2 3/4m antibody staining was found in meniscus tissue, possibly owing to the polyclonal nature of the collagen 2 3/4m antibody. Meniscus contains 98% type I collagen (Sun *et al.*, 2012). However it also has small amounts of collagen type II, thus it is possible that the epitope is recognised, even when the porcine menisci analysed was not visibly degraded (Brindle *et al.*, 2001).

The observed staining of the meniscus suggests that the construct also has applicability for meniscus repair. OA is a disease of the whole joint including the menisci (Sun *et al.*, 2012). Grades of meniscal tears have been shown to be correlated with the severity of cartilage lesions and changes in OA meniscal cell expression compared to normal suggests menisci may be actively involved in the OA disease process (Pabbruwe *et al.*, 2010; Sun *et al.*, 2012). Meniscal tears that are located within the avascular regions have been shown to have a limited capacity for repair, suggesting a cellular therapy could be an attractive option for meniscal repair. Pabbruwe *et al.* demonstrated the integration of meniscal interfaces through an MSC-seeded collagen membrane (Pabbruwe *et al.*, 2010). In a similar approach, through application of the construct, where even a different antibody more specific for menisci may be applied, the enhanced retention of MSCs at a meniscal tear may contribute to repair efficacy and prevent further degeneration of the joint.

An observational, qualitative approach was used to assess the RGDStBAb construct binding to the cell surface in chapter 3. Ideally a quantitative method would have been advantageous in order to assess the number of constructs binding the MSC surface at one time. Unsuccessful attempts were made using flow cytometry and a cell-based ELISA approach to address this question (O'Kennedy and Reading, 1990; Repp *et al.*, 2003). One method that might have provided valuable data is surface plasmon resonance (SPR)

to establish binding coefficients of the construct with MSCs (Leonard *et al.*, 2004). This would have provided robust quantitative information but was beyond the scope of the current project; however, this application may be valuable for future validation.

The stereological approach to quantifying MSCs on the cartilage surface was developed to allow a 3D measure of cells across the surface (Curtin, 2009; Garcia *et al.*, 2007). Within this project, refinements of this method were made to eliminate subjectivity and aid identification of delivered MSCs to the cartilage surface by labelling MSCs with PKH26 or cell tracker red fluorescence. Additionally, using Image J to manually count cells reduced duplicates of counts. In chapter 4, bias was also eliminated through assisted relabelling of images and randomisation.

The RGD component of the antibody-peptide construct naturally causes cell-cell adherence. RGDSt bound to one cell, encompassing more than one RGD available sequence will then bind to integrin receptors of another cell. RGD binding to integrin receptors also stimulates an increase in integrin expression, further amplifying the process (Humphries *et al.*, 2006; Ruoslahti, 1996). The two-step incubation used also enables this cell-cell adherence. RGDSt is incubated alone first with MSCs to enable efficient binding of RGD to the MSC surface prior to the addition of the biotinylated antibody. *In vitro*, this cell-cell adherence did not appear to restrict the efficiency of the RGDStBAb construct and likely contributed to increasing the numbers of cells retained. Conversely, cell-cell adherence may have also limited individual cell binding, where cell retention was dependant on only a few cells bound to the cartilage. It will be interesting to observe whether this cell-cell adherence will have any adverse effects for cellular delivery *in vivo*. Additionally, whether direct cell adherence to cartilage is required or whether indirect increased cellular retention through cell-cell contact and trophic release is sufficient for repair will need to be elucidated *in vivo*.

Potential future *in vitro* experiments that will provide additional information on the binding nature of the construct may include an RGD peptide block on

the cartilage explant prior to addition of the construct. This will provide information on the role the RGDSt plays as part of the construct in binding to the cartilage. Further analysis of the specific nature of the antibody might be elucidated by performing a stereological count of MSCs binding to explants of other tissues such as meniscus and muscle. Further, an alternative MSC retention method may be achieved by pre-incubating the cartilage explants first with the coll 2 3/4m antibody, followed by an application of MSCs incubated with RGDSt.

An antibody-peptide construct was tailored for application to degraded articular cartilage as a method of enhancing MSC retention at the diseased tissue. In a previous study of antibody targeting for cartilage repair, Dennis *et al.* targeted chondrocytes through antibody linked protein G (Dennis *et al.*, 2004). Thus, the antibody-peptide construct is a unique example of a construct with not only bispecific potential, but also an example for localising MSCs to degraded cartilage. The use of an RGD peptide provides a construct with a wide application to other cell types and further, linkage through a streptavidin/biotin bridge allows the flexibility of any biotinylated antibody specific to the target tissue to be used. The construct also provides possible functionality through the RGD peptide, shown to influence MSC adhesion and differentiation. Experiments demonstrated biocompatibility of the construct with MSCs, further highlighting the potential of the designed construct as a regenerative tool.

5.4 Regulatory Aspects for Clinical Translation

An important aspect of any applied research is to consider how the technology might be applied in the clinical setting. This would be a requirement in the initial design of a therapy, since for example, designing a method of localising cells that then has to be later modified significantly to adapt to a clinical setting would be both time consuming and costly. Additionally, the new technology will need to demonstrate superiority over the clinical standard in order to have a place within the clinic. The current

clinical standard for cartilage being microfracture, suggests that any new therapy that requires regulatory approval and higher cost will inevitably need to demonstrate superior efficacy.

With an aim of an easy route to market technology, pullulan was chosen as a suitable bioadhesive to investigate for clinical translation, based on its history of safe use and FDA approval for a variety of applications within the pharmaceutical and food industry (Coviello *et al.*, 2007; Leathers, 2003; Rekha and Sharma, 2007). The simple arthroscopic application of pullulan to cartilage as an adhesive, also suggests how close the material could be to clinical translation. *In vivo* studies will confirm retention time of the material within the joint and whether further modifications to the material need to be made. There are many examples of modified pullulan currently being tested and depending on the modification, should not add significantly to the regulatory route (Akiyoshi *et al.*, 1998; Autissier *et al.*, 2007; Bae *et al.*, 2011; Bruneel and Schacht, 1995; Coviello *et al.*, 2007; Wong *et al.*, 2011).

As part of the design specifications of the antibody-peptide construct, a less complex regulatory route was favourable where possible. Delivery of a cell therapy alone for cartilage has a regulatory route, defined by FDA criteria of ‘minimally manipulated vs. more than minimal manipulation’ (Centeno and Faulkner, 2011). The addition of a further biologic in the form of an antibody-peptide construct, adds an additional regulatory challenge, extending to a definition of a ‘therapeutic biological product’ (FDA, 2009). A first requirement for any biologic is for biocompatibility, already demonstrated *in vitro* with MSCs; subsequently, this would be followed by biocompatibility with cartilage and the synovial joint *in vivo*.

The development and design of the antibody-peptide construct highlights the limitations that arise in terms of regulatory hurdles with more complex design (Bulman *et al.*, 2012). The combined components of the current RGDStBAb design would need regulatory consideration for future application. The RGD peptide is currently in use in various forms in clinical trials (Haubner *et al.*, 2001; Schafer, 1996), e.g. delta-24-RGD is a current

biologic in clinical trials for treatment of recurrent gliomas (clinicaltrials.gov, 2013). Similarly, the streptavidin-biotin interaction has also been employed in clinical trials. In a phase II trial, streptavidin-conjugated NRLU-10 mAB (NR-LU-10 recognising an antigen on epithelial tumours) was administered and localised to tumours, followed by administration of yttrium-90-biotin (Chivers *et al.*, 2011; Grana *et al.*, 2002; Knox *et al.*, 2000). Encouraging clinical trial results for both RGD and streptavidin-biotin for cancer therapeutics suggest their potential use in developing a cartilage treatment.

To remove the use of a chemical linker for conjugating streptavidin to RGD, it is possible that a genetic engineering or 'recombinant' approach could be used, creating a streptavidin molecule engineered/fused with RGD (Carter, 2001; Cloutier *et al.*, 2000; Dubel *et al.*, 1995; Kipriyanov *et al.*, 1995). However, chemical crosslinking has been used in clinical trials for bispecific antibody constructs (Doppalapudi *et al.*, 2010; Repp *et al.*, 2003). The coll 2 3/4m antibody to date has only been used for *in vitro* diagnostic testing (Hollander *et al.*, 1994) and has no prior testing *in vivo*.

Based on the current literature and clinical trials, the current antibody-peptide design is already potentially clinically acceptable. Since the bioadhesive approach is currently not specific to cartilage, the more complex antibody-peptide design with targeting specificity may ultimately be more effective. As for other areas of research, such as cancer therapeutics, the cartilage field might also require more complex technologies such as these for efficacy. Cartilage is a multicomplex, organised tissue that currently has no treatment that results in hyaline cartilage. Traditional regenerative therapies, such as application of a cell-seeded scaffold, have been shown to date to not provide the requirements for efficacy (Brittberg, 2008; Gudas *et al.*, 2005; Iwasa *et al.*, 2009; Knutsen *et al.*, 2007). It is therefore important to look to other fields for ideas to develop and advance the state of the art within the cartilage field (Bulman *et al.*, 2012; Carlson *et al.*, 2007; Dinauer *et al.*, 2005; Janssen *et al.*, 2002; Lum *et al.*, 2005). This will consequently encompass more regulatory challenges and hurdles that need to be accepted and overcome by

not only the governing regulatory bodies but also researchers in the field (Bulman *et al.*, 2012; Mason, 2005).

5.5 Conclusion

Pullulan, the RGDStBAb targeting construct and RGDSt alone demonstrated methods of enhancing MSC adhesion to degraded cartilage, including biocompatibility and beneficial functional responses. Both pullulan and RGDSt may be applied for enhancing cellular retention in any context, with a possible easier regulatory and cost route to market. However, for specificity a tailored construct like the RGDStBAb would be a more attractive choice.

5.6 Future *In Vivo* Experiments

A next-step for the approaches discussed for localising MSCs to cartilage, is to assess not only retention and specificity *in vivo*, but also efficacy and toxicity of the MSCs in combination with the technologies. The *ex vivo* explant model was appropriate for observing cell retention. Under the dynamic conditions created by a rocking platform and only a small explant surface area, MSCs demonstrated an enhanced binding with the various localisation technologies compared to MSCs alone, suggesting the superior potential of the technologies tested.

In previous explant culture experiments using a human explant model system with MSCs, it was reported that chondrogenic matrix deposition was evident after 14 days in chondrogenic culture media (Curtin, 2009). However, limitations to an *ex vivo* model include an absence of external load naturally found *in vivo* that also influence the cartilage repair process and further environmental cues not present within *in vitro* culture (Smith, 2007). Due to limitations in studying efficacy *ex vivo*, an *in vivo* model would be more suitable, providing the external influences that are absent in an artificial environment. Although, *in vitro* models of mechanical load have also been developed (Buschmann *et al.*, 1999; Parkkinen *et al.*, 1992; Smith, 2007), an

in vivo study would provide more value, with the ideal environmental conditions for demonstrating efficacy.

5.7 *In Vivo* in a Mouse Model

For preliminary screening of new therapies, mice are considered to be an ideal pre-clinical model due to the low costs, maintenance and space required for keeping them over larger species (Chu *et al.*, 2010; Glasson *et al.*, 2007). Transgenic mouse models of OA exist that are usually characterised by a set of specific symptoms and do not always represent the general and progressive disease process of OA (Glasson *et al.*, 2007; Glasson *et al.*, 2008). Surgical models are therefore favoured since they can replicate the clinical situation of starting from a single lesion within the joint and progressing to OA (Glasson *et al.*, 2007).

Glasson *et al.* performed anterior cruciate ligament transection (ACLT) and destabilisation of the medial meniscus (DMM) in 129/SvEv mouse knee joints. The ACLT procedure demonstrated severe OA with subchondral bone erosion and required high surgical proficiency in the mouse model, inducing too severe/end stage OA not suitable for a pre-clinical model. The less invasive procedure of DMM, resulted in lesions on the weight-bearing regions of the medial tibial plateau and femoral condyles and progressed from mild to severe over a period of 8 weeks post-surgery (Glasson *et al.*, 2007). The location and severity of the lesions following DMM surgery were consistent with those observed in aged spontaneous mouse models of OA, however, the DMM model is considered to be more consistent than spontaneous OA models such as the STR/ort model (Glasson *et al.*, 2007; Glasson *et al.*, 2008).

In a future study, the DMM mouse model could be used for demonstrating MSC localisation and efficacy to the degraded cartilage (Cullen, 2010). Despite some studies showing tolerance of hMSCs in mice (Mansilla *et al.*, 2005), it would be envisaged that the DMM mouse model would be performed in a nude mouse model with the use of human MSCs for long

term study of MSC retention. Alternatively, murine MSCs may be used in a non-nude DMM model.

One of the main issues in cell transplantation is locating the destination of infused cells (Allers *et al.*, 2004). An *in vivo* analysis of the number of MSCs retained within the cartilage, with and without the localisation methods using pullulan, RGDSt or RGDStBAb, their functional contribution to the repair of the tissue and efficacy of repair would be of interest to evaluate and compare. Cells may be fluorescently tracked *in vivo* to assess both retention and contribution to newly formed tissue. In addition, biocompatibility of the localisation methods with the cartilage tissue and within the synovial joint as a whole will be demonstrated.

5.8 The Future of Cartilage Repair

Owing to the complexity of articular cartilage in terms of graded zonality and hierarchical organisation, it is likely that combinatorial therapeutic approaches are required for efficacious repair (Bulman *et al.*, 2012). Often the simplest and most regulatory favourable idea is favoured with a quick route to market over more complex technologies; however to repair cartilage, it may be that the complex idea is the most suitable and efficacious. Future repair strategies for cartilage must consider the mechanical properties and biological functions of native cartilage. Current strategies lack some of the required properties and thus combining approaches might provide the most suitable repair interface (Bulman *et al.*, 2012).

It will be valuable for future cartilage studies to consider cellular retention, within the three basic elements of tissue engineering, whether it is through native progenitor infiltration into scaffolds encompassing a retention method or through transplanted progenitors localised and/or encapsulated within materials. Whether through increasing cell numbers retained at a surface of repair by localisation methods, an increase in either cellular building blocks and/or trophic factor release, increasing native progenitor tissue repair will

improve the current lack of cellular engraftment and completion of repair within a cartilage defect or scaffold. In addition, through specificity of localisation, repair might be tailored through an organisational approach. Cells might be placed or orientated through antibodies or peptides according to the tissue hierarchy (Bulman *et al.*, 2012; Klein *et al.*, 2009; Nguyen *et al.*, 2011) or functional peptides might be used to determine and control the transplanted, native progenitor or tissue differentiation and response (Grzesiak *et al.*, 1997; Hubbell, 2003; Jeschke *et al.*, 2002; Khatayevich *et al.*, 2010; You *et al.*, 2011).

Bibliography

Abbasi, A.M., Chester, K.A., Talbot, I.C., Macpherson, A.S., Boxer, G., Forbes, A., Malcolm, A.D., and Begent, R.H. (1993). CD44 is associated with proliferation in normal and neoplastic human colorectal epithelial cells. *Eur J Cancer* 29A, 1995-2002.

Abramson, S.B. (2007). Basic Arthritis Research
<http://www.med.nyu.edu/medicine/labs/abramsonlab/basic-arth-research.html>.

Aggarwal, S., and Pittenger, M.F. (2005). Human mesenchymal stem cells modulate allogeneic immune cell responses. *Blood* 105, 1815-1822.

Aigner, T., Bertling, W., Stoss, H., Weseloh, G., and von der Mark, K. (1993). Independent expression of fibril-forming collagens I, II, and III in chondrocytes of human osteoarthritic cartilage. *J Clin Invest* 91, 829-837.

Aigner, T., Fundel, K., Saas, J., Gebhard, P.M., Haag, J., Weiss, T., Zien, A., Obermayr, F., Zimmer, R., and Bartnik, E. (2006). Large-scale gene expression profiling reveals major pathogenetic pathways of cartilage degeneration in osteoarthritis. *Arthritis Rheum* 54, 3533-3544.

Aigner, T., Haag, J., Martin, J., and Buckwalter, J. (2007). Osteoarthritis: aging of matrix and cells--going for a remedy. *Curr Drug Targets* 8, 325-331.

Aigner, T., and McKenna, L. (2002). Molecular pathology and pathobiology of osteoarthritic cartilage. *Cell Mol Life Sci* 59, 5-18.

Aigner, T., Stoss, H., Weseloh, G., Zeiler, G., and von der Mark, K. (1992). Activation of collagen type II expression in osteoarthritic and rheumatoid cartilage. *Virchows Arch B Cell Pathol Incl Mol Pathol* 62, 337-345.

Aigner, T., and Stove, J. (2003). Collagens--major component of the physiological cartilage matrix, major target of cartilage degeneration, major tool in cartilage repair. *Adv Drug Deliv Rev* 55, 1569-1593.

Aigner, T., Zhu, Y., Chansky, H.H., Matsen, F.A., 3rd, Maloney, W.J., and Sandell, L.J. (1999). Reexpression of type IIA procollagen by adult articular chondrocytes in osteoarthritic cartilage. *Arthritis Rheum* 42, 1443-1450.

Akiyoshi, K., Kobayashi, S., Shichibe, S., Mix, D., Baudys, M., Kim, S.W., and Sunamoto, J. (1998). Self-assembled hydrogel nanoparticle of

cholesterol-bearing pullulan as a carrier of protein drugs: complexation and stabilization of insulin. *J Control Release* 54, 313-320.

Alberts, B., Bray, D., Lewis, J., Raff, M., Roberts, K., and Watson, J.D. (1994). *Molecular Biology of the Cell*, Third edn (Garland Publishing).

Allers, C., Sierralta, W.D., Neubauer, S., Rivera, F., Minguell, J.J., and Conget, P.A. (2004). Dynamic of distribution of human bone marrow-derived mesenchymal stem cells after transplantation into adult unconditioned mice. *Transplantation* 78, 503-508.

Alon, R., Bayer, E.A., and Wilchek, M. (1990). Streptavidin contains an RYD sequence which mimics the RGD receptor domain of fibronectin. *Biochem Biophys Res Commun* 170, 1236-1241.

Alon, R., Bayer, E.A., and Wilchek, M. (1992). Cell-adhesive properties of streptavidin are mediated by the exposure of an RGD-like RYD site. *Eur J Cell Biol* 58, 271-279.

Alon, R., Hershkovich, R., Bayer, E.A., Wilchek, M., and Lider, O. (1993). Streptavidin blocks immune reactions mediated by fibronectin-VLA-5 recognition through an Arg-Gly-Asp mimicking site. *Eur J Immunol* 23, 893-898.

Amini, A.A., and Nair, L.S. (2012). Injectable hydrogels for bone and cartilage repair. *Biomed Mater* 7, 024105.

Anamelechi, C.C., Clermont, E.E., Brown, M.A., Truskey, G.A., and Reichert, W.M. (2007). Streptavidin binding and endothelial cell adhesion to biotinylated fibronectin. *Langmuir* 23, 12583-12588.

Ap Gwynn, I., Wade, S., Ito, K., and Richards, R.G. (2002). Novel aspects to the structure of rabbit articular cartilage. *Eur Cell Mater* 4, 18-29.

Archer, C.W., Williams, R., Nelson, L., and Khan, I.M. (2012). Articular Cartilage-Derived Stem Cells: Identification, Characterisation and their Role in Spontaneous Repair. *Rheumatology* 53, 5.

Arner, E.C. (2002). Aggrecanase-mediated cartilage degradation. *Curr Opin Pharmacol* 2, 322-329.

Ashwell, M.S., O'Nan, A.T., Gonda, M.G., and Mente, P.L. (2008). Gene expression profiling of chondrocytes from a porcine impact injury model. *Osteoarthritis Cartilage* 16, 936-946.

- Atala, A., and Lanza, R.P., eds. (2002). *Methods of Tissue Engineering* (Oxford, Elsevier).
- Augello, A., Tasso, R., Negrini, S.M., Cancedda, R., and Pennesi, G. (2007). Cell therapy using allogeneic bone marrow mesenchymal stem cells prevents tissue damage in collagen-induced arthritis. *Arthritis Rheum* 56, 1175-1186.
- Aurich, M., Poole, A.R., Reiner, A., Mollenhauer, C., Margulis, A., Kuettner, K.E., and Cole, A.A. (2002). Matrix homeostasis in aging normal human ankle cartilage. *Arthritis Rheum* 46, 2903-2910.
- Autissier, A., Letourneur, D., and Le Visage, C. (2007). Pullulan-based hydrogel for smooth muscle cell culture. *J Biomed Mater Res A* 82, 336-342.
- Bae, H., Ahari, A.F., Shin, H., Nichol, J.W., Hutson, C.B., Masaeli, M., Kim, S.H., Aubin, H., Yamanlar, S., and Khademhosseini, A. (2011). Cell-laden microengineered pullulan methacrylate hydrogels promote cell proliferation and 3D cluster formation. *Soft Matter* 7, 1903-1911.
- Bai, X., Xiao, Z., Pan, Y., Hu, J., Pohl, J., Wen, J., and Li, L. (2004). Cartilage-derived morphogenetic protein-1 promotes the differentiation of mesenchymal stem cells into chondrocytes. *Biochem Biophys Res Commun* 325, 453-460.
- Bakker, A.C., van de Loo, F.A., van Beuningen, H.M., Sime, P., van Lent, P.L., van der Kraan, P.M., Richards, C.D., and van den Berg, W.B. (2001). Overexpression of active TGF-beta-1 in the murine knee joint: evidence for synovial-layer-dependent chondro-osteophyte formation. *Osteoarthritis Cartilage* 9, 128-136.
- Baragi, V.M., Becher, G., Bendele, A.M., Biesinger, R., Bluhm, H., Boer, J., Deng, H., Dodd, R., Essers, M., Feuerstein, T., *et al.* (2009). A new class of potent matrix metalloproteinase 13 inhibitors for potential treatment of osteoarthritis: Evidence of histologic and clinical efficacy without musculoskeletal toxicity in rat models. *Arthritis Rheum* 60, 2008-2018.
- Barry, F., Boynton, R., Murphy, M., Haynesworth, S., and Zaia, J. (2001a). The SH-3 and SH-4 antibodies recognize distinct epitopes on CD73 from human mesenchymal stem cells. *Biochem Biophys Res Commun* 289, 519-524.
- Barry, F., Boynton, R.E., Liu, B., and Murphy, J.M. (2001b). Chondrogenic differentiation of mesenchymal stem cells from bone marrow:

differentiation-dependent gene expression of matrix components. *Exp Cell Res* 268, 189-200.

Barry, F.P., Boynton, R.E., Haynesworth, S., Murphy, J.M., and Zaia, J. (1999). The monoclonal antibody SH-2, raised against human mesenchymal stem cells, recognizes an epitope on endoglin (CD105). *Biochem Biophys Res Commun* 265, 134-139.

Bartholomew, A., Sturgeon, C., Siatskas, M., Ferrer, K., McIntosh, K., Patil, S., Hardy, W., Devine, S., Ucker, D., Deans, R., *et al.* (2002). Mesenchymal stem cells suppress lymphocyte proliferation in vitro and prolong skin graft survival in vivo. *Exp Hematol* 30, 42-48.

Bartlett, W., Skinner, J.A., Gooding, C.R., Carrington, R.W., Flanagan, A.M., Briggs, T.W., and Bentley, G. (2005). Autologous chondrocyte implantation versus matrix-induced autologous chondrocyte implantation for osteochondral defects of the knee: a prospective, randomised study. *J Bone Joint Surg Br* 87, 640-645.

Bassaganya-Riera, J., DiGuardo, M., Viladomiu, M., de Horna, A., Sanchez, S., Einerhand, A.W., Sanders, L., Hontecillas, R. (2011). Soluble fibers and resistant starch ameliorate disease activity in interleukin-10-deficient mice with inflammatory bowel disease. *J Nutr* 141, 1318-25.

Bavaresco, L., Bernardi, A., Braganhol, E., Cappellari, A.R., Rockenbach, L., Farias, P.F., Wink, M.R., Delgado-Canedo, A., and Battastini, A.M. (2008). The role of ecto-5'-nucleotidase/CD73 in glioma cell line proliferation. *Mol Cell Biochem* 319, 61-68.

Bayer, E.A., Ben-Hur, H., and Wilchek, M. (1990). Isolation and properties of streptavidin. *Methods Enzymol* 184, 80-89.

Bayer, E.A., and Wilchek, M. (1990). Protein biotinylation. *Methods Enzymol* 184, 138-160.

Becerra, J., Andrades, J.A., Guerado, E., Zamora-Navas, P., Lopez-Puertas, J.M., and Reddi, A.H. (2010). Articular cartilage: structure and regeneration. *Tissue Eng Part B Rev* 16, 617-627.

Bentley, G., Biant, L.C., Vijayan, S., Macmull, S., Skinner, J.A., and Carrington, R.W. (2012). Minimum ten-year results of a prospective randomised study of autologous chondrocyte implantation versus

mosaicplasty for symptomatic articular cartilage lesions of the knee. *J Bone Joint Surg Br* 94, 504-509.

Bertolo, A., Thiede, T., Aebli, N., Baur, M., Ferguson, S.J., and Stoyanov, J.V. (2011). Human mesenchymal stem cell co-culture modulates the immunological properties of human intervertebral disc tissue fragments in vitro. *Eur Spine J* 20, 592-603.

Beyth, S., Borovsky, Z., Mevorach, D., Liebergall, M., Gazit, Z., Aslan, H., Galun, E and Rachmilewitz, J. (2005). Human mesenchymal stem cells alter antigen-presenting cell maturation and induce T-cell unresponsiveness. *Blood* 105, 2214-2219.

Billinghurst, R.C., Dahlberg, L., Ionescu, M., Reiner, A., Bourne, R., Rorabeck, C., Mitchell, P., Hambor, J., Diekmann, O., Tschesche, H., *et al.* (1997). Enhanced cleavage of type II collagen by collagenases in osteoarthritic articular cartilage. *J Clin Invest* 99, 1534-1545.

Biomet (2013). ChonDux for Filling Full Thickness Cartilage Defects in the Femoral Condyle of the Knee
<http://clinicaltrials.gov/ct2/show/NCT01110070>.

Blain, E.J., Gilbert, S.J., Wardale, R.J., Capper, S.J., Mason, D.J., and Duance, V.C. (2001). Up-regulation of matrix metalloproteinase expression and activation following cyclical compressive loading of articular cartilage in vitro. *Arch Biochem Biophys* 396, 49-55.

Bobis, S., Jarocha, D., and Majka, M. (2006). Mesenchymal stem cells: characteristics and clinical applications. *Folia Histochem Cytobiol* 44, 215-230.

Boot-Handford, R.P., Tuckwell, D.S., Plumb, D.A., Rock, C.F., and Poulson, R. (2003). A novel and highly conserved collagen (pro(α)1(XXVII)) with a unique expression pattern and unusual molecular characteristics establishes a new clade within the vertebrate fibrillar collagen family. *J Biol Chem* 278, 31067-31077.

Bouffi, C., Thomas, O., Bony, C., Giteau, A., Venier-Julienne, M.C., Jorgensen, C., Montero-Menei, C., and Noel, D. (2010). The role of pharmacologically active microcarriers releasing TGF-β3 in cartilage formation in vivo by mesenchymal stem cells. *Biomaterials* 31, 6485-6493.

Brindle, T., Nyland, J., and Johnson, D.L. (2001). The meniscus: review of basic principles with application to surgery and rehabilitation. *J Athl Train* 36, 160-169.

Brittberg, M. (1999). Autologous chondrocyte transplantation. *Clin Orthop Relat Res*, S147-155.

Brittberg, M. (2008). Autologous chondrocyte implantation--technique and long-term follow-up. *Injury* 39 *Suppl 1*, S40-49.

Brittberg, M., Sjogren-Jansson, E., Lindahl, A., and Peterson, L. (1997). Influence of fibrin sealant (Tisseel) on osteochondral defect repair in the rabbit knee. *Biomaterials* 18, 235-242.

Brooks, P.C., Montgomery, A.M., Rosenfeld, M., Reisfeld, R.A., Hu, T., Klier, G., and Cheresh, D.A. (1994). Integrin alpha v beta 3 antagonists promote tumour regression by inducing apoptosis of angiogenic blood vessels. *Cell* 79, 1157-1164.

Brooks, P.C., Stromblad, S., Sanders, L.C., von Schalscha, T.L., Aimes, R.T., Stetler-Stevenson, W.G., Quigley, J.P., and Cheresh, D.A. (1996). Localisation of matrix metalloproteinase MMP-2 to the surface of invasive cells by interaction with integrin alpha v beta 3. *Cell* 85, 683-693.

Brown, R.A., and Jones, K.L. (1990). The synthesis and accumulation of fibronectin by human articular cartilage. *J Rheumatol* 17, 65-72.

Browne, J.E., and Branch, T.P. (2000). Surgical alternatives for treatment of articular cartilage lesions. *J Am Acad Orthop Surg* 8, 180-189.

Bruneel, D., and Schacht, E. (1995). End Group Modification of Pullulan. *Polymer* 36, 169-172.

Buchanan, W.W. (2003). William Hunter (1718-1783). *Rheumatology* 42, 1260-1261.

Buhring, H.J., Battula, V.L., Treml, S., Schewe, B., Kanz, L., and Vogel, W. (2007). Novel markers for the prospective isolation of human MSC. *Ann N Y Acad Sci* 1106, 262-271.

Bulman, S.E., Barron, V., Coleman, C.M., and Barry, F. (2012). Enhancing the Mesenchymal Stem Cell Therapeutic Response: Cell Localisation and Support for Cartilage Repair. *Tissue Eng Part B Rev*.

Burrage, P.S., Mix, K.S., and Brinckerhoff, C.E. (2006). Matrix metalloproteinases: role in arthritis. *Front Biosci* 11, 529-543.

Buschmann, M.D., Kim, Y.J., Wong, M., Frank, E., Hunziker, E.B., and Grodzinsky, A.J. (1999). Stimulation of aggrecan synthesis in cartilage explants by cyclic loading is localized to regions of high interstitial fluid flow. *Arch Biochem Biophys* 366, 1-7.

Butch, A.W. (2000). Dilution protocols for detection of hook effects/prozone phenomenon. *Clin Chem* 46, 1719-1721.

Buttner, F.H., Hughes, C.E., Margerie, D., Lichte, A., Tschesche, H., Caterson, B., and Bartnik, E. (1998). Membrane type 1 matrix metalloproteinase (MT1-MMP) cleaves the recombinant aggrecan substrate rAgg1mut at the 'aggrecanase' and the MMP sites. Characterization of MT1-MMP catabolic activities on the interglobular domain of aggrecan. *Biochem J* 333 (Pt 1), 159-165.

Campbell, I.D., and Humphries, M.J. (2012). Integrin structure, activation, and interactions. *Cold Spring Harb Perspect Biol* 3.

Cao, B., Zheng, B., Jankowski, R.J., Kimura, S., Ikezawa, M., Deasy, B., Cummins, J., Epperly, M., Qu-Petersen, Z., and Huard, J. (2003). Muscle stem cells differentiate into haematopoietic lineages but retain myogenic potential. *Nat Cell Biol* 5, 640-646.

Caplan, A.I. (2009a). New era of cell-based orthopedic therapies. *Tissue Eng Part B Rev* 15, 195-200.

Caplan, A.I. (2009b). Why are MSCs therapeutic? New data: new insight. *J Pathol* 217, 318-324.

Carlson, C.B., Mowery, P., Owen, R.M., Dykhuizen, E.C., and Kiessling, L.L. (2007). Selective tumour cell targeting using low-affinity, multivalent interactions. *ACS Chem Biol* 2, 119-127.

Caron, J.P., Fernandes, J.C., Martel-Pelletier, J., Tardif, G., Mineau, F., Geng, C., and Pelletier, J.P. (1996). Chondroprotective effect of intraarticular injections of interleukin-1 receptor antagonist in experimental osteoarthritis. Suppression of collagenase-1 expression. *Arthritis Rheum* 39, 1535-1544.

Carrington, J.L. (2005). Aging bone and cartilage: cross-cutting issues. *Biochem Biophys Res Commun* 328, 700-708.

Carter, P. (2001). Improving the Efficacy of Antibody-based Cancer Therapies. *Nature Reviews* 1, 12.

- Caterson, B., Flannery, C.R., Hughes, C.E., and Little, C.B. (2000). Mechanisms involved in cartilage proteoglycan catabolism. *Matrix Biol* 19, 333-344.
- CDC (2010). Prevalence of doctor-diagnosed arthritis and arthritis-attributable activity limitation --- United States, 2007-2009. *MMWR Morb Mortal Wkly Rep* 59, 1261-1265.
- Centeno, C.J., and Faulkner, S. (2011). The Use of Mesenchymal Stem Cells in Orthopaedics: Review of the Literature, Current Research, and Regulatory Landscape. *Journal of American Physicians and Surgeons* 16, 7.
- Chen, A., Zheng, G., and Tykocinski, M.L. (2000). Hierarchical costimulator thresholds for distinct immune responses: application of a novel two-step Fc fusion protein transfer method. *J Immunol* 164, 705-711.
- Chen, F.H., and Tuan, R.S. (2008). Mesenchymal stem cells in arthritic diseases. *Arthritis Res Ther* 10, 223.
- Chen, J., Wang, C., Lu, S., Wu, J., Guo, X., Duan, C., Dong, L., Song, Y., Zhang, J., Jing, D., *et al.* (2005). In vivo chondrogenesis of adult bone-marrow-derived autologous mesenchymal stem cells. *Cell Tissue Res* 319, 429-438.
- Cheng, K., Li, T.S., Malliaras, K., Davis, D.R., Zhang, Y., and Marban, E. (2010). Magnetic targeting enhances engraftment and functional benefit of iron-labelled cardiosphere-derived cells in myocardial infarction. *Circ Res* 106, 1570-1581.
- Cheung, N.K., Cheung, I.Y., Kushner, B.H., Ostrovskaya, I., Chamberlain, E., Kramer, K., and Modak, S. (2012). Murine anti-GD2 monoclonal antibody 3F8 combined with granulocyte-macrophage colony-stimulating factor and 13-cis-retinoic acid in high-risk patients with stage 4 neuroblastoma in first remission. *J Clin Oncol* 30, 3264-3270.
- Chiang, H., and Jiang, C.C. (2009). Repair of articular cartilage defects: review and perspectives. *J Formos Med Assoc* 108, 87-101.
- Chivers, C.E., Koner, A.L., Lowe, E.D., and Howarth, M. (2011). How the biotin-streptavidin interaction was made even stronger: investigation via crystallography and a chimaeric tetramer. *Biochem J* 435, 55-63.
- Chivers, R.A.W., R.G (1997). The strength of adhesive-bonded tissue joints. *International Journal of Adhesion and Adhesives* 17, 127-132.

Cho, S.K., Bourdeau, A., Letarte, M., and Zuniga-Pflucker, J.C. (2001). Expression and function of CD105 during the onset of hematopoiesis from Flk1(+) precursors. *Blood* 98, 3635-3642.

Christian, W., Johnson, T.S., and Gill, T.J. (2008). In vitro and in vivo cell tracking of chondrocytes of different origin by fluorescent PKH26 and CFMDA. *J Biomedical Science and Engineering* 1, 6.

Chu, C.R., Szczodry, M., and Bruno, S. (2010). Animal models for cartilage regeneration and repair. *Tissue Eng Part B Rev* 16, 105-115.

Chubinskaya, S., Huch, K., Mikecz, K., Cs-Szabo, G., Hasty, K.A., Kuettner, K.E., and Cole, A.A. (1996). Chondrocyte matrix metalloproteinase-8: up-regulation of neutrophil collagenase by interleukin-1 beta in human cartilage from knee and ankle joints. *Lab Invest* 74, 232-240.

Chubinskaya, S., Mikhail, R., Deutsch, A., and Tindal, M.H. (2001). ADAM-10 protein is present in human articular cartilage primarily in the membrane-bound form and is upregulated in osteoarthritis and in response to IL-1alpha in bovine nasal cartilage. *J Histochem Cytochem* 49, 1165-1176.

Clark, J.O.E., and Hemsley, W. (1994). Chemistry: Mini Dictionary. In *Chemistry*, J.O.E. Clark, and W. Hemsley, eds. (Edinburgh, Harrap Nooks Ltd).

clinicaltrials.gov (2013). <http://clinicaltrials.gov/>.

Cloutier, S.M., Couty, S., Terskikh, A., Marguerat, L., Crivelli, V., Pugnieres, M., Mani, J.C., Leisinger, H.J., Mach, J.P., and Deperthes, D. (2000). Streptabody, a high avidity molecule made by tetramerization of in vivo biotinylated, phage display-selected scFv fragments on streptavidin. *Mol Immunol* 37, 1067-1077.

Coleman, C.M., Curtin, C., Barry, F.P., O'Flatharta, C., and Murphy, J.M. (2010). Mesenchymal stem cells and osteoarthritis: remedy or accomplice? *Hum Gene Ther* 21, 1239-1250.

Coleman, C.M., and Tuan, R.S. (2003). Functional role of growth/differentiation factor 5 in chondrogenesis of limb mesenchymal cells. *Mech Dev* 120, 823-836.

Colter, D.C., Sekiya, I., and Prockop, D.J. (2001). Identification of a subpopulation of rapidly self-renewing and multipotential adult stem cells in

colonies of human marrow stromal cells. *Proc Natl Acad Sci U S A* 98, 7841-7845.

Conca, K.R., and Yang, T.C.S. (1993). Edible food barrier coatings. In *Biodegradable Polymers and Packaging*, C. Ching, D.L. Kaplan, and E.L. Thomas, eds. (Lancaster: Technomic).

Connelly, J.T., Garcia, A.J., and Levenston, M.E. (2007). Inhibition of in vitro chondrogenesis in RGD-modified three-dimensional alginate gels. *Biomaterials* 28, 1071-1083.

Conway, J.G., Wakefield, J.A., Brown, R.H., Marron, B.E., Sekut, L., Stimpson, S.A., McElroy, A., Menius, J.A., Jeffreys, J.J., Clark, R.L., *et al.* (1995). Inhibition of cartilage and bone destruction in adjuvant arthritis in the rat by a matrix metalloproteinase inhibitor. *J Exp Med* 182, 449-457.

Corcione, A., Benvenuto, F., Ferretti, E., Giunti, D., Cappiello, V., Cazzanti, F., Risso, M., Gualandi, F., Mancardi, G.L., Pistoia, V., *et al.* (2006). Human mesenchymal stem cells modulate B-cell functions. *Blood* 107, 367-372.

Coviello, T., Matricardi, P., Marianecchi, C., and Alhaique, F. (2007). Polysaccharide hydrogels for modified release formulations. *J Control Release* 119, 5-24.

Cullen, E. (2010). Migration and Engraftment of Mesenchymal Stem Cells in a Destabilised Medial Meniscal Model of Osteoarthritis. Phase I: model establishment. In *Medicine* (Galway, National University of Ireland, Galway).

Curtin, C. (2009). Cellular Therapy for Cartilage Repair: Strategies for Targeting. In *Regenerative Medicine Institute (Remedi)* (Galway, National University of Ireland, Galway), pp. 185.

d'Ayala, G.G., Malinconico, M., and Laurienzo, P. (2008). Marine derived polysaccharides for biomedical applications: chemical modification approaches. *Molecules* 13, 2069-2106.

D'Souza, S.E., Ginsberg, M.H., and Plow, E.F. (1991). Arginyl-glycyl-aspartic acid (RGD): a cell adhesion motif. *Trends Biochem Sci* 16, 246-250.

da Silva Meirelles, L., Caplan, A.I., and Nardi, N.B. (2008). In search of the in vivo identity of mesenchymal stem cells. *Stem Cells* 26, 2287-2299.

Dahlberg, L., Billingham, R.C., Manner, P., Nelson, F., Webb, G., Ionescu, M., Reiner, A., Tanzer, M., Zukor, D., Chen, J., *et al.* (2000). Selective

enhancement of collagenase-mediated cleavage of resident type II collagen in cultured osteoarthritic cartilage and arrest with a synthetic inhibitor that spares collagenase 1 (matrix metalloproteinase 1). *Arthritis Rheum* 43, 673-682.

Danisovic, L., Varga, I., Zamborsky, R., and Bohmer, D. (2012). The tissue engineering of articular cartilage: cells, scaffolds and stimulating factors. *Exp Biol Med (Maywood)* 237, 10-17.

De Bari, C., and Dell'Accio, F. (2008). Cell therapy: a challenge in modern medicine. *Biomed Mater Eng* 18, S11-17.

De Bari, C., Dell'Accio, F., Tylzanowski, P., and Luyten, F.P. (2001). Multipotent mesenchymal stem cells from adult human synovial membrane. *Arthritis Rheum* 44, 1928-1942.

Dejica, V.M., Mort, J.S., Lavery, S., Antoniou, J., Zukor, D.J., Tanzer, M., and Poole, A.R. (2012). Increased type II collagen cleavage by cathepsin K and collagenase activities with aging and osteoarthritis in human articular cartilage. *Arthritis Res Ther* 14, R113.

Dejica, V.M., Mort, J.S., Lavery, S., Percival, M.D., Antoniou, J., Zukor, D.J., and Poole, A.R. (2008). Cleavage of type II collagen by cathepsin K in human osteoarthritic cartilage. *Am J Pathol* 173, 161-169.

Dennis, J.E., Cohen, N., Goldberg, V.M., and Caplan, A.I. (2004). Targeted delivery of progenitor cells for cartilage repair. *J Orthop Res* 22, 735-741.

Dequeker, J., and Luyten, F.P. (2008). The history of osteoarthritis-osteoarthrosis. *Ann Rheum Dis* 67, 5-10.

Devine, S.M., Bartholomew, A.M., Mahmud, N., Nelson, M., Patil, S., Hardy, W., Sturgeon, C., Hewett, T., Chung, T., Stock, W., *et al.* (2001). Mesenchymal stem cells are capable of homing to the bone marrow of non-human primates following systemic infusion. *Exp Hematol* 29, 244-255.

Di Nicola, M., Carlo-Stella, C., Magni, M., Milanese, M., Longoni, P.D., Matteucci, P., Grisanti, S., and Gianni, A.M. (2002). Human bone marrow stromal cells suppress T-lymphocyte proliferation induced by cellular or nonspecific mitogenic stimuli. *Blood* 99, 3838-3843.

Diamandis, E.P., and Christopoulos, T.K. (1991). The biotin-(strept)avidin system: principles and applications in biotechnology. *Clin Chem* 37, 625-636.

Diaz-Romero, J., Gaillard, J.P., Grogan, S.P., Nestic, D., Trub, T., and Mainil-Varlet, P. (2005). Immunophenotypic analysis of human articular chondrocytes: changes in surface markers associated with cell expansion in monolayer culture. *J Cell Physiol* 202, 731-742.

Dinauer, N., Balthasar, S., Weber, C., Kreuter, J., Langer, K., and von Briesen, H. (2005). Selective targeting of antibody-conjugated nanoparticles to leukemic cells and primary T-lymphocytes. *Biomaterials* 26, 5898-5906.

Docheva, D., Haasters, F., and Schieker, M. (2008). Mesenchymal Stem Cells and Their Cell Surface Receptors. *Current Rheumatology Reviews* 4, 6.

Docheva, D., Popov, C., Mutschler, W., and Schieker, M. (2007). Human mesenchymal stem cells in contact with their environment: surface characteristics and the integrin system. *J Cell Mol Med* 11, 21-38.

Dominici, M. (2008). General MSC discussion, S. Bulman, ed.

Dominici, M.L.B., K; Mueller, I; Slaper-Cortenbach, I; Marini F,C; Krause, D,S; Deans, R,J; Keating, A; Prockop D, J and Horwitz, E,M. (2006). Minimal criteria for defining multipotent mesenchymal stromal cells. The International Society for Cellular Therapy position statement. *Cytotherapy* 8, 315-317.

Donkerwolcke, M., Burny, F., and Muster, D. (1998). Tissues and bone adhesives--historical aspects. *Biomaterials* 19, 1461-1466.

Doppalapudi, V.R., Huang, J., Liu, D., Jin, P., Liu, B., Li, L., Desharnais, J., Hagen, C., Levin, N.J., Shields, M.J., *et al.* (2010). Chemical generation of bispecific antibodies. *Proc Natl Acad Sci U S A* 107, 22611-22616.

Dowthwaite, G.P., Bishop, J.C., Redman, S.N., Khan, I.M., Rooney, P., Evans, D.J., Haughton, L., Bayram, Z., Boyer, S., Thomson, B., *et al.* (2004). The surface of articular cartilage contains a progenitor cell population. *J Cell Sci* 117, 889-897.

Dubel, S., Breitling, F., Kontermann, R., Schmidt, T., Skerra, A., and Little, M. (1995). Bifunctional and multimeric complexes of streptavidin fused to single chain antibodies (scFv). *J Immunol Methods* 178, 201-209.

Dubey, P.K., Mishra, V., Jain, S., Mahor, S., and Vyas, S.P. (2004). Liposomes modified with cyclic RGD peptide for tumour targeting. *J Drug Target* 12, 257-264.

Duffy, M.M., Pindjakova, J., Hanley, S.A., McCarthy, C., Weidhofer, G.A., Sweeney, E.M., English, K., Shaw, G., Murphy, J.M., Barry, F.P., *et al.* (2011). Mesenchymal stem cell inhibition of T-helper 17 cell- differentiation is triggered by cell-cell contact and mediated by prostaglandin E2 via the EP4 receptor. *Eur J Immunol* *41*, 2840-2851.

Emadedin, M., Aghdami, N., Taghiyar, L., Fazeli, R., Moghadasali, R., Jahangir, S., Farjad, R., and Baghaban Eslaminejad, M. (2012). Intra-articular injection of autologous mesenchymal stem cells in six patients with knee osteoarthritis. *Arch Iran Med* *15*, 422-428.

Embry Flory, J.J., Fosang, A.J., and Knudson, W. (2006). The accumulation of intracellular ITEGE and DIPEN neopeptides in bovine articular chondrocytes is mediated by CD44 internalization of hyaluronan. *Arthritis Rheum* *54*, 443-454.

English, K., Barry, F.P., and Mahon, B.P. (2008). Murine mesenchymal stem cells suppress dendritic cell migration, maturation and antigen presentation. *Immunol Lett* *115*, 50-58.

FDA (2009). Drugs
<http://www.fda.gov/Drugs/DevelopmentApprovalProcess>.

Feng, Y., Jin, X., Dai, G., Liu, J., Chen, J., and Yang, L. (2011). In vitro targeted magnetic delivery and tracking of superparamagnetic iron oxide particles labelled stem cells for articular cartilage defect repair. *J Huazhong Univ Sci Technolog Med Sci* *31*, 204-209.

Fernandes, J.C., Caron, J.P., Martel-Pelletier, J., Jovanovic, D., Mineau, F., Tardif, G., Otterness, I.G., and Pelletier, J.P. (1997). Effects of tenidap on the progression of osteoarthritic lesions in a canine experimental model. Suppression of metalloprotease and interleukin-1 activity. *Arthritis Rheum* *40*, 284-294.

Fisher, J.E., Caulfield, M.P., Sato, M., Quartuccio, H.A., Gould, R.J., Garsky, V.M., Rodan, G.A., and Rosenblatt, M. (1993). Inhibition of osteoclastic bone resorption in vivo by echistatin, an "arginyl-glycyl-aspartyl" (RGD)-containing protein. *Endocrinology* *132*, 1411-1413.

Flannery, C.R., Zollner, R., Corcoran, C., Jones, A.R., Root, A., Rivera-Bermudez, M.A., Blanchet, T., Gleghorn, J.P., Bonassar, L.J., Bendele, A.M., *et al.* (2009). Prevention of cartilage degeneration in a rat model of

osteoarthritis by intraarticular treatment with recombinant lubricin. *Arthritis Rheum* 60, 840-847.

Fonsatti, E., Altomonte, M., Nicotra, M.R., Natali, P.G., and Maio, M. (2003). Endoglin (CD105): a powerful therapeutic target on tumour-associated angiogenic blood vessels. *Oncogene* 22, 6557-6563.

Fosang, A.J., Last, K., Fujii, Y., Seiki, M., and Okada, Y. (1998). Membrane-type 1 MMP (MMP-14) cleaves at three sites in the aggrecan interglobular domain. *FEBS Lett* 430, 186-190.

Fosang, A.J., Last, K., Stanton, H., Golub, S.B., Little, C.B., Brown, L., and Jackson, D.C. (2010). Neoepitope antibodies against MMP-cleaved and aggrecanase-cleaved aggrecan. *Methods Mol Biol* 622, 312-347.

Fosang, A.J., Last, K., Stanton, H., Weeks, D.B., Campbell, I.K., Hardingham, T.E., and Hembry, R.M. (2000). Generation and novel distribution of matrix metalloproteinase-derived aggrecan fragments in porcine cartilage explants. *J Biol Chem* 275, 33027-33037.

Fosang, A.J., Stanton, H., Little, C.B., and Atley, L.M. (2003). Neoepitopes as biomarkers of cartilage catabolism. *Inflamm Res* 52, 277-282.

Frauenstuh, S., Reichmann, E., Ibold, Y., Goetz, P.M., Sittinger, M., and Ringe, J. (2007). A microcarrier-based cultivation system for expansion of primary mesenchymal stem cells. *Biotechnology progress* 23, 187-193.

Freed, L.E., Vunjak-Novakovic, G., and Langer, R. (1993). Cultivation of cell-polymer cartilage implants in bioreactors. *Journal of cellular biochemistry* 51, 257-264.

Frenkel, S.R., and Di Cesare, P.E. (2004). Scaffolds for articular cartilage repair. *Ann Biomed Eng* 32, 26-34.

Fuerst, M., Bertrand, J., Lammers, L., Dreier, R., Echtermeyer, F., Nitschke, Y., Rutsch, F., Schafer, F.K., Niggemeyer, O., Steinhagen, J., *et al.* (2009). Calcification of articular cartilage in human osteoarthritis. *Arthritis Rheum* 60, 2694-2703.

Garcia, Y., Breen, A., Burugapalli, K., Dockery, P., and Pandit, A. (2007). Stereological methods to assess tissue response for tissue-engineered scaffolds. *Biomaterials* 28, 175-186.

Genes, N.G., Rowley, J.A., Mooney, D.J., and Bonassar, L.J. (2004). Effect of substrate mechanics on chondrocyte adhesion to modified alginate surfaces. *Arch Biochem Biophys* 422, 161-167.

Gerasimou, A., Ramella, R., Brero, A., Boero, O., Sheiban, I., Levi, R., and Gallo, M.P. (2009). Homing of annexin-labelled stem cells to apoptotic cells. *Cell Mol Biol Lett* 14, 100-112.

Giannini, S., Battaglia, M., Buda, R., Cavallo, M., Ruffilli, A., and Vannini, F. (2009a). Surgical treatment of osteochondral lesions of the talus by open-field autologous chondrocyte implantation: a 10-year follow-up clinical and magnetic resonance imaging T2-mapping evaluation. *Am J Sports Med* 37 *Suppl 1*, 112S-118S.

Giannini, S., Buda, R., Vannini, F., Cavallo, M., and Grigolo, B. (2009b). One-step bone marrow-derived cell transplantation in talar osteochondral lesions. *Clin Orthop Relat Res* 467, 3307-3320.

Glasson, S.S., Blanchet, T.J., and Morris, E.A. (2007). The surgical destabilization of the medial meniscus (DMM) model of osteoarthritis in the 129/SvEv mouse. *Osteoarthritis Cartilage* 15, 1061-1069.

Glasson, S.S., Resmini, C., and Morris, E. (2008). UTILITY OF THE STR/ORT MOUSE MODEL OF SPONTANEOUS OA. In *Osteoarthritis and Cartilage*, pp. S47-S48.

Glennie, M.J., and Johnson, P.W. (2000). Clinical trials of antibody therapy. *Immunol Today* 21, 403-410.

Goldring, M.B., and Goldring, S.R. (2007). Osteoarthritis. *J Cell Physiol* 213, 626-634.

Gole, M.D., Poulsen, D., Marzo, J.M., Ko, S.H., and Ziv, I. (2004). Chondrocyte viability in press-fit cryopreserved osteochondral allografts. *J Orthop Res* 22, 781-787.

Gooding, C.R., Bartlett, W., Bentley, G., Skinner, J.A., Carrington, R., and Flanagan, A. (2006). A prospective, randomised study comparing two techniques of autologous chondrocyte implantation for osteochondral defects in the knee: Periosteum covered versus type I/III collagen covered. *Knee* 13, 203-210.

Goodman, S.L., Holzemann, G., Sulyok, G.A., and Kessler, H. (2002). Nanomolar small molecule inhibitors for $\alpha_6\beta_6$, $\alpha_5\beta_5$, and $\alpha_3\beta_3$ integrins. *J Med Chem* 45, 1045-1051.

Goshima, J., Goldberg, V.M., and Caplan, A.I. (1991). The osteogenic potential of culture-expanded rat marrow mesenchymal cells assayed in vivo in calcium phosphate ceramic blocks. *Clin Orthop Relat Res*, 298-311.

Grana, C., Chinol, M., Robertson, C., Mazzetta, C., Bartolomei, M., De Cicco, C., Fiorenza, M., Gatti, M., Caliceti, P., and Paganelli, G. (2002). Pretargeted adjuvant radioimmunotherapy with yttrium-90-biotin in malignant glioma patients: a pilot study. *Br J Cancer* 86, 207-212.

Grenfell, W. (1924). *Yourself and Your Body* (London, Hodder and Stroughton Ltd).

Gronthos, S., and Simmons, P.J. (1995). The growth factor requirements of STRO-1-positive human bone marrow stromal precursors under serum-deprived conditions in vitro. *Blood* 85, 929-940.

Grzesiak, J.J., Pierschbacher, M.D., Amodeo, M.F., Malaney, T.I., and Glass, J.R. (1997). Enhancement of cell interactions with collagen/glycosaminoglycan matrices by RGD derivatization. *Biomaterials* 18, 1625-1632.

Gudas, R., Gudaite, A., Pocius, A., Gudiene, A., Cekanauskas, E., Monastyreckiene, E., and Basevicius, A. (2012). Ten-year follow-up of a prospective, randomized clinical study of mosaic osteochondral autologous transplantation versus microfracture for the treatment of osteochondral defects in the knee joint of athletes. *Am J Sports Med* 40, 2499-2508.

Gudas, R., Kalesinskas, R.J., Kimtys, V., Stankevicius, E., Toliusis, V., Bernotavicius, G., and Smailys, A. (2005). A prospective randomized clinical study of mosaic osteochondral autologous transplantation versus microfracture for the treatment of osteochondral defects in the knee joint in young athletes. *Arthroscopy* 21, 1066-1075.

Gudas, R., Stankevicius, E., Monastyreckiene, E., Pranys, D., and Kalesinskas, R.J. (2006). Osteochondral autologous transplantation versus microfracture for the treatment of articular cartilage defects in the knee joint in athletes. *Knee Surg Sports Traumatol Arthrosc* 14, 834-842.

Gumbiner, B.M. (1996). Cell adhesion: the molecular basis of tissue architecture and morphogenesis. *Cell* 84, 345-357.

Gundersen, H.J.G., Bagger, P., Bendtsen, T.F., Evans, S.M., Korbo, L., Marcussen, N., Moller, A., Nielsen, K., Nyengaard, J.R., Pakkenberg, B., *et al.* (1988). The new stereological tools: disector, fractionator, nucleator and point sampled intercepts and their use in pathological research and diagnosis, review article. *APMIS* 96, 857-881.

Haleem, A.M., Singergy, A.A., Sabry, D., Atta, H.M., Rashed, L.A., Chu, C.R., El Shewy, M.T., Azzam, A., and Abdel Aziz, M.T. (2010). The Clinical Use of Human Culture-Expanded Autologous Bone Marrow Mesenchymal Stem Cells Transplanted on Platelet-Rich Fibrin Glue in the Treatment of Articular Cartilage Defects: A Pilot Study and Preliminary Results. *Cartilage* 1, 253-261.

Hall, B.K., and Miyake, T. (2000). All for one and one for all: condensations and the initiation of skeletal development. *Bioessays* 22, 138-147.

Hambach, L., Neureiter, D., Zeiler, G., Kirchner, T., and Aigner, T. (1998). Severe disturbance of the distribution and expression of type VI collagen chains in osteoarthritic articular cartilage. *Arthritis Rheum* 41, 986-996.

Hangody, L., Vasarhelyi, G., Hangody, L.R., Sukosd, Z., Tibay, G., Bartha, L., and Bodo, G. (2008). Autologous osteochondral grafting--technique and long-term results. *Injury* 39 *Suppl* 1, S32-39.

Hansen, O.M., Foldager, C.B., Christensen, B.B., Everland, H., and Lind, M. (2012). Increased chondrocyte seeding density has no positive effect on cartilage repair in an MPEG-PLGA scaffold. *Knee Surg Sports Traumatol Arthrosc.*

Haubner, R., Wester, H.J., Weber, W.A., Mang, C., Ziegler, S.I., Goodman, S.L., Senekowitsch-Schmidtke, R., Kessler, H., and Schwaiger, M. (2001). Noninvasive imaging of alpha(v)beta3 integrin expression using 18F-labelled RGD-containing glycopeptide and positron emission tomography. *Cancer Res* 61, 1781-1785.

Hayashi, M., Muneta, T., Ju, Y.J., Mochizuki, T., and Sekiya, I. (2008). Weekly intra-articular injections of bone morphogenetic protein-7 inhibits osteoarthritis progression. *Arthritis Res Ther* 10, R118.

Haynesworth, S.E., Baber, M.A., and Caplan, A.I. (1996). Cytokine expression by human marrow-derived mesenchymal progenitor cells in vitro: effects of dexamethasone and IL-1 alpha. *J Cell Physiol* 166, 585-592.

Haynesworth, S.E., Goldberg, V.M., and Caplan, A.I. (1994). Diminution of the number of mesenchymal stem cells as a cause for skeletal aging. In *Musculoskeletal Soft-tissue Aging: Impact on Mobility*. In *Handbook of Stem Cells*, BuckwalterJA, GoldbergVM, and Y. WooSL-Y, eds. (Rosemont, American Academy of Orthopaedic Surgeons), pp. 79-87.

Henson, F.M., and Vincent, T. (2007). Chondrocyte outgrowth into a gelatin scaffold in a single impact load model of damage/repair - effect of BMP-2. *BMC Musculoskelet Disord* 8, 120.

Henson, F.M.D., Bowe, E.A., and M.E., D. (2005). Promotion of the intrinsic damage–repair response in articular cartilage by fibroblastic growth factor-2. *Osteoarthritis and Cartilage* 13, 537-544.

Hermanson, G.T. (2008). *Bioconjugate Techniques*, 2nd edn (Academic Press Inc).

Hermansson, M., Sawaji, Y., Bolton, M., Alexander, S., Wallace, A., Begum, S., Wait, R., and Saklatvala, J. (2004). Proteomic analysis of articular cartilage shows increased type II collagen synthesis in osteoarthritis and expression of inhibin betaA (activin A), a regulatory molecule for chondrocytes. *J Biol Chem* 279, 43514-43521.

Hersel, U., Dahmen, C., and Kessler, H. (2003). RGD modified polymers: biomaterials for stimulated cell adhesion and beyond. *Biomaterials* 24, 4385-4415.

Ho, S.T., Cool, S.M., Hui, J.H., and Hutmacher, D.W. (2010). The influence of fibrin based hydrogels on the chondrogenic differentiation of human bone marrow stromal cells. *Biomaterials* 31, 38-47.

Ho, W., Tawil, B., Dunn, J.C., and Wu, B.M. (2006). The behavior of human mesenchymal stem cells in 3D fibrin clots: dependence on fibrinogen concentration and clot structure. *Tissue Eng* 12, 1587-1595.

Hollander, A.P., Heathfield, T.F., Webber, C., Iwata, Y., Bourne, R., Rorabeck, C., and Poole, A.R. (1994). Increased damage to type II collagen in osteoarthritic articular cartilage detected by a new immunoassay. *J Clin Invest* 93, 1722-1732.

Hollander, A.P., Pidoux, I., Reiner, A., Rorabeck, C., Bourne, R., and Poole, A.R. (1995). Damage to type II collagen in aging and osteoarthritis starts at the articular surface, originates around chondrocytes, and extends into the cartilage with progressive degeneration. *J Clin Invest* 96, 2859-2869.

Homandberg, G.A. (1999). Potential regulation of cartilage metabolism in osteoarthritis by fibronectin fragments. *Front Biosci* 4, D713-730.

Homandberg, G.A., Hui, F., Wen, C., Purple, C., Bewsey, K., Koepp, H., Huch, K., and Harris, A. (1997). Fibronectin-fragment-induced cartilage chondrolysis is associated with release of catabolic cytokines. *Biochem J* 321 (Pt 3), 751-757.

Homandberg, G.A., and Wen, C. (1998). Exposure of cartilage to a fibronectin fragment amplifies catabolic processes while also enhancing anabolic processes to limit damage. *J Orthop Res* 16, 237-246.

Horton, W.E., Jr., Yagi, R., Lavery, D., and Weiner, S. (2005). Overview of studies comparing human normal cartilage with minimal and advanced osteoarthritic cartilage. *Clin Exp Rheumatol* 23, 103-112.

Horwitz, E.M., Gordon, P.L., Koo, W.K., Marx, J.C., Neel, M.D., McNall, R.Y., Muul, L., and Hofmann, T. (2002). Isolated allogeneic bone marrow-derived mesenchymal cells engraft and stimulate growth in children with osteogenesis imperfecta: Implications for cell therapy of bone. *Proc Natl Acad Sci U S A* 99, 8932-8937.

Horwitz, E.M., Prockop, D.J., Fitzpatrick, L.A., Koo, W.W., Gordon, P.L., Neel, M., Sussman, M., Orchard, P., Marx, J.C., Pyeritz, R.E., *et al.* (1999). Transplantability and therapeutic effects of bone marrow-derived mesenchymal cells in children with osteogenesis imperfecta. *Nat Med* 5, 309-313.

Huang, G., Zhou, Z., Srinivasan, R., Penn, M.S., Kottke-Marchant, K., Marchant, R.E., and Gupta, A.S. (2008). Affinity manipulation of surface-conjugated RGD peptide to modulate binding of liposomes to activated platelets. *Biomaterials* 29, 1676-1685.

Huang, J.I., Kazmi, N., Durbhakula, M.M., Hering, T.M., Yoo, J.U., and Johnstone, B. (2005). Chondrogenic potential of progenitor cells derived from human bone marrow and adipose tissue: a patient-matched comparison. *J Orthop Res* 23, 1383-1389.

Hubbell, J.A. (2003). Materials as morphogenetic guides in tissue engineering. *Curr Opin Biotechnol* 14, 551-558.

Hulejova, H., Baresova, V., Klezl, Z., Polanska, M., Adam, M., and Senolt, L. (2007). Increased level of cytokines and matrix metalloproteinases in osteoarthritic subchondral bone. *Cytokine* 38, 151-156.

Humphries, J.D., Byron, A., and Humphries, M.J. (2006). Integrin ligands at a glance. *Journal of Cell Science* 119, 3.

Humphries, M.J. (2000). Integrin structure. *Biochem Soc Trans* 28, 311-339.

Hung, S.C., Pochampally, R.R., Chen, S.C., Hsu, S.C., and Prockop, D.J. (2007). Angiogenic effects of human multipotent stromal cell conditioned medium activate the PI3K-Akt pathway in hypoxic endothelial cells to inhibit apoptosis, increase survival, and stimulate angiogenesis. *Stem Cells* 25, 2363-2370.

Hunter, D.J., Li, J., LaValley, M., Bauer, D.C., Nevitt, M., DeGroot, J., Poole, R., Eyre, D., Guermazi, A., Gale, D., *et al.* (2007). Cartilage markers and their association with cartilage loss on magnetic resonance imaging in knee osteoarthritis: the Boston Osteoarthritis Knee Study. *Arthritis Res Ther* 9, R108.

Hunziker, E.B. (2009). The elusive path to cartilage regeneration. *Adv Mater* 21, 3419-3424.

Huxley-Jones, J., Robertson, D.L., and Boot-Handford, R.P. (2007). On the origins of the extracellular matrix in vertebrates. *Matrix Biol* 26, 2-11.

Hwang, D.S., Sim, S.B., and Cha, H.J. (2007). Cell adhesion biomaterial based on mussel adhesive protein fused with RGD peptide. *Biomaterials* 28, 4039-4046.

Hynes, R.O. (1999). Cell adhesion: old and new questions. *Trends Cell Biol* 9, M33-37.

Ichinose, S., Yamagata, K., Sekiya, I., Muneta, T., and Tagami, M. (2005). Detailed examination of cartilage formation and endochondral ossification using human mesenchymal stem cells. *Clin Exp Pharmacol Physiol* 32, 561-570.

Ishiura, Y., Kotani, N., Yamashita, R., Yamamoto, H., Kozutsumi, Y., and Honke, K. (2010). Anomalous expression of Thy1 (CD90) in B-cell

lymphoma cells and proliferation inhibition by anti-Thy1 antibody treatment. *Biochem Biophys Res Commun* 396, 329-334.

Issa, R.I., Engebretson, B., Rustom, L., McFetridge, P.S., and Sikavitsas, V.I. (2011). The effect of cell seeding density on the cellular and mechanical properties of a mechanostimulated tissue-engineered tendon. *Tissue Eng Part A* 17, 1479-1487.

Iwasa, J., Engebretsen, L., Shima, Y., and Ochi, M. (2009). Clinical application of scaffolds for cartilage tissue engineering. *Knee Surg Sports Traumatol Arthrosc* 17, 561-577.

Jabbari, E., and Khandemhosseini, A. (2010). *Biologically-Responsive Hybrid Biomaterials: A reference for Material Scientists and Bioengineers* (Springer).

Jain, M., Kamal, N., and Batra, S.K. (2007). Engineering antibodies for clinical applications. *Trends Biotechnol* 25, 307-316.

Janssen, M.L., Oyen, W.J., Dijkgraaf, I., Massuger, L.F., Frielink, C., Edwards, D.S., Rajopadhye, M., Boonstra, H., Corstens, F.H., and Boerman, O.C. (2002). Tumour targeting with radiolabelled alpha(v)beta(3) integrin binding peptides in a nude mouse model. *Cancer Res* 62, 6146-6151.

Jasti, B.L., X; Cleary, G (2003). Recent Advances in Mucoadhesive Drug Delivery Systems. *Pharmatech*, 194-196.

Jeong, Y.I., Nah, J.W., Na, H.K., Na, K., Kim, I.S., Cho, C.S., and Kim, S.H. (1999). Self-assembling nanospheres of hydrophobized pullulans in water. *Drug Dev Ind Pharm* 25, 917-927.

Jeschke, B., Meyer, J., Jonczyk, A., Kessler, H., Adamietz, P., Meenen, N.M., Kantlehner, M., Goepfert, C., and Nies, B. (2002). RGD-peptides for tissue engineering of articular cartilage. *Biomaterials* 23, 3455-3463.

Jin, H.J., Park, S.K., Oh, W., Yang, Y.S., Kim, S.W., and Choi, S.J. (2009). Down-regulation of CD105 is associated with multi-lineage differentiation in human umbilical cord blood-derived mesenchymal stem cells. *Biochem Biophys Res Commun* 381, 676-681.

Johnson, L.L. (2001). Arthroscopic abrasion arthroplasty: a review. *Clin Orthop Relat Res*, S306-317.

- Johnstone, B., Hering, T.M., Caplan, A.I., Goldberg, V.M., and Yoo, J.U. (1998). In vitro chondrogenesis of bone marrow-derived mesenchymal progenitor cells. *Exp Cell Res* 238, 265-272.
- Jones, E.A., Kinsey, S.E., English, A., Jones, R.A., Straszynski, L., Meredith, D.M., Markham, A.F., Jack, A., Emery, P., and McGonagle, D. (2002). Isolation and characterization of bone marrow multipotential mesenchymal progenitor cells. *Arthritis Rheum* 46, 3349-3360.
- Jones, K.L., Brown, M., Ali, S.Y., and Brown, R.A. (1987). An immunohistochemical study of fibronectin in human osteoarthritic and disease free articular cartilage. *Ann Rheum Dis* 46, 809-815.
- Kafienah, W., Bromme, D., Buttle, D.J., Croucher, L.J., and Hollander, A.P. (1998). Human cathepsin K cleaves native type I and II collagens at the N-terminal end of the triple helix. *Biochem J* 331 (Pt 3), 727-732.
- Karp, J.M., and Leng Teo, G.S. (2009). Mesenchymal stem cell homing: the devil is in the details. *Cell Stem Cell* 4, 206-216.
- Kaya, G., Rodriguez, I., Jorcano, J.L., Vassalli, P., and Stamenkovic, I. (1997). Selective suppression of CD44 in keratinocytes of mice bearing an antisense CD44 transgene driven by a tissue-specific promoter disrupts hyaluronate metabolism in the skin and impairs keratinocyte proliferation. *Genes Dev* 11, 996-1007.
- Kean, T.J., Duesler, L., Young, R.G., Dadabayev, A., Olenyik, A., Penn, M., Wagner, J., Fink, D.J., Caplan, A.I., and Dennis, J.E. (2011). Development of a peptide-targeted, myocardial ischemia-homing, mesenchymal stem cell. *J Drug Target* 20, 23-32.
- Khaldoyanidi, S., Denzel, A., and Zoller, M. (1996). Requirement for CD44 in proliferation and homing of hematopoietic precursor cells. *J Leukoc Biol* 60, 579-592.
- Khan, I.M., Williams, R., and Archer, C.W. (2009). One flew over the progenitor's nest: migratory cells find a home in osteoarthritic cartilage. *Cell Stem Cell* 4, 282-284.
- Khatayevich, D., Gungormus, M., Yazici, H., So, C., Cetinel, S., Ma, H., Jen, A., Tamerler, C., and Sarikaya, M. (2010). Biofunctionalization of materials for implants using engineered peptides. *Acta Biomater* 6, 4634-4641.

Kibria, G., Hatakeyama, H., Ohga, N., Hida, K., and Harashima, H. (2011). Dual-ligand modification of PEGylated liposomes shows better cell selectivity and efficient gene delivery. *J Control Release* 153, 141-148.

Kim, C., Ye, F., and Ginsberg, M.H. (2011a). Regulation of integrin activation. *Annu Rev Cell Dev Biol* 27, 321-345.

Kim, I.L., Mauck, R.L., and Burdick, J.A. (2011b). Hydrogel design for cartilage tissue engineering: a case study with hyaluronic acid. *Biomaterials* 32, 8771-8782.

Kimoto, T., Shibuya, T., and Shiobara, S. (1997). Safety studies of a novel starch, pullulan: chronic toxicity in rats and bacterial mutagenicity. *Food Chem Toxicol* 35, 323-329.

Kinnaird, T., Stabile, E., Burnett, M.S., Lee, C.W., Barr, S., Fuchs, S., and Epstein, S.E. (2004). Marrow-derived stromal cells express genes encoding a broad spectrum of arteriogenic cytokines and promote in vitro and in vivo arteriogenesis through paracrine mechanisms. *Circ Res* 94, 678-685.

Kipriyanov, S.M., Dubel, S., Breitling, F., Kontermann, R.E., Heymann, S., and Little, M. (1995). Bacterial expression and refolding of single-chain Fv fragments with C-terminal cysteines. *Cell Biophys* 26, 187-204.

Kisiday, J., Jin, M., Kurz, B., Hung, H., Semino, C., Zhang, S., and Grodzinsky, A.J. (2002). Self-assembling peptide hydrogel fosters chondrocyte extracellular matrix production and cell division: implications for cartilage tissue repair. *Proc Natl Acad Sci U S A* 99, 9996-10001.

Klein, T.J., Rizzi, S.C., Reichert, J.C., Georgi, N., Malda, J., Schuurman, W., Crawford, R.W., and Hutmacher, D.W. (2009). Strategies for zonal cartilage repair using hydrogels. *Macromol Biosci* 9, 1049-1058.

Klein, T.J., Schumacher, B.L., Schmidt, T.A., Li, K.W., Voegtline, M.S., Masuda, K., Thonar, E.J., and Sah, R.L. (2003). Tissue engineering of stratified articular cartilage from chondrocyte subpopulations. *Osteoarthritis Cartilage* 11, 595-602.

Kluba, T., Fiedler, K., Kunze, B., Ipach, I., and Suckel, A. (2012). Fibrin sealants in orthopaedic surgery: practical experiences derived from use of QUIXIL(R) in total knee arthroplasty. *Arch Orthop Trauma Surg* 132, 1147-1152.

Knox, S.J., Goris, M.L., Tempero, M., Weiden, P.L., Gentner, L., Breitz, H., Adams, G.P., Axworthy, D., Gaffigan, S., Bryan, K., *et al.* (2000). Phase II trial of yttrium-90-DOTA-biotin pretargeted by NR-LU-10 antibody/streptavidin in patients with metastatic colon cancer. *Clin Cancer Res* 6, 406-414.

Knutsen, G., Drogset, J.O., Engebretsen, L., Grontvedt, T., Isaksen, V., Ludvigsen, T.C., Roberts, S., Solheim, E., Strand, T., and Johansen, O. (2007). A randomized trial comparing autologous chondrocyte implantation with microfracture. Findings at five years. *J Bone Joint Surg Am* 89, 2105-2112.

Ko, I.K., Kean, T.J., and Dennis, J.E. (2009). Targeting mesenchymal stem cells to activated endothelial cells. *Biomaterials* 30, 3702-3710.

Ko, I.K., Kim, B.G., Awadallah, A., Mikulan, J., Lin, P., Letterio, J.J., and Dennis, J.E. (2010). Targeting improves MSC treatment of inflammatory bowel disease. *Mol Ther* 18, 1365-1372.

Kobayashi, M., Squires, G.R., Mousa, A., Tanzer, M., Zukor, D.J., Antoniou, J., Feige, U., and Poole, A.R. (2005). Role of interleukin-1 and tumour necrosis factor alpha in matrix degradation of human osteoarthritic cartilage. *Arthritis Rheum* 52, 128-135.

Koc, O.N., Gerson, S.L., Cooper, B.W., Dyhouse, S.M., Haynesworth, S.E., Caplan, A.I., and Lazarus, H.M. (2000). Rapid hematopoietic recovery after coinfusion of autologous-blood stem cells and culture-expanded marrow mesenchymal stem cells in advanced breast cancer patients receiving high-dose chemotherapy. *J Clin Oncol* 18, 307-316.

Koc, O.N., Peters, C., Aubourg, P., Raghavan, S., Dyhouse, S., DeGasperi, R., Kolodny, E.H., Yoseph, Y.B., Gerson, S.L., Lazarus, H.M., *et al.* (1999). Bone marrow-derived mesenchymal stem cells remain host-derived despite successful hematopoietic engraftment after allogeneic transplantation in patients with lysosomal and peroxisomal storage diseases. *Exp Hematol* 27, 1675-1681.

Koelling, S., Kruegel, J., Irmer, M., Path, J.R., Sadowski, B., Miro, X., and Miosge, N. (2009). Migratory chondrogenic progenitor cells from repair tissue during the later stages of human osteoarthritis. *Cell Stem Cell* 4, 324-335.

Koga, H., Engebretsen, L., Brinchmann, J.E., Muneta, T., and Sekiya, I. (2009). Mesenchymal stem cell-based therapy for cartilage repair: a review. *Knee Surg Sports Traumatol Arthrosc* 17, 1289-1297.

Koga, H., Muneta, T., Ju, Y.J., Nagase, T., Nimura, A., Mochizuki, T., Ichinose, S., von der Mark, K., and Sekiya, I. (2007). Synovial stem cells are regionally specified according to local microenvironments after implantation for cartilage regeneration. *Stem Cells* 25, 689-696.

Koga, H., Shimaya, M., Muneta, T., Nimura, A., Morito, T., Hayashi, M., Suzuki, S., Ju, Y.J., Mochizuki, T., and Sekiya, I. (2008). Local adherent technique for transplanting mesenchymal stem cells as a potential treatment of cartilage defect. *Arthritis Res Ther* 10, R84.

Kok, R.J., Schraa, A.J., Bos, E.J., Moorlag, H.E., Asgeirsdottir, S.A., Everts, M., Meijer, D.K., and Molema, G. (2002). Preparation and functional evaluation of RGD-modified proteins as alpha(v)beta(3) integrin directed therapeutics. *Bioconjug Chem* 13, 128-135.

Kon, E., Gobbi, A., Filardo, G., Delcogliano, M., Zaffagnini, S., and Marcacci, M. (2009). Arthroscopic second-generation autologous chondrocyte implantation compared with microfracture for chondral lesions of the knee: prospective nonrandomized study at 5 years. *Am J Sports Med* 37, 33-41.

Krampera, M., Glennie, S., Dyson, J., Scott, D., Laylor, R., Simpson, E., and Dazzi, F. (2003). Bone marrow mesenchymal stem cells inhibit the response of naive and memory antigen-specific T cells to their cognate peptide. *Blood* 101, 3722-3729.

Kretlow, J.D., Jin, Y.Q., Liu, W., Zhang, W.J., Hong, T.H., Zhou, G., Baggett, L.S., Mikos, A.G., and Cao, Y. (2008). Donor age and cell passage affects differentiation potential of murine bone marrow-derived stem cells. *BMC Cell Biol* 9, 60.

Kriangkum, J., Xu, B., Nagata, L.P., Fulton, R.E., and Suresh, M.R. (2001). Bispecific and bifunctional single chain recombinant antibodies. *Biomol Eng* 18, 31-40.

Krzeski, P., Buckland-Wright, C., Balint, G., Cline, G.A., Stoner, K., Lyon, R., Beary, J., Aronstein, W.S., and Spector, T.D. (2007). Development of musculoskeletal toxicity without clear benefit after administration of PG-

116800, a matrix metalloproteinase inhibitor, to patients with knee osteoarthritis: a randomized, 12-month, double-blind, placebo-controlled study. *Arthritis Res Ther* 9, R109.

Kumar, A.S., and Mody, K. (2009). Microbial Exopolysaccharides: Variety and Potential Applications. In *Microbial Production of Biopolymers and Polymer Precursors: Applications and Perspectives*, B.H.A. Rehm, ed. (Caister Academic Press).

Kuroda, K., Fujimoto, K., Sunamoto, J., and Akiyoshi, K. (2002). Hierarchical Self-Assembly of Hydrophobically Modified Pullulan in Water: Gelation by Networks of Nanoparticles. *Langmuir* 18, 6.

Kuroda, R., Ishida, K., Matsumoto, T., Akisue, T., Fujioka, H., Mizuno, K., Ohgushi, H., Wakitani, S., and Kurosaka, M. (2007). Treatment of a full-thickness articular cartilage defect in the femoral condyle of an athlete with autologous bone-marrow stromal cells. *Osteoarthritis Cartilage* 15, 226-231.

Kurz, B., Lemke, A.K., Fay, J., Pufe, T., Grodzinsky, A.J., and Schunke, M. (2005). Pathomechanisms of cartilage destruction by mechanical injury. *Ann Anat* 187, 473-485.

Kushner, B.H., Kramer, K., and Cheung, N.K. (2001). Phase II trial of the anti-G(D2) monoclonal antibody 3F8 and granulocyte-macrophage colony-stimulating factor for neuroblastoma. *J Clin Oncol* 19, 4189-4194.

Le Blanc, K., Frassoni, F., Ball, L., Locatelli, F., Roelofs, H., Lewis, I., Lanino, E., Sundberg, B., Bernardo, M.E., Remberger, M., *et al.* (2008). Mesenchymal stem cells for treatment of steroid-resistant, severe, acute graft-versus-host disease: a phase II study. *Lancet* 371, 1579-1586.

Leathers, T.D. (2003). Biotechnological production and applications of pullulan. *Appl Microbiol Biotechnol* 62, 468-473.

Leathers, T.D. (2005). *Pullulan* (Wiley).

Lee, B.P., Messersmith, P.B., Israelachvili, J.N., and Waite, J.H. (2011). Mussel-Inspired Adhesives and Coatings. *Annu Rev Mater Res* 41, 99-132.

Lee, C.H., Cook, J.L., Mendelson, A., Moioli, E.K., Yao, H., and Mao, J.J. (2010). Regeneration of the articular surface of the rabbit synovial joint by cell homing: a proof of concept study. *Lancet* 376, 440-448.

- Lee, C.R., Grad, S., Gorna, K., Gogolewski, S., Goessl, A., and Alini, M. (2005). Fibrin-polyurethane composites for articular cartilage tissue engineering: a preliminary analysis. *Tissue Eng* 11, 1562-1573.
- Lee, H.J., Choi, B.H., Min, B.H., and Park, S.R. (2009). Changes in surface markers of human mesenchymal stem cells during the chondrogenic differentiation and dedifferentiation processes in vitro. *Arthritis Rheum* 60, 2325-2332.
- Lee, M.S., Trindade, M.C., Ikenoue, T., Schurman, D.J., Goodman, S.B., and Smith, R.L. (2002). Effects of shear stress on nitric oxide and matrix protein gene expression in human osteoarthritic chondrocytes in vitro. *J Orthop Res* 20, 556-561.
- Lee, R.J., Fang, Q., Davol, P.A., Gu, Y., Sievers, R.E., Grabert, R.C., Gall, J.M., Tsang, E., Yee, M.S., Fok, H., *et al.* (2007). Antibody targeting of stem cells to infarcted myocardium. *Stem Cells* 25, 712-717.
- Lehr, C.M. (1996). From sticky stuff to sweet receptors--achievements, limits and novel approaches to bioadhesion. *Eur J Drug Metab Pharmacokinet* 21, 139-148.
- Leonard, P., Hearty, S., Quinn, J., and O'Kennedy, R. (2004). A generic approach for the detection of whole *Listeria monocytogenes* cells in contaminated samples using surface plasmon resonance. *Biosens Bioelectron* 19, 1331-1335.
- Leung, S.-H., Leone, R.S., Kumar, L.D., Kulkarni, N., and Sorg, A.F. (2006). Fast dissolving orally consumable films, U.P. Office, ed. (USA).
- Levitz, S.M. (2010). Innate recognition of fungal cell walls. *PLoS Pathog* 6, e1000758.
- Li, W.J., Danielson, K.G., Alexander, P.G., and Tuan, R.S. (2003). Biological response of chondrocytes cultured in three-dimensional nanofibrous poly(epsilon-caprolactone) scaffolds. *J Biomed Mater Res A* 67, 1105-1114.
- Li, Y., Xu, L., and Olsen, B.R. (2007a). Lessons from genetic forms of osteoarthritis for the pathogenesis of the disease. *Osteoarthritis Cartilage* 15, 1101-1105.
- Li, Y.M., Schilling, T., Benisch, P., Zeck, S., Meissner-Weigl, J., Schneider, D., Limbert, C., Seufert, J., Kassem, M., Schutze, N., *et al.* (2007b). Effects

of high glucose on mesenchymal stem cell proliferation and differentiation. *Biochem Biophys Res Commun* 363, 209-215.

Liao, H.T., Chen, C.T., Chen, C.H., Chen, J.P., and Tsai, J.C. (2011). Combination of guided osteogenesis with autologous platelet-rich fibrin glue and mesenchymal stem cell for mandibular reconstruction. *J Trauma* 70, 228-237.

Liechty, K.W., MacKenzie, T.C., Shaaban, A.F., Radu, A., Moseley, A.M., Deans, R., Marshak, D.R., and Flake, A.W. (2000). Human mesenchymal stem cells engraft and demonstrate site-specific differentiation after in utero transplantation in sheep. *Nat Med* 6, 1282-1286.

Lin, Y.T., Tang, C.H., Chuang, W.J., Wang, S.M., Huang, T.F., and Fu, W.M. (2005). Inhibition of adipogenesis by RGD-dependent disintegrin. *Biochem Pharmacol* 70, 1469-1478.

Lipman, N.S., Jackson, L.R., Trudel, L.J., and Weis-Garcia, F. (2005). Monoclonal versus polyclonal antibodies: distinguishing characteristics, applications, and information resources. *ILAR J* 46, 258-268.

Little, C.B., Hughes, C.E., Curtis, C.L., Janusz, M.J., Bohne, R., Wang-Weigand, S., Taiwo, Y.O., Mitchell, P.G., Otterness, I.G., Flannery, C.R., *et al.* (2002). Matrix metalloproteinases are involved in C-terminal and interglobular domain processing of cartilage aggrecan in late stage cartilage degradation. *Matrix Biol* 21, 271-288.

Liu, X., Jin, X., and Ma, P.X. (2011). Nanofibrous hollow microspheres self-assembled from star-shaped polymers as injectable cell carriers for knee repair. *Nat Mater* 10, 398-406.

Loeser, R.F. (2000). Chondrocyte integrin expression and function. *Biorheology* 37, 109-116.

Lorenzo, P., Bayliss, M.T., and Heinegard, D. (2004). Altered patterns and synthesis of extracellular matrix macromolecules in early osteoarthritis. *Matrix Biol* 23, 381-391.

Lum, H.E., Miller, M., Davol, P.A., Grabert, R.C., Davis, J.B., and Lum, L.G. (2005). Preclinical studies comparing different bispecific antibodies for redirecting T cell cytotoxicity to extracellular antigens on prostate carcinomas. *Anticancer Res* 25, 43-52.

Lum, L.G., Fok, H., Sievers, R., Abedi, M., Quesenberry, P.J., and Lee, R.J. (2004). Targeting of Lin-Sca+ hematopoietic stem cells with bispecific antibodies to injured myocardium. *Blood Cells Mol Dis* 32, 82-87.

Maheshwari, G., Brown, G., Lauffenburger, D.A., Wells, A., and Griffith, L.G. (2000). Cell adhesion and motility depend on nanoscale RGD clustering. *J Cell Sci* 113 (Pt 10), 1677-1686.

Maheshwari, G., Wells, A., Griffith, L.G., and Lauffenburger, D.A. (1999). Biophysical integration of effects of epidermal growth factor and fibronectin on fibroblast migration. *Biophys J* 76, 2814-2823.

Majumdar, M.K., Thiede, M.A., Mosca, J.D., Moorman, M., and Gerson, S.L. (1998). Phenotypic and functional comparison of cultures of marrow-derived mesenchymal stem cells (MSCs) and stromal cells. *J Cell Physiol* 176, 57-66.

Manfredini, M., Zerbinati, F., Gildone, A., and Faccini, R. (2007). Autologous chondrocyte implantation: a comparison between an open periosteal-covered and an arthroscopic matrix-guided technique. *Acta Orthop Belg* 73, 207-218.

Mann, B.K., and West, J.L. (2002). Cell adhesion peptides alter smooth muscle cell adhesion, proliferation, migration, and matrix protein synthesis on modified surfaces and in polymer scaffolds. *J Biomed Mater Res* 60, 86-93.

Mano, J.F., Silva, G.A., Azevedo, H.S., Malafaya, P.B., Sousa, R.A., Silva, S.S., Boesel, L.F., Oliveira, J.M., Santos, T.C., Marques, A.P., *et al.* (2007). Natural origin biodegradable systems in tissue engineering and regenerative medicine: present status and some moving trends. *J R Soc Interface* 4, 999-1030.

Mansilla, E., Marin, G.H., Sturla, F., Drago, H.E., Gil, M.A., Salas, E., Gardiner, M.C., Piccinelli, G., Bossi, S., Petrelli, L., *et al.* (2005). Human mesenchymal stem cells are tolerized by mice and improve skin and spinal cord injuries. *Transplant Proc* 37, 292-294.

Mara, C.S., Sartori, A.R., Duarte, A.S., Andrade, A.L., Pedro, M.A., and Coimbra, I.B. (2011). Periosteum as a source of mesenchymal stem cells: the effects of TGF-beta3 on chondrogenesis. *Clinics (Sao Paulo)* 66, 487-492.

Marko, K., Ligeti, M., Mezo, G., Mihala, N., Kutnyanszky, E., Kiss, E., Hudecz, F., and Madarasz, E. (2008). A novel synthetic peptide polymer with cyclic RGD motifs supports serum-free attachment of anchorage-dependent cells. *Bioconjug Chem* *19*, 1757-1766.

Martinez, C., Hofmann, T.J., Marino, R., Dominici, M., and Horwitz, E.M. (2007). Human bone marrow mesenchymal stromal cells express the neural ganglioside GD2: a novel surface marker for the identification of MSCs. *Blood* *109*, 4245-4248.

Mason, C. (2005). Stem cells are big news, but are they big business? *Med Device Technol* *16*, 25.

Mason, C. (2007). Regenerative medicine 2.0. *Regen Med* *2*, 11-18.

Mason, C., and Manzotti, E. (2010). Regenerative medicine cell therapies: numbers of units manufactured and patients treated between 1988 and 2010. *Regen Med* *5*, 307-313.

Matsumoto, T., Okabe, T., Ikawa, T., Iida, T., Yasuda, H., Nakamura, H., and Wakitani, S. (2010). Articular cartilage repair with autologous bone marrow mesenchymal cells. *J Cell Physiol* *225*, 291-295.

Mauck, R.L., Wang, C.C., Oswald, E.S., Ateshian, G.A., and Hung, C.T. (2003). The role of cell seeding density and nutrient supply for articular cartilage tissue engineering with deformational loading. *Osteoarthritis Cartilage* *11*, 879-890.

Medcalf, N. (2011). A new business model for cell-based therapeutics. In *Engineering* (Galway, National University of Ireland, Galway), pp. 186.

Meirelles Lda, S., Fontes, A.M., Covas, D.T., and Caplan, A.I. (2009). Mechanisms involved in the therapeutic properties of mesenchymal stem cells. *Cytokine Growth Factor Rev* *20*, 419-427.

Millard, M., Odde, S., and Neamati, N. (2011). Integrin targeted therapeutics. *Theranostics* *1*, 154-188.

Moerman, E.J., Teng, K., Lipschitz, D.A., and Lecka-Czernik, B. (2004). Aging activates adipogenic and suppresses osteogenic programs in mesenchymal marrow stroma/stem cells: the role of PPAR-gamma2 transcription factor and TGF-beta/BMP signaling pathways. *Aging Cell* *3*, 379-389.

Mohtai, M., Gupta, M.K., Donlon, B., Ellison, B., Cooke, J., Gibbons, G., Schurman, D.J., and Smith, R.L. (1996). Expression of interleukin-6 in osteoarthritic chondrocytes and effects of fluid-induced shear on this expression in normal human chondrocytes in vitro. *J Orthop Res* 14, 67-73.

Mokbel, A.N., El Tookhy, O.S., Shamaa, A.A., Rashed, L.A., Sabry, D., and El Sayed, A.M. (2011). Homing and reparative effect of intra-articular injection of autologous mesenchymal stem cells in osteoarthritic animal model. *BMC Musculoskelet Disord* 12, 259.

Mort, J.S., Flannery, C.R., Makkerh, J., Krupa, J.C., and Lee, E.R. (2003). Use of anti-neoepitope antibodies for the analysis of degradative events in cartilage and the molecular basis for neoepitope specificity. *Biochem Soc Symp*, 107-114.

Muellner, T., Knopp, A., Ludvigsen, T.C., and Engebretsen, L. (2001). Failed autologous chondrocyte implantation. Complete atraumatic graft delamination after two years. *Am J Sports Med* 29, 516-519.

Murphy, J.M., Fink, D.J., Hunziker, E.B., and Barry, F.P. (2003). Stem cell therapy in a caprine model of osteoarthritis. *Arthritis Rheum* 48, 3464-3474.

Mythri, G.K., Kavitha, M., Rupesh Kumar, S., and Jagadeesh, S. (2011). Novel Mucoadhesive Polymers –A Review. *Journal of Applied Pharmaceutical Science* 1, 5.

Nair, V., Kumar, D.A., Prakash, G., Jacob, S., and Agarwal, A. (2009). Bilateral spontaneous in-the-bag anterior subluxation of PCIOL managed with glued IOL technique: A case report. *Eye Contact Lens* 35, 215-217.

Nakamura, Y., Muguruma, Y., Yahata, T., Miyatake, H., Sakai, D., Mochida, J., Hotta, T., and Ando, K. (2006). Expression of CD90 on keratinocyte stem/progenitor cells. *Br J Dermatol* 154, 1062-1070.

Nallamotheu, R., Wood, G.C., Pattillo, C.B., Scott, R.C., Kiani, M.F., Moore, B.M., and Thoma, L.A. (2006). A tumour vasculature targeted liposome delivery system for combretastatin A4: design, characterization, and in vitro evaluation. *AAPS PharmSciTech* 7, E32.

Naumann, A., Dennis, J.E., Awadallah, A., Carrino, D.A., Mansour, J.M., Kastenbauer, E., and Caplan, A.I. (2002). Immunochemical and mechanical characterization of cartilage subtypes in rabbit. *J Histochem Cytochem* 50, 1049-1058.

Nehrer, S., Breinan, H.A., Ramappa, A., Hsu, H.P., Minas, T., Shortkroff, S., Sledge, C.B., Yannas, I.V., and Spector, M. (1998). Chondrocyte-seeded collagen matrices implanted in a chondral defect in a canine model. *Biomaterials* *19*, 2313-2328.

Nejadnik, H., Hui, J.H., Feng Choong, E.P., Tai, B.C., and Lee, E.H. (2010). Autologous bone marrow-derived mesenchymal stem cells versus autologous chondrocyte implantation: an observational cohort study. *Am J Sports Med* *38*, 1110-1116.

Nelson, F., Dahlberg, L., Lavery, S., Reiner, A., Pidoux, I., Ionescu, M., Fraser, G.L., Brooks, E., Tanzer, M., Rosenberg, L.C., *et al.* (1998). Evidence for altered synthesis of type II collagen in patients with osteoarthritis. *J Clin Invest* *102*, 2115-2125.

Nemeth, K., Leelahavanichkul, A., Yuen, P.S., Mayer, B., Parmelee, A., Doi, K., Robey, P.G., Leelahavanichkul, K., Koller, B.H., Brown, J.M., *et al.* (2009). Bone marrow stromal cells attenuate sepsis via prostaglandin E(2)-dependent reprogramming of host macrophages to increase their interleukin-10 production. *Nat Med* *15*, 42-49.

Neuhold, L.A., Killar, L., Zhao, W., Sung, M.L., Warner, L., Kulik, J., Turner, J., Wu, W., Billingham, C., Meijers, T., *et al.* (2001). Postnatal expression in hyaline cartilage of constitutively active human collagenase-3 (MMP-13) induces osteoarthritis in mice. *J Clin Invest* *107*, 35-44.

Nguyen, L.H., Kudva, A.K., Saxena, N.S., and Roy, K. (2011). Engineering articular cartilage with spatially-varying matrix composition and mechanical properties from a single stem cell population using a multi-layered hydrogel. *Biomaterials* *32*, 6946-6952.

Nicodemus, G.D., and Bryant, S.J. (2008). Cell encapsulation in biodegradable hydrogels for tissue engineering applications. *Tissue Eng Part B Rev* *14*, 149-165.

Nixon, A.J., Haupt, J.L., Frisbie, D.D., Morisset, S.S., McIlwraith, C.W., Robbins, P.D., Evans, C.H., and Ghivizzani, S. (2005). Gene-mediated restoration of cartilage matrix by combination insulin-like growth factor-I/interleukin-1 receptor antagonist therapy. *Gene Ther* *12*, 177-186.

Nuttelman, C.R., Mortisen, D.J., Henry, S.M., and Anseth, K.S. (2001). Attachment of fibronectin to poly(vinyl alcohol) hydrogels promotes

NIH3T3 cell adhesion, proliferation, and migration. *J Biomed Mater Res* 57, 217-223.

O'Driscoll, S.W. (1999). Articular cartilage regeneration using periosteum. *Clin Orthop Relat Res*, S186-203.

O'Hara, B.P., Urban, J.P., and Maroudas, A. (1990). Influence of cyclic loading on the nutrition of articular cartilage. *Ann Rheum Dis* 49, 536-539.

O'Kennedy, R.J., and Reading, C.L. (1990). Rapid simple cell suspension enzyme-linked immunosorbent assay to demonstrate and measure antibody binding. *Analyst* 115, 1145-1146.

Orozco, L., Munar, A., Soler, R., Alberca, M., Soler, F., Huguet, M., Sentis, J., Sanchez, A., and Garcia-Sancho, J. (2013). Treatment of Knee Osteoarthritis With Autologous Mesenchymal Stem Cells: A Pilot Study. *Transplantation* 95, 1535-1541.

Otterness, I.G., Downs, J.T., Lane, C., Bliven, M.L., Stukenbrok, H., Scampoli, D.N., Milici, A.J., and Mezes, P.S. (1999). Detection of collagenase-induced damage of collagen by 9A4, a monoclonal C-terminal neopeptide antibody. *Matrix Biol* 18, 331-341.

Pabbruwe, M.B., Kafienah, W., Tarlton, J.F., Mistry, S., Fox, D.J., and Hollander, A.P. (2010). Repair of meniscal cartilage white zone tears using a stem cell/collagen-scaffold implant. *Biomaterials* 31, 2583-2591.

Pankov, R., and Yamada, K.M. (2002). Fibronectin at a glance. *J Cell Sci* 115, 3861-3863.

Parekkadan, B., van Poll, D., Suganuma, K., Carter, E.A., Berthiaume, F., Tilles, A.W., and Yarmush, M.L. (2007). Mesenchymal stem cell-derived molecules reverse fulminant hepatic failure. *PLoS One* 2, e941.

Parkkinen, J.J., Lammi, M.J., Helminen, H.J., and Tammi, M. (1992). Local stimulation of proteoglycan synthesis in articular cartilage explants by dynamic compression in vitro. *J Orthop Res* 10, 610-620.

Patel, S., Rodriguez-Merchan, E.C., and Haddad, F.S. (2010). The use of fibrin glue in surgery of the knee. *J Bone Joint Surg Br* 92, 1325-1331.

Pearle, A.D., Warren, R.F., and Rodeo, S.A. (2005). Basic science of articular cartilage and osteoarthritis. *Clin Sports Med* 24, 1-12.

Pei, M., He, F., and Vunjak-Novakovic, G. (2008). Synovium-derived stem cell-based chondrogenesis. *Differentiation* 76, 1044-1056.

Pelletier, J.P., Caron, J.P., Evans, C., Robbins, P.D., Georgescu, H.I., Jovanovic, D., Fernandes, J.C., and Martel-Pelletier, J. (1997). In vivo suppression of early experimental osteoarthritis by interleukin-1 receptor antagonist using gene therapy. *Arthritis Rheum* 40, 1012-1019.

Pelletier, J.P., McCollum, R., Cloutier, J.M., and Martel-Pelletier J. (1995). Synthesis of metalloproteases and interleukin 6 (IL-6) in human osteoarthritic synovial membrane is an IL-1 mediated process. *J Rheumatol Suppl.* 43, 109-114.

Pelttari, K., Winter, A., Steck, E., Goetzke, K., Hennig, T., Ochs, B.G., Aigner, T., and Richter, W. (2006). Premature induction of hypertrophy during in vitro chondrogenesis of human mesenchymal stem cells correlates with calcification and vascular invasion after ectopic transplantation in SCID mice. *Arthritis Rheum* 54, 3254-3266.

Peters, J.H., Carsons, S., Yoshida, M., Ko, F., McDougall, S., Loreda, G.A., and Hahn, T.J. (2003). Electrophoretic characterization of species of fibronectin bearing sequences from the N-terminal heparin-binding domain in synovial fluid samples from patients with osteoarthritis and rheumatoid arthritis. *Arthritis Res Ther* 5, R329-339.

Pfaff, M., Tangemann, K., Muller, B., Gurrath, M., Muller, G., Kessler, H., Timpl, R., and Engel, J. (1994). Selective recognition of cyclic RGD peptides of NMR defined conformation by alpha IIb beta 3, alpha V beta 3, and alpha 5 beta 1 integrins. *J Biol Chem* 269, 20233-20238.

Phillips, J., Drumm, A., Harrison, P., Bird, P., Bhamra, K., Berrie, E., and Hale, G. (2001). Manufacture and quality control of CAMPATH-1 antibodies for clinical trials. *Cytotherapy* 3, 233-242.

Phipatanakul, W.P., VandeVord, P.J., Teitge, R.A., and Wooley, P.H. (2004). Immune response in patients receiving fresh osteochondral allografts. *Am J Orthop (Belle Mead NJ)* 33, 345-348.

Phitak, T., Pothacharoen, P., Settakorn, J., Poompimol, W., Caterson, B., and Kongtawelert, P. (2012). Chondroprotective and anti-inflammatory effects of sesamin. *Phytochemistry* 80, 77-88.

Pittenger, M.F., Mackay, A.M., Beck, S.C., Jaiswal, R.K., Douglas, R., Mosca, J.D., Moorman, M.A., Simonetti, D.W., Craig, S., and Marshak, D.R.

- (1999). Multilineage potential of adult human mesenchymal stem cells. *Science* 284, 143-147.
- Ponte, A.L., Marais, E., Gally, N., Langonne, A., Delorme, B., Herault, O., Charbord, P., and Domenech, J. (2007). The in vitro migration capacity of human bone marrow mesenchymal stem cells: comparison of chemokine and growth factor chemotactic activities. *Stem Cells* 25, 1737-1745.
- Poole, A.R., Kobayashi, M., Yasuda, T., Lavery, S., Mwale, F., Kojima, T., Sakai, T., Wahl, C., El-Maadawy, S., Webb, G., *et al.* (2002). Type II collagen degradation and its regulation in articular cartilage in osteoarthritis. *Ann Rheum Dis* 61 *Suppl* 2, ii78-81.
- Poole, A.R., Kojima, T., Yasuda, T., Mwale, F., Kobayashi, M., and Lavery, S. (2001). Composition and structure of articular cartilage: a template for tissue repair. *Clin Orthop Relat Res*, S26-33.
- Poole, A.R., Nelson, F., Dahlberg, L., Tchetina, E., Kobayashi, M., Yasuda, T., Lavery, S., Squires, G., Kojima, T., Wu, W., *et al.* (2003). Proteolysis of the collagen fibril in osteoarthritis, 2003/11/01 edn.
- Poole, A.R., Rosenberg, L.C., Reiner, A., Ionescu, M., Bogoch, E., and Roughley, P.J. (1996). Contents and distributions of the proteoglycans decorin and biglycan in normal and osteoarthritic human articular cartilage. *J Orthop Res* 14, 681-689.
- Poole, C.A., Ayad, S., and Gilbert, R.T. (1992). Chondrons from articular cartilage. V. Immunohistochemical evaluation of type VI collagen organisation in isolated chondrons by light, confocal and electron microscopy. *J Cell Sci* 103 (Pt 4), 1101-1110.
- Porter, J.R., Henson, A., Ryan, S., and Popat, K.C. (2009). Biocompatibility and mesenchymal stem cell response to poly(epsilon-caprolactone) nanowire surfaces for orthopedic tissue engineering. *Tissue Eng Part A* 15, 2547-2559.
- Pratt, C.W., and Cornely, K. (2004). *Essential Biochemistry* (Wiley International).
- Punwar, S., and Khan, W.S. (2011). Mesenchymal stem cells and articular cartilage repair: clinical studies and future direction. *Open Orthop J.* 5 *Suppl* 2, 296-301.
- Quintavalla, J., Uziel-Fusi, S., Yin, J., Boehnlein, E., Pastor, G., Blancuzzi, V., Singh, H.N., Kraus, K.H., O'Byrne, E., and Pellas, T.C. (2002).

Fluorescently labelled mesenchymal stem cells (MSCs) maintain multilineage potential and can be detected following implantation into articular cartilage defects. *Biomaterials* 23, 109-119.

Quirici, N., Soligo, D., Bossolasco, P., Servida, F., Lumini, C., and Deliliers, G.L. (2002). Isolation of bone marrow mesenchymal stem cells by anti-nerve growth factor receptor antibodies. *Exp Hematol* 30, 783-791.

Ramamurthi, A., and Vesely, I. (2002). Smooth muscle cell adhesion on crosslinked hyaluronan gels. *J Biomed Mater Res* 60, 195-205.

Rasmusson, I., Uhlin, M., Le Blanc, K., and Levitsky, V. (2007). Mesenchymal stem cells fail to trigger effector functions of cytotoxic T lymphocytes. *J Leukoc Biol* 82, 887-893.

Re'em, T., Tsur-Gang, O., and Cohen, S. (2010). The effect of immobilized RGD peptide in macroporous alginate scaffolds on TGFbeta1-induced chondrogenesis of human mesenchymal stem cells. *Biomaterials*.

Rekha, M.R., and Sharma, C.P. (2007). Pullulan as a Promising Biomaterial for Biomedical Applications: A Perspective. *Trends Biomater Artif Organs* 20, 116-121.

Rekha, M.R., and Sharma, C.P. (2009). Blood compatibility and in vitro transfection studies on cationically modified pullulan for liver cell targeted gene delivery. *Biomaterials* 30, 6655-6664.

Repp, R., van Ojik, H.H., Valerius, T., Groenewegen, G., Wieland, G., Oetzel, C., Stockmeyer, B., Becker, W., Eisenhut, M., Steininger, H., *et al.* (2003). Phase I clinical trial of the bispecific antibody MDX-H210 (anti-FcgammaRI x anti-HER-2/neu) in combination with Filgrastim (G-CSF) for treatment of advanced breast cancer. *Br J Cancer* 89, 2234-2243.

Rezvan, A., Ni, C.W., Alberts-Grill, N., and Jo, H. (2011). Animal, in vitro, and ex vivo models of flow-dependent atherosclerosis: role of oxidative stress. *Antioxid Redox Signal* 15, 1433-1448.

Ricote, M., Li, A.C., Willson, T.M., Kelly, C.J., and Glass, C.K. (1998). The peroxisome proliferator-activated receptor-gamma is a negative regulator of macrophage activation. *Nature*. 391, 79-82.

Rizkalla, G., Reiner, A., Bogoch, E., and Poole, A.R. (1992). Studies of the articular cartilage proteoglycan aggrecan in health and osteoarthritis.

Evidence for molecular heterogeneity and extensive molecular changes in disease. *J Clin Invest* 90, 2268-2277.

Robinson, M.J., Osorio, F., Rosas, M., Freitas, R.P., Schweighoffer, E., Gross, O., Verbeek, J.S., Ruland, J., Tybulewicz, V., Brown, G.D., *et al.* (2009). Dectin-2 is a Syk-coupled pattern recognition receptor crucial for Th17 responses to fungal infection. *J Exp Med* 206, 2037-2051.

Rogue, A.B., Firke, S.N., Gaikewad, S.B., Gunjkar, V.N., Vadvalkar, S.M., (2011). Bioadhesive Polymer: Review. *Journal of Pharmaceutical and Biomedical Sciences* 5, 5.

Rosen, A.B., Kelly, D.J., Schuldt, A.J., Lu, J., Potapova, I.A., Doronin, S.V., Robichaud, K.J., Robinson, R.B., Rosen, M.R., Brink, P.R., *et al.* (2007). Finding fluorescent needles in the cardiac haystack: tracking human mesenchymal stem cells labelled with quantum dots for quantitative in vivo three-dimensional fluorescence analysis. *Stem Cells* 25, 2128-2138.

Ruegg, C., Yilmaz, A., Bieler, G., Bamat, J., Chaubert, P., and Lejeune, F.J. (1998). Evidence for the involvement of endothelial cell integrin α V β 3 in the disruption of the tumour vasculature induced by TNF and IFN- γ . *Nat Med* 4, 408-414.

Ruoslahti, E. (1996). RGD and other recognition sequences for integrins. *Annu Rev Cell Dev Biol* 12, 697-715.

Sackstein, R., Merzaban, J.S., Cain, D.W., Dagia, N.M., Spencer, J.A., Lin, C.P., and Wohlgemuth, R. (2008). Ex vivo glycan engineering of CD44 programs human multipotent mesenchymal stromal cell trafficking to bone. *Nat Med* 14, 181-187.

Saijo, S., Ikeda, S., Yamabe, K., Kakuta, S., Ishigame, H., Akitsu, A., Fujikado, N., Kusaka, T., Kubo, S., Chung, S.H., *et al.* (2010). Dectin-2 recognition of alpha-mannans and induction of Th17 cell differentiation is essential for host defense against *Candida albicans*. *Immunity* 32, 681-691.

Saijo, S., and Iwakura, Y. (2011). Dectin-1 and Dectin-2 in innate immunity against fungi. *Int Immunol* 23, 467-472.

Sakaguchi, Y., Sekiya, I., Yagishita, K., and Muneta, T. (2005). Comparison of human stem cells derived from various mesenchymal tissues: superiority of synovium as a cell source. *Arthritis Rheum* 52, 2521-2529.

- Salinas, C.N., and Anseth, K.S. (2008). The enhancement of chondrogenic differentiation of human mesenchymal stem cells by enzymatically regulated RGD functionalities. *Biomaterials* 29, 2370-2377.
- Salinas, C.N., Cole, B.B., Kasko, A.M., and Anseth, K.S. (2007). Chondrogenic differentiation potential of human mesenchymal stem cells photoencapsulated within poly(ethylene glycol)-arginine-glycine-aspartic acid-serine thiol-methacrylate mixed-mode networks. *Tissue Eng* 13, 1025-1034.
- Salter, D.M. (1993). Tenascin is increased in cartilage and synovium from arthritic knees. *Br J Rheumatol* 32, 780-786.
- Samuels, J., Krasnokutsky, S., and Abramson, S.B. (2008). Osteoarthritis: a tale of three tissues. *Bull NYU Hosp Jt Dis* 66, 244-250.
- Sandell, L.J., and Aigner, T. (2001). Articular cartilage and changes in arthritis. An introduction: cell biology of osteoarthritis. *Arthritis Res* 3, 107-113.
- Sandy, J.D., and Verscharen, C. (2001). Analysis of aggrecan in human knee cartilage and synovial fluid indicates that aggrecanase (ADAMTS) activity is responsible for the catabolic turnover and loss of whole aggrecan whereas other protease activity is required for C-terminal processing in vivo. *Biochem J* 358, 615-626.
- Sarkar, D., Vemula, P.K., Teo, G.S., Spelke, D., Karnik, R., Wee le, Y., and Karp, J.M. (2008). Chemical engineering of mesenchymal stem cells to induce a cell rolling response. *Bioconjug Chem* 19, 2105-2109.
- Sarkar, D., Vemula, P.K., Zhao, W., Gupta, A., Karnik, R., and Karp, J.M. (2010). Engineered mesenchymal stem cells with self-assembled vesicles for systemic cell targeting. *Biomaterials* 31, 5266-5274.
- Sato, K., Yang, X.L., Yudate, T., Chung, J.S., Wu, J., Luby-Phelps, K., Kimberly, R.P., Underhill, D., Cruz, P.D., Jr., and Ariizumi, K. (2006). Dectin-2 is a pattern recognition receptor for fungi that couples with the Fc receptor gamma chain to induce innate immune responses. *J Biol Chem* 281, 38854-38866.
- Sato, M., Uchida, K., Nakajima, H., Miyazaki, T., Guerrero, A.R., Watanabe, S., Roberts, S., and Baba, H. (2012). Direct transplantation of mesenchymal

stem cells into the knee joints of Hartley strain guinea pigs with spontaneous osteoarthritis. *Arthritis Res Ther* 14, R31.

Schafer, A.I. (1996). Antiplatelet therapy. *Am J Med* 101, 199-209.

Schinhan, M., Gruber, M., Dorotka, R., Pilz, M., Stelzeneder, D., Chiari, C., Rossler, N., Windhager, R., and Nehrer, S. (2013). Matrix-associated autologous chondrocyte transplantation in a compartmentalized early stage of osteoarthritis. *Osteoarthritis Cartilage* 21, 217-225.

Schraa, A.J., Kok, R.J., Moorlag, H.E., Bos, E.J., Proost, J.H., Meijer, D.K., de Leij, L.F., and Molema, G. (2002). Targeting of RGD-modified proteins to tumour vasculature: a pharmacokinetic and cellular distribution study. *Int J Cancer* 102, 469-475.

Schulze-Tanzil, G., de Souza, P., Merker, H.J., and Shakibaei, M. (2001). Co-localisation of integrins and matrix metalloproteinases in the extracellular matrix of chondrocyte cultures. *Histol Histopathol* 16, 1081-1089.

Schumacher, B.L., Block, J.A., Schmid, T.M., Aydelotte, M.B., and Kuettner, K.E. (1994). A novel proteoglycan synthesized and secreted by chondrocytes of the superficial zone of articular cartilage. *Arch Biochem Biophys* 311, 144-152.

Sekiya, I., Larson, B.L., Vuoristo, J.T., Reger, R.L., and Prockop, D.J. (2005). Comparison of effect of BMP-2, -4, and -6 on in vitro cartilage formation of human adult stem cells from bone marrow stroma. *Cell Tissue Res* 320, 269-276.

Sen, M., Wankowski, D.M., Garlie, N.K., Siebenlist, R.E., Van Epps, D., LeFever, A.V., and Lum, L.G. (2001). Use of anti-CD3 x anti-HER2/neu bispecific antibody for redirecting cytotoxicity of activated T cells toward HER2/neu+ tumours. *J Hematother Stem Cell Res* 10, 247-260.

Serini, G., Valdembri, D., and Bussolino, F. (2006). Integrins and angiogenesis: a sticky business. *Exp Cell Res* 312, 651-658.

Shaikh, R., Raj Singh, T.R., Garland, M.J., Woolfson, A.D., and Donnelly, R.F. (2011). Mucoadhesive drug delivery systems. *J Pharm Bioallied Sci* 3, 89-100.

Shakibaei, M., Abou-Rebyeh, H., and Merker, H.J. (1993). Integrins in ageing cartilage tissue in vitro. *Histol Histopathol* 8, 715-723.

- Shakibaei, M., Csaki, C., and Mobasheri, A. (2008). Diverse roles of integrin receptors in articular cartilage. *Adv Anat Embryol Cell Biol* 197, 1-60.
- Shakibaei, M., and Merker, H.J. (1999). Beta1-integrins in the cartilage matrix. *Cell Tissue Res* 296, 565-573.
- Shakibaei, M., Zimmermann, B., and Merker, H.J. (1995). Changes in integrin expression during chondrogenesis in vitro: an immunomorphological study. *J Histochem Cytochem* 43, 1061-1069.
- Silbert, J.E., and Sugumaran, G. (2002). Biosynthesis of chondroitin/dermatan sulfate. *IUBMB Life* 54, 177-186.
- Silva, E.A., and Mooney, D.J. (2004). Synthetic extracellular matrices for tissue engineering and regeneration. *Curr Top Dev Biol* 64, 181-205.
- Singh, P., Carraher, C., and Schwarzbauer, J.E. (2010). Assembly of fibronectin extracellular matrix. *Annu Rev Cell Dev Biol* 26, 397-419.
- Singh, R.S., Ganganpreet, K.S and Kennedy, J.F. (2008). Pullulan: Microbial sources, production and applications. *Carbohydrate Polymers* 73, 515-531.
- Sittinger, M., Bujia, J., Minuth, W.W., Hammer, C., and Burmester, G.R. (1994). Engineering of cartilage tissue using bioresorbable polymer carriers in perfusion culture. *Biomaterials* 15, 451-456.
- Smith, R.L. (2007). Mechanical Loading Effects on Articular Cartilage Matrix Metabolism and Osteoarthritis. In *Osteoarthritis, Inflammation and Degradation: A Continuum*, J. Buckwalter, M. Lotz, and J.F. Stoltz, eds. (IOS Press), pp. 14-30.
- Smith, R.L., Lin, J., Trindade, M.C., Shida, J., Kajiyama, G., Vu, T., Hoffman, A.R., van der Meulen, M.C., Goodman, S.B., Schurman, D.J., *et al.* (2000). Time-dependent effects of intermittent hydrostatic pressure on articular chondrocyte type II collagen and aggrecan mRNA expression. *J Rehabil Res Dev* 37, 153-161.
- Smolarczyk, R., Cichon, T., Graja, K., Hucz, J., Sochanik, A., and Szala, S. (2006). Antitumour effect of RGD-4C-GG-D(KLAKLAK)₂ peptide in mouse B16(F10) melanoma model. *Acta Biochim Pol* 53, 801-805.
- Sotiropoulou, P.A., Perez, S.A., Gritzapis, A.D., Baxevanis, C.N., and Papamichail, M. (2006). Interactions between human mesenchymal stem cells and natural killer cells. *Stem Cells* 24, 74-85.

Spaggiari, G.M., Capobianco, A., Abdelrazik, H., Becchetti, F., Mingari, M.C., and Moretta, L. (2008). Mesenchymal stem cells inhibit natural killer-cell proliferation, cytotoxicity, and cytokine production: role of indoleamine 2,3-dioxygenase and prostaglandin E2. *Blood* *111*, 1327-1333.

Squires, G.R., Okouneff, S., Ionescu, M., and Poole, A.R. (2003). The pathobiology of focal lesion development in aging human articular cartilage and molecular matrix changes characteristic of osteoarthritis. *Arthritis Rheum* *48*, 1261-1270.

Stagg, J., Divisekera, U., Duret, H., Sparwasser, T., Teng, M.W., Darcy, P.K., and Smyth, M.J. (2011). CD73-deficient mice have increased antitumour immunity and are resistant to experimental metastasis. *Cancer Res* *71*, 2892-2900.

Steadman, J.R., Rodkey, W.G., and Briggs, K.K. (2002). Microfracture to treat full-thickness chondral defects: surgical technique, rehabilitation, and outcomes. *J Knee Surg* *15*, 170-176.

Steinwachs, M.R., Guggi, T., and Kreuz, P.C. (2008). Marrow stimulation techniques. *Injury* *39 Suppl 1*, S26-31.

Stoop, R. (2008). Smart biomaterials for tissue engineering of cartilage. *Injury* *39 Suppl 1*, S77-87.

Stoop, R., van der Kraan, P.M., Buma, P., Hollander, A.P., Poole, A.R., and van den Berg, W.B. (1999). Denaturation of type II collagen in articular cartilage in experimental murine arthritis. Evidence for collagen degradation in both reversible and irreversible cartilage damage. *J Pathol* *188*, 329-337.

Sun, Y., Mauerhan, D.R., Kneisl, J.S., James Norton, H., Zinchenko, N., Ingram, J., Hanley, E.N., Jr., and Gruber, H.E. (2012). Histological examination of collagen and proteoglycan changes in osteoarthritic menisci. *Open Rheumatol J* *6*, 24-32.

Sundelacruz, S., and Kaplan, D.L. (2009). Stem cell- and scaffold-based tissue engineering approaches to osteochondral regenerative medicine. *Semin Cell Dev Biol* *20*, 646-655.

Sutherland, I.W. (1998). Novel and established applications of microbial polysaccharides. *Trends Biotechnol* *16*, 41-46.

Sutton, S., Clutterbuck, A., Harris, P., Gent, T., Freeman, S., Foster, N., Barrett-Jolley, R., and Mobasher, A. (2009). The contribution of the

synovium, synovial derived inflammatory cytokines and neuropeptides to the pathogenesis of osteoarthritis. *Vet J* 179, 10-24.

Tagalakis, A.D., Grosse, S.M., Meng, Q.H., Mustapa, M.F., Kwok, A., Salehi, S.E., Tabor, A.B., Hailes, H.C., and Hart, S.L. (2010). Integrin-targeted nanocomplexes for tumour specific delivery and therapy by systemic administration. *Biomaterials* 32, 1370-1376.

Tarone, G., Galetto, G., Prat, M., and Comoglio, P.M. (1982). Cell surface molecules and fibronectin-mediated cell adhesion: effect of proteolytic digestion of membrane proteins. *J Cell Biol* 94, 179-186.

Tchetina, E.V., Squires, G., and Poole, A.R. (2005). Increased type II collagen degradation and very early focal cartilage degeneration is associated with upregulation of chondrocyte differentiation related genes in early human articular cartilage lesions. *J Rheumatol* 32, 876-886.

Tetlow, L.C., Adlam, D.J., and Woolley, D.E. (2001). Matrix metalloproteinase and proinflammatory cytokine production by chondrocytes of human osteoarthritic cartilage: associations with degenerative changes. *Arthritis Rheum* 44, 585-594.

ThermoScientific. SMCC and Sulfo-SMCC
www.thermo.com/pierce.

Tilg, H., Trehu, E., Atkins, M.B., Dinarello, C.A., and Mier, J.W. (1994). Interleukin-6 (IL-6) as an anti-inflammatory cytokine: induction of circulating IL-1 receptor antagonist and soluble tumour necrosis factor receptor p55. *Blood* 83, 113-118.

Ting, V., Sims, C.D., Brecht, L.E., McCarthy, J.G., Kasabian, A.K., Connelly, P.R., Elisseff, J., Gittes, G.K., and Longaker, M.T. (1998). In vitro prefabrication of human cartilage shapes using fibrin glue and human chondrocytes. *Ann Plast Surg* 40, 413-420; discussion 420-411.

Tins, B.J., McCall, I.W., Takahashi, T., Cassar-Pullicino, V., Roberts, S., Ashton, B., and Richardson, J. (2005). Autologous chondrocyte implantation in knee joint: MR imaging and histologic features at 1-year follow-up. *Radiology* 234, 501-508.

Togel, F., Weiss, K., Yang, Y., Hu, Z., Zhang, P., and Westenfelder, C. (2007). Vasculotropic, paracrine actions of infused mesenchymal stem cells

are important to the recovery from acute kidney injury. *Am J Physiol Renal Physiol* 292, F1626-1635.

Tognana, E., Padera, R.F., Chen, F., Vunjak-Novakovic, G., and Freed, L.E. (2005). Development and remodeling of engineered cartilage-explant composites in vitro and in vivo. *Osteoarthritis Cartilage* 13, 896-905.

Traggiati, E., Volpi, S., Schena, F., Gattorno, M., Ferlito, F., Moretta, L., and Martini, A. (2008). Bone marrow-derived mesenchymal stem cells induce both polyclonal expansion and differentiation of B cells isolated from healthy donors and systemic lupus erythematosus patients. *Stem Cells* 26, 562-569.

Trochon, V., Mabilat, C., Bertrand, P., Legrand, Y., Smadja-Joffe, F., Soria, C., Delpech, B., and Lu, H. (1996). Evidence of involvement of CD44 in endothelial cell proliferation, migration and angiogenesis in vitro. *Int J Cancer* 66, 664-668.

Trzeciak, T., Kruczynski, J., Jaroszewski, J., and Lubiatowski, P. (2006). Evaluation of cartilage reconstruction by means of autologous chondrocyte versus periosteal graft transplantation: an animal study. *Transplant Proc* 38, 305-311.

Tsai, W.B., and Wang, M.C. (2005). Effect of an avidin-biotin binding system on chondrocyte adhesion, growth and gene expression. *Biomaterials* 26, 3141-3151.

Tzianabos, A.O. (2000). Polysaccharide immunomodulators as therapeutic agents: structural aspects and biologic function. *Clin Microbiol Rev.* 13, 523-33.

Umlauf, D., Frank, S., Pap, T., and Bertrand, J. (2010). Cartilage biology, pathology, and repair. *Cell Mol Life Sci* 67, 4197-4211.

Valdes, A.M., Van Oene, M., Hart, D.J., Surdulescu, G.L., Loughlin, J., Doherty, M., and Spector, T.D. (2006). Reproducible genetic associations between candidate genes and clinical knee osteoarthritis in men and women. *Arthritis Rheum* 54, 533-539.

Vankemmelbeke, M., Dekeyser, P.M., Hollander, A.P., Buttle, D.J., and Demeester, J. (1998). Characterization of helical cleavages in type II collagen generated by matrixins. *Biochem J* 330 (Pt 2), 633-640.

Venn, G., Nietfeld, J.J., Duits, A.J., Brennan, F.M., Arner, E., Covington, M., Billingham, M.E., and Hardingham T.E. (1993). Elevated synovial fluid

levels of interleukin-6 and tumor necrosis factor associated with early experimental canine osteoarthritis. *Arthritis Rheum.* 36,:819-26.

Vinatier, C., Bouffi, C., Merceron, C., Gordeladze, J., Brondello, J.M., Jorgensen, C., Weiss, P., Guicheux, J., and Noel, D. (2009). Cartilage tissue engineering: towards a biomaterial-assisted mesenchymal stem cell therapy. *Curr Stem Cell Res Ther* 4, 318-329.

Vinod, K.R., T., R.R., S., S., Banji., D., and B., V.R. (2012). Critical Review on Mucoadhesive Drug Delivery Systems. *Hygeia: Journal for Drugs and Medicines* 4, 21.

Visna, P., Pasa, L., Cizmar, I., Hart, R., and Hoch, J. (2004). Treatment of deep cartilage defects of the knee using autologous chondrograft transplantation and by abrasive techniques--a randomized controlled study. *Acta Chir Belg* 104, 709-714.

Vonwil, D., Schuler, M., Barbero, A., Strobel, S., Wendt, D., Textor, M., Aebi, U., and Martin, I. (2010). An RGD-restricted substrate interface is sufficient for the adhesion, growth and cartilage forming capacity of human chondrocytes. *Eur Cell Mater* 20, 316-328.

Wagers, A.J., and Weissman, I.L. (2004). Plasticity of adult stem cells. *Cell* 116, 639-648.

Wakitani, S., Goto, T., Pineda, S.J., Young, R.G., Mansour, J.M., Caplan, A.I., and Goldberg, V.M. (1994). Mesenchymal cell-based repair of large, full-thickness defects of articular cartilage. *J Bone Joint Surg Am* 76, 579-592.

Wakitani, S., Imoto, K., Yamamoto, T., Saito, M., Murata, N., and Yoneda, M. (2002). Human autologous culture expanded bone marrow mesenchymal cell transplantation for repair of cartilage defects in osteoarthritic knees. *Osteoarthritis Cartilage* 10, 199-206.

Wakitani, S., Kawaguchi, A., Tokuhara, Y., and Takaoka, K. (2008). Present status of and future direction for articular cartilage repair. *J Bone Miner Metab* 26, 115-122.

Wakitani, S., Mitsuoka, T., Nakamura, N., Toritsuka, Y., Nakamura, Y., and Horibe, S. (2004). Autologous bone marrow stromal cell transplantation for repair of full-thickness articular cartilage defects in human patellae: two case reports. *Cell Transplant* 13, 595-600.

Wakitani, S., Nawata, M., Tensho, K., Okabe, T., Machida, H., and Ohgushi, H. (2007). Repair of articular cartilage defects in the patello-femoral joint with autologous bone marrow mesenchymal cell transplantation: three case reports involving nine defects in five knees. *J Tissue Eng Regen Med* 1, 74-79.

Wakitani, S., Okabe, T., Horibe, S., Mitsuoka, T., Saito, M., Koyama, T., Nawata, M., Tensho, K., Kato, H., Uematsu, K., *et al.* (2011). Safety of autologous bone marrow-derived mesenchymal stem cell transplantation for cartilage repair in 41 patients with 45 joints followed for up to 11 years and 5 months. *J Tissue Eng Regen Med* 5, 146-150.

Walker, G.D., Fischer, M., Gannon, J., Thompson, R.C., Jr., and Oegema, T.R., Jr. (1995). Expression of type-X collagen in osteoarthritis. *J Orthop Res* 13, 4-12.

Wang, D.A., Varghese, S., Sharma, B., Strehin, I., Fermanian, S., Gorham, J., Fairbrother, D.H., Cascio, B., and Elisseeff, J.H. (2007). Multifunctional chondroitin sulphate for cartilage tissue-biomaterial integration. *Nat Mater* 6, 385-392.

Wang, Y., Zhao, L., Smas, C., and Sul, H.S. (2010). Pref-1 interacts with fibronectin to inhibit adipocyte differentiation. *Mol Cell Biol* 30, 3480-3492.

Welman, A.D., and Maddox, I.S. (2003). Exopolysaccharides from lactic acid bacteria: perspectives and challenges. *Trends Biotechnol* 21, 269-274.

Westacott, C.I., and Sharif, M. (1996). Cytokines in osteoarthritis: mediators or markers of joint destruction? *Semin Arthritis Rheum* 25, 254-272.

Wilke, M.M., Nydam, D.V., and Nixon, A.J. (2007). Enhanced early chondrogenesis in articular defects following arthroscopic mesenchymal stem cell implantation in an equine model. *J Orthop Res* 25, 913-925.

Williams, R.J., 3rd, Dreese, J.C., and Chen, C.T. (2004). Chondrocyte survival and material properties of hypothermically stored cartilage: an evaluation of tissue used for osteochondral allograft transplantation. *Am J Sports Med* 32, 132-139.

Wong, M., Wuethrich, P., Eggli, P., and Hunziker, E. (1996). Zone-specific cell biosynthetic activity in mature bovine articular cartilage: a new method using confocal microscopic stereology and quantitative autoradiography. *J Orthop Res* 14, 424-432.

Wong, V.W., Rustad, K.C., Glotzbach, J.P., Sorkin, M., Inayathullah, M., Major, M.R., Longaker, M.T., Rajadas, J., and Gurtner, G.C. (2011). Pullulan hydrogels improve mesenchymal stem cell delivery into high-oxidative-stress wounds. *Macromol Biosci* *11*, 1458-1466.

Wu, W., Billingham, R.C., Pidoux, I., Antoniou, J., Zukor, D., Tanzer, M., and Poole, A.R. (2002). Sites of collagenase cleavage and denaturation of type II collagen in aging and osteoarthritic articular cartilage and their relationship to the distribution of matrix metalloproteinase 1 and matrix metalloproteinase 13. *Arthritis Rheum* *46*, 2087-2094.

Xing, Z., Gaudie, J., Cox, G., Baumann, H., Jordana, M., Lei, X.F., and Achong, M.K. (1998). IL-6 is an antiinflammatory cytokine required for controlling local or systemic acute inflammatory responses. *J Clin Invest* *101*, 311-320.

Yagi, H., Soto-Gutierrez, A., Parekkadan, B., Kitagawa, Y., Tompkins, R.G., Kobayashi, N., and Yarmush, M.L. (2010). Mesenchymal stem cells: Mechanisms of immunomodulation and homing. *Cell Transplant* *19*, 667-679.

Yamada, Y., Boo, J.S., Ozawa, R., Nagasaka, T., Okazaki, Y., Hata, K., and Ueda, M. (2003). Bone regeneration following injection of mesenchymal stem cells and fibrin glue with a biodegradable scaffold. *J Craniomaxillofac Surg* *31*, 27-33.

Yang, Y., Rossi, F.M., and Putnins, E.E. (2007). Ex vivo expansion of rat bone marrow mesenchymal stromal cells on microcarrier beads in spin culture. *Biomaterials* *28*, 3110-3120.

Yao, Z., Nakamura, H., Masuko-Hongo, K., Suzuki-Kurokawa, M., Nishioka, K., and Kato, T. (2004). Characterisation of cartilage intermediate layer protein (CILP)-induced arthropathy in mice. *Ann Rheum Dis* *63*, 252-258.

Yasuda, T. (2006). Cartilage destruction by matrix degradation products. *Mod Rheumatol* *16*, 197-205.

Yasumoto, T., Bird, J.L., Sugimoto, K., Mason, R.M., and Bayliss, M.T. (2003). The G1 domain of aggrecan released from porcine articular cartilage forms stable complexes with hyaluronan/link protein. *Rheumatology (Oxford)* *42*, 336-342.

Yegutkin, G.G., Marttila-Ichihara, F., Karikoski, M., Niemela, J., Laurila, J.P., Elima, K., Jalkanen, S., and Salmi, M. (2011). Altered purinergic signaling in CD73-deficient mice inhibits tumour progression. *Eur J Immunol* *41*, 1231-1241.

You, M., Peng, G., Li, J., Ma, P., Wang, Z., Shu, W., Peng, S., and Chen, G.Q. (2011). Chondrogenic differentiation of human bone marrow mesenchymal stem cells on polyhydroxyalkanoate (PHA) scaffolds coated with PHA granule binding protein PhaP fused with RGD peptide. *Biomaterials* *32*, 2305-2313.

Young, D.A., Lakey, R.L., Pennington, C.J., Jones, D., Kevorkian, L., Edwards, D.R., Cawston, T.E., and Clark, I.M. (2005). Histone deacetylase inhibitors modulate metalloproteinase gene expression in chondrocytes and block cartilage resorption. *Arthritis Res Ther* *7*, R503-512.

Zack, M.D., Arner, E.C., Anglin, C.P., Alston, J.T., Malfait, A.M., and Tortorella, M.D. (2006). Identification of fibronectin neoepitopes present in human osteoarthritic cartilage. *Arthritis Rheum* *54*, 2912-2922.

Zhang, Y., Yang, Y., Hong, H., and Cai, W. (2011). Multimodality molecular imaging of CD105 (Endoglin) expression. *Int J Clin Exp Med* *4*, 32-42.

Zheng, M.H., Willers, C., Kirilak, L., Yates, P., Xu, J., Wood, D., and Shimmin, A. (2007). Matrix-induced autologous chondrocyte implantation (MACI): biological and histological assessment. *Tissue Eng* *13*, 737-746.

Zhou, H., Guo, M., Bian, C., Sun, Z., Yang, Z., Zeng, Y., Ai, H., and Zhao, R.C. (2010). Efficacy of bone marrow-derived mesenchymal stem cells in the treatment of sclerodermatous chronic graft-versus-host disease: clinical report. *Biol Blood Marrow Transplant* *16*, 403-412.

Zitzmann, S., Ehemann, V., and Schwab, M. (2002). Arginine-glycine-aspartic acid (RGD)-peptide binds to both tumour and tumour-endothelial cells in vivo. *Cancer Res* *62*, 5139-5143.

Zuk, P.A., Zhu, M., Ashjian, P., De Ugarte, D.A., Huang, J.I., Mizuno, H., Alfonso, Z.C., Fraser, J.K., Benhaim, P., and Hedrick, M.H. (2002). Human adipose tissue is a source of multipotent stem cells. *Mol Biol Cell* *13*, 4279-4295.